รายงานวิจัยฉบับสมบูรณ์

โครงการ **การศึกษาความเฉพาะเจาะจงของตัวเร่งปฏิกิริยาที่มีผลต่อการผลิตผลิตภัณฑ์ที่ได้จากการไพโรไลซิสยางรถยนต์ใช้แล้ว**

โดย รองศาสตราจารย์ ดร. ศิริรัตน์ จิตการค้า

พฤษภาคม 2554

สัญญาเลขที่ **RMU5180037**

รายงานวิจัยฉบับสมบูรณ์

โครงการ การศึกษาความเฉพาะเจาะจงของตัวเร่งปฏิกิริยาที่มีผลต่อการผลิตผลิตภัณฑ์ที่ได้จากการไพโรไลซิสยางรถยนต์ใช้แล้ว

รองศาสตราจารย์ ดร. ศิริรัตน์ จิตการค้า

วิทยาลัยปิโตรเลียมและปิโตรเคมี
จุฬาลงกรณ์มหาวิทยาลัย

สนับสนุนโดยสำนักงานกองทุนสนับสนุนการวิจัย
และสำนักงานคณะกรรมการการอุดมศึกษา

(ความเห็นในรายงานนี้เป็นของผู้วิจัย สกว. และ สกอ. ไม่จำเป็นต้องเห็นด้วยเสมอไป)

กิตติกรรมประกาศ

ผู้วิจัยได้รับเงินทุนสนับสนุนงานวิจัยจาก สำนักงานกองทุนสนับสนุนการวิจัย หรือ สกว. ในหัวข้อที่เกี่ยวข้องกับ การผลิตน้ำมันเชื้อเพลิงทางเลือกและสารตั้งต้นที่มีคุณค่าในอุตสาหกรรมปิโตรเคมีจากกระบวนการไพโรไลซิสยางรถยนต์หมดสภาพโดยใช้ตัวเร่งปฏิกิริยาร่วมในกระบวนการ มาตั้งแต่เริ่มต้นทำงานวิจัยในฐานะอาจารย์ใหม่ จนมาจนกระทั่งบัดนี้ ผู้วิจัยก็ได้รับทุนต่อเนื่อง จากสำนักงานกองทุนสนับสนุนการวิจัย (สกว.) และ สำนักงานคณะกรรมการการอุดมศึกษา (สกอ.) ในทุนเพิ่มขีดความสามารถด้านการวิจัยของอาจารย์รุ่นกลางในสถาบันอุดมศึกษา ผู้วิจัยจึงขอขอบพระคุณสำนักงานกองทุนสนับสนุนการวิจัย และสำนักงานคณะกรรมการการอุดมศึกษา ที่ได้สนับสนุนเงินทุนวิจัยแก่ผู้วิจัยเป็นอย่างดีเสมอมา ซึ่งทำให้สามารถวางรากฐานงานวิจัยของตนเอง เพื่อเป็นส่วนเล็กๆ ส่วนหนึ่งในการผลิตผลงานประเภทต่างๆ ให้กับวงการการศึกษา นอกจากนี้ ผู้วิจัยขอขอบพระคุณบุคลากรของทั้งสององค์กรดังกล่าว ที่ช่วยสนับสนุนการดำเนินงานต่างๆ ให้ลุล่วงได้อย่างสะดวก ถูกต้อง และรวดเร็ว

ทั้งนี้ งานวิจัยในหลายๆ ด้านของผู้วิจัย รวมถึงทางด้านเปลี่ยนขยะยางรถยนต์เป็นพลังงานนี้ จะไม่สำเร็จลุล่วงได้เลยถ้าปราศจากการสนับสนุนร่วมกันในด้านเงินทุน เครื่องมือ และอื่นๆ จาก ศูนย์ความเป็นเลิศแห่งชาติด้านปิโตรเลียม ปิโตรเคมี และวัสดุขั้นสูง วิทยาลัยปิโตรเลียมและปิโตรเคมี จุฬาลงกรณ์มหาวิทยาลัย และบุคลากรของหน่วยงานดังกล่าว ผู้วิจัยจึงขอขอบพระคุณมา ณ โอกาสนี้ นอกจากนี้ ผู้วิจัยขอกราบขอบพระคุณ รองศาสตราจารย์ ดร. สุจิตรา วงศ์เกษมจิตต์ หัวหน้าหน่วยปฏิบัติการวิจัยการสังเคราะห์และการประยุกต์สารโลหะอินทรีย์ จุฬาฯ ที่กรุณาให้คำปรึกษาในงานวิจัยด้านการสังเคราะห์ตัวรองรับประเภท Mesopore อีกทั้งขอขอบคุณนิสิตปริญญาโทและเอก ซึ่งมีรายนามในด้านหลังของรายงานฉบับนี้ ที่ได้ช่วยเหลือและให้ข้อมูล รวมทั้งใช้กำลังใจและกำลังกายในการสนับสนุนการทำงานวิจัยในเรื่องนี้ สุดท้ายนี้ ความดีที่อาจจะเกิดจากผลงานวิจัยนี้ ผู้เขียนขอมอบแด่บิดา มารดา และผู้มีพระคุณทุกท่านที่เปรียบเสมือนบิดามารดา ที่ช่วยอบรมเลี้ยงดู และให้การศึกษาแก่ผู้เขียนมา

บทคัดย่อ

รหัสโครงการ: RMU5180037

ชื่อโครงการ: การศึกษาความเฉพาะเจาะจงของตัวเร่งปฏิกิริยาที่มีผลต่อการผลิตผลิตภัณฑ์ที่ได้จากการไพโรไลซิสยางรถยนต์ใช้แล้ว

ชื่อนักวิจัย: รองศาสตราจารย์ ดร. ศิริรัตน์ จิตการค้า
วิทยาลัยปิโตรเลียมและปิโตรเคมี
จุฬาลงกรณ์มหาวิทยาลัย

Email Address: sirirat.j@chula.ac.th

ระยะเวลาโครงการ: 15 พฤษภาคม พ.ศ. 2551 ถึง 14 พฤษภาคม พ.ศ. 2554

ในการวิจัยด้านการไพโรไลซิสยางรถรถยนต์หมดสภาพนี้ ผู้วิจัยได้ทดสอบตัวเร่งปฏิกิริยาหลากหลายชนิดที่ใช้ร่วมในกระบวนการ โดยตัวเร่งดังกล่าวมีองค์ประกอบเป็นโลหะหนึ่งในชนิดต่อไปนี้คือ แพลทตินัม พัลเลเดียม รูธีเนียม รีเนียม โรเดียม และเงิน ซึ่งถูกบรรจุอยู่บนตัวรองรับ 3 ประเภทคือ ประเภทที่มีคุณสมบัติเป็นกรด เป็นเบส และประเภทที่มีรูพรุนขนาดมีโซ ซึ่งก็คือ เอชเบตา เอชมอร์ เอชวาย เคแอล เอสบีเอ-1 และเอ็มซีเอ็ม เพื่อตรวจสอบความเฉพาะเจาะจงในการผลิตผลิตภัณฑ์ต่างๆ เช่น ก๊าซเชื้อเพลิง น้ำมันเชื้อเพลิง และสารปิโตรเคมีประเภทต่างๆ จากการทดลองพบว่า โลหะแทบจะทุกตัวโดยเฉพาะแพลทตินัมและพัลเลเดียม ที่ใช้นั้นช่วยเพิ่มผลผลิตของน้ำมันเชื้อเพลิงชนิดเบา อีกทั้งยังลดปริมาณโพลาร์อะโรมาติกส์และแอสฟัสทีนในน้ำมันอีกด้วย รูธีเนียมช่วยเพิ่มการผลิตสารโอเลฟินส์เบาได้อย่างเฉพาะเจาะจงโดยเฉพาะเมื่อบรรจุลงไปบนตัวรองรับเอชมอร์และเอ็มซีเอ็ม อีกทั้งพบว่าโลหะเงินมีศักยภาพอย่างมากในการผลิตก๊าซหุงต้มในปริมาณที่สูง นอกจากนี้ ผลงานวิจัยแสดงให้เห็นว่า ตัวเร่งปฏิกิริยาที่บรรจุโลหะโรเดียมและรีเนียมสามารถผลิตสารประกอบโมโนอะโรมาติกส์ในน้ำมันในปริมาณสูงอย่างเฉพาะเจาะจงอีกด้วย

คำหลัก: ยางรถยนต์, ไพโรไลซิส, โลหะ, ซีโอไลท์, น้ำมัน, สารปิโตรเคมี

Abstract

Project Code: RMU5180037

Project Title: Selectivity of Catalysts toward the Production of Various Products Obtained from Pyrolysis of Waste Tire

Investigator: Dr. Sirirat Jitkarnka
Associate Professor
The Petroleum and Petrochemical College
Chulalongkorn University

Email Address: sirirat.j@chula.ac.th

Project Period: 15 May 2008 - 14 May 2011

On waste tire pyrolysis, this work investigated the selectivity of various catalysts composed of metals (Pt, Pd, Ru, Re, Rh, and Ag) and three types of supports; acid, base, and mesoporous supports (HBETA, HMOR, HY, KL, SBA-1, and MCMs) toward the production of various products such as valuable gases, oils, and some petrochemicals. As a result, most of metal-supported catalysts, especially Pt- and Pd-loaded ones, improved light oil production with low contents of polar-aromatics and asphaltene. Ru catalysts selectively produced light olefins, especially when loaded on HMOR and MCMs. Ag-supported catalysts were found promising in producing cooking gases. Moreover, some catalysts such as Rh- and Re-loaded ones selectively produced a high mono-aromatic content in oil.

Keywords: Waste tire, Pyrolysis, Metals, Zeolites, Oils, Petrochemicals

Table of Contents

Chapter		Page
	Acknowledgements	๓
	Abstract (Thai)	๔
	Abstract (English)	๕
1	**Introduction**	**1**
2	**Background and Literature Reviews**	**7**
	2.1 Tires and Waste Tire Problems	7
	2.2 Pyrolysis of Waste Tire	10
	2.2.1 Mechanistic Study	11
	2.2.2 Pyrolytic Oil	12
	2.2.3 Effects of Pyrolysis Conditions	13
	2.2.4 Catalytic Pyrolysis of Waste Tire	14
	2.3. Noble Metal-Supported Catalysts	24
	2.3.1 Monometallic Catalysts	24

Dr. Sirirat Jitkarnka
Associate Professor
The Petroleum and Petrochemical College
Chulalongkorn University

2.3.2 Bimetallic Catalysts 31

2.4. Objectives and Scope 33

3 Methodology 35

3.1. Samples, Materials, and Chemicals 35

3.1.1 Waste Tire Samples 35

3.1.2 Materials and Chemicals 36

3.2 Catalyst Preparation 37

3.3 Pyrolysis of Waste Tire 38

3.3.1 Pyrolysis 38

3.3.2 Product Characterization 39

3.3.3 Catalyst Characterization 43

4 Effects of Acid Supports 46

4.1. Characterization of Acid Zeolites 46

4.2 Pyrolysis of Waste Tire 48

4.2.1 Product Yields 48

4.2.2 Gas Compositions 49

4.2.3 Petroleum fractions 50

4.2.4 Molecular Composition in oils 52

4.2.5 Petrochemical Yields 62

5 Effects of Metals on Acid Supports 64

5.1. Pt-Loaded Catalysts 65

5.1.1 Product Yields 65

5.1.2 Gas Compositions 66

5.1.3 Petroleum fractions 67
5.1.4 Molecular Composition in oils 68
5.1.5 Petrochemical Yields 69
5.1.6 Polar-aromatic reduction 70
5.2 Pd-Loaded Catalysts 84
5.2.1 Product Yields 84
5.2.2 Gas Compositions 85
5.2.3 Petroleum fractions 86
5.2.4 Molecular Composition in oils 88
5.2.5 Petrochemical Yields 89
5.2.6 Effects of Pd loading amount and loading technique 89
5.3 Ru-Loaded Catalysts 100
5.3.1 Product Yields 101
5.3.2 Gas Compositions 102
5.3.3 Petroleum fractions 103
5.3.4 Molecular Composition in oils 104
5.3.5 Petrochemical Yields 105
5.3.6 Effect of Ru Loading Amount 106
5.4 Ag-Loaded Catalysts 119
5.4.1 Product Yields 120
5.4.2 Gas Compositions 121
5.4.3 Petroleum fractions 122
5.4.4 Molecular Composition in oils 124
5.4.5 Petrochemical Yields 128
5.4.6 Sulfur removal from oil 129
5.5 Rh-Loaded Catalysts 132

5.5.1 Product Yields 132
5.5.2 Gas Compositions 133
5.5.3 Petroleum fractions 134
5.5.4 Molecular Composition in oils 136
5.5.5 Petrochemical Yields 137
5.6 Re-Loaded Catalysts 137
5.6.1 Product Yields 138
5.6.2 Gas Compositions 138
5.6.3 Petroleum fractions 140
5.6.4 Molecular Composition in oils 141
5.6.5 Petrochemical Yields 143

6 Effects of Basic Support and Metals on Basic Support 145
6.1. Characterization of Metal-loaded KL Catalysts 147
6.2 Pyrolysis of Waste Tire 147
6.2.1 Product Yields 147
6.2.2 Gas Compositions 148
6.2.3 Petroleum fractions 151
6.2.4 Molecular Composition in oils 152
6.2.5 Petrochemical Yields 156

7 Mesoporous Supports and Role of Ruthenium 158
7.1. SBA-1 158
7.1.1. SBA-1 as a support 159
7.1.2 Roles of ruthenium during catalytic pyrolysis of waste tire 160
7.1.3 Influences of catalyst preparation 165

7.1.4 Influences of ruthenium particle size 169

7.1.5 Conclusions 173

7.2 MCM-41 174

7.2.1 Catalyst characterization 175

7.2.2 Pyrolysis products 178

7.2.3. Conclusions 187

7.3 MCM-48 188

7.3.1 Catalyst characterization 188

7.3.2 Pyrolysis Products 189

7.3.3 Conclusions 195

8 Conclusions and Recommendations 196

8.1 Selectivity of acid supports 197

8.2 Selectivity of metals on acid supports 198

8.3 Selectivity of basic support and metals on basic support 204

8.4 Selectivity of mesoporous supports and the roles of rhutenium 206

8.5 Recommendations for future work 208

References 209

Outputs of the Project 230

1

Introduction

Nowadays, the rapid growth of the population and the economics in the world generates the large amount of tires. The world production of waste tire is approximate $6x10^6$ tons/year, and nearly 70% of these wastes are simply dumped in an open or in the land fill (Galvagno *et al.*, 2002). Likewise, Shulmam in 2002 reported that large numbers of waste tires were generated: 2.5 x 10^6 tons per year in the European Union, 2.5 x 10^6 tons per year in the North America, and $1x10^6$ tons per year in Japan. In 2004, the biggest consumption was in China, which produced $4.2x10^6$ tons. This, together with the fact that tires are designed to be resistant to chemical, biological and physical degradation, has been causing serious environmental problems. Owing to the low bulk density, they occupy large volumes (about 75% of the space) and, if buried, disrupt the integrity of landfill sites.

Dr. Sirirat Jitkarnka
Associate Professor
The Petroleum and Petrochemical College
Chulalongkorn University

Moreover, fires at tire deposits are very difficult to control, and generate high levels of pollution to the soil, atmosphere, and waters (San Miguel *et al.,* 2006).

The nature of the tire is the thermoset rubbers which individual chain has been chemically linked by covalent bonds during the polymerization process. The typical passenger tire is composed of 14% wt natural rubber, 27% wt synthetic rubber, 28% wt carbon block, 14-15% wt steel and 16-17% wt fabric, accelerators, antiozonants etc. The average weight is about 25 lbs of new tires and 20 lbs for used tires. There are several techniques used to eliminate and recycle the used tires such as retreading, reclaiming, incineration, grinding, gasification, landfill etc.. However, all of them have some limitations. The pyrolysis process which is the thermal decomposition of rubber polymer to lower molecular weight products (liquid and gases) in the absence of oxygen has been currently interesting for used tire pyrolysis because these products can be useful as fuels and chemicals feed stock. There are 4 new technologies are being developed: (1) **Microwave pyrolysis** which requires shorter heating time and more uniform heat transfer to the objects than conventional heating method, (2) **Ultrasonic devulcanization** which uses sonic energy to break down sulfur-carbon chemical bonds in tires and rubber tires to transform from solid to a highly viscous fluid within milliseconds, (3) **Supercritical fluid depolymerization** which supercritical water is used to depolymerize the rubber compounds to lower molecular weights with requires lower temperature and shorter processing times and (4) **Use of special catalysts** which can reduce processing time and temperature to decompose the tire rubbers with no significant of new equipment.

In many countries, the environmental regulations concerning the waste tire are becoming more and more stringent. This waste hierarchy favors the valorization and recycling alternatives. Thus, over recent years, tire pyrolysis, a recycling process, has attracted renewed significant attention. It essentially involves decomposition of the tire components by exposure to high temperatures in the absence of oxygen. The result is a carbonized char, condensable oil, and a gas fraction. The char can be used as low-grade carbon black, as a solid fuel, or may be upgraded to activated carbon

(Williams and Brindle, 2003), whereas the gas contains mainly hydrocarbons (C_1- C_5), hydrogen with a relative high content (Barbooti *et al*, 2004), and a low concentration of H_2S (Berrueco *et al.*, 2005). The tire-derived oil is a complex mixture of hydrocarbons with a high amount of aromatics (Cunliffe and Williams, 1998).

The tire-derived oil was reported to have a high calorific value of about 41-44 MJ/kg (Cunliffe and Williams, 1998). In addition, its property is similar, to a certain extent, to that of commercial petroleum naphtha (Benellal *et al.*, 1995). When it was used as a fuel by mixing with a reference fuel in a diesel engine, a reliable operation could be achieved up to 70% of this oil in the blend (Murugan *et al.,* 2009). However, higher smoke, hydrocarbon (HC) and CO emissions were recorded. Also, oil sticking was occasionally found on the nozzle stem and sac. These phenomena were believed to come from the high concentration of aromatics, especially the high concentration of polycyclic HCs (Murugan *et al.*, 2009). In addition, there are considerable amounts of sulfur-containing compounds such as thiophene, benzothiophene, and their derivatives found in the tire-derived oil (Williams and Bottrill, 1995; Pakdel *et al.*, 2001), consecutively limiting its applications as a direct-usable fuel due to the serious problem of SO_2 emission and a decrease in the efficiency of the engine. Unfortunately, no study has been found so far on dealing with aromatic reduction, particularly poly- and polar-aromatics (PPAHs) in order to make the tire-derived oil applicable as a high quality fuel. Instead, the catalytic pyrolysis of waste tire has sometimes been focused on the possibility of aromatic production.

One well-known catalyst is zeolites, which have been widely used in technologies such as adsorption, separation, and catalysis. For zeolite applications, their efficiency is made possible by specific properties, such as high surface area, molecular sieve characteristics, high adsorption capacity and well-defined active sites. Zeolites can be classified in terms of their channel size as having ultra large (>12) membered rings (MR), medium (10-MR) and small (8-MR) rings. The number of tetrahedral atoms (T: Si, Al, P, Ge, etc.) in the ring defines and limits the pore aperture of their largest channels. The more rapid diffusion of reactant and products

is better obtained within large-pore tri-directional zeolite (Blasco *et al.*, 2004). Recently, synthesis attempts have been directed to an additional new zeolite, which has large pore openings, and large and ultralarge rings, like a series of new large-pore tri-dimensional (Si,Ge)-zeolite called the ITQ series, such as ITQ-21. It is a new zeolite, containing Si, Ge and optionally Al as the framework cation. This material presents a unique pore topology formed by nearby spherical large cavities of 1.18 nm diameter joined to six other neighboring cavities by circular 12-ring pore windows with an aperture of 0.74 nm, which results in a three-directional channel system of fully interconnected passageways. This new zeolite, because of these new properties, could lead to some improved catalysts for oil refinery (Corma *et al.*, 2002). Williams and Brindle (2002, 2003a, 2003b) investigated the pyrolysis of waste tire using ZSM-5 and Y zeolites with different Si:Al ratios and pore diameters to see the influences of zeolite structure, catalyst temperature, and catalyst-to-tire ratio on the yield and compositions of the tire-derived oil. Boxiong *et al.* (2007a) studied the effects of USY and ZSM-5 on the compositions of the light fractions. Overall, higher aromatic concentrations could be obtained with using zeolites having higher acidity and larger pore diameter, and also with higher catalyst-to-tire ratios.

Bifunctional catalysts have been extensively studied for the reduction of aromatics in fuel (Lugstein *et al.*, 1999). Metals can catalyze the hydrogenation of the feedstock, making it more reactive for cracking and removing heteroatoms (sulfur, oxygen) (Ali *et al.*, 2002). And, a high level of aromatic hydrogenation at moderate hydrogen pressures can be achieved with noble metals catalysts (Eliche-Quesada *et al.*, 2006a, 2006b). This intrinsically-high hydrogenation activity might also help reducing steric effects that impede the direct elimination of the sulfur heteroatom (Pecoraro and Chianelli, 1981) in the hydrodesulfurization (HDS). However, noble metals display a low resistance to sulfur poisoning, thus limiting their applications. The sulfur tolerance of a noble metal-supported catalyst may be enhanced by (i) using acidic carriers (Barbier *et al.*, 1990), (ii) changing the metal particle size, or (iii) alloying with other metals (Lee and Rhee, 1998). Consequently, the activity of noble metal-supported catalysts depends strongly on the type of the support (Onyestyak *et*

al., 2002), the metal dispersion, and also the metallic nature (Castellon *et al.*, 2004).

The purpose of the work was to investigate the influences of various noble metal-supported catalysts (Pt, Ru, Rh, Pd, Ag, and Re supported on HBETA, HMOR, HY, KL, SBA-1, MCM-41, and MCM-48) on the yields and nature of the products obtained from waste tire pyrolysis. The pyrolysis was carried out in a bench-scale autoclave reactor from room temperature to the final temperature of 500°C (for the pyrolysis zone) and 350°C (for the catalytic zone) with the heating rate of 10°C/min in the atmospheric pressure. Other parameters; particle size, holding time, N_2 flow rate, the amount of sample and catalysts were fixed at 8-18 mesh, 90 min, 30 ml/min, 30 g, and 7.5 g, respectively.

2

Background and Literature Reviews

2.1 Tires and Waste Tire Problems

Typically, a tire composes of natural rubber (NR), styrene-butadiene rubber (SBR), and butadiene rubber (BR) (Williams and Besler, 1995). The rubber chains are cross-linked by sulfur after vulcanization. Sulfur may be present in the vulcanization network in a number of ways such as monosulfide, disulfide, or polysulfide (Blow and Hepburn, 1982). It may also be present as dependent sulfides, or cyclic sulfides. The content (wt%) of sulfur in the tire depends on the manufacture, but generally in the range of 1-2% (Blow and Hepburn, 1982). **Table 2.1** summarizes the typical composition of a tire (Qu *et al.,* 2006).

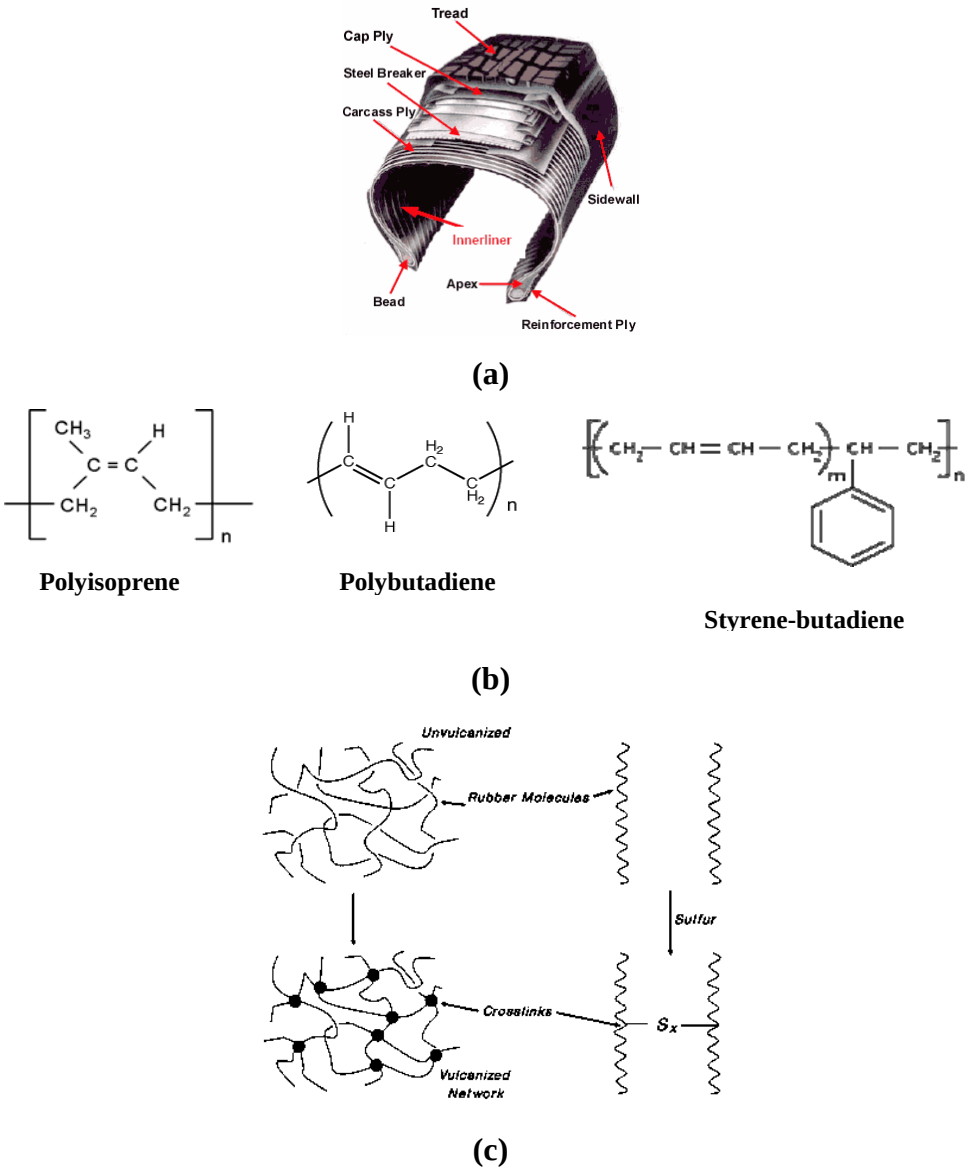

Figure 2.1 (a) Tire structure (www.mindfully.org), (b) Rubbers composition (http://en.wikipedia.org/wiki/Styrene-butadiene), and (c) Vulcanization (www.eng-forum.com/articles/tires...res2.htm)

Table 2.1 A typical composition of a passenger tire (Qu *et al.,* 2006)

	Natural	Syrene-Butadiene Rubber	Butadiene

	Rubber		**Rubber**
wt%	58	27	15

Table 2.2 Chemical compositions and function in tire manufacture

Material	**Function**
Natural rubber or polyisoprene	The basic elastomer in tire making
Styrene-butadiene co-polymer (SBR)	For substitution in the part of natural rubber base on the comparative of materials cost
Polybutadiene	For combination with other rubbers due to its low heat-build up properties
Halobutyl rubber	For the tubeless inner liner compounds
Carbon Black	For reinforcement and abrasion resistance.
Silica	For high performance tire
Sulphur	For cross-linking the rubber molecules in the vulcanization process
Vulcanizing Accelerators	Speed up the vulcanization
Activators	An assister for the vulcanization, such as zinc oxide
Antioxidants and antiozonants	A preventer of sidewall cracking due to the action of sunlight and ozone

Due to the growing population, the world demand of tire keeps increasing. Consequently, over $6x10^6$ tons of waste tire are globally produced annually (Galvagno *et al.,* 2002). This, together with the fact that tires are designed to be resistant to chemical, biological and physical degradation, has been causing serious environmental problems. Owing to the low bulk density of this waste, it occupies

large volumes and, if buried, disrupts the integrity of landfill sites. Moreover, fires at tire deposits are very difficult to control and generate high levels of pollution to the soil, atmosphere and water (San Miguel *et al.,* 2006). For those reasons, the environmental regulations concerning the waste tire become more and more stringent. This waste hierarchy favors the valorization and recycling alternatives. At the same time, the gradually depletion of petroleum reserves has created interest in finding alternative source of energy. Thus, over recent years, tire pyrolysis, a recycling process, has attracted renewed significant attention.

2.2 Pyrolysis of Waste Tire

Pyrolysis of waste tire essentially involves the degradation of the tire components by exposure to high temperatures in the absence of oxygen. The result is a carbonized char, condensable oil and a gas fraction. The yields and nature of these products depend on many factors *e.g.* temperature, the size of tire particle, the type of reactors, pressure…, etc. The oil and gas can be used as fuels or chemical feedstock, whereas the solid residue can be recycled in worthwhile applications such as smokeless fuel, carbon black or low-grade activated carbon. The main products of waste tire pyrolysis consist of gas product, liquid oil, and char. The properties of these products are shown in **Table 2.3**.

Table 2.3 The properties of main products obtained from tire pyrolysis (http://www.ciwmb.ca.gov/Publications/Tires/43296029.doc)

Product	Composition	Properties
Gas (10-30%)	Hydrocarbon mixture, low sulfur content	Calorific value of 19-45 MJ m^{-3} (500-1,200 Btu ft^{-3})
Oil (38-55%)	Contains less than 1% sulfur	Calorific value of 42 MJ kg^{-3} (18,000 Btu lb^{-3})

Char (33-38%)	Contains 2-3% sulfur and approx. 4-5% zinc	Calorific value of 28-33 MJ kg^{-3} (12,000-14,000 Btu lb^{-3})

2.2.1 Mechanistic Study

Chen and Qian (2000) investigated the decomposition of polybutadiene under different temperatures. At lower temperatures, the rubber is decomposed mainly by scission, followed by unzipping to yield monomers, whereas at higher temperatures, the hydrogen transfer reaction takes place, and chain scission mainly occurrs at the β-positions accompanied by cyclization and aromatization.

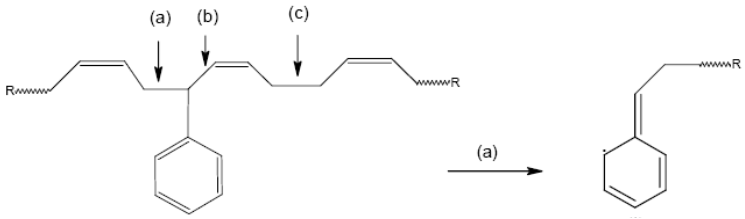

Scheme 2.1 SBR decomposition (Choi, 2000)

In the pyrolysis of natural rubber (NR), the β-scission is also much more preferable because of the low bond dissociation energy, leaving the allylic radicals (Chen and Qian, 2002). For SBR, the thermal degradation is favored at the position (a) than (c) in **Scheme 2.1** as suggested by Choi (Choi, 2000), and no product resulted from the dissociation at the position (b) was observed.

The complex structure of tire makes it difficult to understand clearly the multi-reactions occurring during tire pyrolysis. However, Jitkarnka *et al.* (2007) proposed that the breakdown of a tire molecule was initialized by breaking S-S bonds, and then spread out along the chains.

2.2.2 Pyrolytic Oil

Among the pyrolysis products, the tire-derived oil has attracted much more attentions due to its high heating value [21], its storage advantage, and its property, which was reported to be similar, to a certain extent, to that of commercial

naphtha (Benellal *et al.*, 1995). Pyrolytic oil is a complex mixture of hydrocarbons (HCs) with high concentration of aromatics, particularly single-ring aromatic HCs (Cunliffe and Williams, 1998). However, this concentration is not high enough to obtain an economically separation process. And, the aromatic property of the tire-derived oil (Benallal *et al.*, 1995), especially its remarkable content of polycyclic HCs, has limited its application as a direct-usable fuel. This is due to the fact that these compounds together with the sulfur-containing compounds found in the oil (Pakdel *et al.*, 2001) cause a lot of smoke, HC and CO emissions, and also oil sticking on the nozzle stem and sac of diesel engine (Murugan *et al.*, 2009).

The formation of polycyclic aromatics during the pyrolysis of waste tire was investigated by Williams and Taylor (1993). They suggested that the pyrolysis of tire led to the production of ethylene, butadiene…, which could react to form cyclic olefins, followed by dehydrogenation to produce aromatic compounds. As a result of subsequent associative reaction, the formation of polycyclic aromatics might occur. A poly-aromatic compound, such as phenathrene, was also formed after the formation of naphthalene, a di-aromatic compound. Moreover, no evidence proving the direct formation of aromatics from cyclization of alkanes was observed.

Pyrolytic oil also has a considerable amount of sulfur-containing compounds, such as benzothiophene, thiophene and their derivatives (Williams and Bottrill, 1995; Pakdel *et al.,* 2001). However, the formation of these compounds during pyrolysis is still remained unelucidated.

2.2.3 Effects of Pyrolysis Conditions

Table 2.4 summarizes the yields of gas and oil generated by waste tire pyrolysis using different reaction systems. Accordingly, the yields are strongly dependent on the type of reactor as well as pyrolysis conditions.

Table 2.4 Yield of pyrolysis products for different systems

Authors	Gas (%wt)	Oil (%wt)	Temperature (°C)	Reactor

Williams *et al.*, 1990	2.4-14.8	3.6-58.8	300-720	Static batch
Laresgoiti *et al.*, 2000	4.8-38.5	7.6-19.3	300-700	Autoclave
Cunliffe and Williams, 1998	4.5-8.9	53.1-58.1	450-600	Static batch
Berrueco *et al.*, 2005	2.4-4.4	30-42.8	400-700	Static batch

Temperature is one of the most important factor controlling the yield and nature of the products evolved in pyrolysis. Therefore, its influences on the degradation of waste tire have been investigated extensively. Generally, it was found that the tire can be completely decomposed at 500°C (Roy *et al.*, 1999; Rodriguez *et al.*, 2001). Pyrolysis at temperatures higher 500°C did not change the yield of the carbonaceous char, except the yield and nature of other products (Laresgoiti *et al.*, 2004). Cunliffe and Williams (1998) observed a decrease in the yield of oil in accordance with an increase in gas yield as the pyrolysis temperature was risen over 600°C. And the concentration of aromatic compounds in oil also increased at the expense of aliphatic hydrocarbons with increasing pyrolysis temperatures. Similar observation was reported by Laresgoiti *et al.* (2004), on which the temperatures were varied in the range of 300°C – 700°C. Pyrolysis temperature also affects the calorific value of the derived oil (Diez *et al.*, 2004). Namely, the oil had high calorific value, and the value increased along with pyrolysis temperature.

Another operating factor that normally found to affect the yield and nature of the obtained products is the residence time, which is typical controlled by the flowrate of the carrier gas. Mastral *et al.* (2000) observed a slight increment in the yield of oil as the velocity of the carrier gas increased. Also, the variation of the flowrate of the carrier gas changed of the oil compositions. However, using different carrier gas insignificantly influenced the yield and compositions of the derived oil. Similarly, the decrease in the yield of oil as the residence time increased was reported by Leung *et al.* (2002) and Barbooti *et al.* (2004), which was attributed to the existence of greater and deeper cracking reactions.

2.2.4 Catalytic Pyrolysis of Waste Tire

Due to the high content of aromatics in the tire-derived oil, catalysts have sometimes been introduced to the pyrolysis, aiming at enhancing the yield of valuable aromatic compounds. Generally, the use of acid zeolite catalyst in the pyrolysis of waste tire increases the yield of gaseous product at the expense of oil yield due to its cracking activity. And, the effect is more pronounced with increasing the amount of acid zeolite catalyst used, *i.e.* increasing the catalyst-to-tire ratio (Boxiong *et al.*, 2007; Williams and Brindle, 2002). And the catalyst-to-tire ratio also affects the compositions of oil and gas products. Boxiong *et al.* (2007b) found that benzene and toluene concentrations peaked at the catalyst-to-tire ratio of 0.5, whereas that of xylenes increased with increasing the value of this ratio.

In petrochemical industry, catalysts have been introduced for reaction improvement and value-added products. Catalysts are used to improve the condition of reaction such as temperature and holding time. Catalysts can reduce the activated energy of reaction. There are many types of catalysts used in petrochemical industry. The properties of catalysts play an important role in the selectivity of products. A zeolite is a commercial catalyst used in petrochemical industry. It is a crystalline material with cross-linked structure of SiO_4 and AlO_4. The crystalline faulting in zeolite structures affects both the catalytic and sorption properties. Using zeolites as catalysts gives many advantages since they can be recovered. The advantages of zeolite catalysts are low cost and higher activity. The zeolite applications are important in cracking refinery process. So, zeolites are commonly used in catalytic operations.

There are several types of zeolites used in cracking reaction due to the difference in the properties of zeolites. The next section introduces the characteristics of four commercial zeolites that were used in this study.

(a) BETA zeolite

BETA zeolite (**Figure 2.2**) is considered as a kind of high silica zeolite with the Si/Al ratio of 13.5. The channel system of BETA zeolite is straight. The pore size of BETA zeolite has three-dimension and has a cross section of 0.76 x 0.64 nm. And, it has an intersecting channel system with 12-membered rings. The structure and channel systems of BETA zeolite are presented in **Figure 2.2**. The introduction of BETA zeolite in petrochemical or petroleum refinery industry is to be used as a catalyst in aromatic alkylation, isomerization, hydrocracking, catalytic cracking, and so on. BETA zeolite has a good selectivity on chain hydrocarbon cracking.

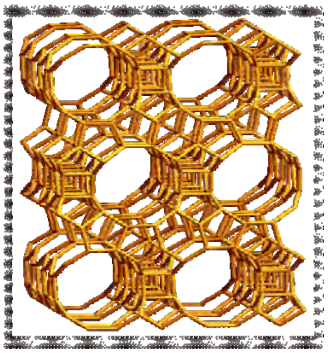

Figure 2.2 BETA zeolite structure (www.chemistry.nus.edu.sg).

(b) Y zeolite

Y zeolite is an intermediate silica zeolite with the Si/Al ratio of 7.5. Y zeolite has the structure as FAU (faujasite). It is considered as three-dimensional pore structure. The pore diameter is 7.4 Å with 12 membered rings. And, this zeolite has surface area approximately 600 m^2/g. The structure and channel system of Y zeolite are presented in **Figure 2.3**. Normally, the application of Y zeolite is used in catalytic cracking. The most importance of this zeolite is used in the acidic form for petroleum refinery catalytic cracking units. The advantage of acidic form can increase the yield of gasoline and diese

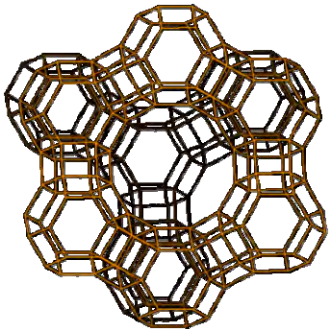

Figure 2.3 Y zeolite structure (www.chemistry.nus.edu.sg).

(c) KL zeolite

KL zeolite is considered as a basic zeolite with the Si/Al ratio of 3.0. It has one-dimension with the straight channel structure of 12-membered rings. The channel of KL zeolite has unique framework topology with an opening of 0.71 nm in diameter. The structure and channel system of KL zeolite are presented in **Figure 2.4**. KL zeolite is a basic catalyst. It acts like an electron donor. This property of KL zeolite can increase the electron density on the metal clusters. There are several researchers who studied the effect of metal loaded on KL zeolite. They reported that KL zeolite was often used as a support for highly dispersed Pt. The Pt/KL was a selective catalyst to produce benzene in the aromatization of n-hexane. The high aromatization activity of the Pt/KL zeolites resulted from the electronic property. Furthermore, the octane number of gasoline fraction can be improved by the basicity of catalyst due to aromatization ability.

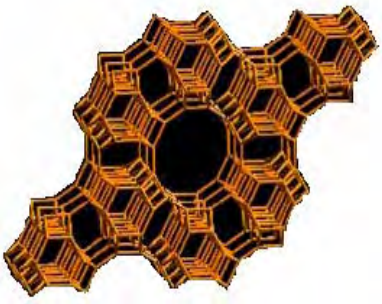

Figure 2.4 KL zeolite structure (www.chemistry.nus.edu.sg).

(d) HMOR zeolite

HMOR zeolite is a moderate acidic zeolite with the Si/Al ratio of 9.5. It has large pore size with an opening of 6.5 Å x 7.0 Å. HMOR zeolite is considered as one-dimensional straight channel structure with 12-membered rings (**Figure 2.5**), and it has surface area is approximately 380 m^2/g. The structure and channel system of HMOR zeolite are presented in Figure 2.5. HMOR zeolites is used as solid acid catalyst and widely used in hydrocracking and hydroisomerization process.

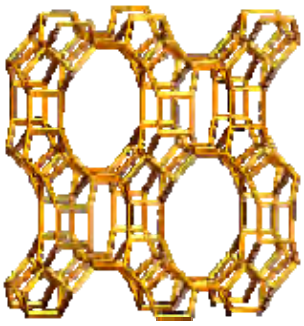

Figure 2.5 HMOR zeolite structure (www.chemistry.nus.edu.sg).

Four commercial catalysts used in the experiment were obtained from Tosoh Company, Singapore are shown in **Table 2.5**.

Table 2.5 The structure of commercial zeolites

Zeolite	Si/Al	Pore size (Å)
USY 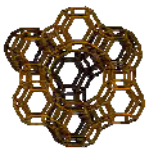	7.5	7.4

BETA 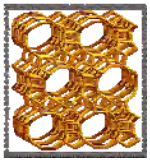	13.5	7.6 x 6.4
HMOR 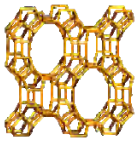	9.5	7 x 6.5
KL	3	7.1

Besides zeolites, mesoporous materials such as MCM and SBA families can be used as supports in many reactions including cracking.

In 1992, the mobil scientists first synthesized the Mobil Composition of Matter series as MCM-41, and MCM-48, which were the most of popular mesoporous molecular sieves. Their surface area is higher than 1,000 m^2/g. Furthermore, they have the pore diameter range between 1.5 to 20 nm, which depends on the condition of synthesis and a kind of surfactant used as the pore-directing agent.

The MCM-41 is a mesoporus silica material, which has one dimension hexagonal pore (**Figure 2.6**). The MCM-48 has three dimensional pores. They have been applied to the catalyst work as a support of heterogeneous catalysts and an adsorbent in waste water treatment. The XRD result of Jang *et al.* (2005) shows that the MCM-48 has plane 211 while the MCM-41 has plane 100 at the same 2-theta value of 2.5. It was confirmed that the MCM-41 has different structure to the MCM-48. The pore size of MCM-48 is between 1.6 nm and 3.8 nm. The XRD patterns of MCM-41 and MCM-48 are shown in **Figure 2.7**.

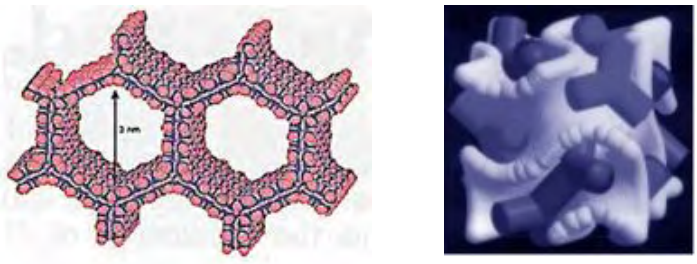

(a) **(b)**

Figure 2.6 Pore structure of the Mobil composition of matter or MCM: (a) MCM-41 (1-D) and (b) MCM-48 (3-D) (http://www.chemistry.wustl.edu/research/lin_group).

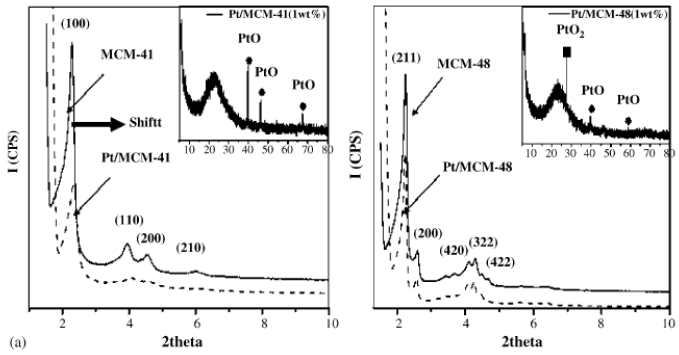

Figure 2.7 XRD results of MCM-41 and MCM-48 with and without platinum loaded (Jang *et al.*, 2005).

Williams and Brindle (2002) studied the catalytic pyrolysis of waste tire using two types of zeolites, Y and ZSM-5, and reported an increase in the concentration of single-ring aromatic hydrocarbons, *i.e.* benzene, toluene and xylene. Y zeolite produced the higher amount of these aromatics with respect to ZSM-5 due to its lower Si:Al ratio and larger pore size. Later, with the aim to obtain much higher concentration of certain single-ring aromatic, Boxiong *et al.* (2007a) used USY and ZSM-5 as catalysts in the pyrolysis of waste tire. The experimental results indicated the high concentrations of benzene, toluene, and xylenes, which could be achieved with USY zeolite. The high concentration of aromatics, particularly poly- and polar-aromatic hydrocarbons (PPAHs), as mentioned earlier, has limited the use of tire-

derived oil as fuel. However, this limitation is still remained unsolved. Actually, no study has been found so far aiming at the reduction of PPAHs in this oil.

Miguel *et al.*, (2006) investigated the effect of various acid catalysts in the conversion of tire rubber into hydrocarbon products. Five catalysts were used in the experiments which are three zeolites (standard ZSM-5, monocrystalline n-ZSM-5 and beta zeolite) and two mesostructured materials (Al-MCM-41 and Al-SBA-15). They found that all zeolite catalysts gave marked selectivity of aromatic species, particularly toluene, m/p-xylene and benzene. While mesostructured catalysts, Al-MCM-41 and Al-SBA-15 exhibited stronger aromatization and benzene alkylation capacity because of their weaker Lewis acid and larger pore size, which provide larger molecules of products. William and Brindle (2002) studied the influence of the temperature in the catalytic pyrolysis with two different pore size catalysts, Y-type zeolite (CBV-400) and ZSM-5, which have pore size of 7.8 Å and 5.6 Å, respectively. They varied the temperature between 430°C and 600°C, and found that Y-type zeolite which has larger pore size and higher surface acidity yielded higher aromatic compounds but lower liquid yields than ZSM-5 catalyst. They noticed that alkyl substituted aromatic compounds decreased with increasing temperature. After that in 2003, they tried to maximize the single ring aromatics from scrap tires pyrolysis using three types of catalysts (ZSM-5, Y-zeolite (CBV-780 and CBV-400)). They concluded that CBV-400 promoted higher yield of all 5 aromatics (benzene, toluene, m/p/o-xylene) than CBV-780 and ZSM-5, respectively, due to higher pore size and lower Si/Al ratio. They also explained that the smaller pore size restricted the hydrocarbons entering the pore structure of catalyst. In addition, they mentioned that higher catalyst/feed ratio provided another pathway to other products and decreased the amount of oil yields. Fan *et al.* (2005) studied a novel catalyst which has excellent olefin reduction without loss in octane number of gasoline. They reported SAPO-11/HMOR/beta/ZSM-5 zeolite gave higher liquid yields, improved gasoline RON because of high iso-paraffins (C5-C6) and arene (C8-C10) and lowered amount of coke deposit on catalysts. They also reported HMOR, H-beta and SAPO-11 were good catalysts for hydroisomerization while HZSM-5 was good for aromatization.

Moreover, they investigated that the stronger acidity favored aromatization, particularly at high temperatures, but lowered stability because of coke formation. In the report of Boxiong *et al.* (2007b), the scrap tires were pyrolysed using the USY zeolite catalyst. They studied the influence of pyrolysis temperature, catalytic temperature, catalyst/tire ratio and heating rate. They found that when the temperature and catalyst/tire ratio were increased, high gas yield and coke formation were observed similar to the report of William and Brindle (2003). Moreover, they found that a high catalyst/tire ratio favored in the increase of the concentration of light naphtha (<160°C) in oils. They also demonstrated that the amount of oil produced using USY zeolite was less than ZSM-5 and Y-zeolite catalysts, but the products from USY zeolite had higher total concentration of benzene, toluene and xylene. Heating rate was also investigated and found to provide aromatics, olefins, and coke formation.

In 2006, Marcilla *et al.* studied the influence of different acid solids in the catalytic pyrolysis of different polymers. The catalysts used in pyrolysis were HZSM-5 zeolite and mesoporous aluminosilicates—MCM-41a and MCM-41b. The MCM-41b had higher acidity. They concluded the activity of acid catalysts depended on pore size, because reactant molecules can easily access to the active site located in the interior of the pores. Furthermore, another factor was acidity. The result showed that the activity of catalyst increased as the acidity increased. In 2008, Torri *et al.* studied on the pyrolytic behavior of cellulose in the presence of MCM-41 mesoporous materials. They used MCM-41 (Si-MCM-41) and Me-MCM-41 catalysts containing different metals (Al, Mg, Ti, Sn or Zr) in the catalyst/cellulose ratio of 1:3. The pyrolytic products were (2H)-furan-3-one, 2-furaldehyde, 5-methyl-2-furaldehyde, 4-hydroxy-5,6-dihydro-pyran-2-one, levoglucosenone, 1-hydroxy-3,6-dioxabicyclo[3.2.1]octan-2-one (LAC), 1,4:3,6-dianhydro-a-D-glucose and levoglucosan. They found mesostructured solids decreased the yields of levoglucosan with respect to non-loading catalysed cellulose, and increased the production of evoglucosenone and LAC. Similarly, Adam *et al.* (2005) studied the pyrolysis of biomass in the presence of Al-MCM-41 type catalysts. They found the effect of

MCM-41 catalyst on the pyrolysis products of spruce wood was related to the size of the pores of the catalyst. Pore size enlargement and transition metal incorporation reduced the yield of acetic acid and water among pyrolysis products. In 2006, Antonakou *et al.* studied Al-MCM-41 as a catalyst in biomass pyrolysis for the production of bio-fuels and chemicals. They found that the production of liquid was decreased compared to non-catalytic runs. The production of gas was comparable or lower, and the production of coke was higher. Reddy and Song (1996) studied the influence of mesoporous zeolite (MCM-41) on polycyclic aromatic conversion. They illustrated that a major advantage of mesoporous Al-MCM-41 catalyst was capable of converting very large molecules into smaller molecules. Aguado *et al.* (2006) studied the catalytic activity of zeolite and mesostructured catalysts in the cracking of pure and waste polyolefins. They found that mesostructured catalysts, Al-MCM-41 and Al-SBA-15, showed stronger aromatization and benzene alkylation capability because of their weaker Lewis acid and larger pore size, which provide larger molecules of products. In 2008, Dũng *et al.* studied the effects of ITQ-21 and ITQ-24 as zeolite additives on the catalytic pyrolytic oil using HMOR. The results were presented that, with increasing the catalyst-to-tire ratio, the gasoline and kerosene yield increased with the reduction of the heavier fractions. The concentration of the saturated hydrocarbons in the pyrolytic oil was found to be higher. Therefore, increasing the catalyst/tire ratio decreased the yield of liquid product.

2.3. Noble Metal-Supported Catalysts

2.3.1 Monometallic Catalysts

Bifunctional catalysts have been extensively studied for the reduction of aromatics in fuel (Lugstein *et al.*, 1999). Metals can catalyze the hydrogenation of the feedstock, making it more reactive for cracking and heteroatoms (sulfur, oxygen) removal (Ali *et al.*, 2002). And a high level of aromatic hydrogenation at moderate hydrogen pressures can be achieved with noble metals catalysts (Eliche-Quesada *et al.*, 2006a; 2006b). This intrinsically-high hydrogenation activity can also help

reducing steric effects that impede the direct elimination of the sulfur heteroatom (Pecoraro and Chianelli, 1981) in the hydrodesulfurization (HDS).

The hydrogenation and ring opening reactions of polycyclic aromatic hydrocarbons has been performed to enhance the quality of diesel oil from the pyrolytic oil products and other oil products by using bifunctional catalysts. Fesi *et al.*, (1999) studied ring opening and dimerization reaction on HZSM-5 and CuZSM-5 zeolites of methyl and dimethyloxiranes. They found that the major transformation pathway were ring opening and dimerization of these reactants to dioxane and dioxolane products and favored on the CuZSM-5 catalyst due to higher activity. In 2001, Weitkamp *et al.* studied the novel catalyst to create C2+ alkane from aromatics. They reported there were two processes to use; namely, a direct route utilizing bifunctional catalyst, and a two-stage routes comprising hydrogenation and followed by ring opening. They found that a good catalyst to produce C2+ alkane in a direct route was Pd/HZSM-5 catalyst. While a two-stage route, ZSM-5 and ZSM-11 were good catalysts to produce C2+ alkane. In 2002, Arribas and Martinez tried to upgrade the quality of diesel by coupling hydrogenation and ring opening of 1-methylnaphthalene using Pt/USY catalyst. They mentioned that the major components of ring opening products (ROP) with high cetane number were C11alkylbenzene, C11cyclohexane and C11cyclopentane. They also mentioned that the selectivity of ROP decreased with increasing Bronsted acidity and the temperatures above 375°C because they rapidly cracked into lower molecular weight products. They found that the maximum yield of ROP obtained from Pt/USY. In 2004, Santikunaporn *et al.* studied the ring opening of decalin and tetralin on HY and Pt/HY zeolite catalysts. They investigated that the production of ring-opening products was greatly enhanced in the presence of Pt. Other noble metals which have the same effect as Pt are Ir, Rh, Ru and Pd, reported by Du *et al.* in 2005. In 1996, Reddy and Song studied the influence of mesoporous zeolite (MCM-41) on polycyclic aromatic conversion. They mentioned that a major advantage of mesoporous Al-MCM-41 catalysts was capable of converting very large molecules.

Pt loading on mesoporous zeolite enhanced the hydrogenation and hydrocracking of large aromatic molecules.

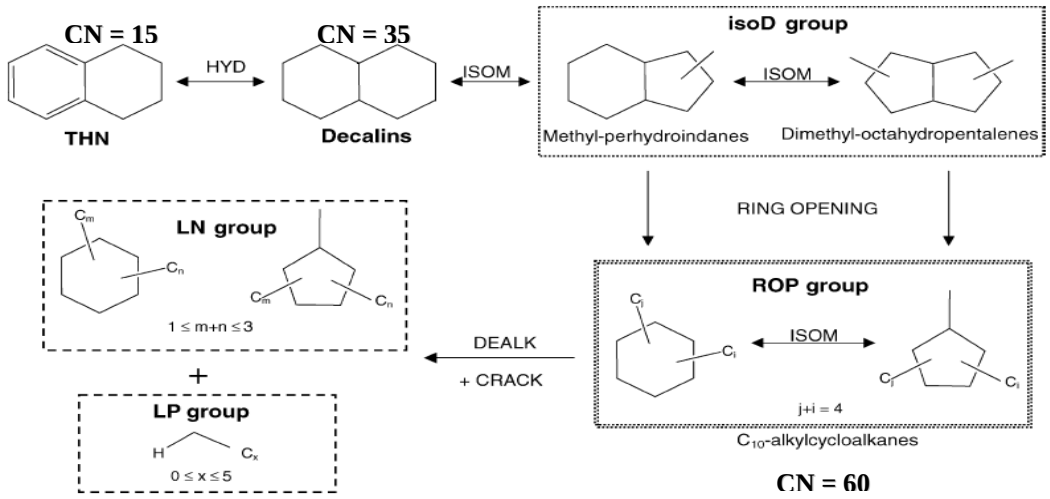

Figure 2.8 Reaction scheme for the ring opening of tetralin on bifunctional catalysts, Pt(Ir)/USY (Arribas *et al.*, 2004a).

The reaction scheme of tetralin on bifunctional catalysts to yield ring opening products is shown in **Figure 2.8**, which was proposed by Arribas *et al.* (2004a). They explained that there were 3 steps to produce ring opening products. Firstly, the aromatic ring of tetralin was hydrogenated on the metal sites of the catalyst to give a mixture of cis- and trans-decalin, and then decalins were isomerized into iso-decalins as shown in the figure. This step involved both metal and acid sites of bifunctional catalyst. Finally, decalin isomers were suffered to ring opening on Bronsted acid sites of the bifunctional catalyst to produce alkylcyclohexanes and alkylcyclopentanes, which have high cetane number.

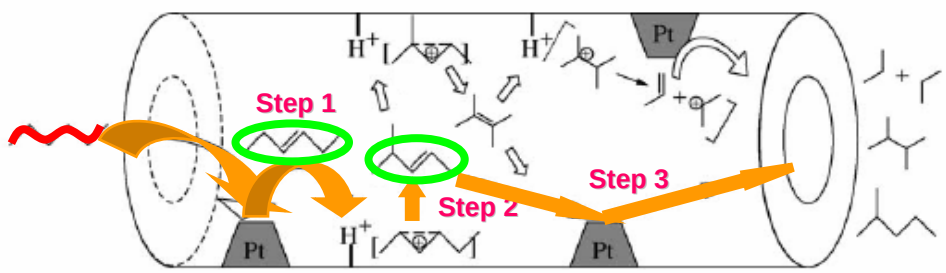

Figure 2.9 Reaction scheme for hydroisomerization of light paraffins on bifunctional catalysts, of Pt/USY(60), Pt/Mordernite(40) and Pt/Beta(50) (Roldan *et al.*, 2005).

However, the other ways to improve the product quality in range of gasoline from waste tires pyrolysis is to increase the octane number by aromatization and hydroisomerization of light paraffins. In 1999, Becue *et al.* investigated the behavior of the different alkali catalysts on the aromatization selectivity. They found that Pt/KL had highest aromatization selectivity. Therefore, octane number of gasoline should be increased with using Pt/KL catalyst. In 2005, Roldan *et al.* studied the influence of acidity and pore geometry on the product distribution in the hydroisomerization of light paraffins. They reported that Pt/USY(60), Pt/Mordernite(40) and Pt/Beta(50) gave high selectivity of isomerized products of light naphtha. Moreover, they showed the step of hydroisomerization process as shown in **Figure 2.9**.

Firstly, the alkane is dehydrogenated to an alkene on the noble metal after that the alkene migrates to the acid site of the support, protonation takes place and then the branched carbocation intermediate is formed. Finally, the formed carbocation is hydrogenated after migration to a metal site to yield a branched alkane or iso-alkane.

Albertazzi *et al.* (2003) studied the hydrogenation of naphthalene with noble metals supported on MCM-41 aluminosilicate catalysts. They found that Rh showed high activity although it favored partial hydrogenation to tetraline than complete hydrogenation to decaline. And, this Rh-supported catalyst can also

catalyze ring-opening and cracking reactions, especially at high temperatures. Similarly, Jacquin *et al.* (2003) observed the high activity of Rh-based catalysts for upgrading diesel. Further, in their work it was reported that decreasing H_2 pressure caused a sudden drop in the yield of high molecular weight products, whereas that of lighter products increased. Besides, Rh-supported catalyst was shown to be a good candidate for the hydrogenolysis cleavage and skeletal rearrangement of C-C bonds (Teschner *et al.*, 2002). The single splitting of C-C bonds was catalyzed at high hydrogen coverage. Decreasing partial pressure of H_2 caused "deepening" of hydrogenolysis, and the hindrance in the re-hydrogenation of the surface intermediates were proposed to explain the successive breakdown of the molecules. It is also worthy mentioned that for very low metal loadings, the carbon-supported rhodium exhibited activities higher than the ruthenium one (Harris and Chianelli, 1984).

Rhenium sulfide was reported to be highly active for the hydrodesulfurization (HDS) reactions, in some cases even higher than the classic Mo and W sulfide, either in the unsupported state (Pecoraro and Chianelli, 1981; Lacroix *et al.*, 1989) or supported on carbon (Ojeda *et al.*, 2005). Nacheff *et al.* (1987) studied the characterization of Re/Al_2O_3 and $Pt\text{-}Re/Al_2O_3$ and their activity in several reactions. Re^o sites were found to be very active for olefin hydrogenation; however, after pre-sulfiding, this hydrogenation activity (of Re/Al_2O_3) was drastically lowered. Besides, Re-supported γ-alumina was an active catalyst promoter for the conversion of hydrocarbon (Okal and Kubicka, 1998).

In 2005, Eliche-Quesada *et al.* studied the hydrogenation and hydrogenolysis/hydrocracking of tetralin in the presence of sulfur, and reported the excellent activity of ruthenium supported on zirconium doped MCM-41. One year later, the same authors found that Ru-supported mesoporous phosphate heterostructures also exhibited high performance for the hydrotreating of aromatics (Eliche-Quesada *et al.*, 2006a; 2006b). Additionally, the catalysts also showed a very good balance between the yields of hydrogenation and hydrogenolysis/hydrocracking products. In the work of Akhmedov and Al-Khowaiter (2000), Ru catalyst was the

most active one for the hydroconversion of hydrocarbon over for a considerable amount of metals-supported catalysts. A high C-C splitting of the tested HCs was also observed for Ru catalyst due to the presence of highly dispersed ruthenium particles on the zeolite support. Gao and Schimidt (1989) showed that the rate of ethane hydrogenolysis could be changed significantly for ruthenium by oxidation and reduction treatments during catalyst preparation. Highly-active sites were formed by oxidation and low temperature reduction. It was believed that the oxidation step may lead to highly dispersed Ru-containing intermediates, which the reduction under reaction conditions may provide very small metal particles.

It is well-accepted that the amount of metal loaded strongly affects the catalytic activity of a metal-supported catalyst. To a certain extent, the catalytic activity generally increases with increasing metal loading. For the HDS of dibenzothiophene, the experimental results of Eliche-Quesada *et al.* (2007) showed an increase in activity when the ruthenium loading was increased up to 7 wt%, whereas the further addition of ruthenium produced a slight decrease. These phenomena were attributed to the fact that high dispersion of ruthenium was obtained and maintained up to 7 wt%, whereas bigger ruthenium crystal was formed with the loading amount higher than 7 wt%. Besides, it was also reported that the excellent hydrogenation of tetraline could be achieved over a catalyst with a high ruthenium content (Eliche-Quesada *et al.*, 2005).

The activity of a noble metal-containing catalyst can also be improved by selecting a proper support. A series of zeolite-catalysts were investigated to determine the support effect for the C-C bond splitting activity of Ru-containg catalysts (Sajkowski *et al.*, 1990; Wu *et al.*, 1990). It was found that these zeolites allowed one to prepare highly dispersed catalysts where most of Ru particles were apparently located on the internal surface of the zeolite crystallites. The increase in activity for these catalysts was mainly due to the presence of highly dispersed Ru particle made possible by the zeolite support. The use of HMOR as a support for Ni and Pt catalysts was reported to exhibit higher activity toward cracking reactions than HBETA zeolite due to its small and one dimensional structure (Escobar *et al.,* 2008).

Also, the crystal size of mordenite is usually larger than that of BETA zeolite, and in the case of cracking it would be more favored over mordenite. A part from zeolite structure, the acid property of the support also plays important role in catalytic activity. Kinger and Vinek (2001) studied the hydroconversion of n-nonane over Ni and Pt containing HMFI, HMOR, and HBETA zeolites, and reported the linear relation between the reaction rate and the number of acid sites. In the same year, noble metal supported on HFAU was proved to be more active than on alumina for toluene hydrogenation, mainly due to the higher acidity of the former support (Chupin *et al.*, 2001). Zheng *et al.* (2008) showed that the activity of Pd-supported on USY for naphthalene hydrogenation in the presence of benzothiophene decreased with increasing SiO_2/Al_2O_3 ratio in the tested range (12 to 80). The beneficial effect of acid sites of the support in the hydrogenation of aromatics with noble metal-supported catalyst is attributed to the hydrogenation of molecules adsorbed on acidic sites by hydrogen spilled-over from the metal sites. It is noted that there generally exists an optimized acid density of the support. In the work of Yasuda *et al.* (1999), the hydrogenation activity of Pd-Pt supported on USY increased with increasing SiO_2/Al_2O_3 ratio, peaked when the ratio was in the 150 - 40 ranges, and then decreased as the ratio increased further. The authors believed that the decrease in both activity and sulfur tolerance, when the SiO_2/Al_2O_3 increased from 40 to 680, may be primarily due to the decrease in the amount of electron-deficient Pd-Pt, resulting from the decrease in Lewis acidity.

Summarily, noble metal supported catalysts can effectively catalyze the hydrogenation of aromatic hydrocarbons. However, one major limit of noble metal is its low resistance to sulfur poisoning. Interestingly, the sulfur tolerance can be enhanced by modifying the physicochemical characteristics of the metal atoms by (i) using acidic carriers (Barbier *et al.*, 1990), (ii) changing the metal particle size, or (iii) alloying with other metals (Lee and Rhee, 1998).

2.3.2 Bimetallic Catalysts

Bimetallic catalysts have been received a great deal of attention because they might exhibit superior activity, selectivity, and deactivation resistance than their corresponding monometallic samples (Sinfelt, 1983; Ponec and Bond, 1995). The variations of catalyst performance are often explained on the basis of electronic and/or geometric effects. The ligand effect speculates the change in adsorption bond strength between chemisorbed adsorbates and surface-active metal atoms. The ensemble theory considers the addition of an inactive metal, resulting in a dilution of the surface-active metal atoms, and then, in a decrease of the active ensemble size. However, the geometric and electronic factors often cannot be easily separated as independent parameters. For instance, the electron bandwidth of the metal, as well as the nature of the exposed planes and the topology of the surface sites, can change with the size of the metallic particle.

In 2002, Crisafulli *et al.* reported that the bimetallic Ni-Ru supported on SiO_2 showed much higher activity and stability than its corresponding mono metallic samples. The different behavior was related to the formation of Ni-Ru cluster on silica and an obvious surface enrichment in nickel, leading to an increase in the metallic dispersion of nickel. Ishihara *et al.* (2005) studied the HDS of sulfur-containing poly-aromatic compounds in light gas oil using noble metal catalysts. They found that, in the case of straight run-light gas oil (SR-LGO), the dibenzothiophen (DBT) HDS activity was remarkably enhanced with using Ru-Rh bimetallic system, revealing a synergistic effect between Rh and Ru. Recently, in the work done by Navarro *et al.* (2009), it was documented 0.5%RuNiMo catalyst was less prone to deactivation than the NiMo reference sample for the HDS of dibenzothiophene. Especially, in the hydrotreatment of a SR-GO, the sulfided 0.5%Ru/NiMo/Al_2O_3 catalyst was proven to be more active in the HDS and HDA reactions than a commercial NiMO/Al_2O_3 catalyst. This high activity was explained by the formation of small particles inducing some preferential exposed planes, favoring hydrogenation properties with the introduction of ruthenium.

Dr. Sirirat Jitkarnka
Associate Professor
The Petroleum and Petrochemical College
Chulalongkorn University

2.4. Objectives and Scope

The objectives of this work were to investigate the influences of various noble metal-supported catalysts on the selectivity or yields and nature of the products obtained from waste tire pyrolysis. The objectives can be classified as follows;-

(a) to study the selectivity of various zeolites on the nature of products or the quality of products,

(b) to study the selectivity of various metals loaded on the zeolites on the nature of products or the quality of products, and

(c) to study why such above catalysts provide such products.

However, in terms of "Products", they mean (i) commercial oils such as gasoline, kerosene, and diesel (gas oil), and/or (ii) commercial gases such as C1 – C4 hydrocarbons, and/or (iii) petrochemicals such as light olefins and aromatics, which can be used a s alternative raw materials for petrochemical industry.

In order to achieve the targets in time, the scope of this work was set as listed below;-

(a) The pyrolysis was carried out in a bench-scale autoclave reactor from room temperature to the final temperature of 500°C (for the pyrolysis zone) and 350°C (for the catalytic zone) with the heating rate of 10°C/min in the atmospheric pressure. Other parameters; particle size, holding time, N_2 flow rate, the amount of sample and catalysts were fixed at 8-18 mesh, 90 min, 30 ml/min, 30 g, and 7.5 g, respectively.

(b) The supports used in this work were specified as HBETA, HMOR, HY, KL, SBA-1, MCM-41, and MCM-48.

(c) The metals used in this work were set as Pt, Ru, Rh, Pd, Ag, and Re.

(d) Gaseous and liquid products were analyzed for their compositions, type, and quantity whereas solid products were only analyzed for their quantity. The quality of all types of products was investigated only if the analysis

instruments would be possibly available and allowed.

3

Methodology

3.1. Samples, Materials, and Chemicals

3.1.1 Waste Tire Samples

The waste tire used in this study was a used passenger car tire (about 50,000 kilometers). To avoid the difference caused by different tires, only one tire was used to prepare the sample. The tire was then cut into pieces by a lab-made up machine and then sieved to obtain the particle sizes of 8-18 mesh.

Table 3.1 summarizes the elemental composition of the waste tire used in this study determined by elemental analysis (LECO, US).

Table 3.1 Elemental composition of waste tire

Element	C	H	S	Other*
%wt	87.4	7.2	1.7	4.7

* Determined by subtraction.

3.1.2 Materials and Chemicals

- Dual Valve Tedlar PVF bag (Cole Palmer)
- Liquid chromatography column (Glass), 650 mm height, 26.6 mm inside diameter
- Silica for liquid chromatography (Particle size 0.063-0.200 ; 70-730 mesh ASTM)
- Neutral alumina for liquid chromatography
- Benzene (C_6H_6, Assay ≥ 99.8 %)
- Diethyl ether ($(C_2H_5)_2O$, Assay ≥ 99.5 %)
- n-pentane ($CH_3(CH_2)_3CH_3$, Assay ≥ 99 %)
- n-hexane ($CH_3(CH_2)_4CH_3$), Assay ≥ 99 %)
- Methanol (CH_3OH, Assay ≥ 99.8 %)
- Carbon disulfide, CS_2
- N_2 gas
- Beta (BEA), Y, Mordenite (MOR), and KL Zeolites (Tosoh Corp., Singapore)
- Rh, Re, Ru, Pt, Pd, and Ag compounds (FLUKA, ALDRICH)
- KBr
- Teflon membranes (FLUKA)

3.2 Catalyst Preparation

Four zeolite catalysts (BEA, USY, HMOR and KL) obtained from Tosoh Company, Singapore were calcined at 500°C for 3 hours with the heating rate of 5°C/min. The other one (Beta) was calcined at 600°C for 5 hours with the heating rate of 2°C/min to remove the organic template from the zeolites. After that, these zeolites were loaded with one of these 6 noble metals; Pt, Pd, Ag, Ru, Re, and Rh

using the incipient wetness impregnation technique. Firstly, the salt solution of each noble metal was individually dropped on the zeolites. And then, the samples were dried in oven at 110°C for 3 hours. Finally, all catalysts were calcined in a furnace at 500°C for 3 hours with the heating rate of 5°C/min to obtain bifunctional catalysts in oxide forms.

To prepare metal-loaded catalysts, these oxide catalysts were reduced with H_2 at 400°C for 1-2 hrs in order to convert the metal oxide forms to metal elements before using in the experiments as shown below.

$$M_xO_y + H_2 \rightarrow M^o + H_2$$

Prior to use, the catalyst powders were pelletized and sieved to the particle size between 300 to 425 μm before being packed in the reactor.

To synthesize SBA-1 (*Santa Barbara Airport* No. 1), a mesoporous molecular sieve, silatrane was first synthesized using the method of Wongkasemjit's group (Charoenpinijkarn *et al.*, 2001). The silatrane precursor was added to a solution containing NaOH, and H_2SO_4, followed by adding a solution of water and cetyl trimethyl ammonium bromide (CTAB) with vigorous stirring (Tanglumlert *et al.,* 2008). Water was added to this mixture prior to aging at room temperature for 2 days to form a white precipitate. The product was filtered and washed with water. Then, the white solid was dried at room temperature and calcined at 580°C for 6 hours (0.5°C/min) to obtain the mesoporous SBA-1.

3.3 Pyrolysis of Waste Tire

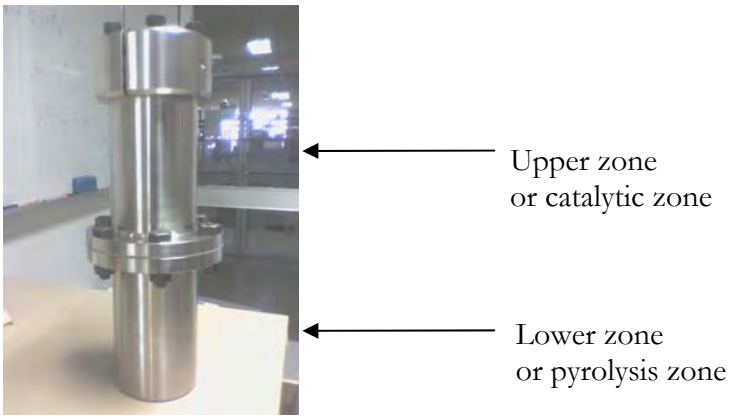

Figure 3.1 Autoclave reactor used in the experiment.

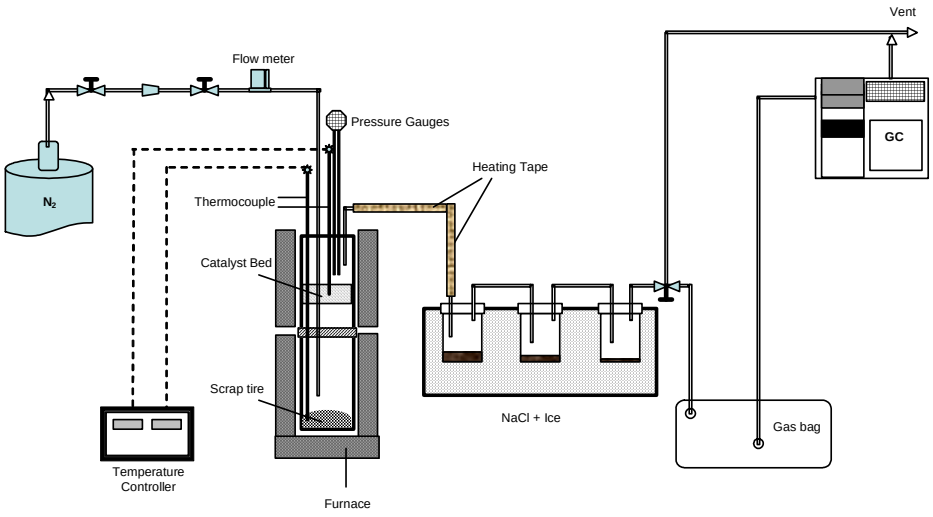

Figure 3.2 Schematic of the pyrolysis process.

3.3.1 Pyrolysis

The autoclave reactor and experimental system are shown in **Figures 3.1 and 3.2**, respectively. A tire sample was pyrolyzed in the lower zone of the reactor from room temperature to a final temperature of 500°C with a heating rate of 10°C/min. This pyrolysis zone was kept at the final temperature for 1 hour to ensure the total conversion of tire. The evolved product was carried by a 25 ml/min nitrogen flow to the upper zone controlled at a desired temperature and packed with

a catalyst. The influences of catalyst were investigated at this zone. The obtained product was next passed through an ice-salt condensing system containing 3 condensers to separate incondensable compounds from the liquid product. The non-condensable products or gaseous products were passed through the condensers and kept in a Tedlar® gas sampling bag. The solid and liquid products were weighed to determine the product distribution. The amount of gas was then determined by mass balance.

3.3.2 Product Characterization

3.3.2.1 SIMDIST GAS Chromatography (SIMDIST GC)

The pyrolytic liquid fraction and petroleum maltenes were analyzed directly by Varian CP-3800 Simulated Distillation Gas chromatography (SIMDIST GC), equipped with FID, using a 15 m x 0.25 mm x 0.25 μm, WCOT fused silica capillary. The following temperature program, according to ASTM D 2887, was used:

Initial temperature	30	°C
Time at initial temperature	0.01	min
Heating rate	20	°C/min
Final temperature	320	°C
Holding time	8.50	min

The outcome from the SIMDIST GC is a true boiling point curve of the oil obtained from the waste tire pyrolysis process which can be cut into petroleum fractions as shown in **Table 3.2**. In some analysis, the curves were also cut into petroleum fractions based on their boiling point, including naphtha (<200°C), kerosene (200°C - 250°C), light gas oil (250°C – 300°C), heavy gas oil (300°C – 370°C), and long residue (>370°C) as listed in **Table 3.3**.

Table 3.2 The boiling point and carbon range of refinery products (Speight, 2002)

Fraction	Carbon range	Boiling point (°C)

Gasoline	C5-C9	15.5 - 149
Kerosene	C10-C13	149 - 232
Gas oil	C14-C20	232 - 343
Light vacuum gas oil	C21-C23	343 - 371
Heavy vacuum gas oil	C24-C50	371 - 566

Table 3.3 Petroleum fractions (Chaiyavech and Grisadanurak, 2000)

Fractions	Boiling point(°C)	Carbon range
Full range naphtha	<200 °C	C5-C10
Kerosene	200-250°C	C10-C14
Light gas oil	250-300°C	C14-C19
Heavy gas oil	300-370°C	C19-C35
Long residue	>370°C	>C35

3.3.2.2 Oil Analysis

The analysis was divided into two steps: the asphaltenes precipitation, and separation of petroleum maltenes by liquid adsorption chromatography. The pyrolytic liquid fraction was first separated into maltanes (n-pentane soluble) compounds and asphaltenes (n-pentane insoluble). Experiments performed to determine the amounts of precipitated asphaltenes consisted of adding a volume of n-pentane to the oil sample in an appropriate flask at the ratio 40:1. After 10 min of ultrasonic shaking, the mixture was left overnight. The solution of n-pentane and deasphalted oil was filtered using a vacuum system with a 0.45-μm filtration Teflon membrane that was previously weighed. The membrane with the precipitated material was dried in a vacuum oven at 0.1 bar and 333 K over 6 hr and finally weighed to determine the precipitated mass of asphaltenes.

In the second step, n-pentane was stripped off from maltenes using a rotary vacuum evaporator in 50°C. Next, the petroleum maltenes was fractionated in a glass column of 650mm x 26.6 mm I.D. Its lower half was packed with neutral alumina which had been activated at 400°C for 8 hr prior to use. The upper half was packed with silica gel. After extraction, the adsorbent was dried at 50°C under vacuum 4.4 kPa for 8 hr. and then activated at 160 °C for 48 hr. The sample of maltenes (4.5 g) was dissolved in 10 cm^3 of hexane and applied to the adsorbent column prewetted with hexane and separated into saturated hydrocarbon, mono-, di-, poly- and polar aromatics compounds by a successive elution with a series of mobile phases that are shown in the Table 3.4. A constant flow-rate of the mobile phase at 20 cm^3 was ensured with a pump. The chromatographic fractions obtained were then stripped of the mobile phases on the rotary vacuum evaporator and dried in a vacuum dryer at 80°C and a pressure of 4.4 kPa to a constant mass. All steps are summarized in **Figure 3.3**.

Table 3.4 Optimized compositions and volumes of mobile phases for fractionation of maltenes using a chromatographic column (Sebor *et al.*, 1999)

Mobile phase	Volume (cm^3)	Prevailing compounds type
Hexane	600	Saturated hydrocarbons
Hexane-benzene (24:1, v/v)	500	Mono-aromatics
Hexane-benzene (22:3, v/v)	500	Di-aromatics
Benzene	500	Poly-aromatics
Benzene-diethyl ether-methanol (1:1:3 v/v)	500	Polar aromatic compounds

3.3.2.3 Gas Chromatography (GC)

Pyrolytic gas fraction was analyzed by a gas chromatograph, Agilent Technologies 6890 Network GC system, using HP-PLOT Q column: 30m x

0.32mm i.d. 20 μm film. FID was used as a detector with He as the carrier gas. The temperature programs were as follows:

Initial temperature	70	°C
Time at initial temperature	8	min
Heating rate	20	°C/min to 200 °C
Holding time	16	min
Final temperature	10	°C/min
Holding time	30	min

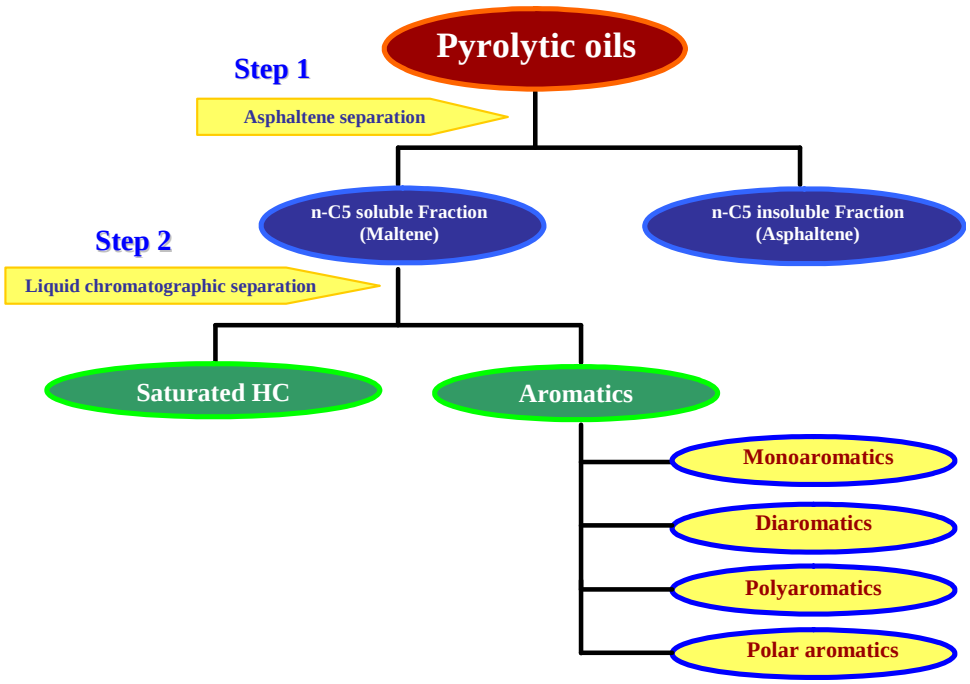

Figure 3.3 Diagram of all steps in the oil analysis.

3.3.3 Catalyst Characterization

(a) Atomic Absorption Spectrometer (AAS)

The amounts of metal loading on any zeolite were obtained by using Atomic Absorption Spectrometer (Varian, SpecterAA 300 model). Aqua regia (3 HCl : 1 HNO_3) was used to digest the ion-exchanged catalyst.

(b) X-ray Diffraction Spectroscopy (XRD)

X-ray diffraction (XRD) patterns were taken by using a Rigaku, Rint X-Ray diffractometer system (RINT 2200) with Cu tube for generating CuKα radiation (1.5406 Å) and nickel filter. In this experiment, XRD was employed to obtain the structure of catalysts and metal dispersion on zeolite supports. A catalyst sample was ground to fine and homogeneous particles, and then packed in glass specimen holder. The data from XRD were collected and recorded by an on-line computer.

(c) Surface Area and Pore Size Distribution

. The specific surface area and the pore size of catalyst were determined by Brun-aueer-emmett-Teller (BET) technique and using Thermo Finnigan, Sorptomatic 1990. This technique was based on the physical adsorption of nitrogen gas at 77°K. The specific surface area and the pore size of catalyst were obtained from the twenty-two-point nitrogen adsorption and desorption isotherm plot. The pore size distribution was calculated using the BJH method.

(d) Temperature Programmed Reduction (TPR)

H_2-TPR profiles of the samples were recorded from room temperature to 600 °C with the heating rate of 10 °C/min using 5%H_2/N_2 after the pretreatment of the samples at 150 °C under helium flow at 30 ml/min for 30 minutes.

(e) Temperature Programming Oxidation (TPO)

Temperature Programming Oxidation can be used to determine the amount and characteristics of coke which deposits on the spent catalysts. The spent catalysts were weight with suitable amounts and placed in the quartz tube. 5% O_2/He was flown through the spent catalyst, while the temperature linearly increased with the heating rate of 10°C/min. The coke was oxidized and the carbon dioxide was generated. This gas was monitored by TCD detector. The exact amount to oxidized coke was calibrated using the pulses of pure CO_2.

(f) Temperature Programmed Desorption (TPD)

TPD analysis was used to characterize the total acidity strength of the catalyst. The catalyst was first pretreated in He at 150 °C for 30 minutes. Then, the system was cooled to 100 °C, and the NH_3 adsorption was performed using 1.13%NH_3/N_2 for 1.5 hours (to make sure that the adsorption of NH_3 completed) followed by the introduction of He (helium flow rate was 30 ml/min) for 30 minutes at 100 °C to remove the physical adsorption of NH_3. Finally, the system was cooled to 50 °C, and then the temperature programmed desorption was started from 50 °C to 900 °C with the heating rate of 10 °C/min.

(g) Transmission Electron Microscope (TEM)

Electron microscopy measurements were performed by using a JEM 2100 Transmission electron microscope (TEM) equipment which operated an accelerating at 200 kV. The sample were prepared by grinding, ultrasonically dispersing in acetone. And then a drop of suspension were evaporated and put on the copper grid. The TEM image were recorded and calculated the particle size diameters from equation $d_{avg} = \sum (n_i d_i)/\sum ni$.

(h) Hydrogen Chemisorption

The samples were pretreated at 150 °C with the heating rate of 10 °C/min for 1 hour; under a flow of helium (helium flow rate was 10 ml/min). Hydrogen chemisorptions of the pretreated samples were carried out at room temperature in a chemisorption system equipped with a TCD. The hydrogen chemisorption was carried out with the hydrogen flow rate of 30 ml/min by hydrogen pulses. The hydrogen pulse was performed by released hydrogen to the system until the chemisorptions completed.

4

Effects of Acid Supports

This chapter discusses the effect of acid zeolites, namely HBETA, HMOR, and HY as acid catalysts, on the pyrolysis products of waste tire. The results are described in terms of product yield, gas composition and yield, true boiling point curves, petroleum fractions, petrochemical yields, carbon number distribution, and the molecular composition of oil.

4.1. Characterization of Acid Zeolites

All zeolites purchased from the Tosoh Company, Singapore have the structures and properties shown in **Table 4.1**. Besides the channel system with 12-membered rings, the three zeolites have approximately the same size of pore opening, which is in the neighborhood of 7 - 7.6 Å. HBETA and HMOR have one thing in common in terms of the pore opening; that is, they have an elliptical pore

opening of 6.4 x 7.6 Å and 6.5 x 7 Å, respectively. HY has a round pore opening of 7.4 Å. It means that the zeolites can be ranked according to their pore opening size as HY>HBETA>HMOR. This rank well corresponds to that on the total pore volume. The surface area can be ranked as HY>HBETA≈HMOR.

Table 4.1 Zeolite properties

Zeolite	Pore Dimen-sion	Membered ring (MR)	Si/Al *	Surface area** (m^2/g)	Pore size* (Å)	Total pore volume *** (cm^3/g)
HBETA	3D	12	13.5	455.4	6.4 x 7.6	0.391
HMOR	1D	12	9.5	462.5	6.5 x 7	0.359
HY	3D	12	7.5	590.4	7.4	0.576

* Provided by Tosoh Company
** BET Method
***BJH method

The Si/Al ratio can relatively indicate the acid properties of zeolites. Usually, a zeolite with the higher Si/Al ratio has less total acidity but higher acid strength. From **Table 4.1**, the Si/Al ratio can be ranked as HBETA>HMOR>HY; therefore, the acid strength can be raked in the same fashion whereas the total acidity is in the inverse ranking.

The advantages of these zeolites can be the followings: (1) they have large pore size and moderate acidity which provide the diffusion of large molecules such as naphthalene etc. entering the pore; therefore, oil products in the ranges of diesel fuel or lighter can be obtained, and (2) mesoporous zeolites can allow faster diffusion of large molecule resulting in preventing re-cracking of ring opening (ROP) substances (giving oil with a high cetane number if containing diesel). This chapter reveals the influences of using these zeolites in the pyrolysis of waste tire.

4.2 Pyrolysis of Waste Tire

4.2.1 Product Yields

The product yield of catalytic pyrolysis with the different zeolites is shown in **Figure 4.1**. The non-catalytic pyrolysis gives 12.4% gas, 14.7% liquid, and 47% solid char. The use of pure zeolites as catalysts can increase the gas product whereas the liquid product decreases as compared to the non-catalytic case. The figure shows that the liquid yields obtained from using zeolites as catalysts were reduced about 3 - 7 %wt in relation to the increase of gas yield due to higher reaction activity of catalysts. Similarly, Williams and Brindle, 2003b explained that catalysts provided other pathways to other products and decreased the amount of oil yields. However, HY catalyst showed the least differences on gas and liquid yields as compared to the non-catalytic pyrolysis. The solid fraction remains constant at about 48%wt yield, indicating that the rubber content in the tire sample is completely decomposed to lower molecular weight products (Miguel *et al.,* 2006).

It was known that acidity plays the important role on cracking, and a high gas production is resulted from high cracking ability. Compared among the pure zeolites, HBETA gives the highest gas yield, followed by HMOR. HY gives a slightly lower gas production than HMOR. The results confirm that the acid strength of the zeolites governs the further cracking of the hydrocarbon fragments evolved from the thermal cracking of the rubber chains of waste tire.

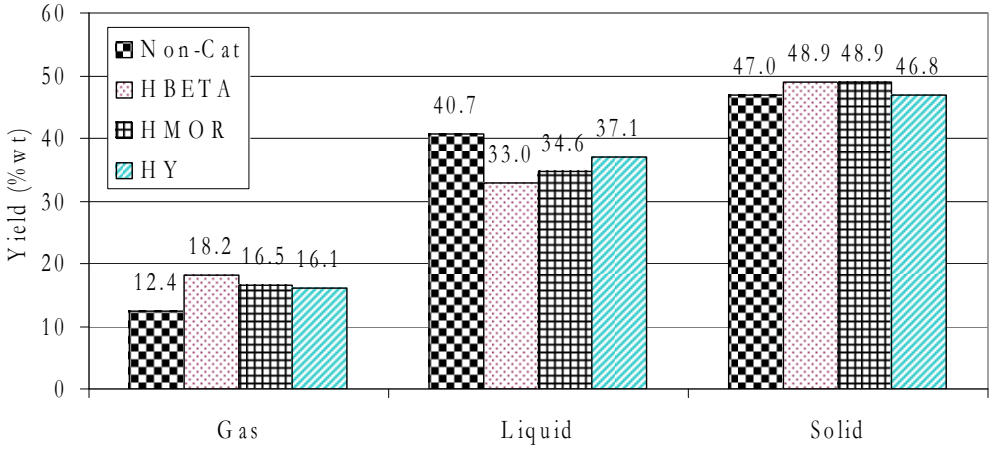

Figure 4.1 Product yields.

4.2.2 Gas Compositions

The gas obtained from tire pyrolysis contains natural gas-like components, but it is much richer in heavy hydrocarbons, unlike a natural gas mainly composed of methane and fixed gases. On the H_2-free basis, the gas from the non-catalytic pyrolysis contains about 17% methane, 8% ethylene, 15% ethane, 9% propylene, 8% propane, 22% mixed C4s, and the rest is the mixture of the heaviers (as shown in **Figure 4.2**).

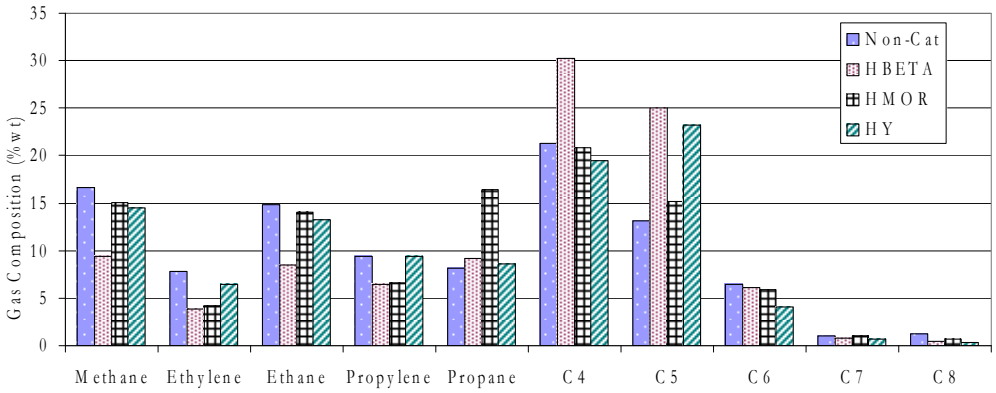

Figure 4.2 Composition of gaseous products.

Figure 4.2 also shows that HBETA zeolite gives tremendously high mixed-C4 and mixed-C5 products. HY also provides a high amount of mixed-C5 products. It can be explained that primary cracking products obtained from the breakdown of polybutadiene and polyisoprene chains are not further cracked to light gases such as methane, C2- and C3-gases. Or, another possible explanation is that the zeolites provide selectivity toward cracking on monomer-monomer bonds in the polymer chains of tire rubbers, resulting in the higher production of mixed-C4 and mixed-C5 products. Normally, a higher molecular weight hydrocarbon gives the higher heating value than a lighter gas. For example, C5 has a higher heating value than C4. Hence, the HBETA zeolite gives the highest heating value of gaseous product because of its high C4 and C5 yields; therefore, it produces the highest price of a natural gas-like gas. Although the dimensional structure (3D) and the pore size of HBETA and HY are similar, HBETA has higher acid strength (higher Si/Al ratio)

than HY. Therefore, HBETA has higher ability to crack mixed-C5 products of polyisoprene or other heavier hydrocarbons to yield mixed-C4. That is the reason why HBETA gives the higher mixed-C4 yield than HY. Moreover, HMOR zeolite produces an apparently high amount of propane with a considerable amount of C4 hydrocarbon as shown in **Figure 4.2**. HMOR is therefore a good catalyst to produce cooking gas (propane and C4).

4.2.3 Petroleum fractions

The quality of oil products can be indicated by a simulated true boiling point curve, which can be obtained from a SIMDIST GC. The results are illustrated in **Figure 4.3**. The lightest oil normally gives the curve to the far most left. From the figure, one can see that HBETA gives the lightest oil, and most of the time, the light oil means the most expensive one. HY gives the heaviest oil but lighter than that obtained from the thermal pyrolysis. These results confirm that the zeolite that has the highest strength of acidity gives the lightest oil, and thus the acidity strength is the factor that governs the cracking of the hydrocarbon fractions of tire.

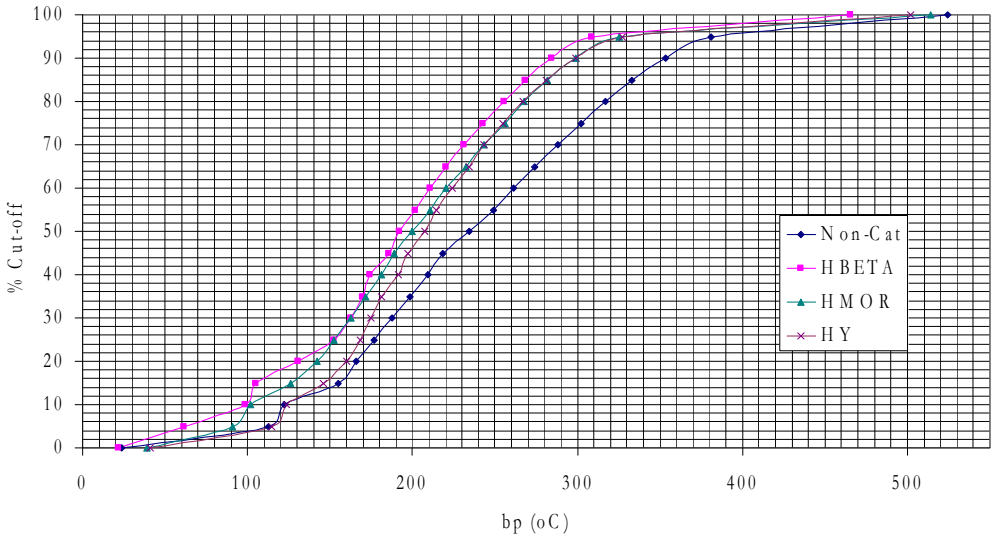

Figure 4.3 True boiling point curves of oils from using acid zeolites**.**

The true boiling point curves can be cut into petroleum fractions according to the boiling point ranges, which are full range naphtha (< 200°C),

kerosene (200-250°C), light gas oil (250-300°C), heavy gas oil (300-370°C), and long residue (>370°C) (Chaiyavech and Grisadanurak, 2000). The result in **Figure 4.4** shows that HBETA zeolite gives the highest full range naphtha production (54% in oil) among all of unloaded zeolites. It can be explained by the highest acid strength of HBETA zeolite, which results in the highest cracking ability to crack heavy fractions to the lightest fractions. HMOR and HY zeolites significantly increase full range naphtha as compared to the non-catalytic case. The order of naphtha production follows that of acid strength.

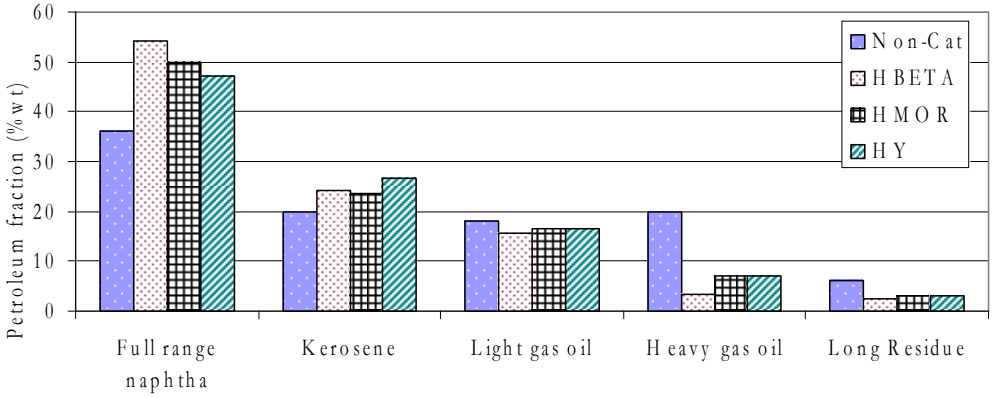

Figure 4.4 Petroleum fractions in oils from using acid zeolites**.**

4.2.4 Molecular Composition in oils

Typically, the pyrolysis of tire generates a lot of aromatic compounds in the oil products, causing a lower cetane number of diesel fraction. Therefore, large pore size catalysts are used because they can allow large molecules, which have large kinetic diameters such as poly-aromatic hydrocarbons to enter the pores.

In this work, the molecular compositions of oils are classified into five fractions including saturated hydrocarbons, mono-aromatics, di-aromatics, poly-aromatics, and polar-aromatics as shown in **Figure 4.5**. BETA zeolite gives the highest amount of saturated hydrocarbons and the consequent lowest total aromatics among all other unloaded zeolites. Especially, it is the only one who can reduce poly-aromaics in the pyrolytic oil. It is possibly caused by the highest acid strength (the highest Si/Al ratio) of BETA zeolite whose protons are strong enough to crack all

types of aromatics, which is resulted in the highest cracking activity. Moreover, with the 3D structure and a high pore opening, HBETA can accept a large molecule like a polyaromatic to enter its pore. However, HBETA and HY zeolite have the same 3D dimensional structure and a comparable pore opening, but HBETA can lower the poly-aromatics whereas HY can not, because HBETA has the higher acid strength. Therefore, HBETA has the higher ability on protonating some aromatic molecules to carbenium ions that can lead to many reactions such as hydrogenation and cracking. All zeolites can reduce polar-aromatics in the pyrolytic oil.

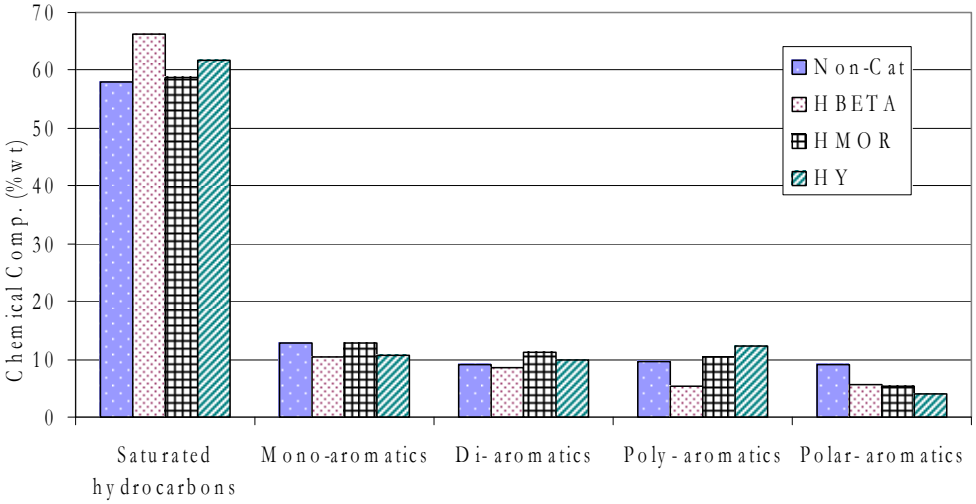

Figure 4.5 Molecular compositions in oils from using acid zeolites**.**

Table 4.2 Desired components in petroleum products

Oil fraction	Key specification	Desired components
Gasoline/Naphtha	Octane number	Isoparaffins, Aromatics
Kerosene	Radiation flame	Aromatics < 22 %vol.
Gas oils	Cetane number	n-Paraffins

Sometimes, in order to determine the oil quality, these compounds must be considered along the range of petroleum fractions. For examples, gas oil fraction should contain a high amount of saturated hydrocarbons in order to have a higher cetane number, and aromatic compounds at an acceptable amount must be

constituted in the range of gasoline in order to obtain the oil with a high octane number. The required components in each range of petroleum fraction are shown in **Table 4.2**.

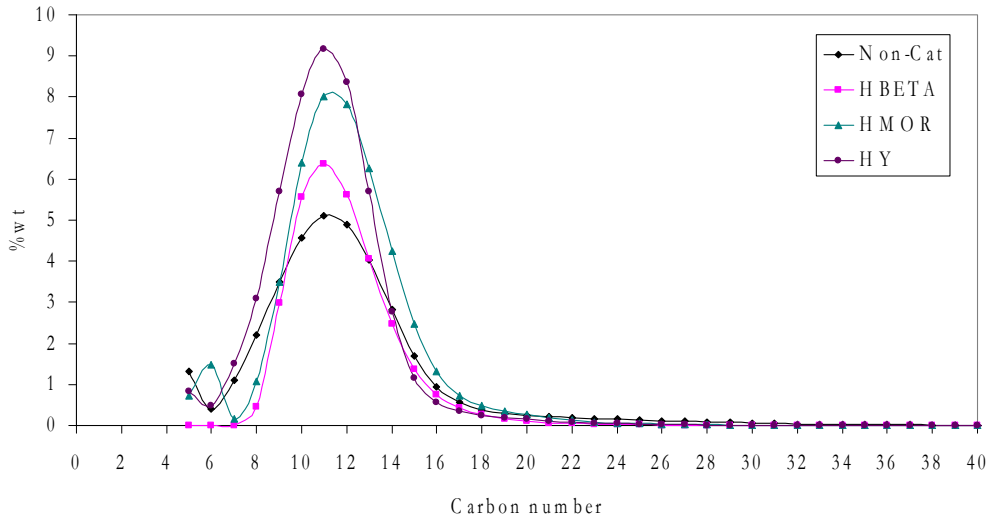

Figure 4.6 Carbon number distribution of saturated hydrocarbons in maltenes obtained from using various zeolites.

Figure 4.6 shows the carbon number distribution of saturated hydrocarbons in maltenes (the pyrolytic oils after asphaltene removal). It is found that most saturated hydrocarbons are distributed in the kerosene fraction for all cases. The average carbon numbers are in the range of C10-C12. The non-catalytic pyrolysis gives the widest distribution of saturated hydrocarbons with the maximum (average carbon number) around C11-C12. The average carbon number slightly shifts to the lower values for all zeolites cases, indicating that the properties of zeolites such as the acidity govern the smaller sizes of saturated hydrocarbons. Namely, the acidity causes the cracking of long/big chains of saturated hydrocarbons to some shorter/smaller ones, or it may also cause the cracking (or other transformations) of the other types of components to shorter/small saturated hydrocarbons. HY gives the oil that has saturated hydrocarbons distributed most in the gasoline range of C5-C9 (Speight, 2002) and full range naphtha (C5-C12

according to Chaiyavech and Grisadanurak, 2000). This indicates that HY yields the highest quality of gasoline/full range naphtha since its oil contains the highest amount of saturated hydrocarbons, although it gives the lowest gasoline/full range naphtha in the oil. In other words, HY gives the lowest fraction of gasoline/full range naphtha with the highest quality.

Likewise, in the kerosene range (C10-C13), HY gives the highest amount of saturated hydrocarbons, followed by HMOR and then HBETA. One may observe that the rank is in the opposite order of that of acid strength, but it follows the rank of acid density of the zeolites. It is expected that the acid density may govern the production of high saturated hydrocarbons in the gasoline and kerosene ranges. However, with considering the fact that the oil from HY contains less amount of full range naphtha and kerosene than HBETA but not the lowest (see **Figure 4.4**), it therefore gives the best quality of the two lightest fractions at a high yield. On the other hand, HBETA gives the highest yield but the lowest quality of the two lightest fractions.

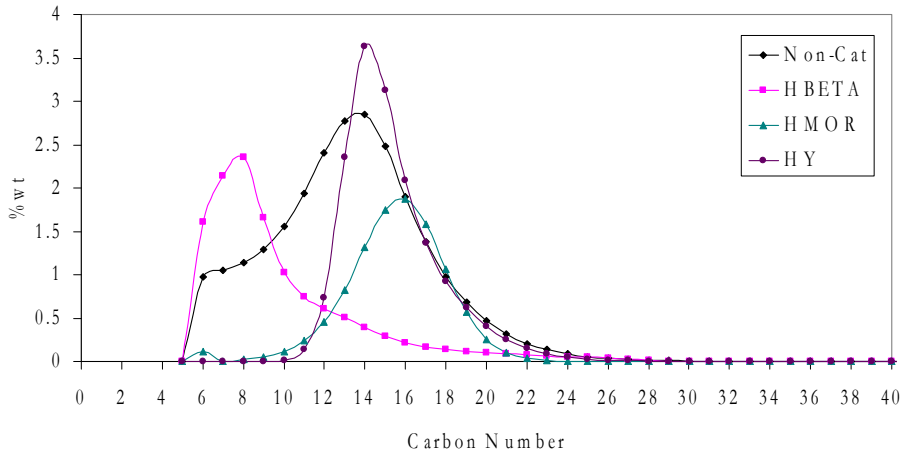

Figure 4.7 Carbon number distribution of mono-aromatics in maltenes obtained from using various zeolites**.**

All zeolites yielded the approximately-equal amount of mono-aromatics in the pyrolytic oils (see **Figure 4.4**). However, mono-aromatics distributions in the oils obtained from the zeolites appear totally different as illustrated in **Figure 4.7**. The

mono-aromatics obtained from the thermal pyrolysis are highly and widest distributed in high amounts in all carbon numbers. Significantly, using the zeolites, the mono-aromatics are distributed more narrowly, especially those from HBETA and HY. HY and HMOR give mono-aromatics highly distributed in the gas oil ranges (C12-C20) whereas HBETA gives those highly distributed in the lighter ranges (naphtha and kerosene; C6-C12). Since the oil obtained from HBETA has much shorter mono-aromatics than those from the other two zeolites, it may used as a catalyst in tire pyrolysis to alternatively produce valuable mono-aromatics (BTXs) for petrochemical industry.

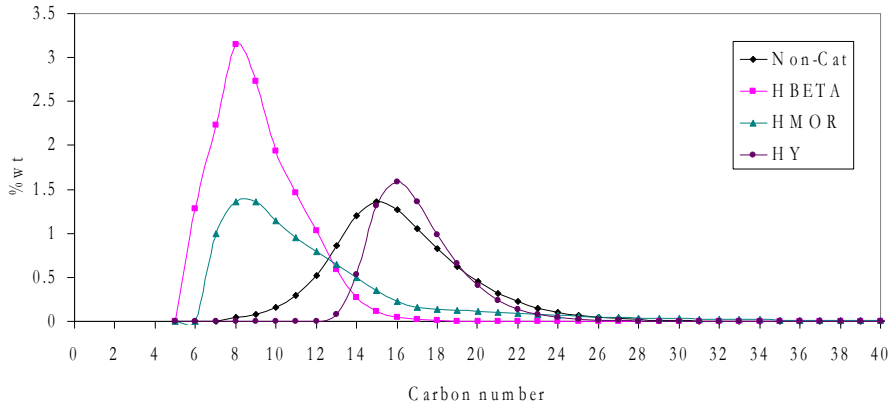

Figure 4.8 Carbon number distribution of di-aromatics in maltenes obtained from using various zeolites**.**

Similarly, di-aromatics obtained from thermal pyrolysis are highly distributed in all carbon numbers with the average around C15-C16 which is in the gas oil range (see **Figure 4.8**). HY also gives the di-aromatics in the gas oil range, but the distribution is narrower. Both HBETA and HMOR give the high distribution of di-aromatics in the full range naphtha with a long tail of distribution to the range of gas oil, indicating the smaller sizes of di-aromatics than those of HY. In the opposite, HBETA produces heavier poly-aromatics than HY and HMOR as shown in **Figure 4.9**, but lighter than those of thermal pyrolysis.

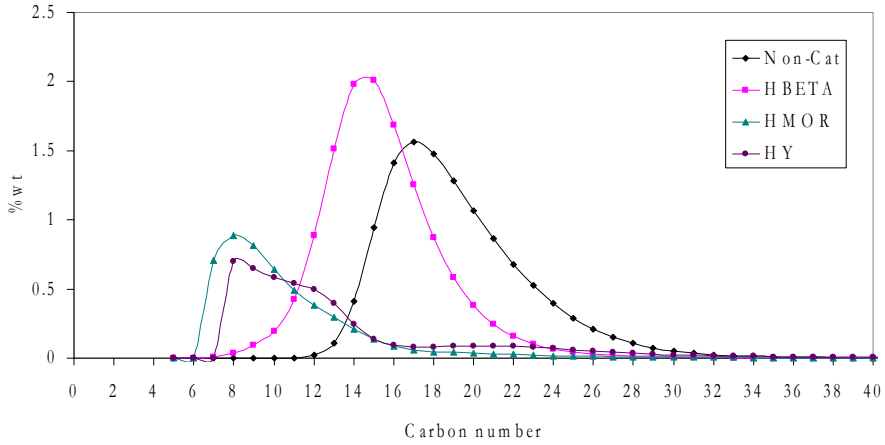

Figure 4.9 Carbon number distribution of poly-aromatics in maltenes obtained from using various zeolites.

Desulfurization is an important process in industry to remove sulfur from petroleum fuels. Due to the fuel quality, it is difficult to satisfy the practical requirement because the environment regulations request a low content of sulfur in oil products. Sulfur content in oil products is an environmental concern because it leads directly to the emission of SO_x when combustion is occurred. Generally, sulfur-containing compounds in oils obtained from waste tire pyrolysis are present in the forms of polar aromatic compounds. In tire manufacture after vulcanization process, sulfur is combined in rubber chains and linked together. Sulfur content in oil products can be present as sulfide, di-sulfide, poly-sulfide, cyclic-sulfides, mercaptans, thiophenes, and free sulfides. When pyrolyzed, the sulfur in tire can be present in the oil in many forms as mentioned, including those present in the aromatic rings in the molecules of oils as so-called "*Polar-aromatics*". In general, polar-aromatics are the aromatics that have a polar atom such as oxygen, nitrogen, and sulfur in the aromatic rings. However, since a tire consists of merely sulfur; therefore, polar-aromatics in the pyrolytic oil are mostly sulfur-containing compounds. Thus, the quantity of polar-aromatics as shown in **Figure 4.4** can roughly or relatively tell how much oil contain sulfur compounds.

Table 4.3 Polar-aromatics production from various zeolites

Samples	Polar-aromatic in oils (%)
Non catalyst	3.65
HBETA	5.95
HMOR	4.10
HY	3.21

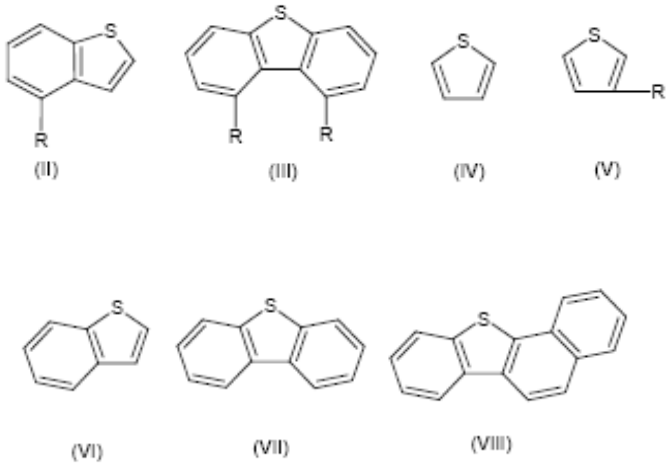

Figure 4.10 Polar-aromatics in pyrolytic oils (Pakdel *et al.,* 2001; Rodriguez *et al.,* 2001; Laresgoiti *et al.,* 2004; and Unapumnuk, 2008).

Table 4.3 summarizes the polar-aromatics content in the oils. All zeolites reduce polar-aromatics in oils, indicating a higher quality of pyrolytic oils obtained. HY gives the lowest amount of polar-aromatic in the oil whereas HBETA gives slightly higher polar-aromatics amount than HMOR. **Figure 4.10** shows several types of polar-aromatics in pyrolytic oils which are found in several literatures (Pakdel *et al.,* 2001, Rodriguez *et al.,* 2001, Laresgoiti *et al.,* 2004, and Unapumnuk, 2008).

Figure 4.11 shows the carbon number distribution of polar-aromatics obtained from various zeolites. In all cases, polar-aromatics are widely distributed from low carbon numbers to high carbon numbers of C40, but highly distributed in

C6-C25. Pyrolysis without a catalyst gives the average carbon number in the range of kerosene, which is around C14 (from **Table 4.4**). The use of catalysts differently shifts carbon number distribution from the non-catalytic case. The average carbon number of polar-aromatics from HBETA is approximately C17 whereas that from HY is around C18. HMOR gives the average carbon number of C15.

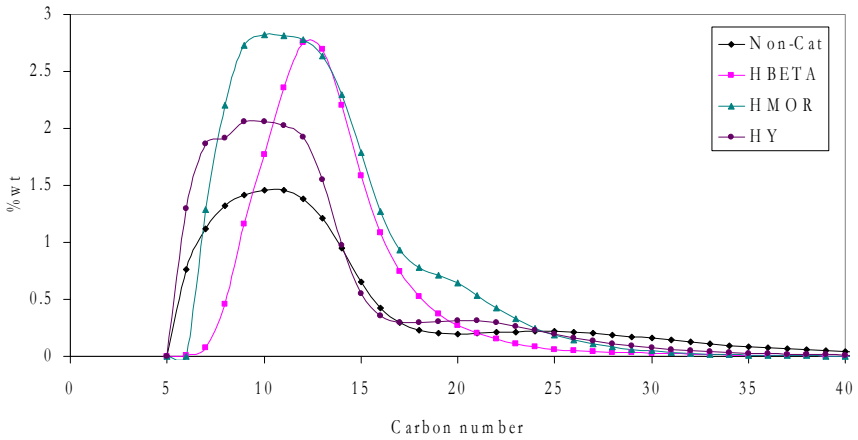

Figure 4.11 Carbon number distribution of polar-aromatics in maltenes obtained from using various zeolites

The sulfur content in the oil product was determined by CHNOS elemental analysis technique. The low amount of sulfur content in an oil product indicates that the oil has high quality. As shown in **Figure 4.12**, the use of zeolites gives a lower quantity of sulfur in the oil than that obtained from the non-catalytic case which gives the oil with 1.38% of sulfur. The use of pure zeolites dramatically decreases the amount of sulfur in the oil products as compared to the non-catalytic case. All zeolites decrease sulfur concentration from 1.38% to 0.94-0.98%. The asphaltene (a very large aromatic molecule in oil) also reduces when the zeolites are used, and it seems that the acid strength plays the role on the asphaltene reduction since the degree of reduction corresponds to the acid strength.

Table 4.4 The average carbon number of polar-aromatics obtained from using different zeolites

Samples	Average Carbon of polar aromatics	Example of sulfur compounds
Non-cat	14.4	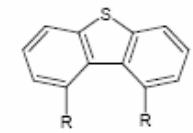
HBETA	16.8	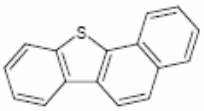
HMOR	15.2	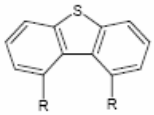
HY	17.8	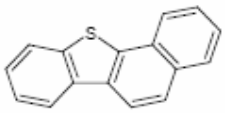

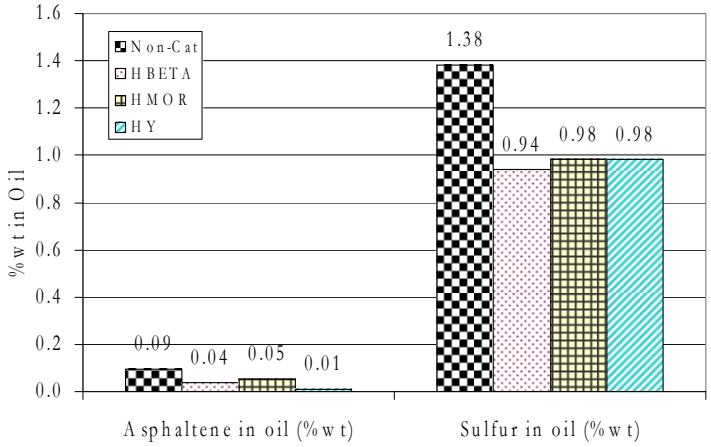

Figure 4.12 Asphalthene and sulfur in oils obtained from using various zeolites

Table 4.5 Sulfur and coke deposition on the spent zeolites

Catalyst	Spent Zeolites	
	Sulfur (%)	Coke formation (g/g catalyst)

HBETA	0.176	0.228
HMOR	0.148	0.148
HY	0.137	0.171

Furthermore, the coke formation on catalysts was determined by the TG/DTA technique. The results are shown in **Table 4.5**. Due to the highest acid strength, the amount of sulfur formation on HBETA is the highest, followed by HMOR and HY, respectively. The coke formation on HBETA is also the highest due to its highest acid strength and its 3D structure which can trap large molecules like coke. However, the dimensional structure of the pore also plays an important role on coke formation. Although HMOR has higher acid strength than HY, but HY has higher coke deposition, because HY has 3D structure whereas HMOR has 1D structure which can less trap coke in its pores.

4.2.5 Petrochemical Yields

Due to the activity, the use of catalysts can increase gaseous products. They have major influence on light olefins and cooking gas production. The gaseous products were analyzed in terms of valuable components such light olefins (ethylene and propylene) and cooking gas (hereby defined as the mixture of propane and mixed C4s) as shown in **Figure 4.13**. The zeolite that increases the light olefins yield is HY, which may be resulted from its lowest acid strength. HBETA and HMOR have a strong enough acid sites that can protonate the olefins, leading to the reduction of olefins as compared to those obtained from the non-catalytic pyrolysis. HY zeolite therefore gives the highest light olefins production. It is also possible that HY zeolite has the highest pore volume (0.5763 cm^3/g), which once heavy primary products can be cracked to light olefins inside the pore, the olefins can diffuse out of the pores of HY so quickly that they are not further cracked to some lighter molecules.

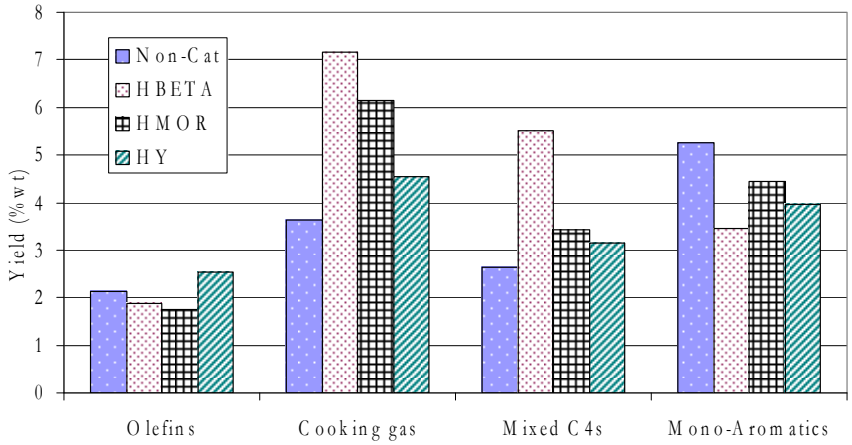

Figure 4.13 Petrochemicals obtained from using various zeolites

The trends of cooking gas and mixed C4s productions are similar on which the productions vary with the acid strength. The higher acid strength, the higher productions are achieved. It is found that the zeolites do not increase the concentration of mono-aromatic compounds in oil (**Figure 4.5**); therefore, with the decrease in oil production with using the zeolites, the yield of mono-aromatics decreases. The pure zeolites thus cannot be used to produce mono-aromatics.

5

Effects of Metals on Acid Supports

Various metals, namely Pt, Pd, Ru, Re, Rd, and Ag were loaded onto the acid zeolites and used as so-called "***Bi-functional catalysts***" in the pyrolysis of waste tire. This chapter discusses the influences of each metal on the yields of products, gas production, petroleum fraction, molecular compositions, and petrochemical production. Since the previous chapter has discussed about the influences of zeolites, only additional information on the effects of each metal are given in this chapter. Each metal has its own characteristics that result in the different characters of tire-derived products. The knowledge on the selectivity of the bi-functional catalysts would allow one to customize the tire-derived products as needed. Moreover, tire pyrolysis may possible be an alternative process to selectively produce petroleum-like oils and some petrochemicals in the future when the world is lacked of petroleum for petroleum and petrochemicals productions.

5.1. Pt-Loaded Catalysts

Pt is an expensive transition metal which no one in the past would have imagined that it could be used as an industrial catalyst. Nowadays, Pt has been known as a good catalyst in many industrial applications such as in ammonia oxidation for the production of sulfuric acid, reforming and cracking of petroleum products, and fuel cells. This work is an attempt to use Pt-loaded catalysts in tire pyrolysis, which is interested in the Pt's selectivity towards the production of some tire-derived products.

5.1.1 Product Yields

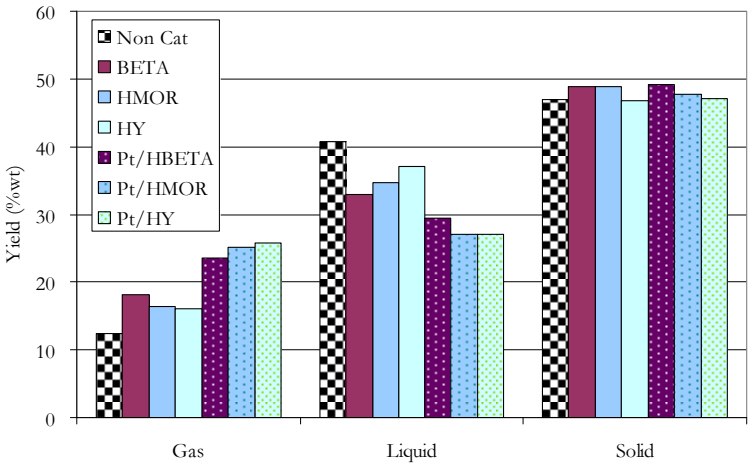

Figure 5.1 Product yields obtained from Pt-loaded catalysts**.**

All Pt-loaded catalysts greatly improve the gas yield by 5% (from HBETA's) to 10% (from HY's) and twice as much as that from the non-catalytic pyrolysis in the expense of the decreases in oil yields in the similar proportions (see **Figure 5.1**). The highest gas yield is obtained when Pt/HY is used as catalyst, and Pt gives the highest improvement of gas yield when loaded on HY zeolite. The increase in gas yield for overall cracking indicates the higher activity in cracking of a catalyst. HY itself has the lowest cracking activity among all zeolites, but Pt/HY has the highest cracking activity. However, the compositions of the gas and the liquid must

be considered for determining the selectivity of the catalysts.

5.1.2 Gas Compositions

The compositions of gases obtained from Pt-loaded catalysts are slightly changed from those obtained from the corresponding zeolites (see **Figure 5.2**).

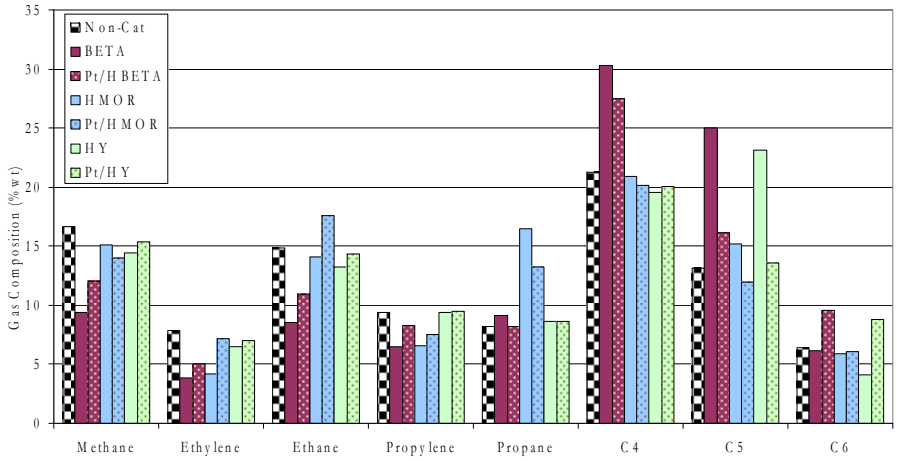

Figure 5.2 Gas compositions from using Pt-loaded catalysts**.**

Pt seems to further increase methane, C2s, propylene, and C6s but decrease propane, C4s, and C5s. Heating value (LHV) of a gaseous product is one of the parameters which can reflect the composition and the quality of a natural gas, and also demonstrate the heat of combustion of a gas product when it is used as a natural gas in the industry. A gas containing of a higher amount of heavy hydrocarbons generally has a higher heating value and then a higher price since the gas is sold according to its heating value. Therefore, it appears that Pt-loaded catalysts can produce a gas with a high heating value. Since Pt loading results in the large increases in gas yield, it may be interesting to consider the yield of each gas component. **Figure 5.3** shows the yields of gases obtained from using Pt-loaded catalysts. One may see that the yield of all gases, except C5s increases by 1-2%.

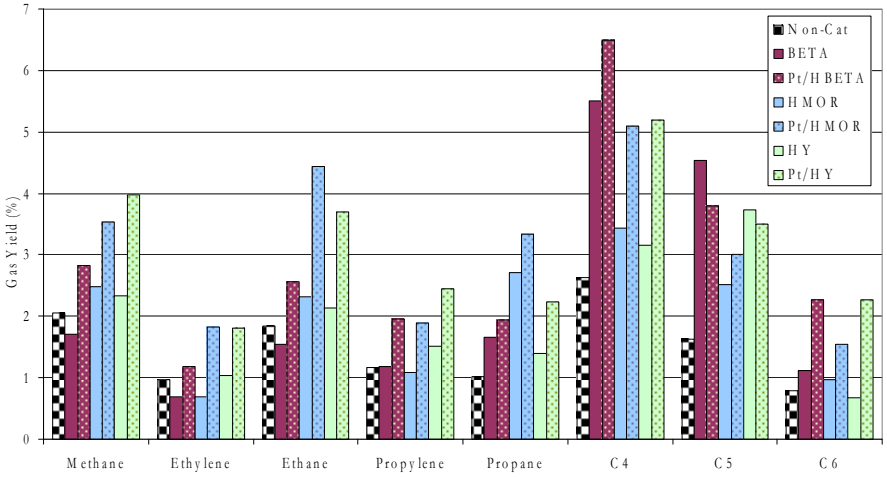

Figure 5.3 Yields of gases obtained from using Pt-loaded catalysts**.**

5.1.3 Petroleum fractions

Simulated true boiling point curves of the maltenes obtained from using Pt-loaded catalysts shown in **Figure 5.4** indicate that with Pt loading the curves shift to the lower boiling points, meaning that all Pt catalysts give lighter oil than all unloaded zeolites. Figure 5.5 reveals that the lightness of the oils is contributed from the increase in naphtha in the oil. The fraction of naphtha in the maltenes is increased by almost 10% (for HBETA case), 28% (for HMOR case), and 20% (for HY case). Pt/HMOR as the best catalyst among all Pt-loaded catalysts gives about 68% naphtha, 20% kerosene, 6% light gas oil, 5%heavy gas oil, and 1% long residue in the oil. **Figure 5.5** also illustrates that the increase of naphtha fraction is resulted from the further cracking of the heavier fractions by Pt loading since all heavier fractions reduce with using the Pt-loaded catalysts.

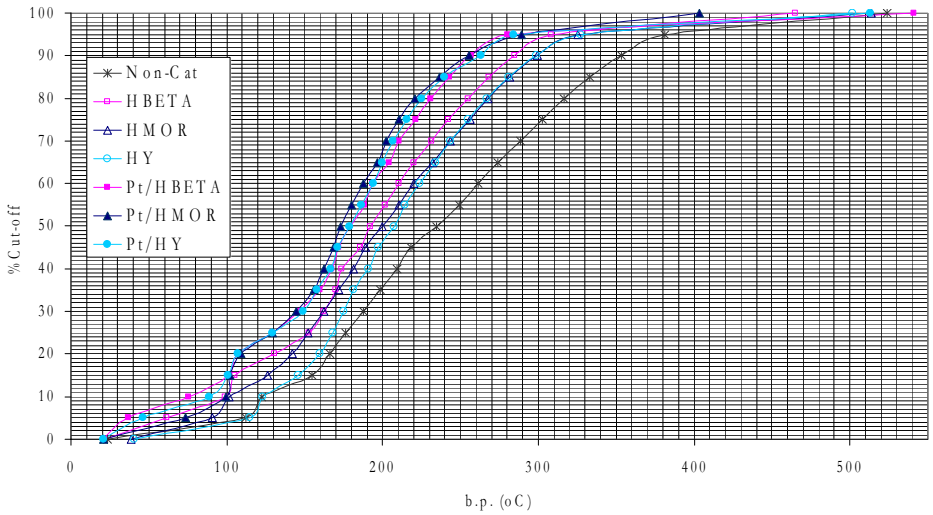

Figure 5.4 Simulated true boiling point curves of maltenes from using Pt-loaded catalysts.

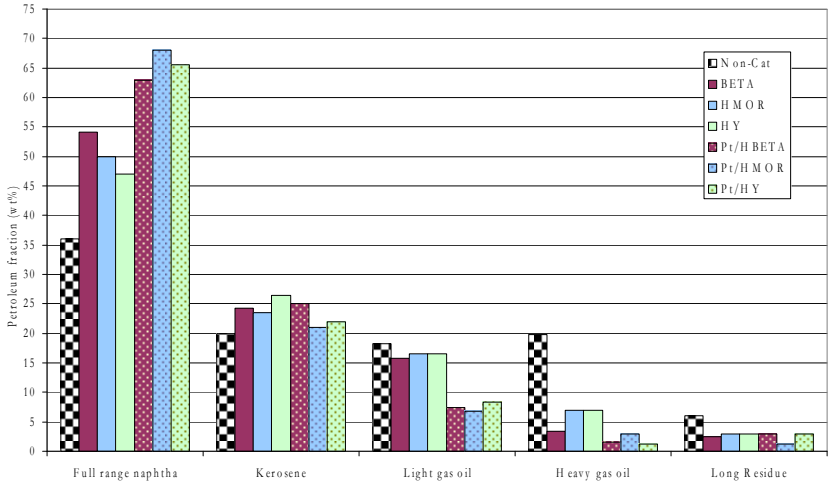

Figure 5.5 Petroleum fractions in maltenes from using Pt-loaded zeolites**.**

5.1.4 Molecular Composition in oils

As compared to HBETA, Pt/HBETA decreases saturated HCs, di-aromatics, and polar-aromatics with the significant increase in mono-aromatics in the oil (**Figure 5.6**). It seems that Pt loading can convert saturated HCs, di-, and polar-aromatics to mono-aromatics. Pt/HY gives some similar results; that is, it decreases saturated HCs and poly-aromatics with the increase of mono-aromatics, indicating

that poly-aromatics are converted to mono-aromatics. Pt/HMOR that gives the oil with the highest amount of naphtha further increases the saturated HCs and mono-aromatics in association with the reduction in all types of aromatics. It means that Pt/HMOR not only gives the highest quantity of naphtha, but also it produces naphtha with the highest quality.

One thing in common all Pt-loaded catalysts have is that they increase mono-aromatic content in the tire-derived oil. It appears that Pt can change aromatic compounds to mono-aromatics and some saturated HCs, possibly via hydrogenolysis, hydrocracking, and ring-opening activity (Santikunaporn *et al.*, 2004; Gault, 1981; Arribas *et al.*, 2004).

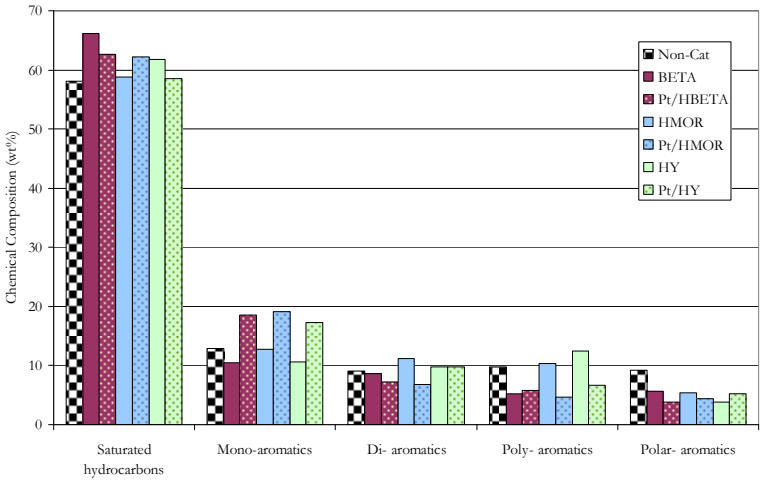

Figure 5.6 Molecular composition in maltenes obtained from using Pt-loaded catalysts**.**

5.1.5 Petrochemical Yields

As compared with the corresponding zeolites, all Pt-loaded catalysts improved the olefins, cooking gas, and mixed C4s productions (**Figure 5.7**), possibly due to the high yield of gas products obtained from using Pt-loaded catalysts. A higher olefins or cooking gas production may be resulted from a higher cracking activity whereas the acidity of the supports plays an important role on the production of mixed C4s.

Dr. Sirirat Jitkarnka
Associate Professor
The Petroleum and Petrochemical College
Chulalongkorn University

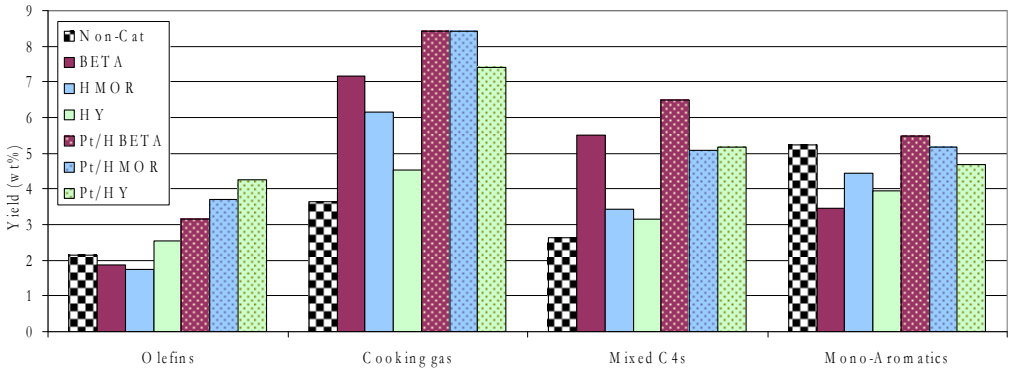

Figure 5.7 Yield of some petrochemicals from using Pt-loaded catalysts**.**

5.1.6 Polar-aromatic reduction

Platinum catalysts have been known as effective desulfurization catalysts (Baldovino-Medrano *et al.*, 2008), and noble metal catalysts are very active for hydrogenation reactions (Williams *et al.*, 2007). For deep HDS, the hydrogenating function of a catalyst is crucial because an initial hydrogenation of the refractory sulfur-containing molecules was found to reduce steric effects that impede the direct elimination of sulfur heteroatoms (McKinley and Emmett, 1957; Pecoraro and Chianelli, 1981). The known poisoning effect of Pt-based catalysts caused by the presence of sulfur-containing compounds in the feed might be overcome by the increase in the support acidity (Stanislays and Cooper, 1994; Du *et al.*, 2005; Yasuda and Yoshimura, 1997; Matsubayashi, *et al.*, 1998; Navarro *et al.,* 2009). Moreover, in 2004, Santikunaporn *et al.* investigated the ring-opening of decalin and tetralin on HY and Pt/HY zeolite catalysts, and found that the production of ring-opening products was increased with the addition of Pt metal.

To our knowledge, there has been no research having conducted to study the effect of pyrolysis temperature and catalysts on the polar-aromatic content in tire-derived oil. Thus, the purposes of this work were to study polar-aromatic formation in the pyrolytic oil obtained from the non-catalytic pyrolysis of waste tire at various temperatures, and to investigate the distinctive effects of Pt-supported HMOR and Pt-supported HBETA catalysts on the polar-aromatic formation (see **Figure 5.6**).

Prior to being able to explain how the catalysts can help reducing polar-aromatic contents, the formation of such compounds needs to be understood. This section is contributed to the discussion about how polar-aromatics can be formed during the pyrolysis of waste tire.

(a) Polar aromatic formation from thermal cracking of tire

The chemistry of sulfur vulcanization is so complex that, even today, only the main stages have been proven. After vulcanization, sulfur was combined in the network in a number of ways. Sulfur may be present as monosulfide, disulfide or polysulfide, but it may also be present as dependent sulfides, or cyclic-mono- and di-sulfides (Blow and Hepburn, 1982). In addition, sulfur was found to attach to the rubber chains almost exclusively at the allylic positions (Mark *et al.*, 1994). Moreover, a typical tire compound contains natural rubber (NR), styrene butadiene rubber (SBR), poly butadiene and butyl rubber (Williams and Besler, 1995). Therefore, the rubber chains of tire should contain the aromatic rings originally from SBR as well as double bonds. In addition, in the SBR, the configuration of styrene monomers could be both block and random. And, the amount of bound styrene (%wt) is in the range from 10 to 45% (Mark *et al.*, 1994), depending on the way the SBR was synthesized.

Several researches have investigated the thermal degradation of different rubbers. In the work of Chen and Qian (2002), it was found that during the pyrolysis of natural rubber, β-scission was much more preferable because of the low bond dissociation energy, leaving the allylic radicals. The thermal cracking of polybutadiene also was reported to occur via β-scission (Blow and Hepburn, 1982). Meanwhile, the thermal degradation of the styrene-butadiene rubber was favored to occur at the position **(a)** than at **(c)** in Scheme 5.1 as suggested by Choi (2000), whereas no product resulted from the dissociation at the position **(b)** was observed. In addition, during the pyrolysis, not only the depolymerization but also the decomposition reaction to produce short chain hydrocarbon occurred (Chen and Qian, 2002).

Dr. Sirirat Jitkarnka
Associate Professor
The Petroleum and Petrochemical College
Chulalongkorn University

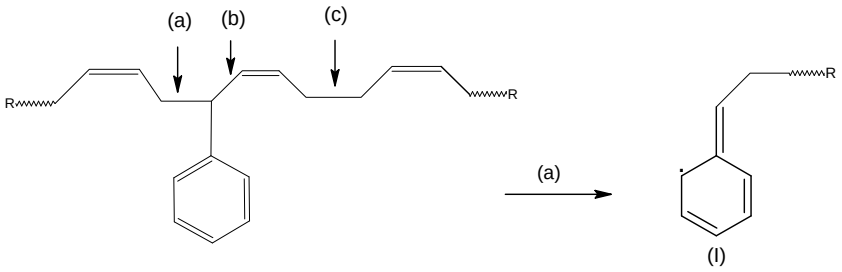

Scheme 5.1 All cracking positions on the SBR chain and the product **(I)** obtained from cracking at the most probable position **(a)** (Uhl *et al.*, 2000)

In the present study, it was found that the polar-aromatics mainly distributed in the heavy fractions of the oils (light and heavy vacuum gas oils), which is in good agreement with some studies (Pakdel *et al.*, 2001; Rodriguez *et al.*, 2001; Laresgoti *et al.*, 2004). Scheme 5.2 shows several polar-aromatics found in the pyrolyzates from various references (Pakdel *et al.*, 2001; Rodriguez *et al.*, 2001; Laresgoti *et al.*, 2004; Unapumnuk *et al.*, 2008).

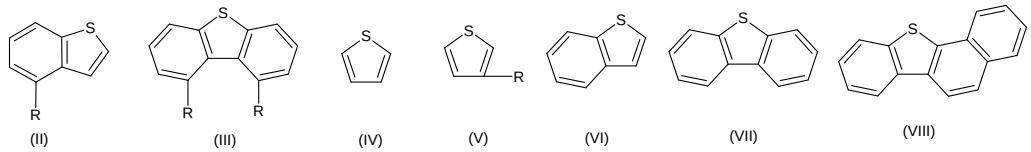

Scheme 5.2 Some polar-aromatics found in pyrolytic oils (Pakdel *et al.*, 2001; Rodriguez *et al.*, 2001; Laresgoti *et al.*, 2004; Unapumnuk *et al.*, 2008)

In order to ease the further discussion about polar-aromatic formation/reduction with respect to the pyrolysis conditions and the presence of catalysts, an example of tire structure is hereby anticipated, as shown in Scheme 5.3, based upon the earlier discussion on the possible cracking positions having been proposed to occur during the pyrolysis of waste tire (Chen and Qian, 2002; Uhl *et al.*, 2000; Choi, 2000) and upon our experimental results.

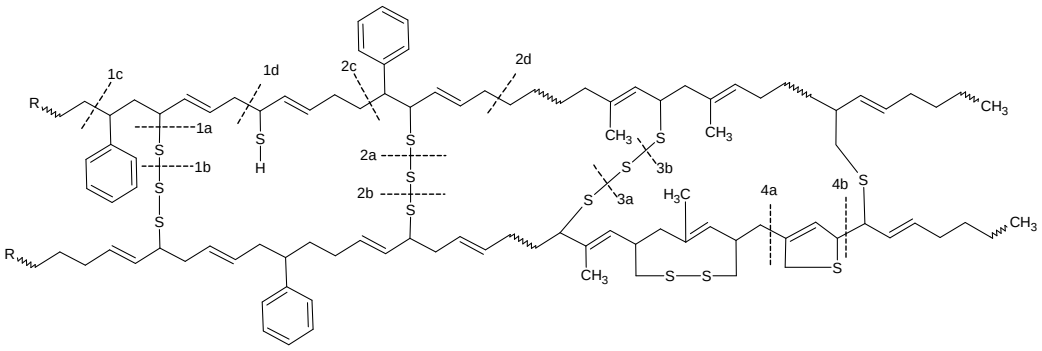

Scheme 5.3 A tire molecule (adapted from Blow and Hepburn, 1982; Williams and Bottrill, 1995; Williams and Besler, 1995) accompanied with the proposed possible cracking positions during pyrolysis (Jitkarnka *et al.*, 2007; Chen and Qian, 2002; Choi, 2000)

The sulfur, which is originally present in the tire rubber approximately by 1.7 %wt (Williams and Brindle, 2003a; 2003b) is the source for the formation of sulfur-containing compounds during pyrolysis. In addition, oxygen is prohibited in pyrolysis. Consequently, polar-aromatics found in pyrolysis oil are mostly sulfur-containing aromatics. In the study of Jitkarnka *et al.* (2007), it was reported that the breakdown of a tire molecule would initially occur at the S – S bonds, and then spread out along the free rubber chains. According to the dissociation energy of the S – S, C – S and C – C bonds, which are 429, 699 and 607 $kJ.mol^{-1}$, respectively (Dean, 1999), the free sulfur might easily be produced by the cracking of tire molecule at the positions **1a**, **1b**, **2a**, **2b**, **3a**, and **3b**.

The thermal cracking reaction could simultaneously occur at any position from **1** to **4**. The scissions occurring at the positions **1 a**, **b**, **c**, and **d** result in the formation of Species **(I)** (Choi, 2000) and some free sulfurs. After that, Species **(I)** might react with the generated free sulfurs under the presence of ethylene *via* the Diels–Alders reaction (Williams and Bottrill, 1995), followed by cyclization and dehydrogenation (Laresgoiti *et al.*, 2004) to form **(II)**. Consequently, Species **(II)** can further react with the produced olefins (Rodriguez *et al.*, 2001), and then again cyclizes yielding Species **(III)** as shown in Scheme 5.4.

Dr. Sirirat Jitkarnka
Associate Professor
The Petroleum and Petrochemical College
Chulalongkorn University

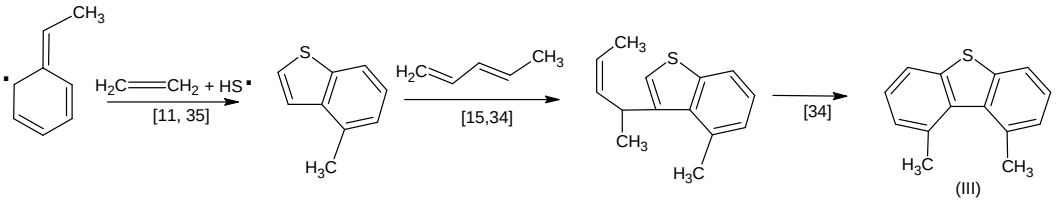

Scheme 5.4 An example of polar aromatic formation via a consecutive reaction with free sulfurs

The production of hydrogen sulfide (Leung *et al.*, 2002; Aylon *et l.,* 2007) in the gas product could be explained by the reactions displayed in Scheme 5.5. Initialized by the simultaneous cracking of tire molecule at positions **1d** and **2c** in **Scheme 3**, the product could then be stabilized by hydrogen coming from potential H–donor structures (Rodriguez *et al.*, 2001), followed by cracking to produce hydrogen sulfide and light olefins such as ethylene and propylene (Dupain *et al.*, 2003).

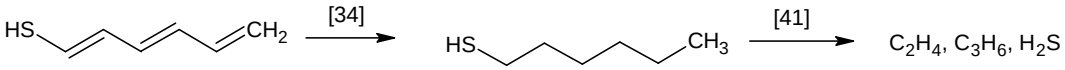

Scheme 5.5 An example of hydrogen sulfide production via hydrogenation followed by cracking

In contrast, with the presence of potential H-donor compounds during the pyrolysis (Rodriguez *et al.*, 2001), the produced H_2S might be added to the olefins generated by the thermal cracking to form thiols, which suffer the cyclization and dehydrogenation into thiophenic compounds (Leflaive *et al.*, 2002; Mizutani *et al.*, 2007).

The cracking of the rubber chain at the positions **2a, b, c** and **d** followed by the free radical stabilization and the cyclization reaction on the chain [44] could lead to the formation of alkyl benzothiophene (**II**). Moreover, thiophene, which could be directly produced via the cracking reaction at positions 4a and 4b, might undergo hydrogen transfer reaction (Rodriguez *et al.*, 2001). And then, the

obtained product subsequently reacts with the available olefins (Valla *et al.*, 2006; Williams and Taylor, 1993), followed by cyclization and dehydrogenation (Rodriguez *et al.*, 2001), generating benzothiophene (**V**). Further reactions could also occur, leading to the formation of polycyclic polar-aromatic compound, **VIII**, as shown in Scheme 5.6.

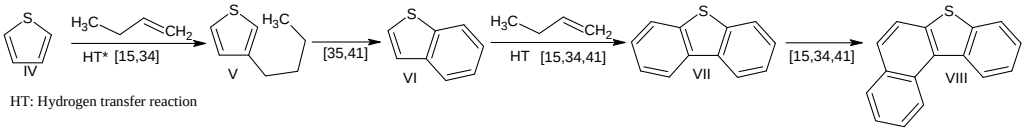

Scheme 5.6 An example of polycyclic polar-aromatic formation initialized by the direct cracking of tire

(b) Effect of temperature on polar aromatic production

The effect of pyrolysis temperature on polar-aromatic production was also investigated in the present study. The results show that under the pyrolysis temperature of 500°C, the amount of polar-aromatics account for approximately 11%wt of the obtained oil product. And, when the pyrolysis temperature increased, the amount of polar-aromatics increased as shown in **Figure 5.8**.

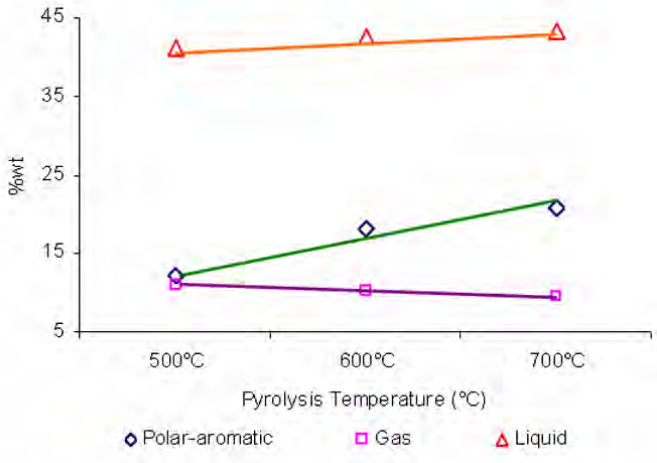

Figure 5.8 Effect of pyrolysis temperature on the yield of gaseous and liquid products in association with the weight-percentage of polar-aromatics in the liquid product.

Dr. Sirirat Jitkarnka
Associate Professor
The Petroleum and Petrochemical College
Chulalongkorn University

From the results, it can be explained that at higher temperatures, more free radicals are generated at a greater rate, so many of them combine one another. As a consequence, more aliphatic chains linked to polar aromatic structures as in Scheme 5.4, and then these chains might undergo cyclization reactions resulting in the production of much heavier polar-aromatic hydrocarbons as in Scheme 5.6. The decrement of gas product as observed in Figure 2 is also the consequence of the poly-aromatic formations. The shift of the peak to the higher carbon number with temperature shown in **Figure 5.9** can be the evidence confirming the formation of bigger size poly-aromatic compounds in the oil products.

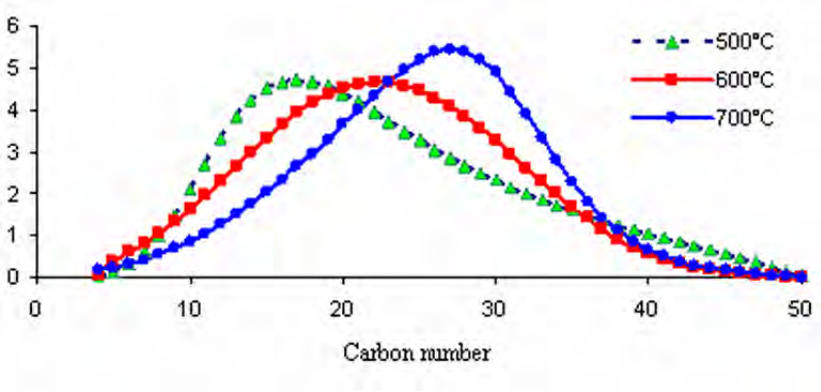

Figure 5.9 Effect Effect of pyrolysis temperature on the carbon number distribution of polar-aromatic compounds.

In summary, the formation of polar-aromatics could mainly be attributed to (i) the combinations of available olefins and free sulfurs, (ii) the combination of sulfur containing compounds with olefins, via the Diels–Alders reactions, and (iii) the direct cracking of tire molecule at where the S atoms are resided. Therefore, in order to reduce polar-aromatics in the pyrolytic oils without the introduction of hydrogen, one can either prevent them from formation via such means or force them by any mean to crack into lower molecules and eventually to hydrogen sulfide as in Scheme 5.5.

(c)Effects of the catalysts

Figure 5.10 shows the percentages of the polar-aromatics in the pyrolytic oils obtained from the experiments run with different catalysts. From the figure, it is clear that HMOR and HBETA zeolites help decrease the amount of polar-aromatics by approximately 30%wt and 50%wt, respectively, as compared to the non catalytic case. The introduction of Pt on the zeolites led to a further decrease in the content of polar-aromatics. And, the lowest polar-aromatic content is observed when Pt/HBETA catalyst was used.

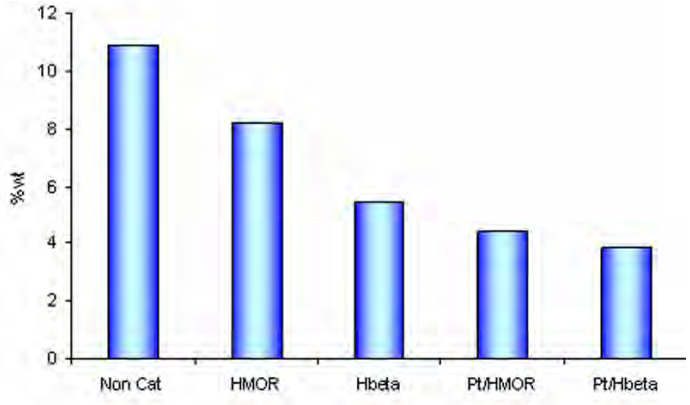

Figure 5.10 Effect of catalysts on the polar-aromatic content in the pyrolytic oils.

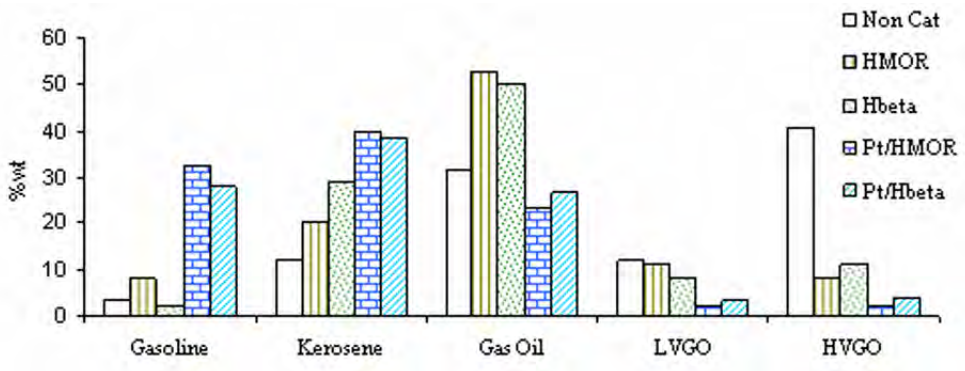

Figure 5.11 Effect of catalyst on polar-aromatic distribution in petroleum fractions.

Figure 5.11 shows the simulated distillation of the obtained polar-aromatic portions, which were cut, according to the boiling points, into gasoline (<149°C), kerosene (149–232°C), gas oil or diesel (232–343°C), light vacuum gas oil

or fuel oil (343–371°C), and heavy vacuum gas oil (>371°C). According to the figure, one can see that polar-aromatics from the non-catalytic pyrolysis are mainly distributed in the range of gas oil and vacuum gas oil. The introduction of the catalysts alters the distribution of polar-aromatics to a range of lighter fractions. Especially, when the bifunctional catalysts were used, polar-aromatic compounds in the HVGO range are decreased remarkably. And, polar-aromatics are highly distributed in the kerosene range, instead of the gas oil range as having occurred when the corresponding zeolites were used. Besides, a small amount of polar-aromatics in the gasoline range is obtained in the case of HBETA. This might be attributed to the fact that HBETA has two channels 7.6x6.4 Å in diameter, and a third channel that is only 5.5x5.5 Å wide (Miguel *et al.,* 2006), so that deep cracking of polar-aromatics might have occurred producing H_2S and light hydrocarbons in the gaseous product.

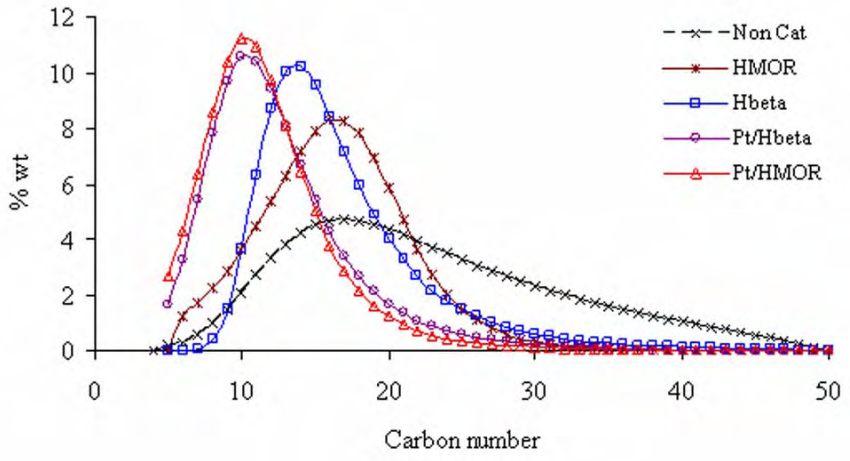

Figure 5.12 Effect of catalysts on the carbon number distribution of polar -aromatic compounds.

Figure 5.12 shows the shift of carbon number distribution of polar-aromatics to lower carbon numbers in conjunction with the narrower distribution when the catalysts were used. Many studies have proven that acid catalysts are able to crack thiophene, benzothiophene, and their derivatives to lower molecular-weight substances (Valla *et al.*, 2006; Li *et al.*, 2008). Once polar-aromatics are formed, acid

catalysts can crack them into smaller molecules, and possibly open aromatic rings, consequently reducing the total amount of the polar-aromatics in the pyrolytic oil.

Table 5.1 Physical and chemical composition of the studied catalysts

Table 1
Physical and chemical composition of the studied catalysts.

Catalyst	Pt (%wt)	Dispersion (%)[a]	Surface area ($m^2 g^{-1}$)	Pore diameter (Å)	Pore volume ($cm^3 g^{-1}$)	Particle size (μm)[b]	Coke ($g g^{-1}$ cat)
HMOR	–	–	372.5 ± 9.3	6.3[c]	0.20[c]	10–12	0.14
HBETA	–	–	618.3	7.5	0.68	3–6	0.22
Pt/HMOR	0.94	30.8	359.8	6.1	0.18	–	0.38
Pt/HBETA	1.01	42.1	608.5	7.1	0.67	–	0.33

[a] Determined by H_2 chemisorption.
[b] Supplied by TOSOH Corp.
[c] Determined by HK method [31].

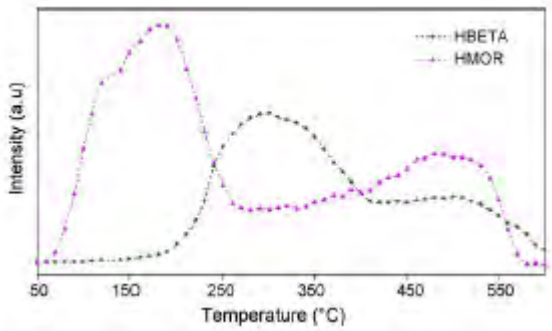

Figure 5.13 NH_3-TPD of HBETA and HMOR.

As presented in this work, among the two zeolites, HBETA exhibits higher activity than HMOR in reducing the size of polar-aromatics as illustrated by the lower average carbon number (**Figure 5.10**) as well as the quantity of the compounds (**Figure 5.8**). The higher activity of HBETA as compared to HMOR might be attributed to its better cracking activity caused by the combination effects of its higher total amount of medium and strong acid sites (**Figure 5.13**), its smaller crystalline (**Table 5.1**), and especially its large sinusoidal pore systems (Lee *et al.*, 2008; Corma *et al.*, 2001). Moreover, its larger pore diameter favors the diffusion of larger molecules into inner pores; thus, a higher amount of reactants including polar-aromatics might be cracked to smaller compounds.

Additionally, it was reported that acid catalysts did not only display the activity on cracking polar-aromatics or sulfur-containing compounds, but also on the cracking of a hydrogenated aromatic intermediate, as in Scheme 5.7a (Corma *et al.*,

2001). Prior to being converted to a polar-aromatic compound, Species (**I**) might be stabilized and cracked to produce lighter HCs, preventing the reactions in Scheme 6 from occurring. In addition, the presence of acid catalysts was found to convert long chain alkylthiophenes to shorter alkyl-thiophenes by cracking the alkyl chain of the former (Corma *et al.*, 2001; Valla *et al.*, 2006) as shown in Scheme 5.7b, resulting in the prevention of the formation of Species **(VI)** from (**V)** as illustrated in Scheme 5.6.

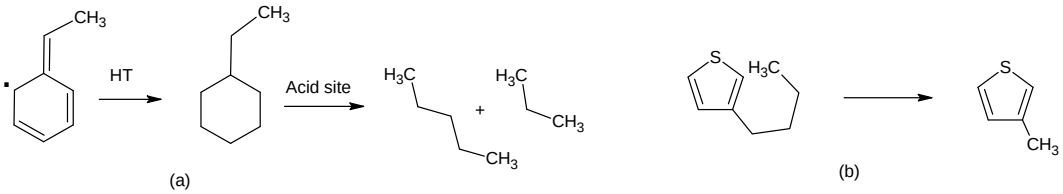

Scheme 5.7 Examples of polar-aromatic reduction by acid catalysts (Corma *et al.*, 2001; Valla *et al.*,2006)

Table 5.1 has shown that HBETA forms the higher amount of coke than HMOR. This could be attributed to the higher total amount of medium and strong acid sites, and particularly its larger pore volume that favors the condensation of an aromatic compound to form coke (Richardeau *et al.*, 2004). Corma and his colleagues (2001) also suggested a possible pathway to form coke from alkyl-benzothiophenes (Species **II**). In addition, the highest amount of coke is produced when the bifunctional catalysts were used, suggesting that possibly polar-aromatics are partially diminished by the formation of coke instead.

As shown in Scheme 5.4, the formation of polar-aromatics involves the interaction with accessible olefins. Consequently, if a catalyst can help eliminating these compounds, the polar-aromatic formation can be prevented. And, interestingly, that was indeed the case when the bifunctional catalysts were used. Although the HBETA zeolite alone displays much higher polar-aromatic reduction than the HMOR zeolite does (**Figure 5.12**); with the introduction of Pt, the polar-aromatic reduction activity of the two emerged bifunctional catalysts is found

comparable. Consequently, the presence of Pt on the surface of the catalyst results in the prevention of polar-aromatic formation. This could be attributed to the high hydrogenation activity of Pt (Williams et al., 2007; Philippou and Anderson, 1997) that helps converting olefins and other unsaturated intermediates to saturated HCs, instead of being combined with one another to form heavier polycyclic polar-aromatic compounds as in Scheme 5.6. In addition, these hydrogenated compounds might further undergo cracking reactions, and then, are converted into lighter polar-aromatics or sulfur-containing compounds or even into H_2S in association with the formation of short-chain hydrocarbons. That explains the shift of the peak to the lower carbon number (**Figure 5.11**) when Pt-supported catalysts were present. Therefore, it is possible that the rate of the hydrogenation catalyzed by Pt metal is faster than the rate of the combination reaction (as in Scheme 5.6 to yield heavier polar-aromatic compounds), leading to the reduction of polar-aromatic compounds in the pyrolytic oils. To visualize the previous explanation, **Scheme 5.8** gives some examples of the prevented and favored reactions if thiophene, reported as a sulfur compound among other thiophene compounds found in tire-derived oil (Pakdel et al., 2001; Rodriguez *et al.*, 2001; Laresgoti *et al.*, 2004; Unapumnuk *et al.*, 2008), is present with the catalysts. Furthermore, as mentioned earlier, the polar-aromatic reduction activity of Pt/HBETA was slightly higher than Pt/HMOR. This could be attributed to the higher surface area of HBETA (**Table 5.1**), resulting in the better dispersion of Pt (**Table 5.1**) (Song and Ma, 2003), and leading to a better hydrogenation activity.

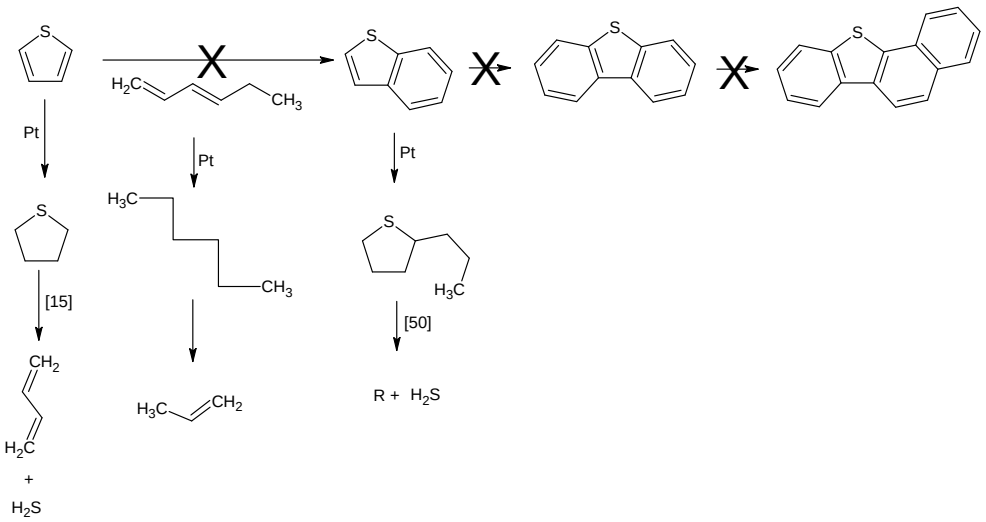

Scheme 5.8 Examples of some prevented and favored reactions by a bifunctional catalyst.

Finally, the bifunctional catalysts can also decrease the amount of polar-aromatic hydrocarbons in the pyrolytic oil via the cracking reactions. Once polar-aromatics are formed, they might be hydrogenated on the Pt sites, followed by cracking on the acid sites, (Can *et al.*, 2007; Contreras *et al.*, 2008).

5.2 Pd-Loaded Catalysts

Pd is one of the metals in a group of elements referred to as "*the Platinum Group Metals (PGMs)*" consisting of palladium, platinum, rhodium, ruthenium, iridium and osmium (Wikipedia, 2011). The PGMs have similar chemical properties, but palladium has the lowest melting point, and has the least dense. Palladium is used as a catalyst in hydrogenation, catalytic converter, and fuel cells. Similar to Pt, Pd is expected to be applicable for tire pyrolysis. The results are discussed as follows.

5.2.1 Product Yields

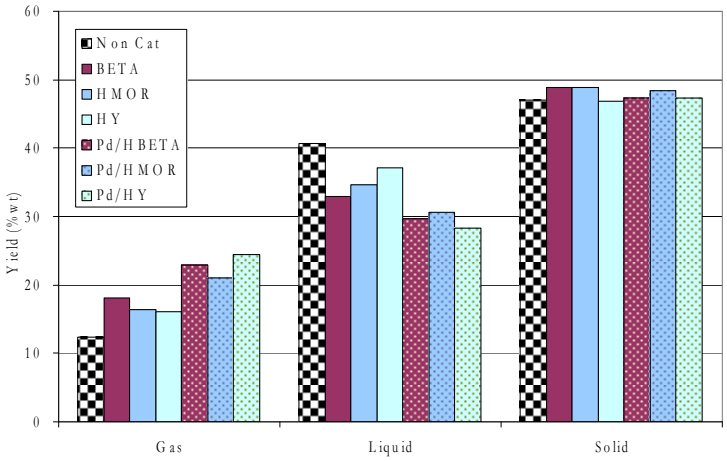

Figure 5.14 Product yields from using Pd-loaded catalysts

Similar to the Pt-loaded catalysts, all Pt-loaded catalysts significantly improve the gas yield by 4% (from HBETA's), 4% (from HMOR's), and 8% (from HY's) in the expense of the decreases in oil yields in the similar proportions (see **Figure 5.14**). The highest gas yield is also obtained with using HY as the support, and Pd gives the highest improvement of gas yield when loaded on HY zeolite. The increase in gas yield for overall cracking indicates the higher activity in cracking of a catalyst. HY itself has the lowest cracking activity among all zeolites, but Pd/HY has the highest cracking activity. However, Pd-loaded catalysts have less cracking activity than the corresponding Pt-loaded catalysts due to the lower gas productions (see Figure 5.1 in comparison with Figure 5.14). The compositions of the gas and the liquid are next considered for determining the selectivity of the catalysts.

5.2.2 Gas Compositions

The compositions of gases obtained from Pd-loaded catalysts are slightly changed from those obtained from the corresponding zeolites (see **Figure 5.15**). Again, the gases obtained from Pd-catalysts are somewhat similar to those from Pt-catalysts (see **Figure 5.2** in comparison with **Figure 5.15**). Only some slight different are observed; for instances, on ethylene and C6s (Pd/HMOR cases).

Dr. Sirirat Jitkarnka
Associate Professor
The Petroleum and Petrochemical College
Chulalongkorn University

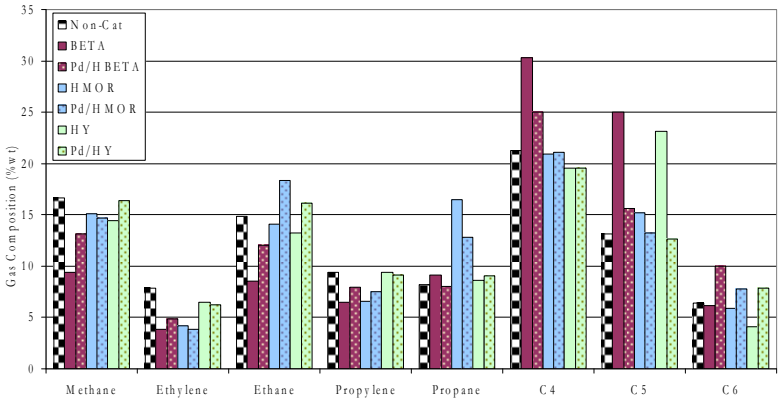

Figure 5.15 Gas compositions from using Pd-loaded catalysts**.**

Pd seems to further increase methane, ethylene, ethane, propylene, and propane from what is produced by the corresponding zeolites, but some still do not reach what is obtained from the non-catalytic case, except ethane and propane given by HMOR. C6s are also more concentrated in the gas products when Pd catalysts are used. Mixed- C4s and C5s are definitely decreased. Since Pd loading results in the increases in the gas yield (**Figure 5.14**) but not as much as Pt loading does, the yield of each gas component can be different. **Figure 5.16** shows the yields of gases obtained from using Pd-loaded catalysts. One may see that the yield of all gases significantly incrases, except C5s, by 1-2%, which is also similar to what is observed from the Pt catalysts cases.

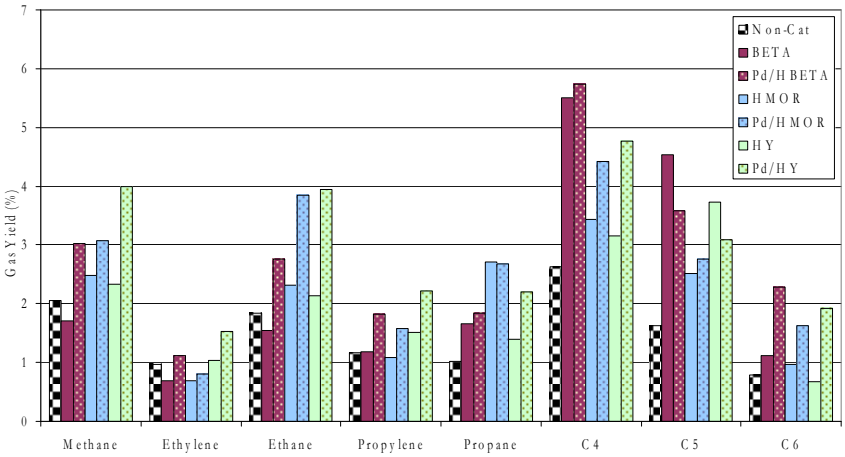

Figure 5.16 Yields of gases obtained from using Pd-loaded catalysts**.**

Dr. Sirirat Jitkarnka
Associate Professor
The Petroleum and Petrochemical College
Chulalongkorn University

5.2.3 Petroleum fractions

Simulated true boiling point curves of the maltenes obtained from using Pd-loaded catalysts shown in **Figure 5.17** indicate that with Pd loading the curves shift to the lower boiling points, meaning that all Pd catalysts give lighter oil than all unloaded zeolites. The lightest oil is obtained from the case when HY is used as the support with Pd loading, unlike the Pt cases in which the lightest oil is obtained when Pt is loaded on HMOR. The lightness of the oils is again contributed from the increase in naphtha in the oils when all Pd-loaded catalysts are introduced (**Figure 5.18**). The fraction of naphtha in the maltenes is increased by only 4% (for HBETA case), 10% (for HMOR case), and 20% (for HY case). Pd/HY as the best catalyst among all Pd-loaded catalysts gives about 68% naphtha, 23% kerosene, 5% light gas oil, 1% heavy gas oil, and 3% long residue in the oil, which is even better than Pt/HMOR (the best one among Pt-loaded catalysts). Likewise, **Figure 5.18** also illustrates that the increase of naphtha fraction is resulted from the further cracking of the heavier fractions (kerosene and both gas oils) by Pd loading since all heavier fractions, except long residue, reduce with using the Pd-loaded catalysts.

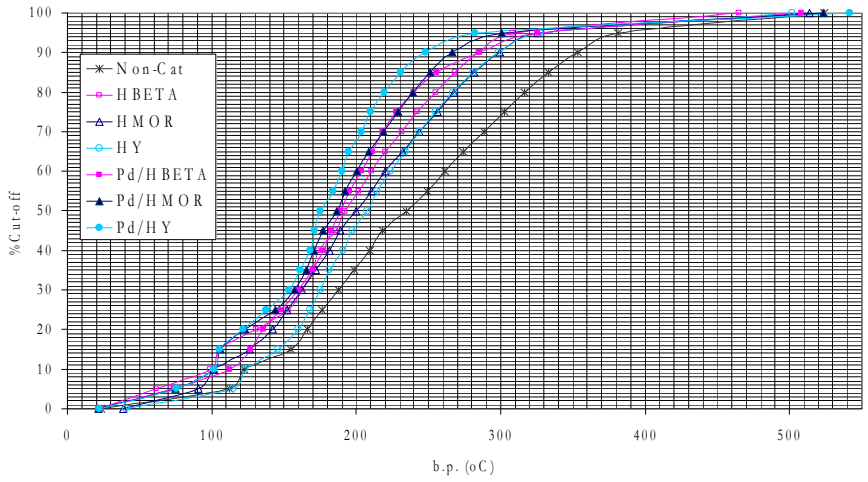

Figure 5.17 Simulated true boiling point curves of maltenes from using Pd-loaded catalysts.

Dr. Sirirat Jitkarnka
Associate Professor
The Petroleum and Petrochemical College
Chulalongkorn University

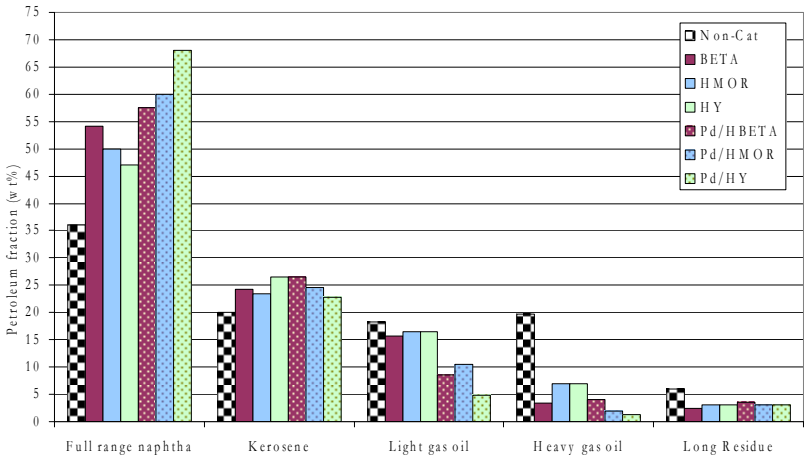

Figure 5.18 Petroleum fractions in maltenes from using Pd-loaded zeolites**.**

5.2.4 Molecular Composition in oils

For all Pd-loaded catalysts, the content of saturated HCs is significantly reduces (**see Figure 5.19**) whereas all aromatics, especially mono-, di-, and polar-aromatics, increase significantly. Poly-aromatics are decreased only when Pd is loaded on HY.

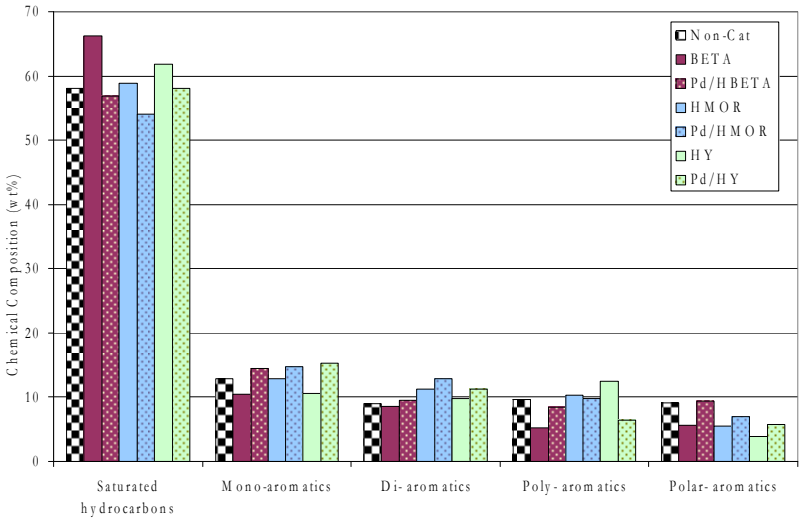

Figure 5.19 Molecular composition in maltenes obtained from using Pd-loaded catalysts**.**

Similar to all Pt-loaded catalysts, one thing all Pd-loaded catalysts

have in common is that they increase mono-aromatic content in the tire-derived oil. However, its effect is not as pronounced as that of Pt, and the pathways seem to be different from those of Pt. Instead, it appears that Pd can change saturated HCs and poly-aromatics to mono- and di-aromatic compounds, possibly via hydrocracking, isomerization (Liu *et al*, 2006), and hydrogenation (Song *et al.*, 2000) activities (without ROP activity) of Pd whereas Pt can produce mono-aromatics and some saturated HCs from aromatic compounds, especially poly- and polar-aromiatics, via its greater ring-opening activity (Santikunaporn *et al.*, 2004; Gault, 1981; Arribas *et al.*, 2004).

5.2.5 Petrochemical Yields

As compared with the corresponding zeolites, all Pd-loaded catalysts improved the olefins, cooking gas, mixed C4s, and mono-aromatics yields (**Figure 5.20**), possibly due to the high yield of gas products obtained from using Pt-loaded catalysts. Again, similar to the Pt catalysts, a higher olefins or cooking gas production may be resulted from a higher cracking activity whereas the acidity of the supports plays an important role on the production of mixed C4s. The mono-aromatic content in oils is improved significantly; however, its yield is slightly improved and not as high as the yield from thermal pyrolysis due to the lower liquid yield than that obtained from the non-catalytic case.

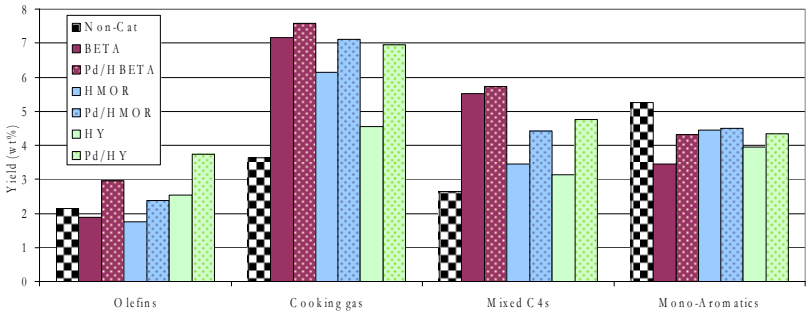

Figure 5.20 Yield of some petrochemicals from using Pd-loaded catalysts**.**

5.2.6 Effects of Pd loading amount and loading technique

The amounts of palladium loading and metal loading method were

investigated for the influences of Pd/H-BETA on product distribution, quality and quantity of oil, represented by the saturated and aromatic hydrocarbons. Several researches have shown the metal loading and the preparation methods (ion-exchange and impregnation) affected to the properties of a catalyst, the selectivity and the activity in hydrogenation, isomerization and hydrotreating reaction. In this work, the influence of metal loading and catalyst preparation technique were studied on the quantity and quality of oil product on pyrolysis of used tire. Especially, the role of the catalyst on upgrading quality by increasing the saturated hydrocarbons and reducing aromatic compound were investigated. The results are discussed as follows.

(a) Catalyst Characterization

The TEM image of Pd/H-BETA catalyst with the Pd content of 0.25 wt.% and 1 wt% confirm the small sizes of palladium particles (**Figure 5.22**). The metal particles are nano-particles, and have a various sizes (3-15 nm). The TEM images also show that larger particle sizes are formed when the amount of metal loading was increased. This same effect has been observed by Lucus *et a.l*, in 2005.

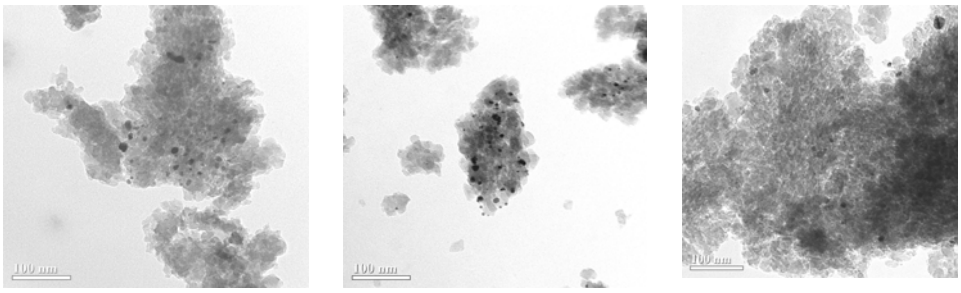

(a) **(b)** **(c)**

Figure 5.22 The TEM image of Pd/H-BETA: (a) 0.25wt% of Pd/H-BETA (impregnated catalyst), and (b) 1.00wt% of Pd/H-BETA (impregnated catalyst) (c) 0.25wt% of Pd/H-BETA (ion-exchanged catalyst)

The ion-exchange technique can produce the catalysts which have a very fine metal particles and higher metal dispersion on H-BETA than incipient impregnation

as shown in the TEM images (**Figure 5.22**). The impregnated catalyst particles have various sizes in the range of 3 to 15 nm. But, the particle sizes of ion-exchanged catalysts almost had same size (4-8 nm). The stronger metal-support interactions of the ion-exchanged catalysts generally give higher dispersion of metal on zeolite than impregnated catalysts. Similarly, the XRD patterns confirmed that metal particle sizes were small, under the lowest detection limit of XRD technique. Moreover, the TEM images also show the location of metal particles. It was found that the metal particles of impregnated catalysts were deposited mostly on the external surfaces. In the case of ion-exchanged catalysts, they were highly distributed on both inside the pore and a few amounts on external surface. The metal particles possibly deposited in the hidden case of H-BETA due to very small metal particles in case of ion-exchange catalysts.

Table 5.2 Surface area of impregnated and ion-exchanged Pd-loaded catalysts

Sample	Pd loading (wt%)	S_{BET} (m^2/g)
H-BETA	-	629.4
Pd/H-BETA (Impregnation)	0.25	558.8
	0.50	597.4
	0.75	537.8
	1.00	567.6
	1.25	519.3
Pd/H-BETA (Ion-exchange)	0.25	610.7
	0.50	610.2
	1.0	611.5

The specific surface area of the impregnated catalysts was decreased when palladium was loaded on the zeolite support as shown in **Table 5.2**. It is possible that the palladium particle might cover the pores of catalyst, and the N_2 gas used in the BET method could not diffuse into the pore. Therefore, the determined surface area was decreased. The effect of palladium loading had no significant change with

the increasing amount of palladium loading.

For ion-exchanged catalysts, the amount of palladium loading did not affect the specific surface area, because the Pd ions were exchanged with protons in the zeolite structure, and the exchange created a very small metal particle clusters which did not cover or block the pore of catalyst. They might be located inside the pore or on the catalyst surface.

(b) Effect of Pd loading amount

The Pd/H-BETA was prepared by an impregnation method, and the amount of palladium loading was varied to 0.25, 0.50, 0.75, 1.00, and 1.25%wt. The final temperature of pyrolysis zone and catalytic zone are 500ºC and 350ºC, respectively. The influence of loading amount onto the H-BETA onto pyrolysis products are reported in this part.

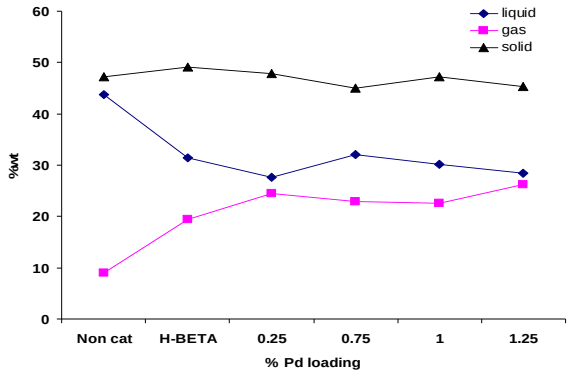

Figure 5.23 Effect of Pd loading amount on product distribution

The product yield of catalytic pyrolysis with the different metal contents is shown in **Figure 5.23**, which shows that the bi-functional catalyst suppresses the liquid yield with the increasing amount of palladium loading. Moreover, the reduction of liquid product is related to the increase of gas product yields. It means that the catalyst cracked the liquid product or high molecular weight hydrocarbons to produce more gas yields. When Pd loading is increased from 0.25 to 0.75 %wt on H-BETA zeolite, the liquid yield rises up. Due to a decrease of specific surface area of the palladium catalysts, it is possible that the increase of palladium

loading slightly reduced the strong acid density of catalyst due to metal particles which partially cover on the acid support (Lucus *et al.*, 2005). Therefore, the cracking activity of bi-functional catalyst was reduced. And then the yields of liquid product were slightly dropped with increasing metal loading up to 1.25%wt. This is because the metal might play greater important role in hydrogenation or ring opening reactions with higher loading percentages. After that the ring opening products might be cracked to lighter products or the gas products on the acid support (H-BETA) of catalyst. Thus, the liquid product is decreased with increasing gas yield.

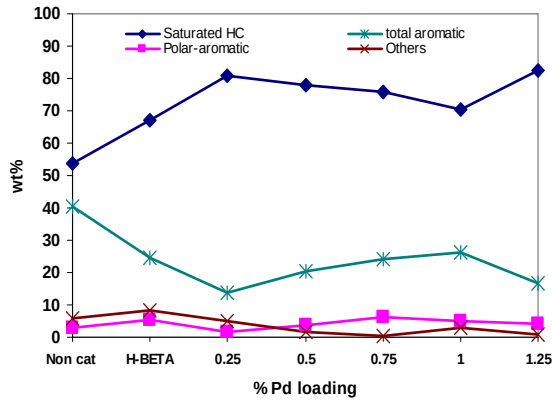

Figure 5.24 Effect of Pd loading amount on molecular compositions in oils

The saturated hydrocarbons and aromatic compounds in maltene fraction were analyzed by using liquid chromatography method. **Figure 5.24** shows the effect of palladium loading on chemical composition in the maltene fractions. The results show that Pd/H-BETA catalysts produce a high fraction of saturated hydrocarbons, and reduce the total aromatic hydrocarbons as compared to the non-catalytic pyrolysis Moreover, the yield of saturated hydrocarbons is slightly dropped with the increase of palladium loading from 0.25wt% to 1.0 wt%. In opposite way, the aromatics are increased with the amount of palladium loading on H-BETA zeolite. From these results, the aromatic compounds might be produced from saturated hydrocarbons. Another supported result is shown in **Figure 5.25**, which is the influence of palladium loading on asphaltene. The amount of asphaltene fraction

is decreased with the increasing percentage of metal loading. For these results, it is possible that the palladium can enhance the hydrogenation and cracking activity of aromatic hydrocarbons. Consequently, the high molecular-weight aromatic compounds (asphaltene) were broken into lower molecular-weight aromatic compounds or the lighter products.

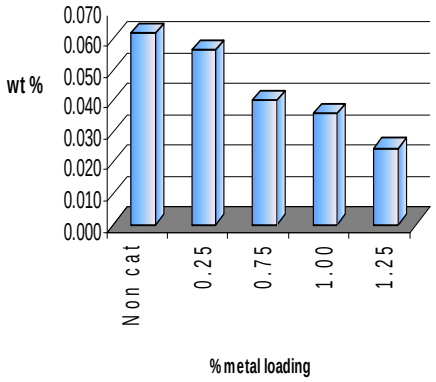

Figure 5.25 Effect of Pd loading amount on the amount of asphaltene in oils

The polar aromatics are the hydrocarbon compounds containing N, O or S, mainly associated with the aromatic structures. The polar aromatic might be formed on the bi-functional catalyst surface. The electron-deficient metal particles created by the strong acid site withdraw the electrons from the noble metal. This decreased the strength of bonding interaction between sulfur and metal particle due to lower acidity of catalyst. Thus, sulfur is split-over on metal sites, and might associate with aromatics to form polar aromatic compounds (Du *et al.*, 2005). In **Figure 5.24**, the polar aromatic hydrocarbons are slightly increased with a increase of palladium loading from 0.25 wt % to 1.0 wt %. This might be related to the metal particle sizes and the amount of metal particles which pertained to the sulfur adsorption site. However, at 1.25 wt % of Pd loading, the polar aromatic slightly decreases. It is possible that 1.25wt% Pd/H-BETA has a larger metal particle which contributed to lower spill-over activity than the other. This effect can increase the strength of sulfur-metal bonding. Thus, the polar aromatic formation was reduced. From above results, it can be concluded that the metal site and the acid site density

had an influence on the polar aromatic formation.

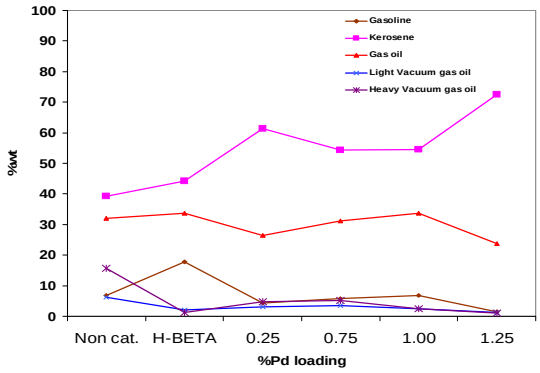

Figure 5.26 Effect of Pd loading amount on petroleum fractions

The quantities of petroleum in maltene fraction are shown in **Figure 5.26**. The bi-functional catalyst can increase the kerosene fractions significantly from 40wt % to 70 wt% because the cracking of heavy hydrocarbons and the pores of the catalyst would be selective with hydrocarbon molecules in kerosene fraction. Similar to Aguado et al., the study on the catalytic pyrolysis of several polyolefins in a batch reactor using different BETA zeolite, showed that the degradation of HDPE had a good selectivity to C5-C12 hydrocarbons (60-70%) (Aguado *et al.*, (2000). However, the gasoline fraction was decreased with the increasing amount of Pd loading. It is possible that the aromatics in gasoline fraction were hydrogenated by metal sites and further cracked to the gas product on the acid sites of bi-functional catalyst. The light and heavy vacuum gas oil fractions decreased with similar trend as gasoline fractions.

From the results of chemical composition and petroleum fraction in maltene, 0.25wt% is the optimum metal loading, because it produced the highest amount of saturated hydrocarbons and lowest aromatic compounds in maltene. It also produced the higher quantity of kerosene fraction.

(b) Effect of Pd loading technique

The properties of noble metal particles are strongly dependent on the preparation procedure such as method for loading metal ion into zeolite (Liu *et al.*, 2006). In this part, the ion-exchange method and incipient wetness impregnation

were investigated. The other parameters such as the catalytic temperature, final pyrolysis temperature, the amount of waste tire, and residence time were fixed at 350°C, 500°C, 10 g, and 25 min , respectively. The effect of palladium loading method on the quality of pyrolysis oil and the amount of petroleum fractions are reported and discussed in this part.

The yield of pyrolysis products obtained from ion-exchanged and impregnated catalysts were similar (**Figure 5.27**). The ion-exchanged catalyst can produce the gas products more than the impregnated catalyst. It is reasonable to assume that the large molecules of hydrocarbons need to be cracked on the external surface of catalyst first, and then the smaller cracked products diffuse inside the pore and react further on the active sites in the pore. From the surface area of both catalysts, the impregnated catalysts possibly have the metal particles covered the pore of zeolite, which might affect to the cracking reaction of hydrocarbons, because they could not diffuse to be cracked further in the pore. On the other hand, the pores of ion-exchanged catalysts are not blocked by metal particles. Therefore, the gas product is higher than that of impregnated catalysts. The solid, liquid, and solid were about 45, 30, and 25 wt%, respectively. It might be possible that the amount of pyrolysis products did not depend on the way to load the metal on the support.

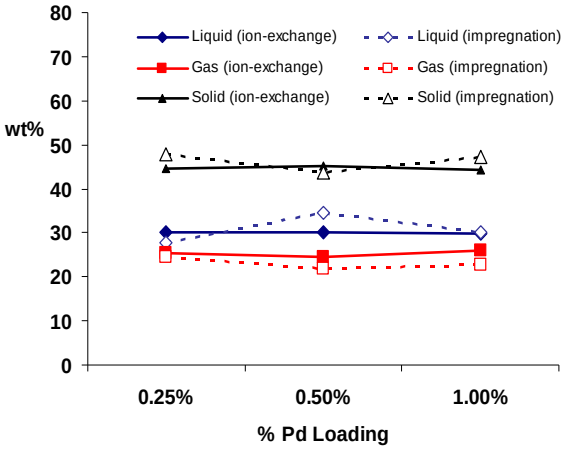

Figure 5.27 Effect of Pd loading technique on product distributions

Dr. Sirirat Jitkarnka
Associate Professor
The Petroleum and Petrochemical College
Chulalongkorn University

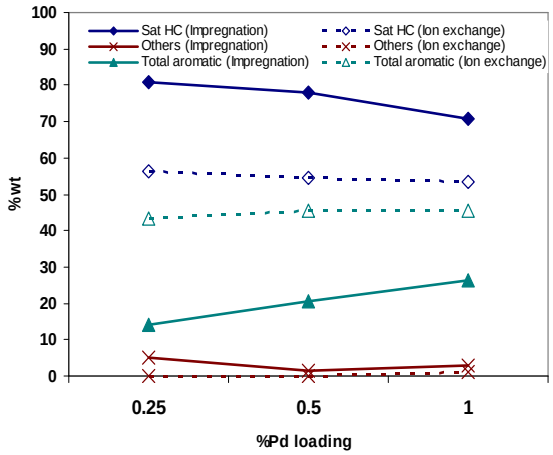

Figure 5.28 Effect of Pd loading technique on the yields of saturated and total aromatic HCs

The quality of pyrolysis was determined by the amount of saturated and aromatic hydrocarbons in the maltene fraction. The effects of metal loading method on quality of pyrolysis oil are shown in **Figure 5.28**. It can be observed that the ion-exchanged catalysts produce lower saturated hydrocarbons and much higher aromatic hydrocarbons than the impregnated catalysts. In fact, very fine metal particles on the ion-exchanged catalysts can well disperse almost inside micropores or mesopores or the main channel, and few amounts are deposited on the external surface of zeolite (**Figure 5.22**). Moreover, the main compositions in pyrolysis oil obtained from thermal degradation of tire such as aromatics (phenantrene, heptadiene, fluorine, naphthalene), alkanes and other hydrocarbons (Dai *et al.*, 2000), are large molecules. And, the large hydrocarbon molecules such as pyrene were hydrogenated mainly on the external surface and in mesopores (Tang *et al.*, 2007). It is possible that the thermal pyrolysis products can hardly diffuse inside the pore of catalyst. Therefore, the ion-exchanged catalysts have less activity on the hydrogenation and ring opening of aromatic compounds than the impregnated catalysts whose metal particles generally deposit on the external surface of zeolite. This might be concluded that the main reactions in reduction of aromatic hydrocarbon are be occurred on the external surface of the catalyst.

The amount of saturated and aromatic hydrocarbons (related to the quality of pyrolysis oil) does not much depend on the amount of metal loading on the ion-exchanged catalysts because these hydrocarbons were not changed with the increasing the palladium loading as shown in **Figure 5.28**.

The effect of loading method on the quantity of petroleum fractions is shown in **Figure 5.29**. It was found that the both catalysts prepared by ion-exchanged and incipient wetness impregnation had similar amount of the petroleum fractions. This indicated that the loading method had a little influence on the quantity of petroleum fractions. However, the oils obtained from impregnated catalysts are composed of the kerosene and the other heavy fractions larger than those obtained from the ion-exchanged catalysts. It might be occurred from the effect of where reactions are taking place. For example, for the impregnation catalysts, the reactions mainly occur at the external surface of mesopores. The secondary reactions of the intermediated products might be occurred, and higher molecular hydrocarbons are formed. On the other hand, the products produced in the ion-exchanged case are limited by the pore size.

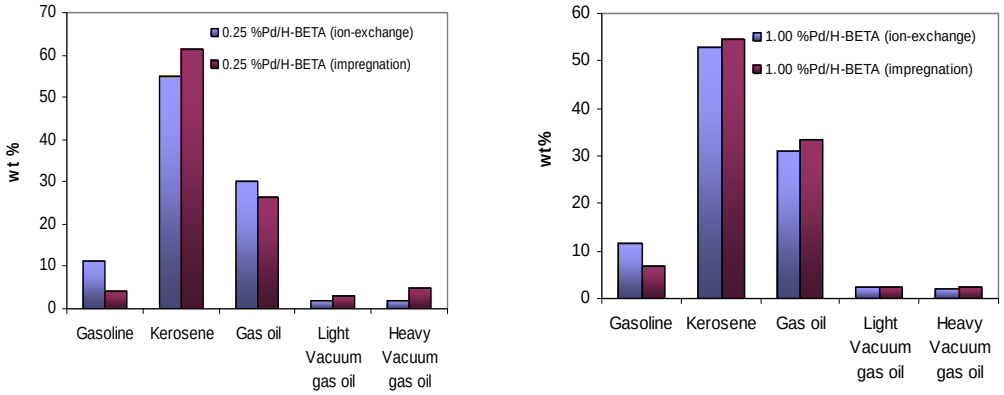

(a) **(b)**

Figure 5.29 Petroleum fractions in maltene obtained from catalytic pyrolysis using: (a) 0.25wt% Pd/H-BETA, and (b) 1.00wt% Pd/H-BETA.

From all of above results, it can be concluded that the chemical compositions in pyrolysis oil are strongly influenced by the metal loading method.

Dr. Sirirat Jitkarnka
Associate Professor
The Petroleum and Petrochemical College
Chulalongkorn University

Moreover, the impregnated catalysts can produce lower saturated hydrocarbon and aromatic contents in pyrolysis oil. Therefore, the impregnation is the suitable method to prepare the catalyst for upgrading oil obtained from tire pyrolysis using Pd/H-BETA catalysts.

In conclusion, the Pd/H-BETA catalyst can reduce aromatic hydrocarbons in the pyrolysis oil, and was selective to produce a large amount of kerosene fraction with higher saturated hydrocarbons. The amount of palladium loading affected to the chemical composition of pyrolysis oil. The saturated hydrocarbons were decreased, and the efficiency of aromatic reduction was also reduced with the increasing palladium loading amount. The optimum of palladium loading was 0.25 wt% on H-BETA zeolite. The influence of catalyst preparation was examined using the impregnation and ion-exchange methods. The impregnated catalysts had a higher activity in reduce-ing aromatic hydrocarbons than the ion-exchange catalysts. The location of metal particles played the important role in the aromatic reduction of Pd/H-BETA zeolite.

5.3 Ru-Loaded Catalysts

Ru is a rare transition metal in the platinum group used in many catalysis applications (both homo- and heterogeneous catalysis) such as the removal of H_2S in oil refineries, olefin metathesis, and a composition in fuel cells. Although it is rare and expensive, it is one of metals in the PMGs; therefore, it was first included in the study for the comparative reason. However, after the results have come out as shown below, it was found to be outstanding and distinctive among the other metals.

5.3.1 Product Yields

Even better than the Pt-loaded catalysts, Ru-loaded catalysts significantly improve the gas yield by 5% (from HBETA's), 15% (from HMOR's), and 7% (from HY's) in the expense of the decreases in oil yields in the similar proportions (see **Figure 5.30**). The highest gas yield is also obtained with using Ru/HMOR, which also gives the highest improvement of gas production among the

other catalysts mentioned earlier. Since the increase in gas yield for overall cracking indicates the higher activity in cracking of a catalyst; therefore, among the other Ru-loaded catalysts, Ru-HMOR has the highest cracking activity. It appears that among Pt, Pd, and Ru, Ru has the highest hydrogenolysis activity that helps the acid sites on the zeolites break C-C bonds. The compositions of the gas and the liquid are next considered for determining the selectivity of the catalysts.

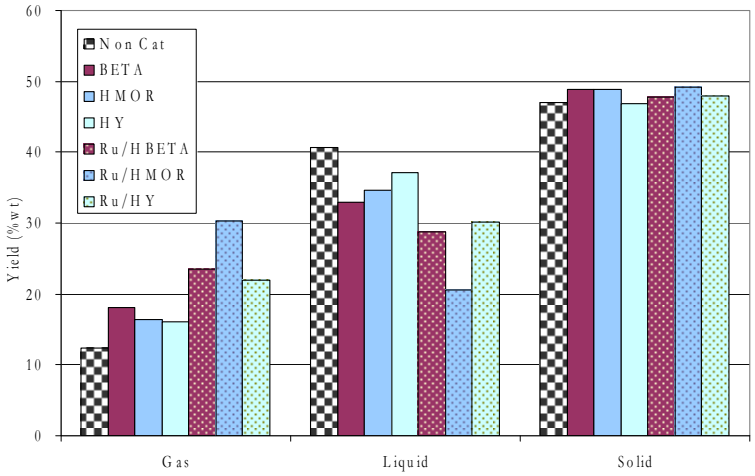

Figure 5.30 Product yields from using Ru-loaded catalysts

5.3.2 Gas Compositions

The compositions of gases obtained from Ru-loaded catalysts are slightly changed from those obtained from the corresponding zeolites (see **Figure 5.31**). Again, the gases obtained from Ru-catalysts are somewhat similar to those from Pt- and Pd-catalysts (see **Figures 5.2**, **5.15**, **and 5.31**). Some distinctive points are observed; especially at Ru/HMOR. Likewise, Ru seems to further increase methane, ethylene, ethane, and propylene from what is produced by the corresponding zeolites. Propane and mixed C4s did not much change. However, some still do not reach what is obtained from the non-catalytic case, except methane and ethane given by HMOR. C6s are also more concentrated in the gas products. Definitely, mixed C5s is the only one whose concentration decreases for all cases, implying that mixed C5s are converted to methane, ethylene, ethane, propylene, and C6s by Ru metal. Since Ru loading results in the increases in the gas yield (**Figure**

5.30) to even a higher extent than Pt loading does, the yield of each gas component can be higher improved. **Figure 5.32** shows the yields of gases obtained from using Ru-loaded catalysts. One may see that the yield of all gases significantly increase, especially in the Ru/HMOR case.

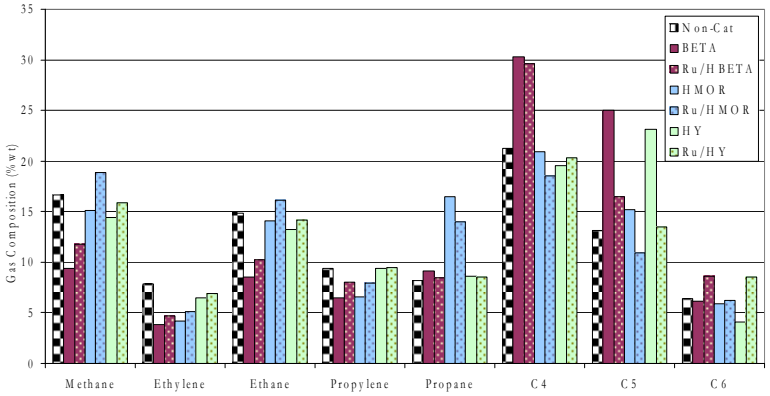

Figure 5.31 Gas compositions from using Ru-loaded catalysts**.**

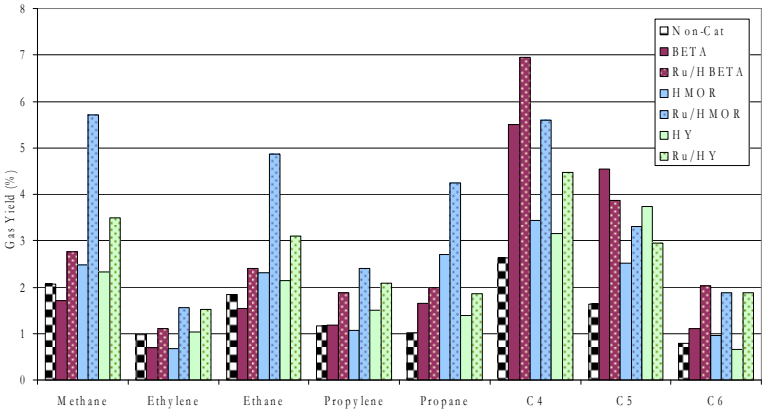

Figure 5.32 Yield of gases from using Ru-loaded catalysts**.**

5.3.3 Petroleum fractions

Simulated true boiling point curves of the maltenes obtained from using Ru-loaded catalysts shown in **Figure 5.33** indicate that with Ru loading the curves shift to the lower boiling points, meaning that all Ru catalysts, except Ru/HBETA, give lighter oil than all unloaded corresponding zeolites. **Figure 5.34**

reveals that the lightness of the oils is contributed from the increase in naphtha in the oil, except the Ru/HBETA case in which the lightness is resulted from the increase in kerosene fraction in the obtained oil. The fraction of naphtha in the maltenes is increased by almost 24% (for HMOR case), and 17% (for HY case). Ru/HMOR as the best catalyst among all Ru-loaded catalysts gives about 74% naphtha, 13% kerosene, 5% light gas oil, 4%heavy gas oil, and 4% long residue in the oil, which is even better than Pt/HMOR that is the best among all Pt-loaded catalysts. **Figure 5.34** also illustrates that the increase of naphtha fraction is resulted from the further cracking of the heavier fractions by Ru loading, except the Ru/HBETA case in which Ru loading can only help cracking the heavier oils to kerosene.

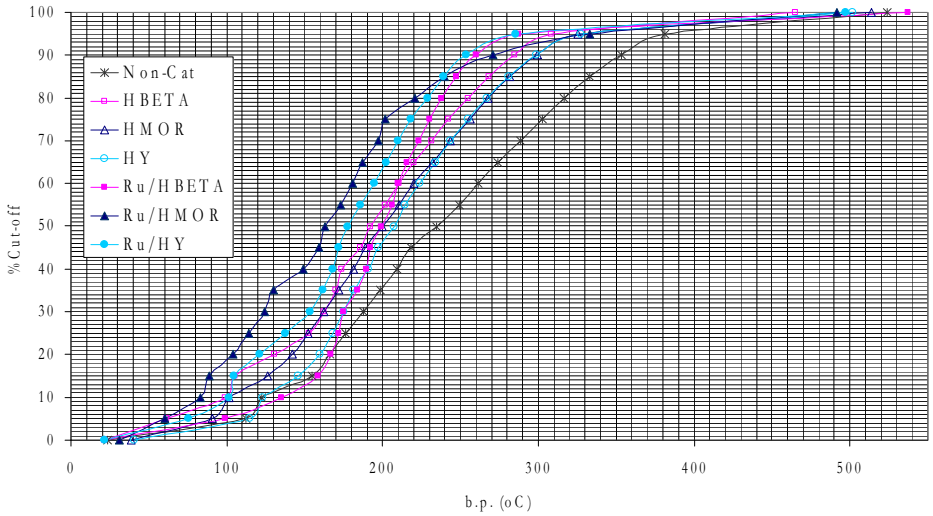

Figure 5.33 Simulated true boiling point curves of maltenes from using Ru-loaded catalysts.

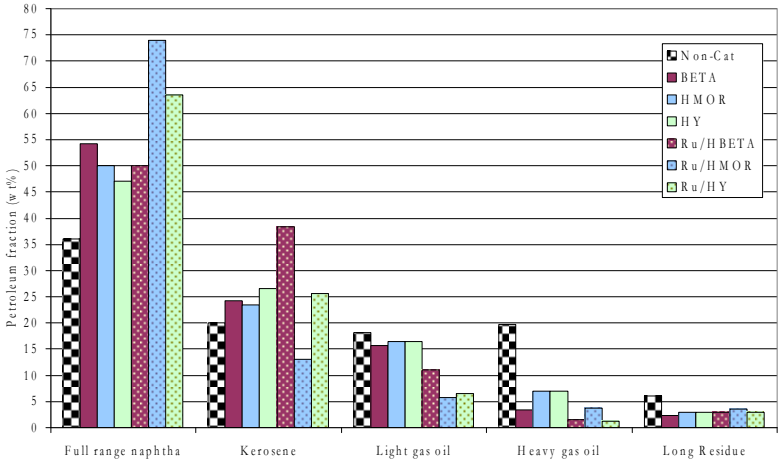

Figure 5.34 Petroleum fractions in maltenes from using Ru-loaded zeolites**.**

5.3.4 Molecular Composition in oils

As compared to the pure zeolites, all Ru-loaded catalyts decreases poly-aromatics with the significant increase in mono- and di-aromatics in the oil (**Figure 5.35**). It seems that Ru loading can convert poly-aromatics to mono- and di-aromatics. Among Ru-catalysts, Ru/HMOR gives some distinguished results as it also gives the distinguishable composition of gas product; that is, it increases saturated HCs whereas the other two Ru-catalysts decrease them, indicating that poly-aromatics are not only converted to mono- and di-aromatics, but also saturated HCs. Ru/HMOR is similar to Pt/HMOR that gives the oil with the highest amount of naphtha further increases the saturated HCs and mono-aromatics in association with the reduction in poly-aromatics. It means that both Ru/HMOR and Pt/HMOR not only give the highest quantity of naphtha, but also it produces naphtha with the highest quality. Similar to Pt-loaded catalysts, one thing all Ru-loaded catalysts have in common is that they increase mono-aromatic content in the tire-derived oil. It appears that Ru as a metal in PMGs can change poly-aromatic compounds to mono-aromatics and some saturated HCs, possibly via hydrogenolysis, hydrocracking, and ring-opening activity (Santikunaporn *et al.*, 2004; Gault, 1981; Arribas *et al.*, 2004), as Pt-loaded catalysts can.

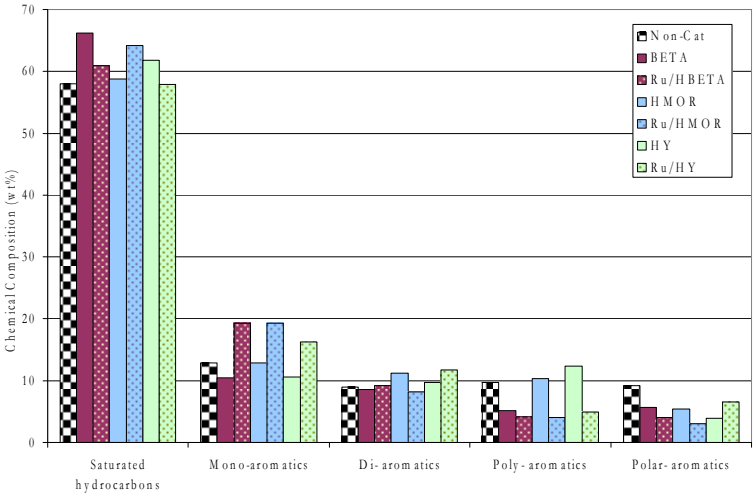

Figure 5.35 Molecular composition in maltenes obtained from using Ru-loaded catalysts**.**

5.3.5 Petrochemical Yields

As compared with the corresponding zeolites, all Ru-loaded catalysts improve the olefins productions (**Figure 5.36**). As mentioned earlier, Ru/HMOR is superior in the production of light olefins, so, it shows the highest production of light olefins in this figure. The other Ru-catalysts, except Ru/HMOR, also improve the yield of cooking gas, mixed C4s, and mono-aromatics. In summary, Ru/HMOR can improve the light olefins production in association with the lightest oil with the best quality. It also gives a high concentration of mono-aromatics in oil, but the yield of mono-aromatics is the lowest among all Ru-loaded catalysts as its oil production is the lowest due to the highest production of gaseous product.

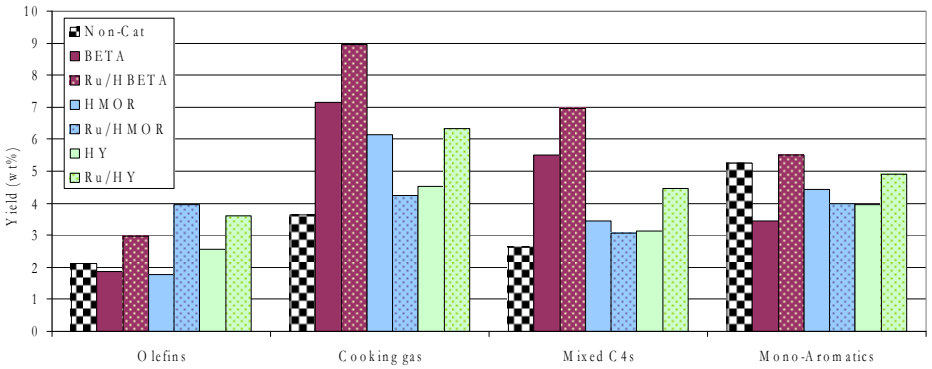

Figure 5.36 Yield of some petrochemicals obtained from using Ru-loaded catalysts**.**

5.3.6 Effect of Ru Loading Amount

Since it was discovered that Ru/HMOR was the most superior catalysts among the other Ru catalysts, the effects of Ru loading amount on the pyrolysis products were investigated. The various amounts of ruthenium were loaded on the HMOR zeolite. The results of all Ru-loaded catalysts, as bifunctional catalysts, with various percentages of Ru are discussed as follows.

(a) Crystal Structure of Catalysts

The XRD patterns of bifunctional catalysts are shown in **Figure 5.37**. It can be observed that every bifunctional catalysts present standard X-ray diffraction patterns according with the topology of mordenite and that the process of ruthenium metal impregnation, and calcinations did not affect the zeolitic structure. The signal for metallic ruthenium was found with a small intensity at $2\theta = 44°$. In addition, no evidence for the ruthenium oxide peak in the prepared catalyst is observed.

Dr. Sirirat Jitkarnka
Associate Professor
The Petroleum and Petrochemical College
Chulalongkorn University

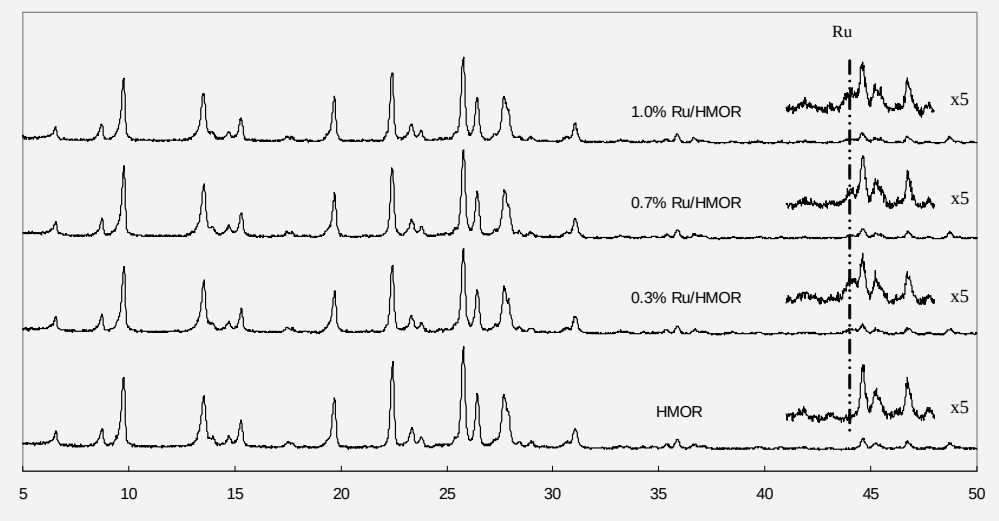

Figure 5.37 XRD patterns of HMOR and Ru/HMOR with different amounts of loading.

(b) Metal Particle Size

The incipient wetness impregnation method provides the metal particle size in the ranges of 5 to 20 nm as shown in The TEM images of Ru/HMOR catalysts in **Figure 5.38**. Moreover, most of the ruthenium particles are well dispersed and located at the outer surface of the zeolite. These results are similar to XRD patterns which small sizes of ruthenium metals are observed. At the high amount of metal loading, some of metal particles are accumulated on the surface of zeolite, and block the pore of the zeolite which might be resulted in the low cracking activity of the catalysts.

(c) Specific Surface Area

The surface area of catalysts was measured by using the BET method. The results are listed in **Table 5.3**. As the ruthenium metal amount increases, the surface area of catalyst is slightly decreased. Moreover, the surface area of catalyst is significantly decreased at 1.2% loading. This can confirm the results of partial pore blocking of zeolite by the agglomeration of ruthenium metal on the catalysts.

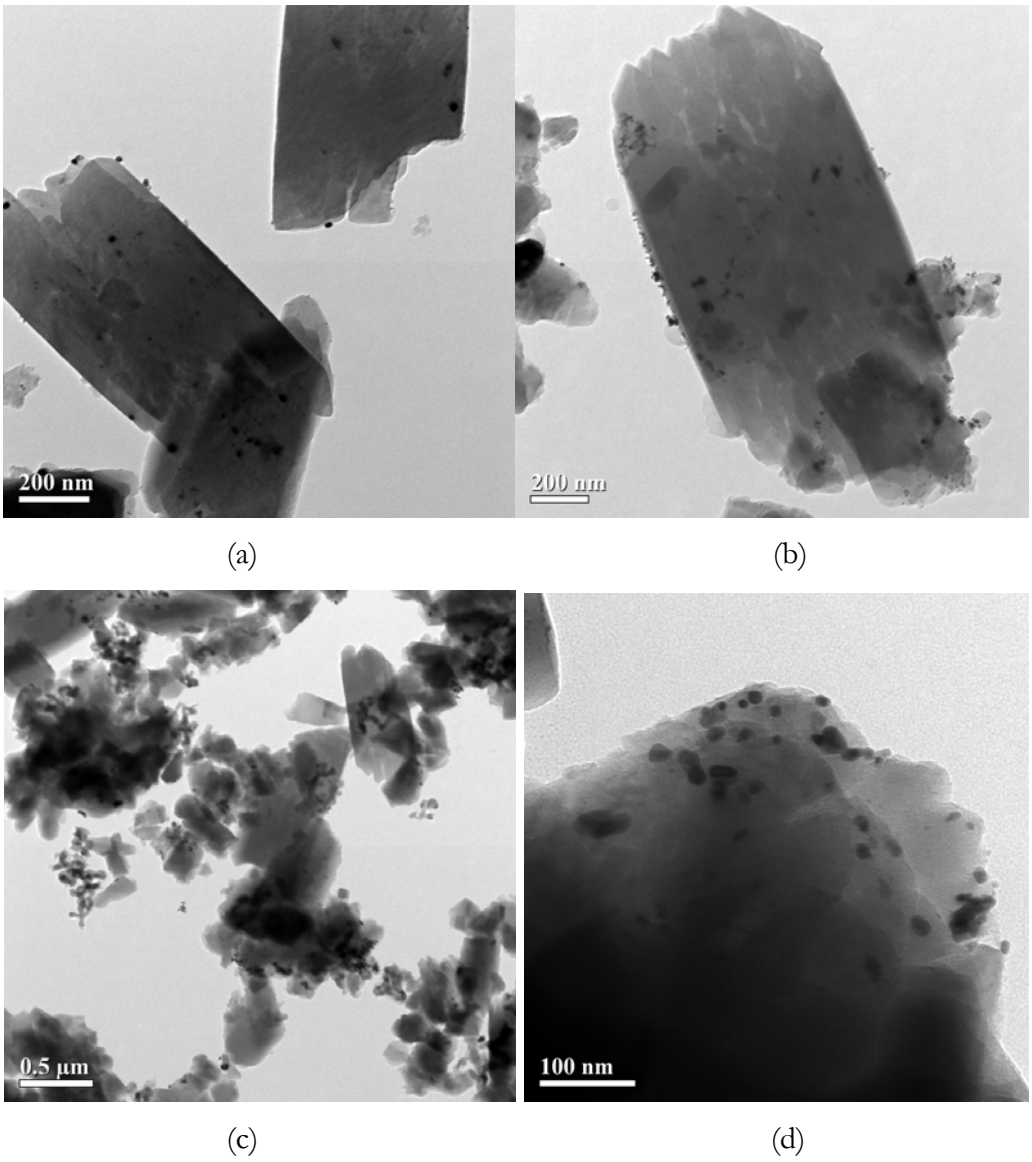

Figure 5.38 The TEM images of Ru/HMOR: (a) 0.3% Ru/HMOR, (b) 0.7% Ru/HMOR, (c) 1.0% Ru/HMOR, and (d) 1.2% Ru/HMOR.

Table 5.3 BET surface area of Ru-loaded catalysts with various percentages of Ru

Catalyst	**%Ru**	**Surface area (m^2/g)**

HMOR	-	462.1
	0.3	449.9
	0.7	437.2
	1	432.7
	1.2	369.9

(d) Product Distributions

Figure 5.39 shows the amount of gas and liquid produced by catalytic pyrolysis as compared to the non-catalytic pyrolysis. It can be investigated that the gas to liquid ratio of catalytic cases are about 2 times higher than non-catalytic case at the same conditions. This means that the amount of gas produced by the bifunctional catalysts is higher than pyrolysis without catalysts because the higher reaction activity of the catalyst cracked the larger molecules to lower product in the form of incondensable-gaseous products. Otherwise, ruthenium loaded on the zeolite can increase thermal cracking activity.

For the different amounts of metal loaded on the zeolite, it was found that the yield to gas increases with the increasing amount of ruthenium reaching the maximum at 0.7% loading, and then decreases at 1.0 and 1.2% loading. This can be suggested that too much loading amount suppresses the reaction activity resulting in the lower amount of gaseous product than low metal loading.

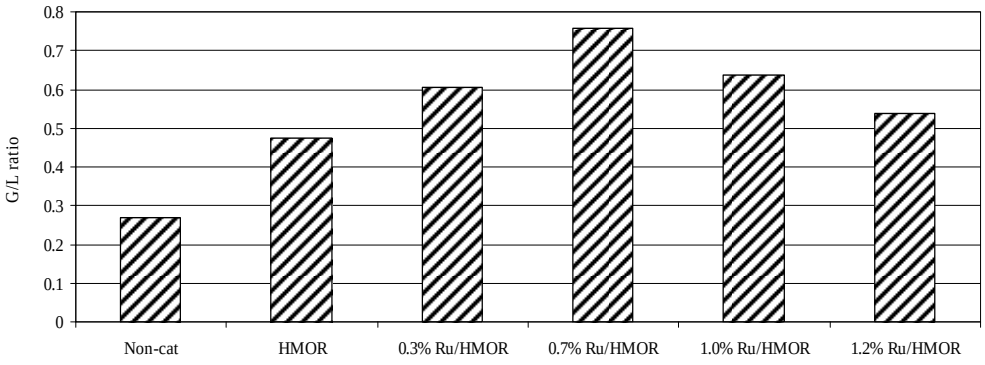

Figure 5.39 Gas to liquid ratio of Ru-loaded catalysts with various %Ru.

The solid yields for both catalytic and non-catalytic cases remain constant at about 47.5 %wt by average because the tire is completely cracked into pyrolysis products in the pyrolysis zone at the same condition and no further cracking of solid product is occurred at the catalytic zone.

(e) Gas Composition

The pyrolysis gas is comprised of methane, ethane, ethylene, propane, propylene, mixed-C_4, mixed-C_5, mixed-C_6, mixed-C_7, and mixed-C_8 hydrocarbons as shown in **Figure 5.40**. With the addition of catalysts, propane increases about 2 times higher than non-catalytic case when the amount of ruthenium increases to the maximum at 0.7% loading whereas ethylene and propylene decrease with increasing metal loading as compared with non-catalytic case. At 1.2% loading, the compositions of light hydrocarbon gases decrease, consequently increasing the heavy hydrocarbon gases such as, mixed-C_5 to mixed-C_8. This is possible that too high metal loading causes the decrease in cracking activity of catalyst, so the yields to lower molecular weight products are decreased at high metal loading.

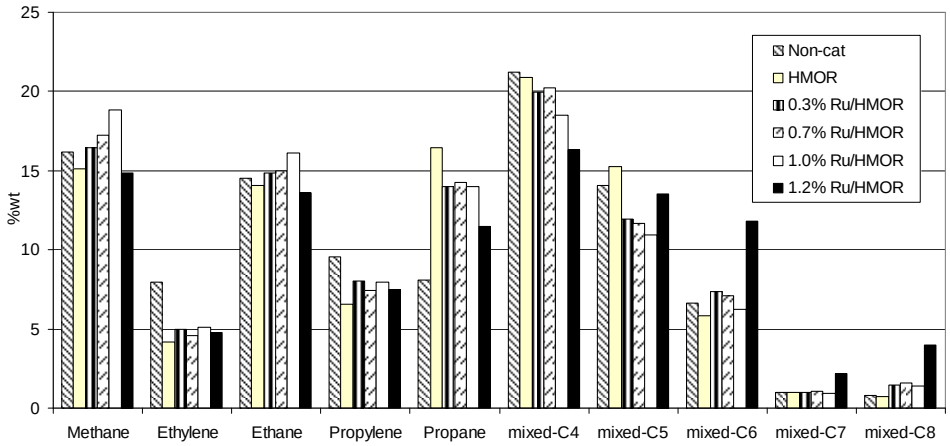

Figure 5.40 Gas compositions from using Ru-loaded catalysts with various %Ru.

Dr. Sirirat Jitkarnka
Associate Professor
The Petroleum and Petrochemical College
Chulalongkorn University

The percentage of metal loading influencing on the gas composition obtained from catalytic pyrolysis can be observed from **Figures 5.40 and 5.41.** The amount of metal loading has a greater influence on the gas distribution than on the yields to gas components. When using the zeolite alone, the selectivity to propane increases about twice as much as obtained from non-catalytic case. As ruthenium loading is increasing, the yield to propane decreases subsequently increasing the light olefins yields. The increase in the amounts of C_2-C_3 compounds and also to methane was reported by Shiraga *et al.* (2007), who studied on the partial oxidation of propane. They found that, in the presence of ruthenium metal, side reactions such as the dehydrogenation of propane, propane cracking, and coke formation could be occurred. These side reactions depending on reactant composition, temperature, residence time, and catalytic system become involved. They suggested that ruthenium metal catalyzed the cracking of propane resulting in high selectivity to methane and C_2-C_3 compounds. That is why the yields to methane, ethylene and propylene are increased when ruthenium metal is loaded.

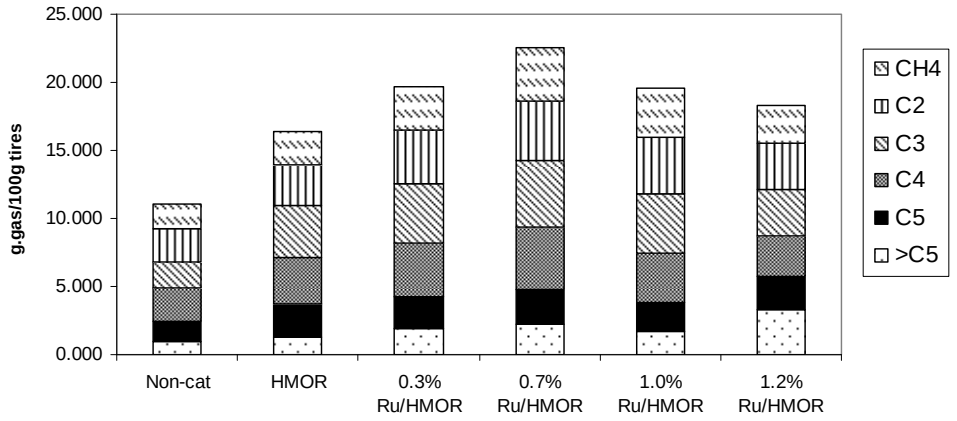

Figure 5.41 Yield of gas components from using Ru-loaded catalysts with various %Ru

Dr. Sirirat Jitkarnka
Associate Professor
The Petroleum and Petrochemical College
Chulalongkorn University

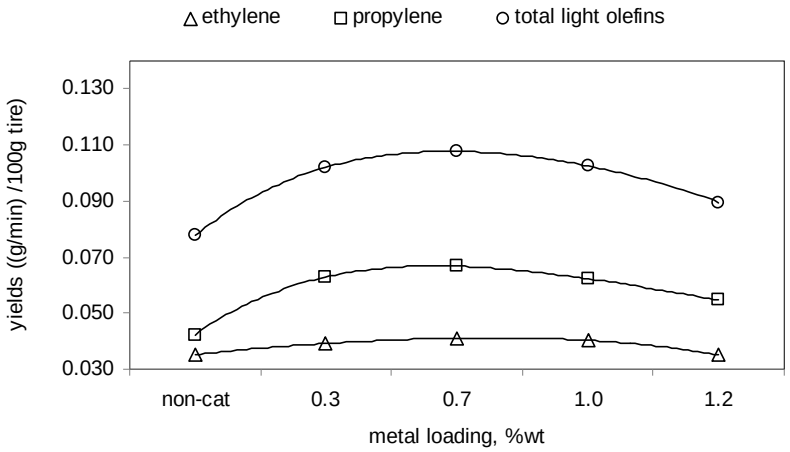

Figure 5.42 Yields of light olefins from using Ru-loaded catalysts with various %Ru

(f) Light Olefins Production

The variation of the yields to light olefins with the percentage of metal loading is shown in **Figure 5.42**. Propylene yield is higher than the yield of ethylene for all catalytic cases. The yield of propylene passes through the maxima at 0.7% loading and then decreases as the amount of metal loading increases. Ethylene yield varies slightly at the low percentages of loading, and then decreases at 1.2% metal loading. Similar results were found by Sha *et al.* (1999) and Basu and Kunzru (1992).

Li *et al.* (2005) also concluded that short residence time was suitable for high total light olefins yields, and it was hard to increase light olefins yields by increasing residence time. Also, to the effect of amount of metal loading, the yields of both components varied slightly as the metal loading increased.

(g) Liquid Analysis

The quantity and quality of petroleum fraction in pyrolysis oil with different weight percentages of metal loading on HMOR are shown in **Figures 5.43 and 5.44**. The boiling point distributions of hydrocarbons in oils were obtained from simulated distillation curves according to ASTM standard method (ASTM D2887,

1989). The main compositions of both catalytic and non-catalytic pyrolysis are gasoline, kerosene, gas oil, and vacuum gas oils.

As compared with the non-catalytic pyrolysis, the yields to heavy fractions such as light vacuum gas oil and heavy vacuum gas oil drastically decrease with using the catalysts as a result of the increases in the yields to gasoline and kerosene. This can be described that the catalytic cracking reaction occurred so that the chains of heavy molecules break down to lower molecular weight products. In addition, the oils products from both non-catalytic and catalytic pyrolysis are distributed in the ranges of C_5 to C_{50}. The carbon number distribution of maltenes obtained from catalytic pyrolysis shows the higher yields of gasoline and kerosene while the lower amount of heavy fractions are produced as shown in **Figure 5.43**. The catalytic pyrolysis can narrow the carbon distribution of pyrolysis oil as compared with non-catalytic pyrolysis. This means that Ru/MOR has very high cracking activity, which is also related to the high yields of gas products as compared with non-catalytic cases as demonstrated above. Similar to Hwang *et al.* (1998), they studied the catalytic degradation of polymer, and found that the carbon distribution of thermal degradation products was distributed in wider ranges than catalytic degradation. Ding *et al.* (1997) also found that the products obtained from the thermal degradation of polyethylene had the carbon number distribution of C_1-C_{27} and above, whereas the catalytic cracking of polyethylene gave the narrow range of distribution of C_1-C_{17}.

For the effects of amount of metal loading on the quantity of petroleum fractions, at a low amount of ruthenium loading, the yield to gas oil is decreased whereas the yields to gasoline and kerosene fractions are increased as shown in **Figure 5.43**. As the amount of metal loading increases, the yield to kerosene is decreased, consequently increasing in the gas oil yield. The other fractions are slightly changed with the amount of metal loading. Moreover, HMOR gave the highest yield of gasoline and the lowest yields of vacuum gas oils. This can be suggested that the zeolite alone has higher cracking activity than using as a bifunctional catalyst. On the other hand, the zeolite alone has higher acidity than zeolite loaded with noble metal. 0.7% loading shows the maximum yield to kerosene

fraction whereas this fraction is started to decrease at 1.0% loading and reaches the minimum at 1.2% loading. In contrary, the gas oil fraction passes through the minimum at 0.7% loading, and reaches maximum at 1.2% loading. This is possible that at high metal loading, partial pore blocking occurs, so that the acidity of external surface of catalyst is decreased resulting in the lower yield to kerosene fraction when compared with low loading or the zeolite alone. These can also be explained by the BET and TEM results shown so far.

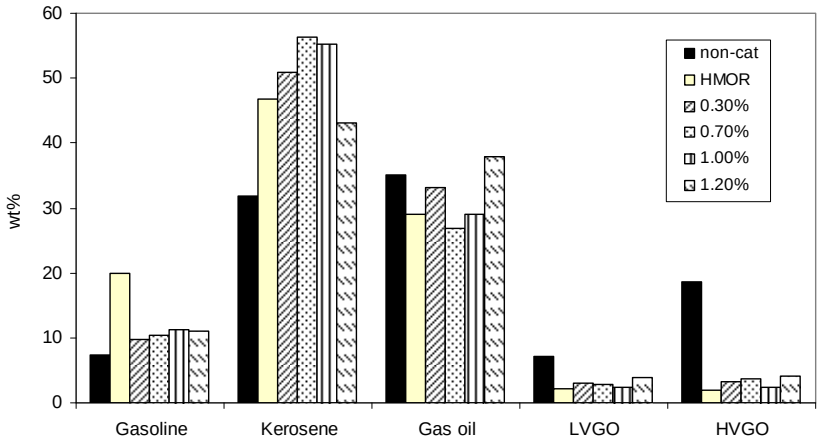

Figure 5.43 Petroleum fractions in maltenes from using Ru-loaded catalysts with various %Ru

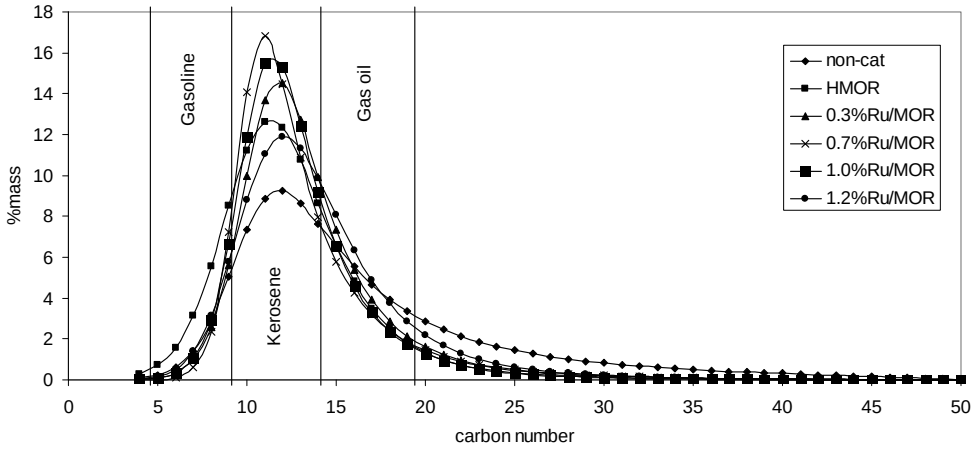

Figure 5.44 Carbon number distribution of maltenes from using Ru-loaded catalysts with various %Ru.

Dr. Sirirat Jitkarnka
Associate Professor
The Petroleum and Petrochemical College
Chulalongkorn University

The quality of pyrolysis oil can be roughly estimated by the amount of chemical compositions in the oil such as, saturated hydrocarbons, mono-aromatics, di-aromatics, poly-aromatics and polar-aromatics in the maltene fractions. The ratio of saturated hydrocarbons and total aromatic hydrocarbons are shown in **Figure 5.45**. It was found that these ratios are comparable for both cases. The increase in the amount of metal causes a slight increase in saturated hydrocarbons, which then decreases as the amount of metal increases. More details on the compositions in aromatic hydrocarbons were investigated and shown in **Figure 5.46**.

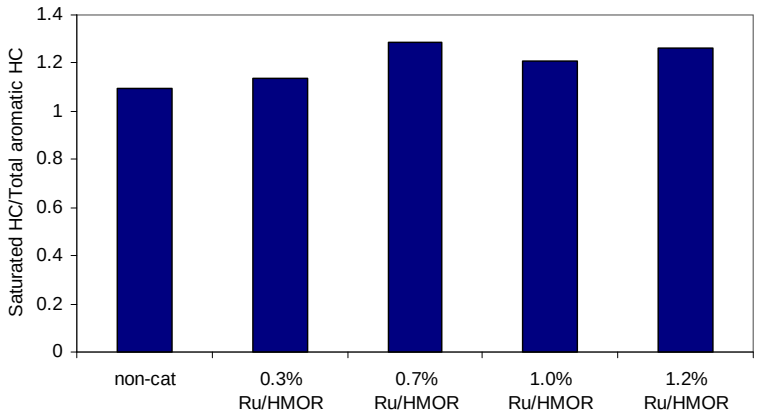

Figure 5.45 The ratio of saturated hydrocarbons to total aromatic hydrocarbons in maltene from using Ru-loaded catalysts with various %Ru.

Dr. Sirirat Jitkarnka
Associate Professor
The Petroleum and Petrochemical College
Chulalongkorn University

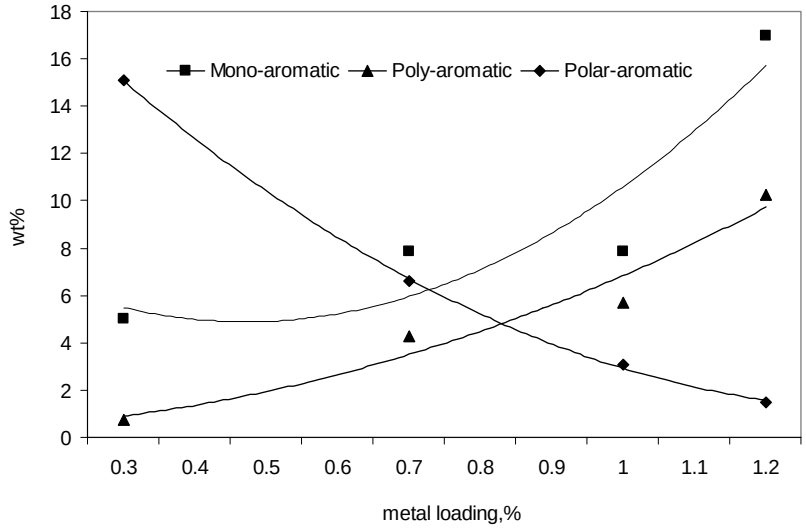

Figure 5.46 Chemical compositions in maltenes from using Ru-loaded catalysts with various %Ru

From **Figure 5.46**, the yield to polar aromatic hydrocarbon decreases whereas the yields to single ring aromatic and poly aromatic hydrocarbons are increased with the increasing of amount of ruthenium loading. Moreover, from the previous section, the yields to light olefins decreased with the increasing amount of metal loading. It is possible that the light olefins molecules combine to form mono-aromatic and poly-aromatic hydrocarbons via the aromatization reaction as reported in the previous section.

Asphaltene reduction in oil products is one criterion to determine which catalyst is better. It was measured from the weight of asphaltene retained on the filter paper after mixing the pyrolyzed oils with n-pentane. The asphaltene can be deposited on the pyrolysis equipment, which can cause problems to the whole process. Therefore, it is more economical to use bifunctional catalysts, which can reduce the amount of asphaltene in oil products.

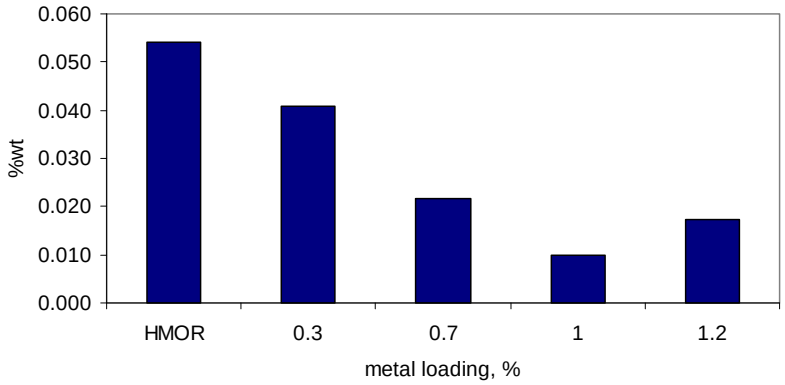

Figure 5.47 Asphaltene reduction from using Ru-loaded catalysts with various %Ru

Figure 5.47 shows the reduction of asphaltene with different amounts of ruthenium loaded on mordenite. It can be observed that the amount of asphaltene decreases with the increasing amount of metal loading as compared with non-catalytic case. In addition, 1.0% ruthenium loading exhibits the highest asphaltene reduction in the experiments.

From the results in this part, it is possible that mono-aromatic and poly-aromatic hydrocarbons are formed directly from the cracked molecules of polar-aromatic hydrocarbons. It is also possible that the light olefins molecules are combined to form single ring aromatics, and the single ring aromatics can also combine with another molecule to form bigger molecules such as, PAHs. On the other hand, the single ring and poly-aromatic hydrocarbons might be possibly formed directly from the cracked molecules of asphaltene, which decreased with the increase of metal loading (Douda *et al.,* 2004).

For the role of ruthenium metal on the pyrolysis product, the low amount of ruthenium loading on the zeolite causes the reaction favor on dehydrogenation reaction resulting in the low amount of paraffins molecule and the increase in light olefins. As the metal contents increases, the hydrogen transfer reaction is dominated resulting in the high amount of paraffins and aromatic hydrocarbons (Betancourt *et al.*, 1998). In addition, from the results that polar-aromatic hydrocarbons decrease as the amount of ruthenium metal increases, it

might be possible that ruthenium metal strongly reacts with sulphur compounds in polar-aromatic molecules resulting in the dissociation of sulphur molecule from polar compounds. Moreover, the ruthenium metal might prevent the formation of polar compounds as reported to have the highest activity for hydrodesulphurization process (Raje *et al.*, 1997).

Figure 5.48 shows the example reaction of the role of ruthenium on the dissociation of sulphur molecule in polar compounds. As the sulphur molecule was removed, the result molecule can be cracked or reacted further to form small aromatic or poly-aromatic compounds, respectively.

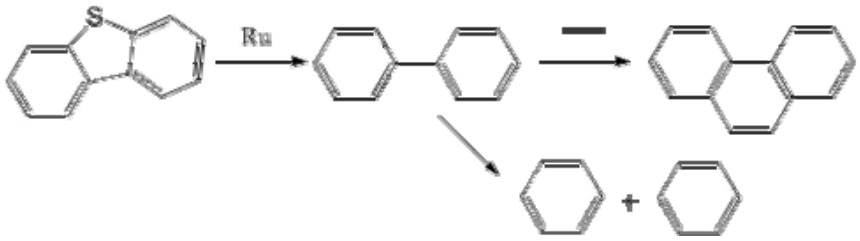

Figure 5.48 Example of mono-aromatic and poly-aromatic formation from polar-aromatic molecule (Ekinci *et al.*, 2002).

5.4 Ag-Loaded Catalysts

Ag-modified zeolites showed high activity in many catalytic processes. Oliveira *et al.* (2009) studied the adsorption desulfurization of model gasoline on NaY zeolites exchanged with Ag(I), Ni(II) and Zn(II). They found that the adsorption capacity for thiophene in the studied samples followed the order: AgY > NiY > ZnY > NaY. The AgY showed the highest adsorption capacity for thiophene (60 - 90% more than the starting material NaY). In the same year, Gong *et al.* studied the deep-desulfurization of gasoline using Ag/BETA. They found that the case of using BETA zeolite alone, it is very inefficient with only 20% sulfur removal, while Ag/BETA can remove 87% sulfur for model gasoline. For actual gasoline, the desulfurization capacity was reduced by about 30%, as compared to the model gasoline

Based on the quality, it is difficult for a tire-derived fuel to satisfy the practical requirement for uses in vehicles because the environment regulations request an ultra low content of sulfur in oils. Sulfur is an environmental concern because it leads directly to the emission of SO_x when combustion is occurred. Desulfurization is an important process in industry to remove sulfur from petroleum fuels. Due to the fuel quality, it is difficult to satisfy the practical requirement because the environment regulations request a low content of sulfur in oil products. Sulfur content in oil products is an environmental concern because it leads directly to the emission of SO_x when combustion is occurred. In tire manufacture after vulcanization process, sulfur is combined in rubber chains and linked together. Sulfur content in oil products might be present as mono-sulfide, di-sulfide, poly-sulfide, cyclic-sulfides and dependent sulfides. Generally, sulfur-containing compounds in oils obtained from waste tire pyrolysis are present in the forms of polar-aromatic compounds. The several types of polar-aromatics in pyrolytic oils are found in several works (Pakdel *et al.,* 2001; Rodriguez *et al.,* 2001; Laresgoiti *et al.,* 2004; Unapumnuk, 2008).

As mentioned above, Ag-modified zeolites were expected to reduce sulfur content in the pyrolytic oils; therefore, Ag was also selected to be one of the metals loaded on the zeolites in this study. Its influences on tire pyrolysis products as well as on the reduction of sulfur in oil were investigated, and the results are discussed below.

5.4.1 Product Yields

The product yield of catalytic pyrolysis using Ag-loaded catalysts is shown in **Figure 5.49**. It is found that all Ag-catalysts further increase the gas fraction, and consequently the liquid fraction decreases as compared to using the corresponding pure zeolites. It can be explained that the presence of Ag metal on zeolites promotes cracking reaction. The fragments evolved from the cracking of the rubber chains of waste tire are further cracked to even lighter products (condensable products to non-condensable products). It seems that non-noble metals like Ag can also help converting heavy molecules to lighter molecules. Ag/HBETA gives the

Dr. Sirirat Jitkarnka
Associate Professor
The Petroleum and Petrochemical College
Chulalongkorn University

highest gas yield among the other Ag catalysts, and it gives the gas yield even higher than Ru/HMOR.

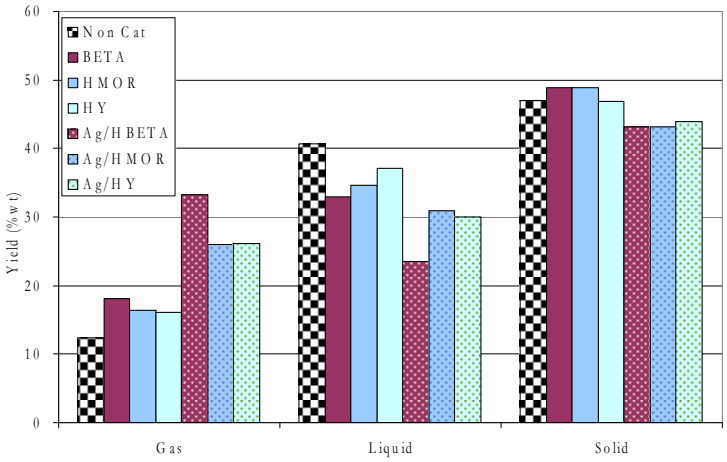

Figure 5.49 Product yields from using Ag-loaded catalysts.

5.4.2 Gas Compositions

Previously, it was found that the compositions of gases obtained from Pt- and Pd-loaded catalysts were slightly changed from those obtained from the corresponding zeolites (see **Figures 5.2 and 5.15**). Ag is the non-noble metal located right next to Pd in the periodical table, so it is interesting to see if Ag would affect the gas composition in the same way as Pd or Pt did. **Figure 5.50** shows the gas composition obtained from using Ag-loaded catalysts.

Like Pd, Pt, and Ru, Ag seems to further increase methane, ethylene, ethane, propylene, and propane from what is produced by the corresponding zeolites. The gas profiles of Ag-laoded catalysts tend to be similar to those of Ru-loaded catalysts. However, unlike the other metals, most gases exceed what is obtained from the non-catalytic case, especially alkanes such as methane, ethane, and propane. Unlike Pd, Ru, and Pt, C6s obtained from Ag are less concentrated in the gas products than those obtained from the pure zeolites. Moreover, the concentration of mixed- C4s significantly increases, leading to the sharp increases in the mixed C4s yield shown in **Figure 5.51**. The yields of all other light gases (up to C4s) are greatly improved when Ag-loaded catalysts are used, especially Ag/HBETA

due to its great increase in the gas yield.

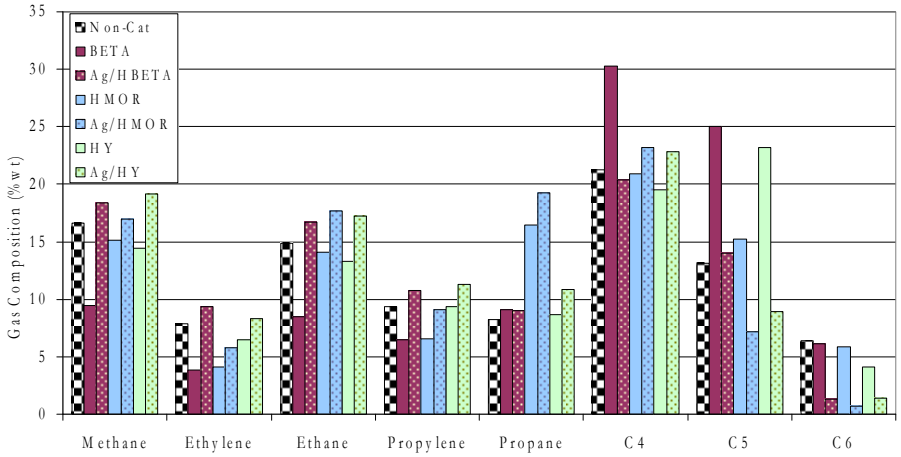

Figure 5.50 Gas compositions from using Ag-loaded catalysts.

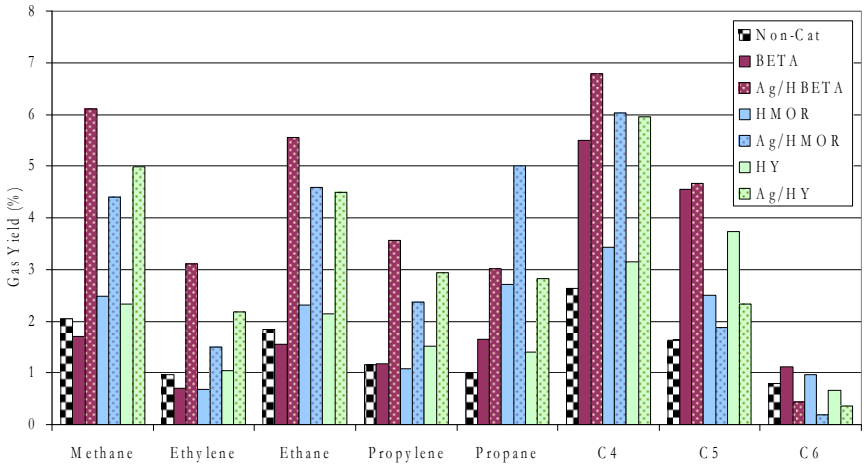

Figure 5.51 Yield of gases from using Ag-loaded catalysts.

5.4.3 Petroleum fractions

Unlike noble metals, all Ag catalysts seem to give heavier oils as indicated in **Figure 5.52** since all true boiling curves after Ag loading shift to the right side of those of pure zeolites. The petroleum fraction cuts shown in **Figure 5.53** give the details on how heavy the oils are produced. When compared to the pure zeolite cases, all Ag-loaded catalysts decrease the light petroleum fractions (full range naphtha) whereas the heavy petroleum fractions (kerosene, gas oil, and long

residue) are increased. However, the naphtha fractions of the Ag loading cases are still higher than that of the non-catalytic case.

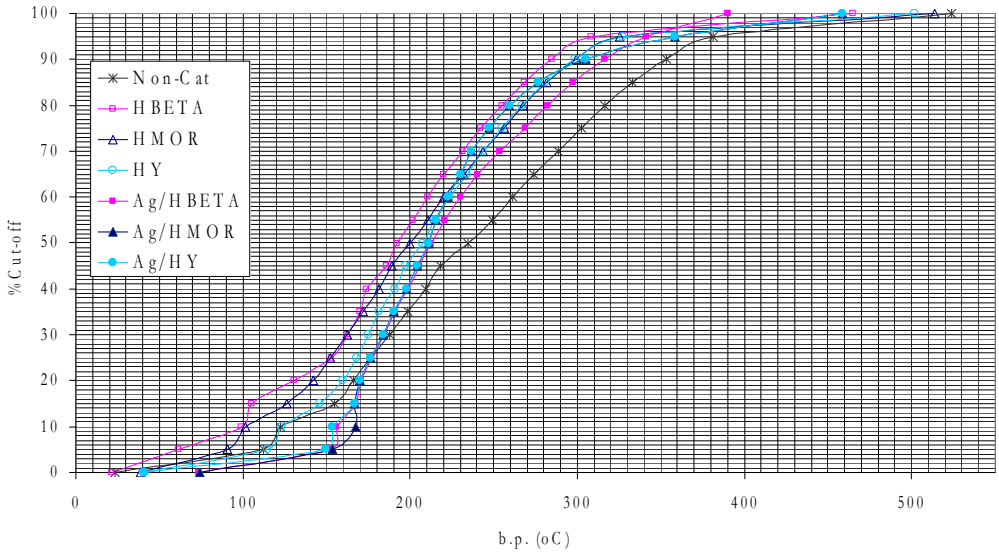

Figure 5.52 True boiling point curves from using Ag-loaded catalysts.

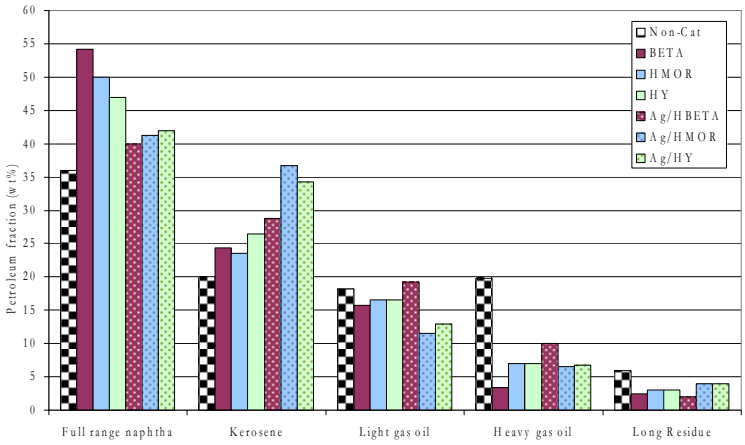

Figure 5.53 Petroleum fractions from using Ag-loaded catalysts.

The observation on which the kerosene fraction increases with the consequent decrease in naphtha fraction, in general, can be possibly explained using two scenarios; (a) the metal loaded suppresses the cracking activity of the parent zeolite, or (b) the metal loaded further cracks or converts the naphtha fraction to kerosene fraction. In the particular Ag cases, after Ag loading, it is found that heavy

gas oil and long residue are maintained, whereas the naphtha and light gas oil decrease with the increase in kerosene. It seems that the naphtha and light gas oil are converted to kerosene fraction. The first scenario; that is, Ag may suppress the cracking activity of the parent zeolites, is not possible in this particular case because from **Figure 5.49** it can be seen that Ag loading assists the parent zeolites in further cracking. As a result, the gas yield increases significantly. Thus, the second scenario may be the explanation. Naphtha fraction may be further cracked to the gas products whereas the increase in kerosene fraction is resulted from the cracking of light gas oil to kerosene. One may see that Ag/HBETA is the one that gives the highest gas yield, and it gives the lowest naphtha among the Ag-loaded catalysts, which supports the second scenario. Moreover, Ag/HBETA gives the highest light gas oil with the lowest kerosene, and these observations confirm the correlation between light gas oil and kerosene as mentioned in the second scenario.

5.4.4 Molecular Composition in oils

Unlike all noble metal-loaded catalysts, Ag-loaded catalysts do not give consensus results, which depend on the zeolite support (**see Figure 5.54**). For examples, Ag on HBETA lowers the saturated HCs; on the other hand, Ag on HMOR increases the saturated HCs whereas Ag on HY maintains them. The molecular composition in oil obtained from Ag catalysts strongly depends on the parent zeolite used as the support. It can be seen that Ag/HBETA gives the higher amount of gas and the poorer quantity and quality of oil, whereas Ag/HY gives the low amount of oil and the higher quantity and better quality of oil. With this observation, one can see that the acidity of the parent zeolites still plays important role on the products besides the Ag metal loaded.

Figure 5.55 shows that Ag/HBETA increases total aromatic compositions whereas saturated hydrocarbons are decreased. The opposite results are found with using Ag/HMOR whereas Ag/Y does not change the ratio. It is possibly caused from the strong interaction between the metal and the support of Ag/HBETA (see **Figure 5.56**), resulting in high hydrogenation and cracking activity. Furthermore, HBETA zeolite is a three-dimensional structure, and has high acid

strength, promoting large molecules to enter the zeolite pores, and then favoring pathways to form aromatics compounds. Additionally, 1%Ag/HMOR increases saturated hydrocarbons, and decreases total aromatics. It is possible that 1%Ag/HMOR has weaker interaction between the metal and the support, so it is easier for Ag on HMOR to react with H_2 (**Figure 5.56**); thus, it can better promote the hydrogenation reaction of unsaturated hydrocarbons to saturated hydrocarbons.

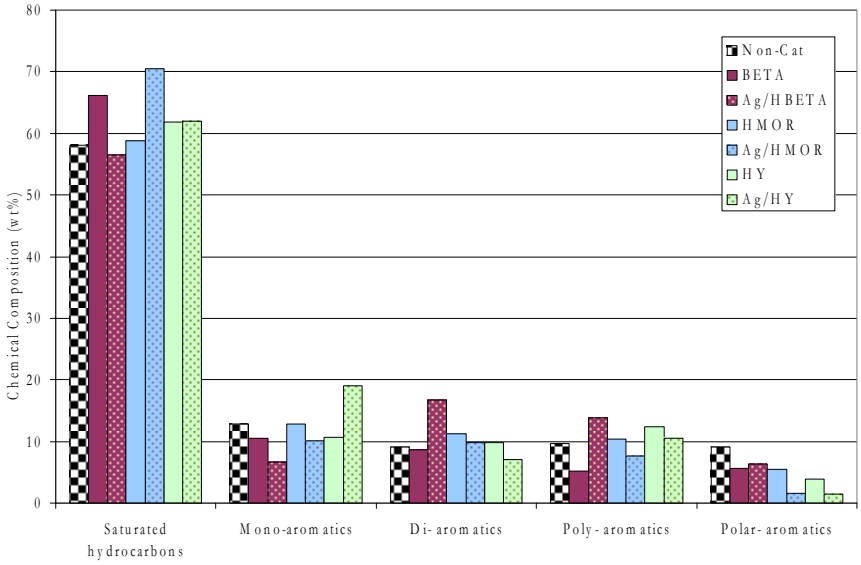

Figure 5.54 Molecular compositions in oils from using Ag-loaded catalysts.

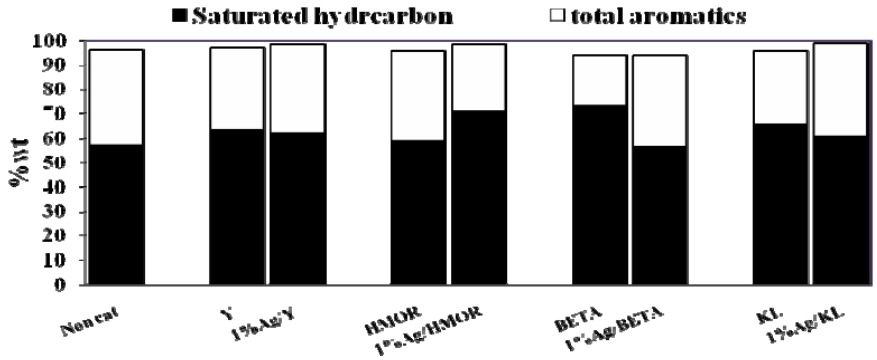

Figure 5.55 Molecular compositions in oils from using Ag-loaded catalysts.

Dr. Sirirat Jitkarnka
Associate Professor
The Petroleum and Petrochemical College
Chulalongkorn University

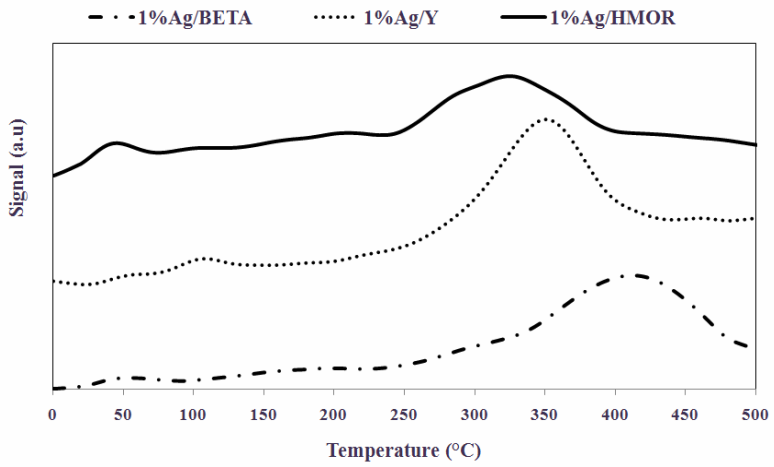

Figure 5.56 H_2-TPR profiles of Ag-loaded catalysts.

Table 5.4 shows the polar-aromatics content in the liquid products. In the cases of Ag loaded on zeolites, Ag/HMOR and Ag/HY tremendously decrease polar-aromatics concentration in maltene as compared to the unloaded zeolites. Ag/HBETA gives the highest amount of polar-aromatics and even higher than the non-catalytic case. It is possible that HBETA has high cracking ability to generate carbocations which create pathways to form aromatic compounds in maltenes. With the strong metal-support interaction, Ag/HBETA further enhances the pathways to polar-aromatic formation.

Table 5.4 Polar-aromatics in oils from using Ag-loaded catalysts

Sample	Polar-aromatic in oil (%)
Non catalyst	3.65
HY	3.21
HMOR	4.10
HBETA	5.95
Ag/HY	1.42
Ag/HMOR	1.54
Ag/HBETA	6.31

Table 5.5 Physical properties of different zeolites loaded with 1%Ag

Catalysts	Pore structure	Specific surface area (m^2/g)	Total pore volume (cm^3/g)	Spent catalysts	
				Sulfur (%)	Coke formation (g/g catalyst)
HBETA	3D	455.4	0.391	0.176	0.228
HMOR	1D	462.5	0.359	0.148	0.142
HY	3D	590.4	0.576	0.137	0.171
Ag/HBETA	3D	406.2	0.244	0.377	0.207
Ag/HMOR	1D	407.1	0.315	0.435	0.147
Ag/Y	3D	579.2	0.380	0.317	0.185

5.4.5 Petrochemical Yields

Ag loaded on all tested zeolites further increases light olefins, cooking gas, and mixed C4s productions as compared to the pure zeolite cases. Ag/HBETA increases about 3.3 times higher light olefins production than HBETA zeolite alone. Ag/HMOR catalyst shows the highest performance since it gives the highest amount of cooking gas (at an apparently-high amount of propane with a considerable amount of C4 hydrocarbons).

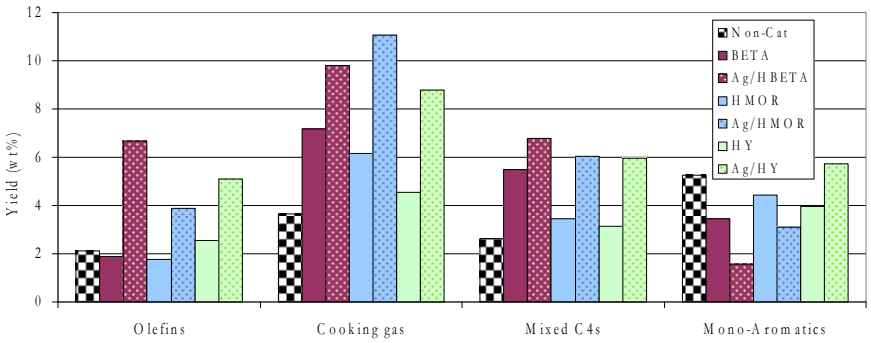

Figure 5.57 Yield of some petrochemicals from using Ag-loaded catalysts.

Moreover, all Ag-loaded catalysts produce a high yield of mixed C4s. Ag/HBETA, which gives the highest yield of olefins, also gives the highest yield of mixed C4s. Ag/Y is the only Ag-loaded catalyst that enhances the mono-aromatic production.

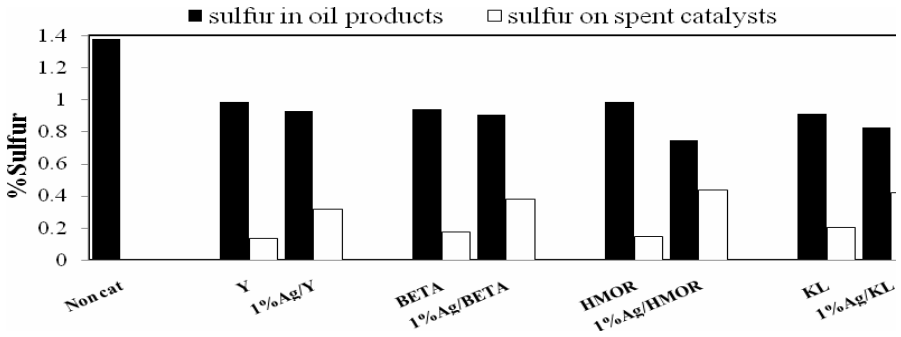

Figure 5.58 Sulfur in oil and on spent Ag-loaded catalysts.

5.4.6 Sulfur removal from oil

The sulfur content in the oil product is determined by CHNOS elemental analysis technique. The low amount of sulfur content in an oil product indicates that the oil has high quality. **Figure 5.58** shows the quantity of sulfur content in the oil products. The use of catalysts gives a lower quantity of sulfur in the oil than that obtained from the non-catalytic case. Pyrolytic oil obtained from using no catalyst contains about 1.38% of sulfur. The use of pure zeolites dramatically decreases the amount of sulfur in the oil products as compared to the non-catalytic case. All unloaded zeolites decrease sulfur concentration from 1.38% to 0.95% (average number from four zeolites). All Ag-loaded zeolites slightly decrease sulfur in the oil. Ag/HMOR catalyst shows a high performance in sulfur removal capacity. It gives the lowest concentration of sulfur in the oil product as compared to the other catalysts. It can decrease from 1.38 wt% to 0.75 wt% of sulfur as compared to the non-catalytic case. Compared with using pure HMOR, Ag/HMOR decreases the amount of sulfur in the oil product from 0.98 wt% to 0.75 wt%. The presence of Ag on HMOR zeolite helps promote desulfurization reaction resulting in the decrease of sulfur concentration in the oil product. It can be suggested that the Ag metal has

Dr. Sirirat Jitkarnka
Associate Professor
The Petroleum and Petrochemical College
Chulalongkorn University

hydrogenolysis activity since it enhances C-S-C bond breaking (Friend and Chen, 1997).

Figure 5.59 shows the carbon number distribution of polar-aromatics. Pyrolysis without a catalyst gives the carbon number distribution in the range of kerosene, which has the average carbon number around C14 (see **Table 5.6**). The use of catalysts differently shifts carbon number distribution from that of the non-catalytic case. For the unloaded catalysts, the zeolites which have 3D structure (Y and BETA) give the carbon number distribution in the range of gas oil (the average carbon number equal to C17 for HBETA and C18 for HY). Moreover, the zeolites with 1D structure (HMOR) give the carbon number distribution in the range of kerosene (the average carbon number equal to C15 for HMOR). It can be implied that pore size of zeolites has the influence on carbon number distribution of polar-aromatics. The one-dimensional structure of zeolites has ability of selectively produce a lighter fraction (such as kerosene fraction) than three-dimensional structure. The carbon number in the cases of HMOR and Y zeolites widely distributes in all fractions.

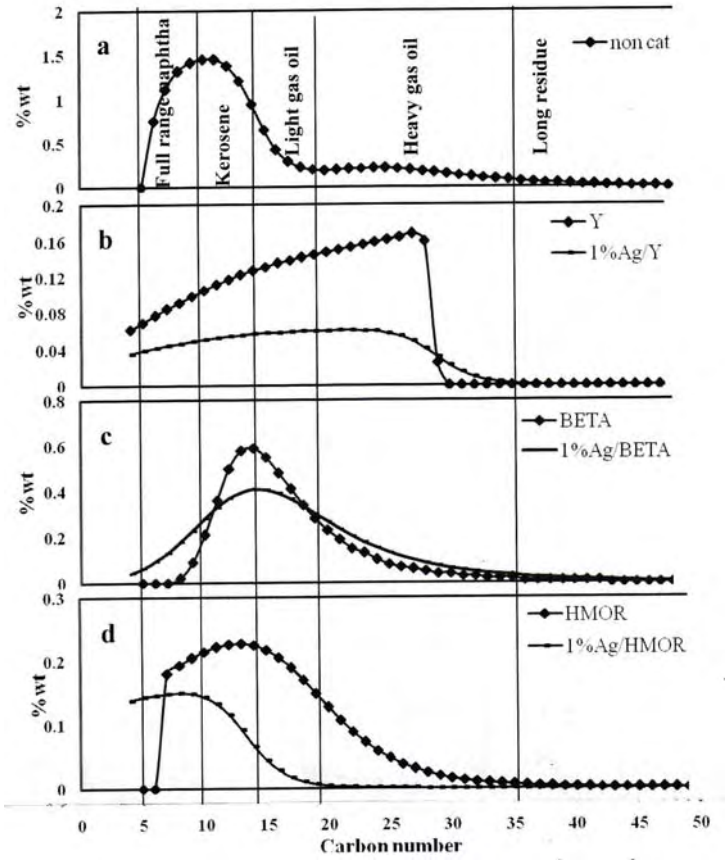

Figure 5.59 Carbon number distribution of polar-aromatics in oils from using Ag-loaded catalysts.

In the cases of Ag loading on zeolits, Ag loaded on HBETA and HY zeolites decreases the amount of polar-aromatics in the same range as using pure HBETA and HY zeolites, confirming that Ag loading help promote sulfur removal from the products. Ag/HMOR shifts the carbon distribution curve from heavy fraction (kerosene) to lighter fraction (naphtha).

Table 5.6 Average carbon number of polar-aromatics obtained from using different zeolites loaded with 1%Ag

Samples	Average Carbon number of polar aromatics	Example of sulfur compounds

Ag/HBETA	17.3	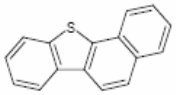
Ag/HMOR	9.1	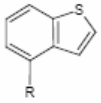
Ag/Y	17.5	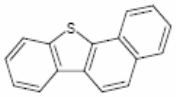

The average of carbon number obtained from using different zeolites loaded with 1%Ag is shown in **Table 5.6**. HBETA and HY zeolites give the average carbon numbers of polar-aromatics lower than that obtained from HMOR zeolite. It might be caused from pore structure since HBETA and HY zeolites have three-dimensional structure having large pore sizes. The large pore size of HBETA and HY zeolites allows large molecules of polar-aromatics formation. Ag/HBETA and Ag/HY give the same average of carbon numbers as the unloaded cases. Ag/HMOR gives the average carbon number lower than that obtained from using pure HMOR.

5.5 Rh-Loaded Catalysts

Rhodium, a noble metal, provides catalytic activity and selectivity in many reactions. It has been reported in several catalytic applications such as the hydrogenolytic ring opening of methylcyclopentane on Rh/Al_2O_3 (Teschner *et al.*, 2000 and 2002) and the hydrogenation of naphthalene (Jacquin *et al.*, 2003; Albertazzi *et al.*, 2003). It was observed that the selectivity to ring opening products and consequently towards fragmentation products ($<C_6$) was resulted from multiple C-C bond ruptures, and the hydrogenolytic cleavage of hydrocarbon C-C bonds was found as a main reaction in the conversion of C_6 alkanes and methyl cyclopentane while C_5-cyclization was a minor reaction. Jacquin *et al.* (2003) reported that at 300°C and atmospheric pressure, rhodium exhibited higher selectivity to hydrogenolysis

and/or ring-opening products than platinum-containing catalysts. In 2009, Barama *et al.* found the most active catalyst for the dry reforming of methane was the Rh/Al-PILC catalyst among Pd, Ni and Ce catalysts. It was suggested that rhodium catalyst can be used in many reactions as an effective catalyst; therefore, it is interesting to investigate how Rh can influence the tire cracking process.

5.5.1 Product Yields

All Rh-loaded catalysts can improve the gas yield by 2% (from HBETA's) to 13% (from HY's) and 2-3 times as much as that from the non-catalytic pyrolysis in the expense of the decreases in oil yields in the similar proportions (see **Figure 5.60**). Besides Ru and Ag, Rh metal appears to be one of the outstanding gas producing catalysts for tire pyrolysis. Similar to Pt/HY, the highest gas yield is obtained when Rh/HY is used as catalyst. In other words, Rh gives the highest improvement of gas yield when loaded on HY zeolite. The increase in gas yield for overall cracking indicates the higher activity in cracking of a catalyst. HY itself has the lowest cracking activity among all zeolites, but Rh/HY and Pt/HY have the highest cracking activity among those loaded on the other parent zeolites. This indicates the obvious contribution from Rh or the other metals.

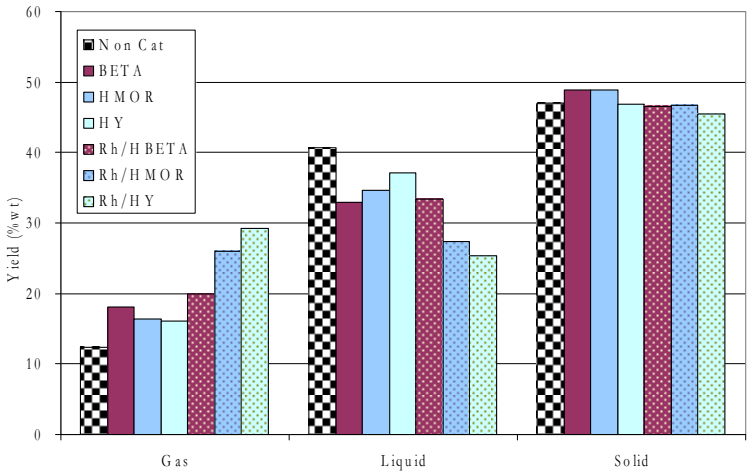

Figure 5.60 Product yields obtained from using Rh-loaded catalysts.

5.5.2 Gas Compositions

Like all metals mentioned earlier, Rh seems to further increase methane, ethylene, ethane, propylene, and propane from what is produced by the corresponding zeolites. The gas profiles of Rh-loaded catalysts tend to be similar to those of Ru- and Ag-loaded catalysts. Two distinguished observations from using Rh-loaded catalysts are that they greatly increase methane and propylene contents and yields (see **Figures 5.61 and 5.62**). However, unlike the other metals, most gases found increasing such as methane and propylene exceed what is obtained from the non-catalytic case. Unlike Pd, Ru, and Pt, C6 HCs obtained from Rh are less concentrated in the gas products than those obtained from the pure zeolites, which is in this case similar to Ag. Moreover, the concentration of mixed- C4s significantly increases, leading to the sharp increases in the mixed C4s yield shown in **Figure 5.62**, which is also the same as of Ag cases. The yields of all other light gases (up to C4s) are greatly improved when Rh-loaded catalysts are used, which is also found similar to Ag-loaded catalysts. Moreover, Rh/HY appears to the most outstanding one among the Rh-loaded catalysts.

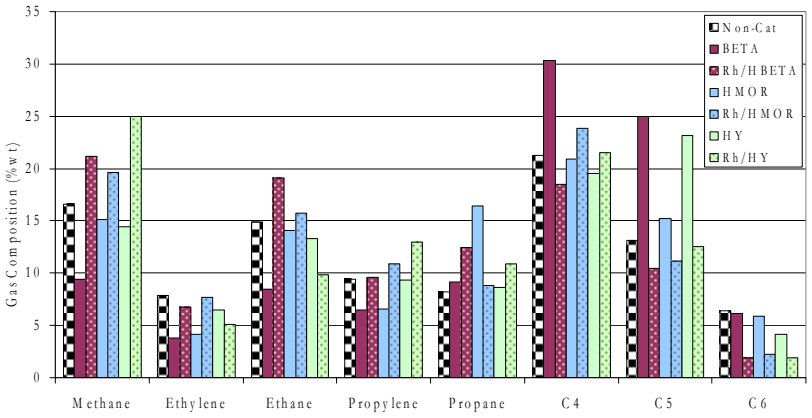

Figure 5.61 Gas compositions obtained from using Rh-loaded catalysts.

Dr. Sirirat Jitkarnka
Associate Professor
The Petroleum and Petrochemical College
Chulalongkorn University

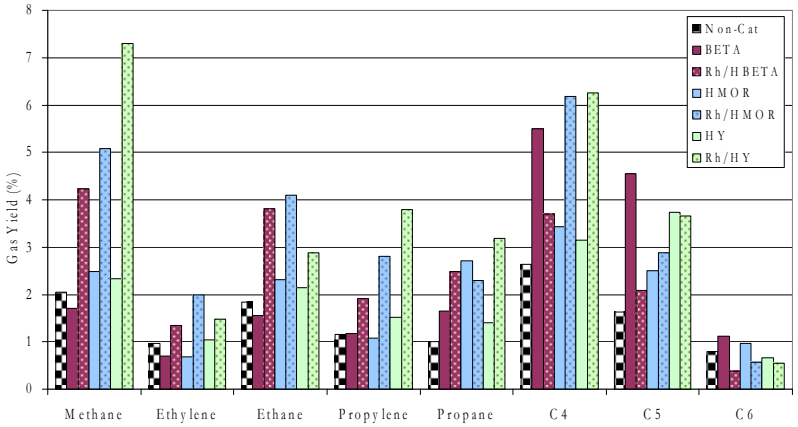

Figure 5.62 Yield of gases obtained from using Rh-loaded catalysts.

5.5.3 Petroleum fractions

Similar to Ag catalysts, all Rh catalysts, except Rh/HY, seem to give heavier oils as indicated in **Figure 5.63** since their true boiling curves after Rh loading shift to the right side of those of pure zeolites. Only the one of Rh/HY shifts to the left, indicating the lighter oil than that of HY.

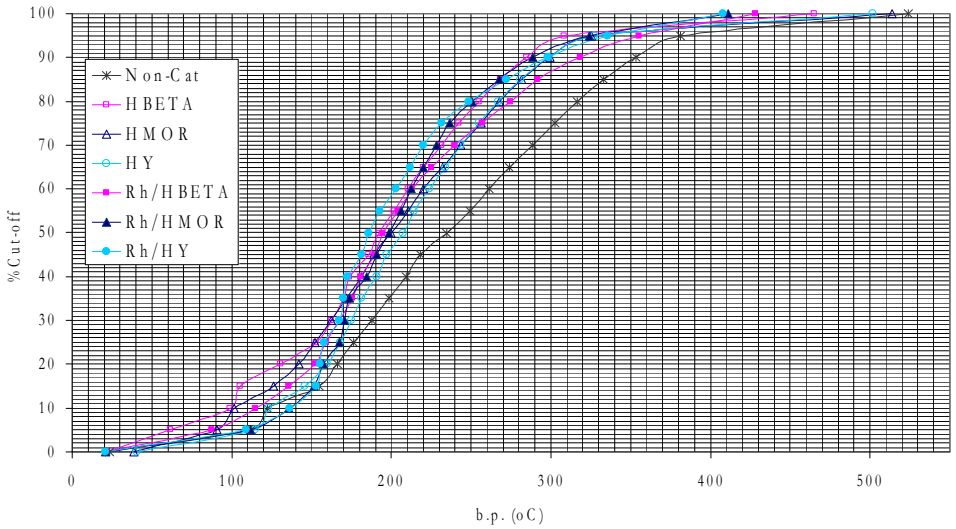

Figure 5.63 True boiling point curves obtained from using Rh-loaded catalysts.

Dr. Sirirat Jitkarnka
Associate Professor
The Petroleum and Petrochemical College
Chulalongkorn University

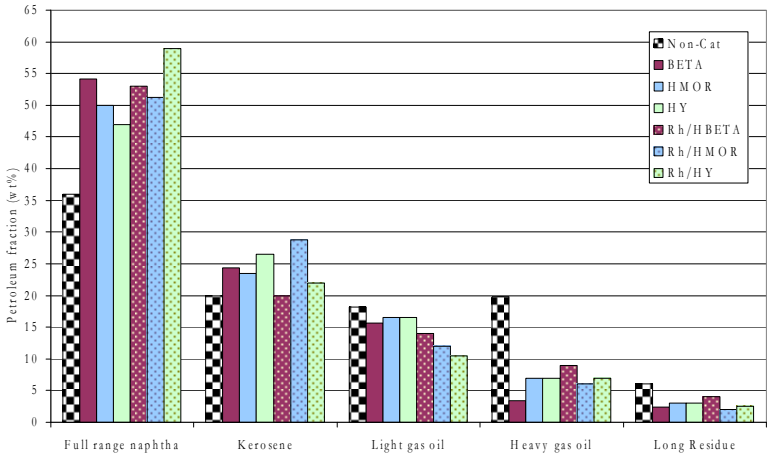

Figure 5.64 Petroleum fractions obtained from using Rh-loaded catalysts.

The petroleum fraction cuts shown in **Figure 5.64** confirm that Rh/HBETA decreases the light petroleum fractions (full range naphtha, kerosene, and light gas oil) whereas the heavy petroleum fractions (heavy gas oil and long residue) are increased. Rh/HMOR decreases naphtha, but increases kerosene whereas the heavier fractions are decreased. Rh/HY gives the most distinctive results; that is, it is the only one among all Rh-loaded catalysts that enhances the naphtha production as well as the gas production as mentioned earlier in this part. Like Ag catalysts, Rh catalysts behave differently, depending on which zeolite is used as the support.

5.5.4 Molecular Composition in oils

Similar to Ag-loaded catalysts, Rh-loaded catalysts do not give consensus results, which depend on the zeolite support (**see Figure 5.65**). For examples, Rh on HBETA lowers the saturated HCs; on the other hand, Ag on HMOR and Ag on HY increase them. The molecular composition in oil obtained from Rh catalysts strongly depends on the parent zeolite used as the support. It appears that Rh/HMOR and Rh/HY give the similar distribution of molecular composition, but Rh/HY gives different pattern. One distinguished outcome that all Rh-loaded catalysts have in common is that they improved mono-aromatic content greatly to almost 20% in oils, and this distinctive outcome has not been found so far

with using other metals loaded on the same parent zeolites.

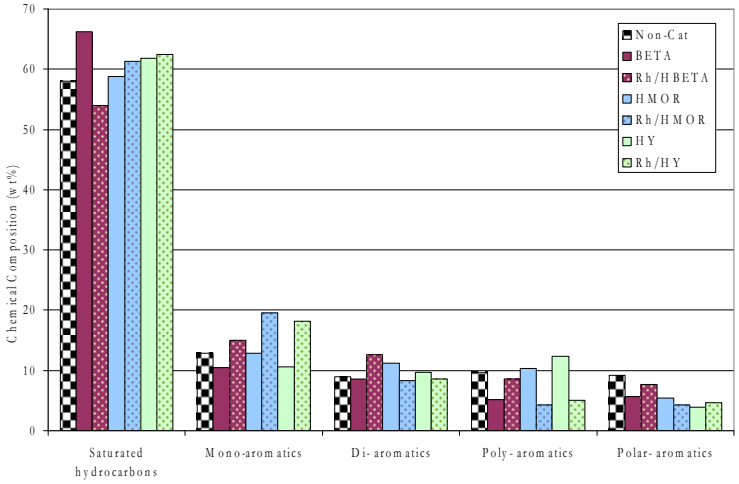

Figure 5.65 Molecular compositions in oils obtained from using Rh-loaded catalysts.

5.5.5 Petrochemical Yields

Rh loaded on all tested zeolites further increases light olefins and mono-aromatic productions as compared to the pure zeolite cases. Rh/HY increases about twice as much light olefins production as HY zeolite alone can, and it gives the highest olefins among all Rh-loaded catalysts. It also appears that Rh/HMOR and Rh/HY give the similar pattern of petroleum yields, but Rh/HY gives different fashion, like in the molecular composition case.

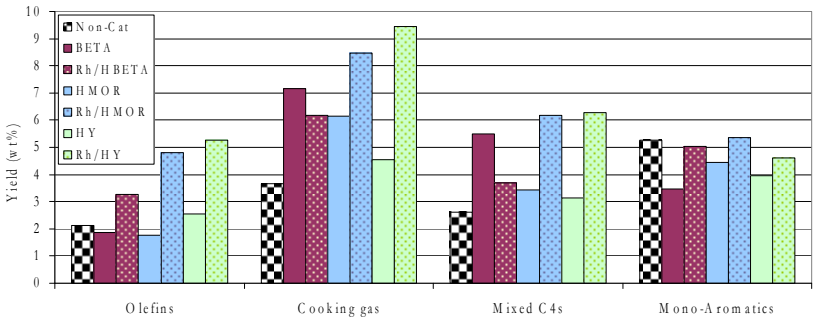

Figure 5.66 Petroleum fractions obtained from using Rh-loaded catalysts.

5.6 Re-Loaded Catalysts

Rhenium-containing catalysts are used for hydrocarbon transition to upgrade product yields; for examples, ethane aromatization (Krogh *et al.*, 2003) with low coking, and the hydrogenation of cyclohexene: CHE (Aboul-Gheil *et al.* 2005). Re metal is usually used with Pt as a bimetallic catalyst such as in the hydroconversions of CHE, which the bimetallic combination of Pd, Ir or Re with platinum supported on HZSM-5 catalyst found to enhance the hydrogenation activity and reduced the temperature of hydrogenation of cyclohexene to cyclohexane compared with only rhenium supported on HZSM-5 (Aboul-Gheit *et al.*, 2005). Moreover, PtRe/HZSM-5 produced the lowest amounts of benzene but the highest toluene and xylenes amounts.

5.6.1 Product Yields

All Re-loaded catalysts can improve the gas yield by 2% (from HMOR's) to 10% (from HY's) in the expense of the decreases in oil yields in the similar proportions (see **Figure 5.67**). Re/HMOR only slightly increases the gas production, indicating that loading Re onto HMOR does not help HMOR to further crack heavy HCs to lighter HCs. Re/HBETA and Re/HY significantly increase the gas production in the similar extent as the other metals can. Moreover, Re seems to be the least active catalyst for cracking in general regardless of the type of support.

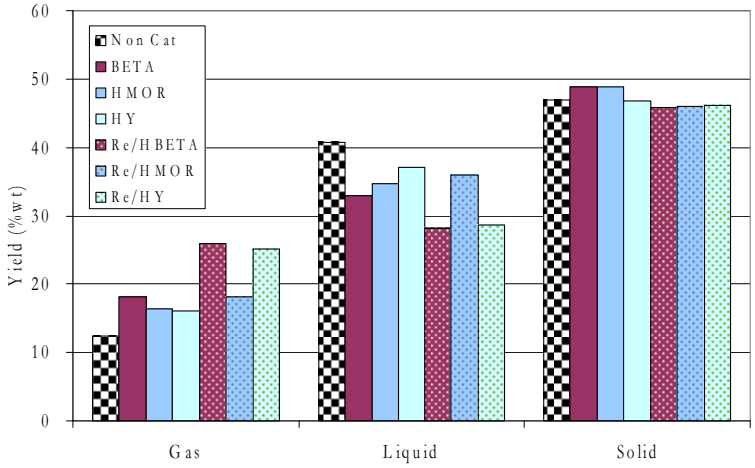

Figure 5.67 Product yields from using Re-loaded catalysts.

Dr. Sirirat Jitkarnka
Associate Professor
The Petroleum and Petrochemical College
Chulalongkorn University

5.6.2 Gas Compositions

Like all metals mentioned earlier, Re seems to further increase methane, ethylene, ethane, propylene, and propane from what is produced by the corresponding zeolites. The gas profiles of Re-loaded catalysts tend to be similar to those of Ru-, Ag- and Rh-loaded catalysts. Similar to Rh catalysts, two distinguished observations from using Re-loaded catalysts are that they significantly increase methane and propylene contents and yields (see **Figures 5.68 and 5.69**) but not as much as those of Rh-loaded catalysts. Also, as Re and Rh catalysts are distinguished from the other metals, most gases found increasing such as methane and propylene exceed what is obtained from the non-catalytic case.

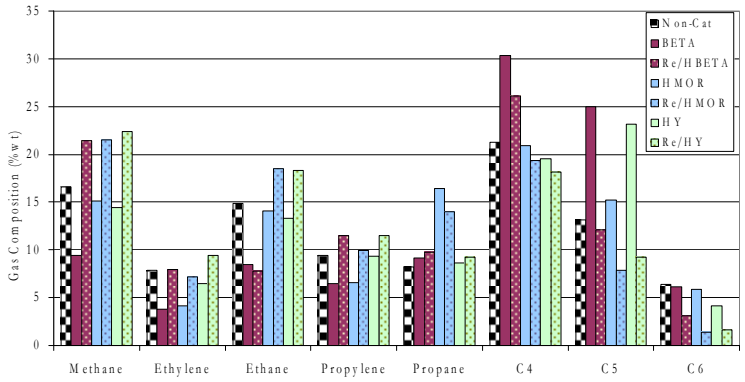

Figure 5.68 Gas compositions from using Re-loaded catalysts.

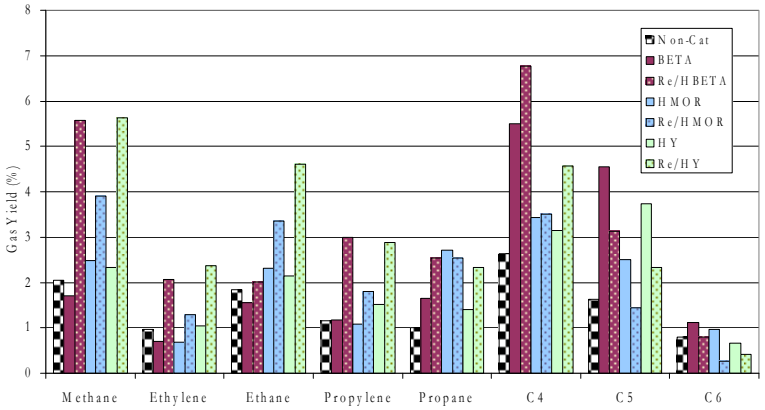

Figure 5.69 Yield of gases from using Re-loaded catalysts.

Dr. Sirirat Jitkarnka
Associate Professor
The Petroleum and Petrochemical College
Chulalongkorn University

Unlike Pd, Ru, and Pt, C6 HCs obtained from Re (so are Rh's and Ag's) are less concentrated in the gas products than those obtained from the pure zeolites. However, the concentration of mixed- C4s decreases, but still results in the sharp increases in the mixed C4s yield shown in **Figure 5.69** because of the high yield of gas product, which is similar to the Ag cases. The yields of all other light gases (up to C4s) are greatly improved when Re-loaded catalysts are used, which is also found similar to Ag- and Rh-loaded catalysts.

5.6.3 Petroleum fractions

Similar to Ag and Rh catalysts, all Re catalysts, except Re/HY, seem to give heavier oils as indicated in **Figure 5.70** since their true boiling curves after Re loading shift to the right side of those of pure zeolites. Only the one of Re/HY shifts to the left, indicating the lighter oil than that of HY.

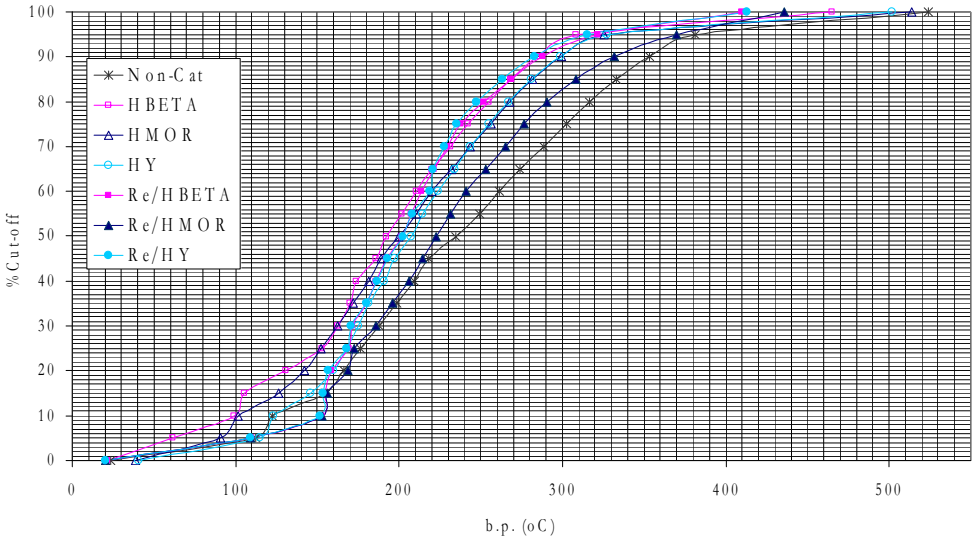

Figure 5.70 True boiling point curves from using Re-loaded catalysts.

The petroleum fraction cuts shown in **Figure 5.71** confirm that both Re/HBETA and Re/HMOR decrease the light petroleum fractions (full range naphtha) whereas the kerosene fraction is increased for all Re-loaded catalysts, which is in this case similar to those of Ag-loaded catalysts. In the Ag cases, after Ag loading, it is found that heavy gas oil and long residue are maintained, whereas the

naphtha and light gas oil decrease with the increase in kerosene. It seems that the naphtha and light gas oil are converted to kerosene fraction. Re/HBETA and Re/HY also appear to follow the same explanation. On the other hand, Re/HMOR decreases naphtha, but increases all heavier fractions (kerosene, gas oils, and long residue). It is implied that loading Re on HMOR suppresses the activity of the parent HMOR. Like Rh/HY, Re/HY gives the most distinctive results; that is, it is the only one among all Re-loaded catalysts that enhances the naphtha productionbut not as much as Rh/HY. Also, similar to Ag and Rh catalysts, Re catalysts behave differently, depending on which zeolite is used as the support.

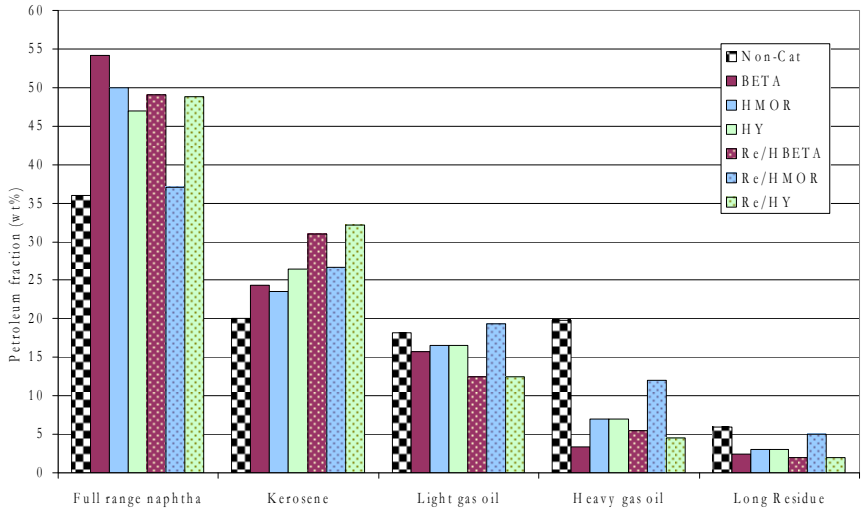

Figure 5.71 Petroleum fractions from using Re-loaded catalysts.

5.6.4 Molecular Composition in oils

Figure 5.65 indicates that all Re-loaded catalysts give the similar distribution of molecular composition, and only slight difference is found on Re/HMOR. Re-loaded catalysts decrease saturated HCs while increases mono-aromatics and polar-aromatics, which are the distinguished outcomes found similar to those of all Rh-loaded catalysts. Re-loaded catalysts, however, improve mono-aromatic content greatly to around 17-18% in oils, which is slightly less than Rh-loaded catalysts. These distinctive outcomes of Re- and Rh- loaded catalysts have not been found so far with using other metals loaded on the same parent zeolites. Since

Re tends to be a selective catalyst fro aromatization (Krogh *et al.*, 2003), it is a rational explanation of why mono-aromatics or other aromatics can be enhanced by Re loading.

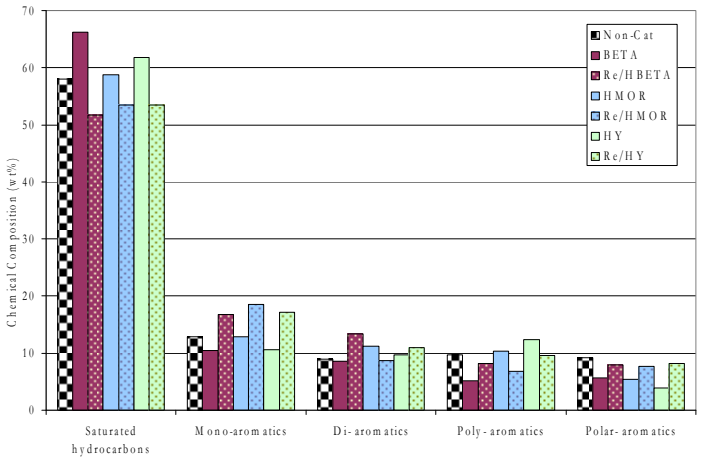

Figure 5.72 Molecular compositions in oils from using Re-loaded catalysts.

Polar-aromatics are the hydrocarbons containing O, N or S, which mainly associate with the aromatic structures (Jada *et al.*, 2003). For tire pyrolysis, S atom actually comes from sulfur in the polymer chains of tires when it is pyrolyzed in the process. O atom might come from; (1) oxygen in the polymer chains of used tire due to tire oxidation (aging) occurred at the sulfur linkages, (2) moisture adsorbed in the pore of catalysts and also on the tire sample, and (3) O atom in the structure of catalysts. And, N comes from N-compounds which are used as additives in tire production.

It was found that polar-aromatics were significantly increased in the presence of some bifunctional catalysts as compared to the pure zeolites and the non-catalyst case. It can be explained that the interaction between the strong acid sites and the small clusters of noble metal results in the electrons being withdrawn from the noble metal; thus, creating an electron-deficient metal particle. This cause can decrease the strength of the bonding interaction between sulfur and metal (Du *et al.*, 2005; Sachtler *et al.*, 1992). Hence, sulfur is splitted-over to acid sites and might associate with the aromatic structures to form polar-aromatic compounds as shown

in **Figure 5.73**. On the other hand, without metals, the strength of sulfur bonding between the surface of pure zeolite and sulfur atom can not be reduced; therefore, polar-aromatic can less occur.

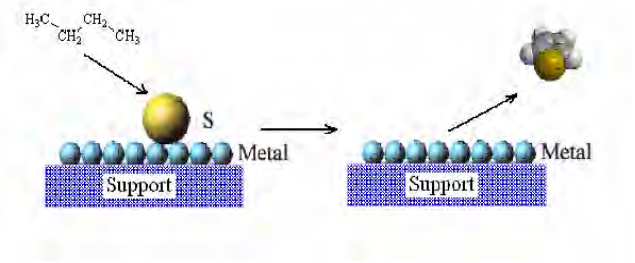

Figure 5.73 Polar-aromatic formation in maltenes (Du *et al.*, 2005).

5.6.5 Petrochemical Yields

Re loaded on all tested zeolites further increases light olefins, mixed C4s, and mono-aromatic productions as compared to the pure zeolite cases, which is also similar to Rh-loaded catalysts. Re/HBETA and Re/HY increase about twice as much light olefins production as the parent zeolites can.

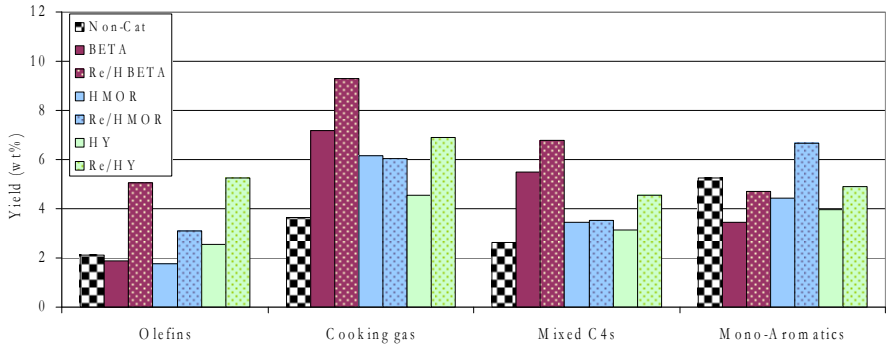

Figure 5.74 Yield of some petrochemicals from using Re-loaded catalysts.

Re/HMOR, which appears to be poor on the production of light olefins, cooking gas, and mixed C4s, is the best catalyst for the production of mono-aromatics. And, **Figure 5.72** indicates that the mono-aromatics may be produced from the conversion of saturated HCs, di- and poly-aromaictics.

6

Effects of Basic Support and Metals on Basic Support

KL zeolite, whose formula is $K_9A_{19}Si_{27}O_{27,}$ has basic properties and one dimensional channel of 12 membered rings with a pore size of 0.71 nm. (Sato *et al.*, 1999). KL zeolite can act as an electron donor and stabilize electron rich metal particles inside the zeolite framework (Alvarez-Rodriguez *et al.*, 2008). It has been used as a support in several studies to improve catalytic activity and selectivity. A highly selective catalyst in the aromatization of n-hexane was found by Barrer and Villiger (1969), who used the platinum catalyst supported on KL zeolite. The influence of different alkali catalysts on the aromatization selectivity was investigated by Becue *et al.* (1999). The highest selectivity on Pt/KL catalyst was achieved, and it enhanced the octane number. The application of KL catalyst on selective hydrogenation reaction has been studied in several researchers. Jacobs *et al.*, 2001

studied the different preparations of Pt/KL catalyst for n-hexane aromatization. They explained that the different methods affected the various results of platinum cluster distribution on the KL support. They also suggested that the vapor phase impregnation was an effective method on KL powder, but not on the extrudates whose efficiency decreased in the presence of the binder material. In 2008, Kumar *et al.*, studied the role of pore size on the aromatization activity of Pt/KL catalyst, which light naphtha was used as a feedstock. It was noted that the pore volume and dispersion was decreased at high metal loading above 0.4wt% because of the Pt agglomeration. No loss in pore volume and surface area was found at low metal loading. In addition, they suggested that the catalyst prepared by incipient wetness impregnation can be an active and stable catalyst for aromatization. The selective hydrogenation was studied by Alvavarez-Rodriguez *et al.* (2005). They found selectivity and activity on the hydrogenation of unsaturated aldehyde by using ruthenium supported on KL zeolite. Later, they further studied the effect of various preparation methods of catalysts, and reported that the Ru/KL catalyst prepared by incipient wetness impregnation showed less reactive but more selective to unsaturated alcohol than the catalyst prepared by treating with $RuCl_3 \cdot xH_2O$. These results related to the size and location of particles in the zeolite framework.

This chapter discusses the effect of basic zeolite, KL, and metal-loaded KL as catalysts, on the pyrolysis products of waste tire. With the activity mentioned above, KL and metal-loaded KL are expected to change the characteristics of the tire-derived products. The basic property of KL is also a key parameter that drives the motivation on selecting KL as a catalyst and support in this work. The results are described in terms of product yield, gas composition and yield, true boiling point curves, petroleum fractions, petrochemical yields, carbon number distribution, and the molecular composition of oil.

6.1. Characterization of Metal-loaded KL Catalysts

As informed by Tosoh Company, Singapore, KL used in this work has the 1D structure, the SiO_2/Al_2O_3 ratio of 6, and the pore size of 7Å. From the BET

method, it is found that the surface area of KL is 297.8 m^2/g. and the total pore volume is 0.392 cm^3/g. The metals loaded are the same ones used in the previous chapter, which are Pt, Pd, Ru, Ag, Rh, and Re. The loaded amount of all metals was fixed at 1% by weight.

6.2 Pyrolysis of Waste Tire

The product yield, gas composition and yield, true boiling point curves, petroleum fractions, petrochemical yields, carbon number distribution, and the molecular composition of oil are discussed in terms of individual metals. The results are discussed below.

6.2.1 Product Yields

The product yield of catalytic pyrolysis with the different zeolites is shown in **Figure 6.1**. The result shows that the presence of KL provides an increase in the gaseous fraction (16%) as compared to the non-catalytic pyrolysis (12.4%). Since the same condition in all experiments was conducted for total conversion of tire, almost constant in solid yields are observed at around 43%. A basic support in general can serve a cracking catalyst, but the cracking mechanism is driven by carbanions, instead of carbenium ions. However, although the cracking activity in most of basic catalyst cases are not as high as that of acid catalysts cases, the selectivity of cracking products may be different and unique; for example, KL was found to be selective to aromatization products such as to BTXs.

All metals, as expected to play the similar role as they did for acid support cases, results in a further increase in gas yield in accordance with a decrease in the yield of liquid product. This result is attributed to the reason that heavy compounds can be attached to the metal sites leading to easier decomposition (C-C cleavage) into lighter compounds. All metals behave the similar way and in the same order as they do on the acid supports. For instances, Pt, Ru, Ag, and Rh are still the top metals that give a high yield of gas product regardless of the support type. Especially, Ag/HBETA, Ag/KL, and Ru/HMOR can produce the gas product with the yields of higher than 30% (33.2%, 30.4%, and 30.3%, respectively).

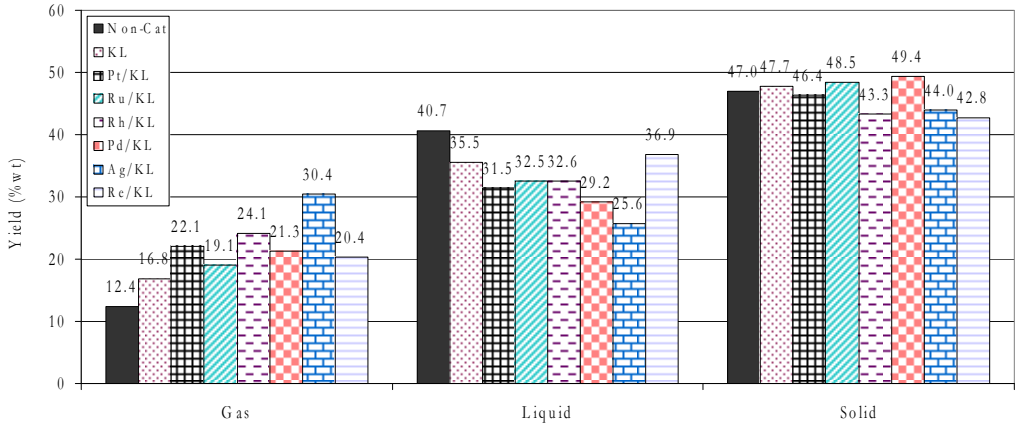

Figure 6.1 Product yields from using metal-loaded KL catalysts.

6.2.2 Gas Compositions

Distinguished from the cases when they are on the acid supports, which the gas compositions alter from support to support and metal to metal, the metals loaded KL give fairly similar gas compositions, as shown in **Figure 6.2**. However, some slight differences are on methane, ethane, and C5+. All metals give almost equal contents of ethylene, propylene, propane, and mixed C4s in the gas products. However, since different metals give different gas yield as shown in **Figure 6.1**, they therefore produce gases at different yields (see **Figure 6.3**), strongly depending on their ability on producing gas. The acid zeolites usually produce a high amount of mixed C4s whereas it appears that the basic zeolites with or without the metal loading do not alter the production of mixed C4s from what the non-catalytic pyrolysis produces.

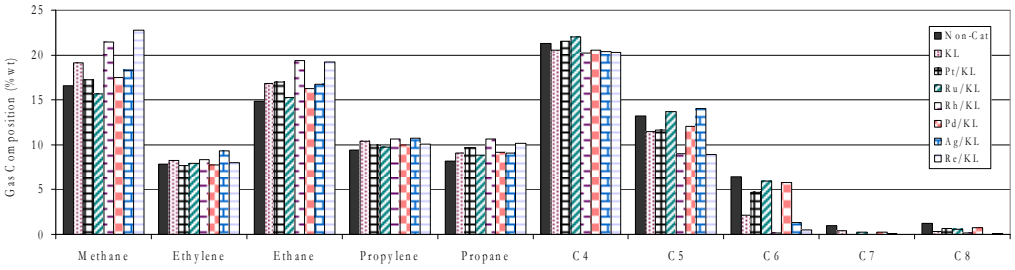

Figure 6.2 Composition of gaseous products from using metal-loaded KL catalysts.

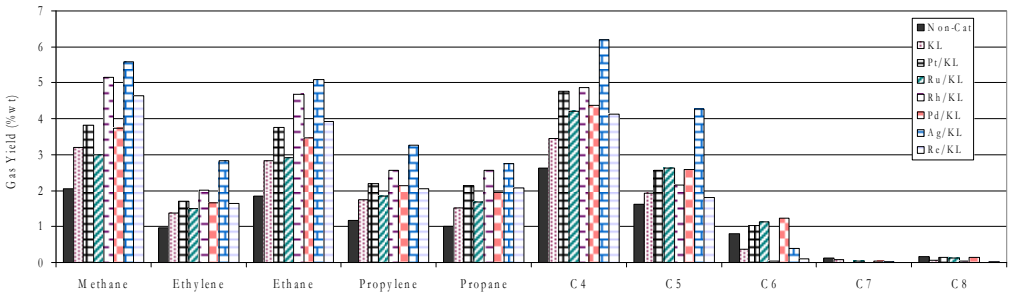

Figure 6.3 Yield of gaseous products from using metal-loaded KL catalysts.

Since Rh/KL is one of the catalysts that have slight differences on the gas compositions (besides Re/KL and Ag/KL), it may be notable to discuss about Rh/KL as the example of these particular cases. Figure 6.2 shows that the role of Rh loaded on KL has the impact on light hydrocarbons; C1, C2, C3 and C4s. Namely, slight increases in C1 as well as C2 and C3 are observed as compared to using KL zeolite. Meanwhile, the amount of unsaturated light hydrocarbons, C2= and C3=, is decreased with the treatment of Rh/KL. Berrueco *et al.* (2005) reported that tire is mainly composed of the rubbers which are polybutadiene and polybutadiene-styrene (SBR). Therefore, light hydrocarbon gases from pyrolysis mostly consist of C1 and C4s as the predominant products, which is in agreement with the observed result as well. However, the presence of Rh results in a decrease in C4s, which might be due to the reason that they are converted to lighter gas like C1. There are several types of reaction take place in the pyrolysis especially decomposition reaction at an elevated temperature which lead to the formation of the fragment of a molecule and free radical species. During pyrolysis, the presence of H free radical as reactive species can also be formed, and then intermediately adsorbed on the active site of catalysts which further undergo the reaction involving H transfer such as hydrogenation and hydrogenolysis. It was found that Rh has the ability in C-C bond breaking at terminal positions and also ability in hydrogenolysis, leading to methane formation (Teschner *et al.*, 2000). In addition, it is worthy mentioned that this metal exhibits activity in hydrogenation reaction, which can be

explained by the hydrogenation of unsaturated light hydrocarbons, C2= and C3=, resulting in a slight increase in hydrogenated products like C2 and C3. However, the gas yield obtained by using Rh/KL is higher than the use of KL alone, which causes a slight increase in C1 as well as C2= and C3= yields and a significant increase in the yield of C2 and C3. In summary, KL does not greatly change the gas compositions, and loading some metals on KL still behaves the same way that KL does. The other metals like Rh, Ag, and Re may slightly alter the gas composition. Besides hydrogenolysis activity, the explanation on how these particular metals can alter the gas compositions whereas the others do not is to be further investigated.

6.2.3 Petroleum fractions

The simulated true boiling point curves shown in **Figure 6.4** indicate that the three metals that give lighter oils than KL are Pd, Pt, and Ru, and those that yields heavier oils than that of KL are Ag, Rh, and Re. These observations can also be found in the cases of acid zeolites, but the order may be different from case to case. Previously, it was found that Ag, Rh, and Re were not those who enhanced the cracking activity of the supports because they produce heavier oil than the parent support can.

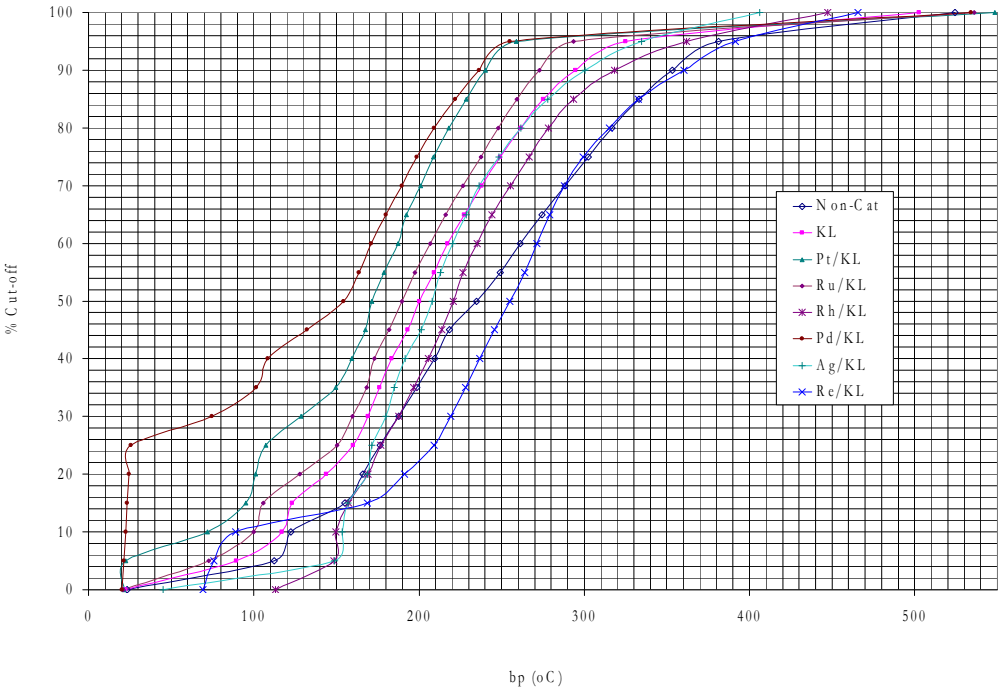

Figure 6.4 True boiling point curves of oils from using metal-loaded KL catalysts.

As discovered so far, Pd was one of the metals that can improve the quality of oil; however, with the KL support Pd seems to give the lightest oil among those produced from Pd loaded on the other supports. **Figure 6.5** shows that Pd/KL produces about 75% naphtha in oil whereas the parent KL results in 50% naphtha in oil. Pd, Pt, and Ru are the supported metals that enhance the naphtha production of KL with reducing the heavier fractions. On the other hand, Ag, Rh, and especially Re suppress the activity.

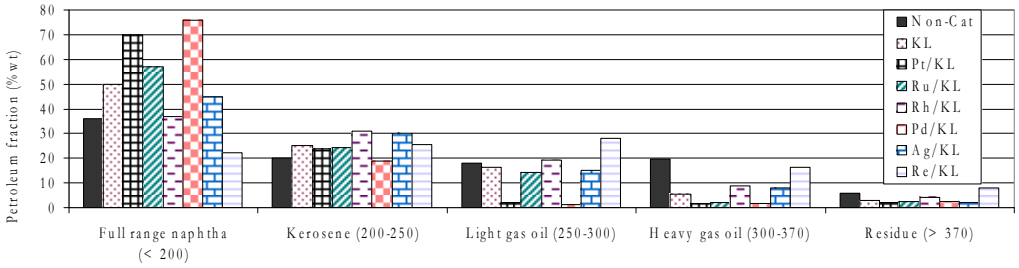

Figure 6.5 Petroleum fractions in oils from using metal-loaded KL catalysts.

6.2.4 Molecular Composition in oils

Fractionations of maltene into chemical classes via the mean of liquid column chromatography are shown in **Figure 6.6**. It reveals that the presence of pure KL results in the same concentrations of saturated hydrocarbons and single-ring aromatic compounds, as those of the non-catalytic case, accompanied by an increase in multi-ring aromatic compounds. When 1% Pt, Re, and especially Rh was loaded on KL, the great amount of mono-aromatics is observed with a consequent lower content of saturated HCs, di- and poly aromatics in oils as compared to KL. Rh/KL gives about 30% mono-aromatics in oil, which is the highest among all catalysts tested in this work.

It has been reported that oil aromaticity is formed by the aromatization of alkene such as C2=, C3= and butadiene produced during tire pyrolysis (Cypres *et al.*, 1987). Then, these compounds are converted to cyclic alkene via cyclisation followed by the dehydrogenation of six carbon atoms to form simple

aromatic compounds and subsequent condensation reactions to form higher poly-aromatics by Diels-Alder reaction, resulting in high C1 and H_2 contents as by products. Moreover, they also reported that at high temperatures, light olefins generated by the deep decomposition of heavier fractions could combine with butadiene to form aromatics and then form high molecular-weight poly-aromatic species by some further reactions of aromatics combined with olefins.

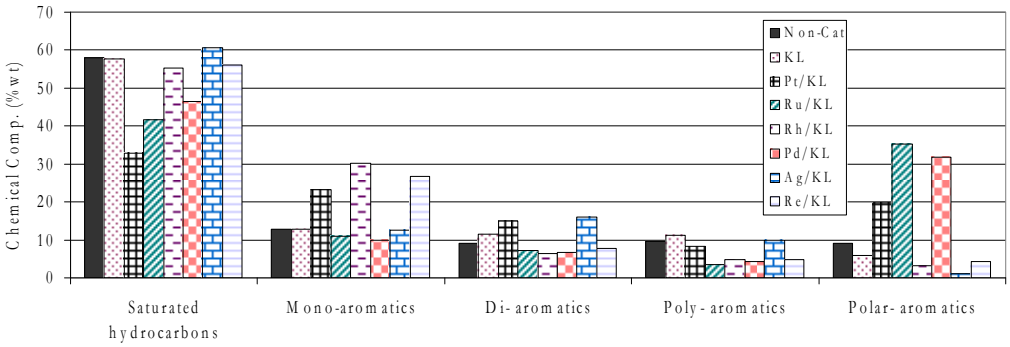

Figure 6.6 Molecular compositions in oils from using acid zeolites

It is widely known that mono-aromatic hydrocarbons have attracted interest in petrochemical industries whereas the presence of poly-cyclic aromatic hydrocarbons is disadvantageous in the view of fuel application and hazardous chemicals. As one can see from the result, the introduction of Rh plays a major role on the formation of mono-aromatic compounds in accordance with the reduction in concentration of multi-ring aromatics. It was noted that Rh metal showed activity in hydrogenation and/or ring opening of hydrocarbons (Albertazzi *et al.*, 2003) while the basic property of KL has shown effect on aromatization reaction (Wakui *et al.*, 1999). For base-catalyzed reaction, it is found that the reactants can act as acid toward catalyst which act as base. KL zeolite which is base catalyst also shows the same activity as explained above. It can abstract H^+ from reactants to form cabanion species and subsequently react with intermediate compounds to form products by several reactions such as isomerization, aromatization and alkylation. For ring-opening reaction, there was no report about the ability of basic catalyst in C-C bond cleavage thus the influence of metal site in those ability is dominant in this study. It

can be assumed that the hydrogenation of poly-aromatics on active site of Rh is the predominant reaction followed by ring opening reaction which leads to a decrease in poly-aromatic compounds. Additionally, it was found that the hydrogenation of poly-cyclic compound is easier than that of single ring aromatics (Corma et al., 1997). This is the reason why the mono-aromatics content continues to increase as the catalysts is applied.

Moreover, the presence of Rh/KL also results in a slight decrease in the concentration of polar-aromatics compared to non-catalytic and pure KL case. It is proven that polar-aromatics found in waste tire pyrolysis is mostly aromatics containing a sulfur because oxygen is not allowed in the pyrolysis (Williams *et al.*,1994). Dung *et al.*, 2009 studied the formation of polar-aromatics in waste tire pyrolysis, and proposed the ways the fraction can be formed. They reported that polar-aromatics can be formed by the combination of olefins with free sulfur or sulfur-containing compounds by Diels-Alders reaction. Moreover, the direct cracking of tire molecules at linked sulfur positions can be occurred. However, the presence of a catalyst can reduce the polar-aromatic formation by the hydrogenation of olefins and unsaturated hydrocarbons to other intermediate products. The reduction in polar-aromatic compounds, when Rh/KL is present, could be attributed to high activity in the hydrogenation property of Rh and the ability in C-S-C bond breaking in the oil molecules. This result is well consistent with the amount of sulfur contents in the oil detected by the elemental analysis technique, which shows the reduction in sulfur with using Rh. It is found that the use of KL and 1%Rh loaded on KL helps decrease sulfur content in the oil by approximately 36 and 75%, respectively, as compared to the non-catalytic case. Additionally, the amount of coke and sulfur deposition on spent Rh/KL catalyst (not shown here) is found higher than using KL alone. These results might be the higher activity for Rh catalyst in polar-aromatics reduction as well as sulfur-containing compound in oil which are either cracked or condensed leading to coke formation. However, these phenomena can cause the catalyst deactivation due to the loss of active sites which is resulted from the formation of aromatic/polymeric type of carbon deposited on Rh and sulfur adsorbed on Rh sites (Lakhapatri *et al.*, 2009).

Figure 6.7 illustrates the comparison of carbon number distribution obtained from using KL and Rh/KL for the investigation of ability in the mono-aromatics production. The non-catalytic case gives a very wide distribution of mono-aromatics with the carbon number average of ~22. The introduction of KL results in a much narrower distribution, and shifts the average carbon to 19. Moreover, Rh/KL further shifts the distribution to an even lower number of 14.4, which the smallest carbon number of around C6-C8 corresponding to benzene, toluene and xylene for instances are also produced.

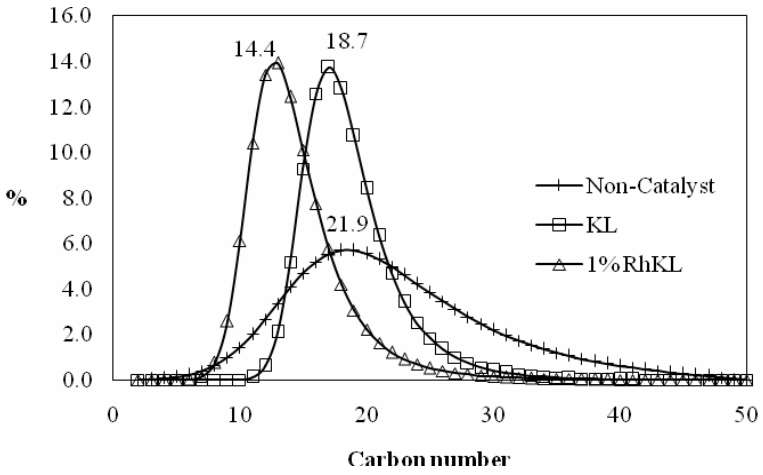

Figure 6.7 Carbon number distribution of mono-aromatics using 1%Rh/KL.

It was found that the addition of Re loading highly increases the amount of mono-aromatics associated with the significant reduction of di- and poly-aromatics. Rhenium catalysts showed the high activity in hydrogenolysis and ring-opening (Carter *et al.*, 1982). Therefore, it is possible that di- and poly-aromatics can be converted to the lighter products such as mono-aromatics via the hydrogenolysis and then the ring-opening function of the catalysts. In addition, Re/KL catalysts can help improve the quality of pyrolytic oil by reducing the amount of asphaltene in the oil product. The result revealed that Re/KL catalysts show the drastic reduction of asphaltene from those of the non-catalytic case (0.2338% in oil) and KL (0.068%) to 0.0337%.

6.2.5 Petrochemical Yields

In terms of yields, the use of all metals can further increase the production of olefins, cooking gas, and mixed C4s of the parent KL zeolite. However, only Pt-, Re-, and Rh-loaded KL catalysts greatly produce mono-aromatics at 7.2% (for Pt/KL) and ~10% (for Re/KL and Rh/KL).

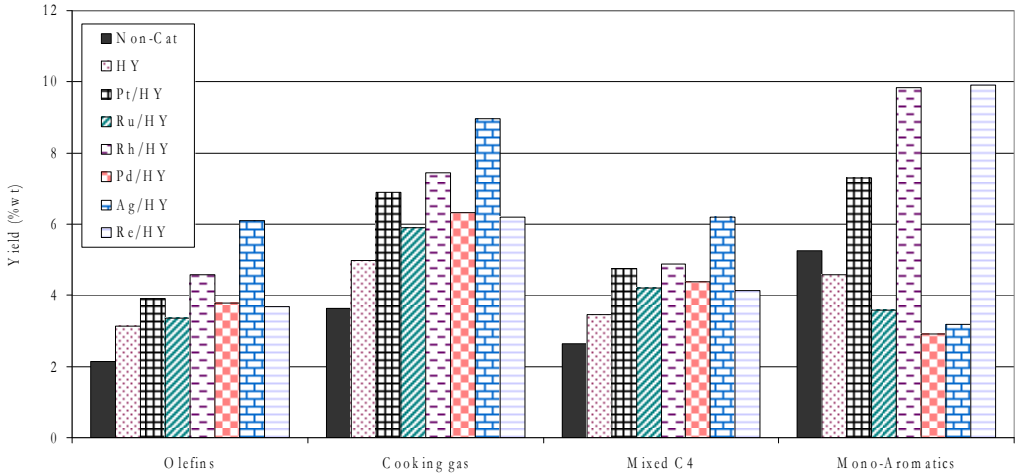

Figure 4.16 Yield of some petrochemicals obtained from using metal-loaded KL catalysts.

Therefore, Re/KL and Rh/KL are found to be promising catalysts for the production of mono-aromatic compounds from waste tire pyrolysis. Consequently, waste tire pyrolysis can be an alternative process to provide alternative sources of raw materials to petrochemical industry when human beings are lack of conventional raw materials obtained from petroleum or other fossil sources.

7

Mesoporous Supports and Role of Ruthenium

7.1. SBA-1

The catalytic pyrolysis of waste tire with Ru/SBA-1 catalysts was studied. The roles of ruthenium were elucidated since the support, a pure silica SBA-1 synthesized via silatrane route, was proven to be catalytically inactive and its structure retained after pyrolysis. Ruthenium clusters increased the yield of gaseous products, approximately 2 times as compared to thermal pyrolysis, at the expense of the liquid yield. They also decreased poly- and polar-aromatics and consequently produced lighter oil. The heating rates (1°C/min, 5°C/min, and 10°C/min) during calcination were found to strongly influence the activity of the Ru/SBA-1 catalysts. The catalyst

Dr. Sirirat Jitkarnka
Associate Professor
The Petroleum and Petrochemical College
Chulalongkorn University

calcined with a heating rate of 5°C/min exhibited the highest activity on poly- and polar-aromatics reduction and light oil production. The highest activity of this catalyst was attributed to its smallest mean ruthenium particle size and its highest sulfur tolerance.

7.1.1. SBA-1 as a support

In order to clearly determine the roles of ruthenium and the effect of calcination rate on the activity of Ru-supported catalyst in the catalytic pyrolysis of waste tires, a selected support should not play any role on chemical reactions. Additionally, to obtain a high metal dispersion for a metal-supported catalyst, the use of a zeolite, especially the one having large surface area, is commonly suggested. Moreover, a pure silica material has been shown to be inactive for the conversion of used tire rubber into hydrocarbon products (Miguel *et al.*, 2006). Consequently, in this study, a silica SBA-1 was first synthesized *via* the silatrane route (Tanglumlert *et al.*, 2008). The accomplishment of the material synthesis was confirmed by XRD and N_2-physical adsorption results. The surface area and pore volume of the synthesized SBA-1 are 1,428 m^2/g and 0.72 cm^3/g, respectively, which are similar to the values from the reference (Tanglumlert *et al.*, 2008).

The experiment results of thermal and catalytic pyrolysis using SBA-1 as a catalyst are depicted in **Figure 7.1**. It can be seen that the yield of solid product is similar in both runs (**Figure 7.1A**). This is because of the fact that the pyrolysis conditions were kept constant and the tire was reported to be completely decomposed at 500°C (Berrueco *et al.*, 2005). As compared to non-catalytic case, the use of SBA-1 insignificantly influences the product yields because the yields of gas and liquid products in the two runs are comparable. In addition, the concentrations of saturated hydrocarbons, mono-, di-, poly- and polar-aromatics, analyzed by liquid adsorption chromatography, of the two derived oils are quite similar (**Figure 7.1B**). Furthermore, the TBP curves of the two oils are mostly overlapped (**Figure 7.1C**). Thus, it is safe to conclude that SBA-1 is catalytically inactive for waste tire pyrolysis.

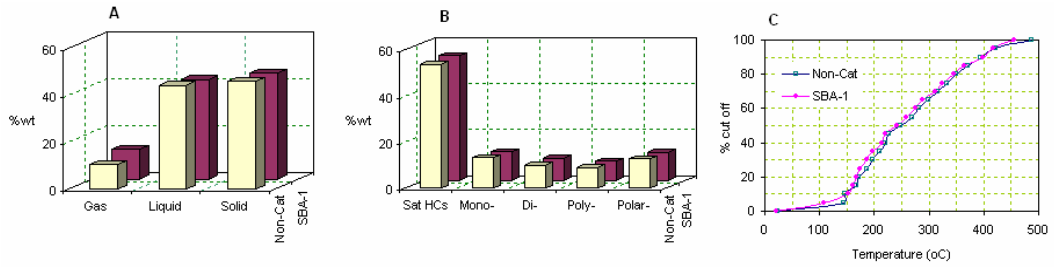

Figure 7.1 Effects of SBA-1 on the pyrolysis products: (A) Product distribution, (B) Liquid compositions, and (C) True boiling point curves.

7.1.2 Roles of ruthenium during catalytic pyrolysis of waste tire

1%Ru-supported SBA-1 catalyst was prepared, and its catalytic activity was tested for understanding the role of ruthenium in the waste tire pyrolysis. The amount of ruthenium loaded on the SBA-1 support is confirmed by ICP analysis. No loss in the crystallinity of the SBA-1 is detected in the XRD pattern of the prepared 1%Ru/SBA-1 sample. Note that the SBA-1 was proven to be catalytically inactive for waste tire pyrolysis; thus, from this point, the influences of 1%Ru/SBA-1 will be presented by comparing directly to the thermal pyrolysis.

The results of experiments with and without 1%Ru/SBA-1 are given in **Figure 7.2**. The results include the product yields, petroleum cuts, and compositions of the derived oils. **Figure 7.2A** shows that 1%Ru/SBA-1 decreases the yield of oil in accordance with an increase in the yield of gaseous products. Namely, the gas yield increases from ~10 %wt to ~20 %wt. **Figure 7.2B** shows the petroleum fractions in the pyrolysis oils. A high concentration of heavy fractions, i.e. residues and gas oil (GO), is observed in the non-catalytic oil. The presence of 1%Ru/SBA-1 catalyst shifts the TBP curves to lower temperature, resulting in the increase in light fractions. The content of light fraction (boiling point < 250°C) increases from approximate 50 wt% to over 70 wt%. **Figure 7.2C** indicates that 1%Ru/SBA-1 strongly influences the compositions of the pyrolysis oils. As compared to non-catalytic oil, the contents of poly- and polar-aromatic hydrocarbons (PPAHs) are much lower. The reduction of these heavy HCs caused by the presence of Ru-based catalysts is further confirmed by observing the results obtained from

FTIR analysis (**Figure 7.2D**). This figure presents the FTIR spectra of the oils in the wave number corresponding to the polycyclic aromatic range (Islas-Flores *et al.*, 2006; Jager *et al.*, 2007). The intensity of peaks at 700cm^{-1} and 740cm^{-1} in the spectrum of the oil produced over 1%Ru/SBA-1 is obviously lower than that of the non-catalytic case, indicating a lower concentration of polycyclic HCs (Jager *et al.*, 2007).

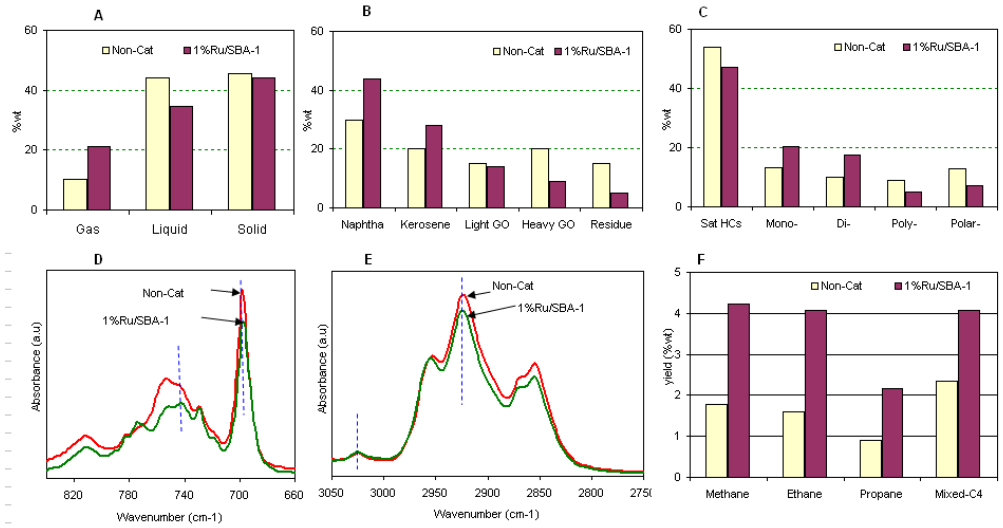

Figure 7.2 Effects of 1%Ru/SBA-1 on the pyrolysis products: (A) Product distribution, (B) Petroleum cuts, (C) Liquid composition, (D) Light alkanes yield.

The formation of PPAHs from the pyrolysis of waste tire was reported to occur through the Diels-Alders reaction and aromatization (Dung *et al.*, 2009; Williams and Taylor, 1993; Williams and Bottrill, 1995). And a poly-aromatic compound, such as phenanthrene, was formed after the formation of naphthalene, a di-aromatic compound. Moreover, no evidence proving the direct formation of aromatics from cyclization of alkanes was observed (Williams and Taylor, 1993). The presence of ruthenium clusters in this study drastically decreases PPAHs (**Figure 7.2C**). Due to the fact that the nature of ruthenium is highly active for catalyzing hydrogenation reaction (Eliche-Quesada *et al.*, 2006); thus, it might decrease PPAHs either by: (i) converting their intermediates to smaller molecules preventing their formation (*first route*), or: (ii) transforming them to other types of molecules, most

likely through hydrogenating (*second route*).

If the first route is really the case, then the content of di-aromatics, intermediates of PPAHs, should be lower with respect to the thermal pyrolysis. However, for 1%Ru/SBA-1 catalyst, the reduction of PPAHs is accompanied with the increase in di-aromatics; thus, the occurrence of the first route is unlikely. Moreover, it has been reported that the hydrogenation of poly-aromatics is more preferable than their di-aromatic intermediates (Jongpatiwut *et al.*, 2004), and generally yields partial hydrogenated products (Jacquin *et al.*, 2003). This, together with the higher concentration of di-aromatics (for 1%Ru/SBA-1) with respect to thermal pyrolysis (**Figure 7.2C**), suggests that the reduction of PPAHs is more likely to occur by the second route. However, it should be noted that no evidence disproving the first route has been found. Therefore, it can be concluded that ruthenium decreases PPAHs by both ways, but the second route is more likely.

The presence of ruthenium clusters also decreases saturates in the derived oil (**Figure 7.2C**). This is well consistent with the results obtained from FTIR analysis (**Figure 7.2E**). The peak at 3030 cm^{-1} corresponds to the C-H stretch aromatic C, whereas the peak at 2920 cm^{-1} belongs to the CH stretch aliphatic (Islas-Flores *et al.*, 2006). And, the ratio between the intensity (I) of peak at 3030 cm^{-1} and 2920 cm^{-1} ($I_{3030cm^{-1}}/I_{2920cm^{-1}}$) is proportional to the relative concentration of saturates in oil (Wang and Griffiths, 1985). It can be seen that as compared to thermal pyrolysis, this ratio increases when 1%Ru/SBA-1 was used, indicating a lower concentration of saturates in the derived oil. Usually, Ru-based catalyst is a good catalyst for hydrogenolysis reaction of hydrocarbons (Eliche-Quesada *et al.*, 2006). And, a consequence of hydrogenolysis generally is the production of light alkanes (Kinger and Vinek, 2001). From the gas analysis from both thermal and catalytic pyrolysis in **Figure 7.2F,** the yields of methane, ethane, propane and mix-C_4 increase dramatically when 1%Ru/SBA-1 was used. Therefore, those saturates might be converted to the light gases, speculatively indicating that the deep hydrogenolysis reactions might have occurred (Akhmedov and Al-Khowaiter, 2000), reducing saturates in the oil.

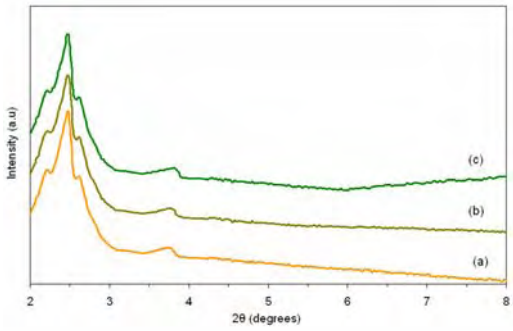

(a)

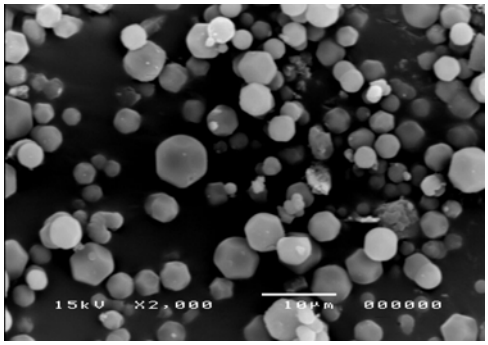

(b)

Figure 7.3 (A) XRD patterns (a) SBA-1, (b) Fresh 1%Ru/SBA-1, and (c) Spent 1%Ru/SBA-1 after coke removal; (B) SEM images: spent 1%Ru/SBA-1 after coke removal

Up to this point, it has been proven that ruthenium cluster strongly influences the pyrolysis products, SBA-1 is catalytically inactive, and there is no loss of the crystallinity of this support after incorporation with ruthenium. However, the topology and/or morphology of a zeolite can be changed during reaction (Wongkerd *et al.*, 2008), which can also be the cause of catalytic activity change (Wongkerd *et al.*, 2008; Lee *et al.*, 2008). Therefore, it is essential to analyze the spent 1%Ru/SBA-1 catalyst to see if any change in the structure of the support has occurred, which would have contributed to the change on the activity. The coke deposited on the spent 1%Ru/SBA-1 was first removed by oxidation. Then, it was subject to analysis by means of XRD and SEM. It can be seen that its XRD pattern is similar to the

fresh catalyst **(Figure 7.3A)**. Actually, no difference can be observed. And, the SEM image of the spent catalysts depicted in **Figure 7.3B** reveals the preservation of the SBA-1 morphology. Therefore, it is safe to conclude that the structure of SBA-1 did not change during pyrolysis. As a consequence, the catalytic activity of 1%Ru/SBA-1 is only attributed to the ruthenium contribution.

Conclusively, ruthenium strongly increases the yield of gas in accordance with a reduction of the oil yield. Moreover, the presence of ruthenium also produces much lighter oil by decreasing poly- and polar-aromatics. Saturates in oil is also lessened possibly due to the high hydrogenolysis activity of ruthenium clusters.

7.1.3 Influences of catalyst preparation

Table 7.1 summarizes the physical-chemical properties of the studied Ru-based catalysts. The catalysts prepared with a calcination rate of 1°C/min, 10°C/min, and 5°C/min are denoted as 4.0Ru/SBA-1, 4.5Ru/SBA-1, and 2.5Ru/SBA-1, respectively. The number in front of the sample name stands for its mean diameter of ruthenium particles obtained from TEM for each rate of calcination. A typical TEM image of the studied catalysts is illustrated in **Figure 7.4**. From ICP analysis, the percentage of Ru in all samples is well consistent with the targeted value. Meanwhile, the surface area and pore volume of all samples decrease with the addition of ruthenium. However, the mean pore diameter of 4.0Ru/SBA-1 and 4.5Ru/SBA-1 samples is higher than that of SBA-1, possibly caused by the blockage of small pores by ruthenium particles leading to the increment of mean diameter. The pore blockage might also be the reason for the reduction in total pore volume.

Table 7.1 Physical-chemical properties of Ru-supported catalysts

Catalyst	Ru	Pore	Surface	Pore	Dispersion	Mean Ru particle size

	(%wt)	volume (cm^3/g)	area (m^2/g)	diameter (nm)	(%)	(nm)*	
						TEM	CO-chemisorption
SBA-1	-	0.72	1428	2.17	-	-	-
4.5Ru/SBA-1	1.02	0.67	1387	2.19	26.6	4.49	4.85
4.0Ru/SBA-1	0.98	0.68	1396	2.22	29.8	3.99	4.33
2.5Ru/SBA-1	0.99	0.71	1405	2.13	48.8	2.56	2.64

*Volume-area mean diameter

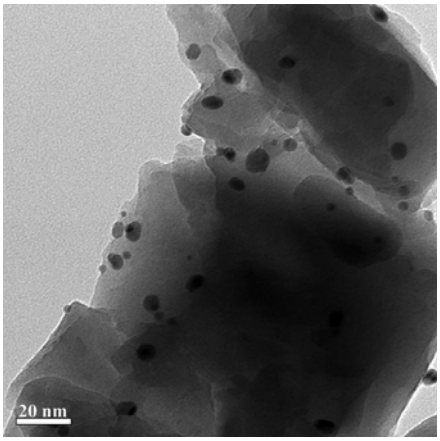

Figure 7.4 TEM image of 4.5Ru/SBA-1.

The metal particle size or the consequent dispersion is strongly dependent on the preparation condition (**Table 7.1**). The sample prepared under the highest heating rate during calcination has the biggest particle size, as determined by CO-chemisorption and TEM. The average particle size obtained from TEM is slightly lower than that obtained from CO-chemisorption for the same sample. However, the trend of the mean ruthenium particle size variation is identical.

H_2-TPR profiles of Ru-supported catalysts are displayed in **Figure 7.5**. From the figure, the two profiles of 2.5Ru/SBA-1 and 4.5Ru/SBA-1 present two overlapped reduction peaks at 195°C and 230°C whereas that of 4.0Ru/SBA-1 shows a narrower peak between the two peaks with a little shoulder at 195°C. The first peak at low temperature (around 195°C) is assigned to the Ru^{3+}/Ru^{o} single step reduction,

whereas the second peak located at high temperature (~ 230°C) comes from the reduction of RuO_2 (Eliche-Quesada *et al.*, 2006). The H_2-consumption curve of 2.5Ru/SBA-1 sample is broad, possibly due to the reduction of highly-dispersed ruthenium species located in different environments; and its high temperature peak is the clearest, indicating a high amount of ruthenium oxide. The signals of the 4.0Ru/SBA-1 and 4.5Ru/SBA-1 are clearly narrower than 2.5Ru/SBA-1, probably due to the poor dispersion of ruthenium in the two samples, leading to the formation of bigger particles, which is well consistent with CO-chemisorption and TEM results (**Table 7.1**). Moreover, all samples have similar ruthenium content; thus, the location of the peaks indicates the degree of metal support interaction. The stronger the metal support interaction, the more difficult it is to reduce the metal. And, a strong interaction between metal and support helps prevent sintering during reaction, resulting in a slower deactivation of the catalyst (Eliche-Quesada *et al.*, 2006). Among all samples, 2.5Ru/SBA-1 has the strongest interaction between metal and support indicated by its highest temperature of the reduction peak. This can be attributed to the smallest clusters of RuO_2 that has strong ruthenium-oxygen-silica interactions (Mazzieri et al., 2003; Komvokis *et al.*, 2009).

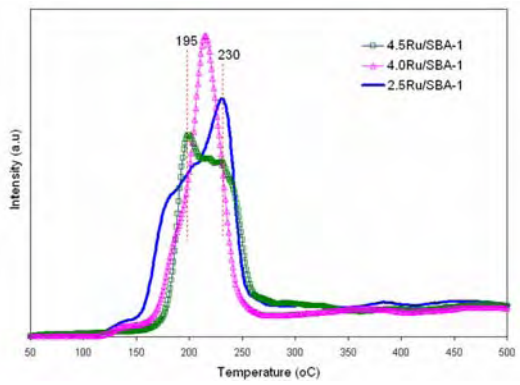

Figure 7.5 TPR-H_2 profiles of calcined Ru/SBA-1 catalysts.

In order to investigate the H_2 uptake of the reduced catalysts, the Ru-supported samples were subjected to TPD-H_2 analysis. The results are displayed in

Figure 7.6. All samples show one hydrogen chemisorption peak locating at a temperature below 200°C. However, the location of the peak is different from sample to sample. The peak of TPD-H_2 profile of 2.5Ru/SBA-1 is located at the highest temperature. Considering the intensity of the peak which is the indication of hydrogen adsorption on the metal sites, the observed trend is 2.5Ru/SBA-1>> 4.0Ru/SBA-1> 4.5Ru/SBA-1. This is well consistent with the results obtained from CO-chemisorption and TEM. Namely, the sample, which shows the higher hydrogen uptake, has smaller ruthenium particles. When the particle is smaller, there exists the greater amount of accessible ruthenium atoms for hydrogen to adsorb; thus, increasing total hydrogen uptake.

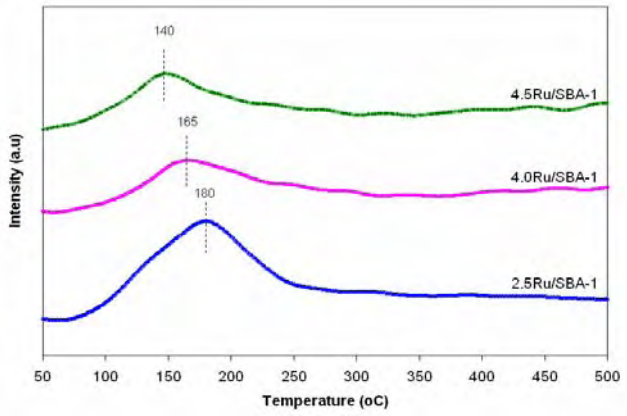

Figure 7.6 TPD-H_2 profiles of Ru/SBA-1 samples: (a) 2.5Ru/SBA-1, (b) 4.0Ru/SBA-1, and (c) 4.5Ru/SBA-1.

7.1.4 Influences of ruthenium particle size

As demonstrated in the previous section, the different heating rates during calcination resulted in the formation of different ruthenium particle sizes on the catalysts. As such, this section presents the influences of ruthenium particle size on the yield and nature of the obtained products, which are summarized in **Figure 7.7**.

Figure 7.7A illustrates the product distribution obtained from using Ru/SBA-1 catalysts having various ruthenium particle sizes. The size of ruthenium

particle strongly affects the yield of gaseous product. The gas yield increases gradually at the expense of the yield of oil with decreasing ruthenium particle size. For instance, the yield of gaseous product increases from around 15 %wt to almost 25 %wt whereas the oil yield drops from around 40 %wt to 30 %wt when the ruthenium particle size decreases from 4.5 nm to 2.5 nm. The influence of ruthenium particle can be further depicted by the petroleum cuts as shown in **Figure 7.7B**. The decrease in ruthenium particle size causes a shift of hydrocarbons from heavy fractions *i.e.* residues and GO to lighter fractions, naphtha and kerosene. And the highest selectivity toward light fractions is observed over the smallest ruthenium particle containing sample, 2.5Ru/SBA-1. **Figure 7.7C** depicts the compositions of the derived oils, which reveals that the sample having the smallest ruthenium particle exhibits the highest activity for the reduction of PPAH compounds in the derived oil. And, increasing ruthenium particle size decreases the activity on PPAH reduction. The mechanism of hydrogenation reaction of aromatics was reported to involve the dissociative adsorption of H_2 on the metal sites (Du *et al.*, 2005). Meanwhile, as revealed from catalyst characterization, the sample having smaller ruthenium particle size possesses higher hydrogen uptake (**Figure 7.6**). Therefore, 2.5Ru/SBA-1 exhibit higher hydrogenation activity as compared to the other Ru-supported catalysts due to its smallest ruthenium particle size (**Table 7.1**). As a consequence, the lowest concentration of PPAHs was detected in the oil obtained from using this catalyst.

As elucidated in the previous section, the ruthenium sites are the active sites for the reduction of PPAHs and saturates in the derived oils, possibly by hydrogenation and hydrogenolysis reactions, respectively. Moreover, the sample with the smallest particle size produces the oil having the highest selectivity toward light fractions, *i.e.* naphtha and kerosene (**Figure 7.7B**), in accordance with the lowest concentration of PPAHs (**Figure 7.7C**). Besides, the yields of light alkane hydrocarbons in gaseous products increase gradually with decreasing ruthenium particle size **(Figure 7.7D**). These observations suggest the existence of greater hydrogenation and hydrogenolysis reactions (Akhmedov and Al-Khowaiter, 2000) as the metal particle size decreases due to the increase of ruthenium specific surface

area. Therefore, it is likely that the decreasing ruthenium particle enhances hydrogenation reactions, then, the hydrogenated species might be further converted into lower molecular weight compounds by thermal cracking and/or hydrogenolysis reactions. That explains the increment in light oil production with decreasing ruthenium particle size. In addition, the greater hydrogenolysis reactions also explain the decrease in saturated HC content in the obtained oils (**Figure 7.7C**). FTIR experiment (not shown here) further confirms the reduction in saturates in oil with decreasing ruthenium particle size.

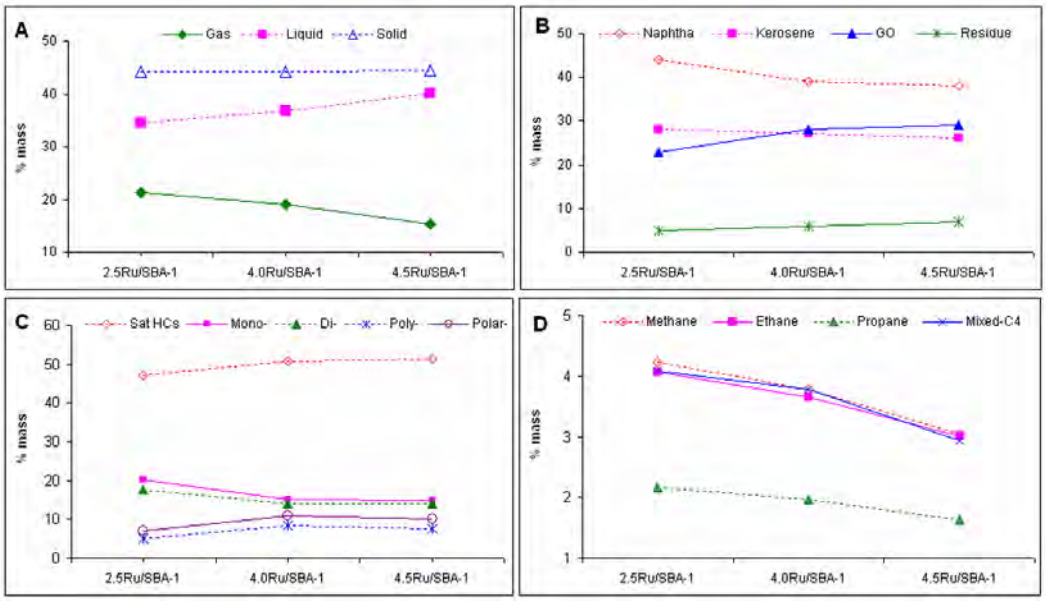

Figure 7.7 Influences of ruthenium particle size on pyrolysis products: (A) Product distribution, (B) Petroleum cuts, (C) Liquid compositions, and (D) Light alkanes yield

The results of TPO experiments of spent SBA-1 and Ru-based catalysts are presented in **Figure 7.8**. SBA-1 sample shows a main oxidation peak at 300°C – 400°C, whereas the TPO curves of all Ru/SBA-1 samples consist of two peaks located at around 300°C and 500°C. The first peak located at low temperature (~300°C) is most likely due to the oxidation of adsorbed hydrocarbon species formed from condensed polycyclic compounds (Zheng *et al.*, 2008) and/or possibly comes from the oxidation of ruthenium metal. And the second peaks at 500°C –

600°C, corresponding to the oxidation of deposited carbon species (Zheng *et al.*, 2008), are obviously distinguishable. In addition, a shift of the second peaks to higher temperature with decreasing ruthenium particle size is observed.

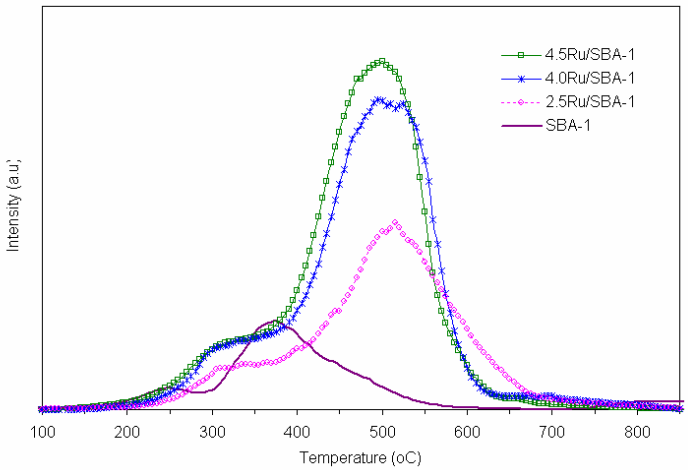

Figure 7.8 TPO profiles of the spent Ru/SBA-1 catalysts

Table 7.2 Coke and sulfur in the spent catalysts

Spent Catalysts	SBA-1	2.5Ru/SBA-1	4.0Ru/SBA-1	4.5Ru/SBA-1
Coke (g/g cat)	0.027	0.061	0.098	0.112
Sulfur (%wt)	-	1.33	1.91	1.99

The quantitative TPO analysis data calculated the temperatures in the range of 250°C – 850°C are shown in **Table 7.2**. It is clearly seen that all Ru-based catalysts produce the higher amount of coke than SBA-1. And, the amount of coke increases in the following order: SBA-1 < 2.5Ru/SBA-1 < 4.0Ru/SBA-1 < 4.5Ru/SBA-1.

Elemental analysis gives the sulfur content in the feed (waste tire) is 1.77±0.01 %wt. Consequently, a considerable amount of sulfur-containing polar-aromatic compounds was produced from waste tire pyrolysis **(Figure 7.7C)**. The sulfur-containing compounds can deactivate the noble metal-supported catalysts by

the strong bonding between sulfur and metal atoms (Eliche-Quesada *et al.*, 2006; Naccache *et al.*, 1973). The metal-support interaction plays an important role in changing the strength of the bonding interaction between sulfur and metal (Jacquin *et al.*, 2003; Naccache *et al.*, 1973; Poondi and Vannice, 1996). In addition, a stronger interaction between metal and support also helps prevent sintering during reaction, resulting in a slower deactivation of the catalyst (Eliche-Quesada *et al.*, 2006). Besides, the sulfur tolerance might also be enhanced by changing the metal particle size (Eliche-Quesada *et al.*, 2006). According to the results of elemental analysis for sulfur contents in the spent catalysts given in **Table 7.2**, 2.5Ru/SBA-1 exhibits the highest sulfur tolerance among Ru-supported catalysts due to its lowest sulfur content, which is probably caused by its strongest interaction between metal and support and smallest ruthenium particle. Consequently, 2.5Ru/SBA-1 exhibits the highest catalytic activity with the least coke formation. The other samples, which have bigger ruthenium particles, display much lower catalytic activity due to their low dispersion and resistance to coke formation.

7.1.5 Conclusions

The roles of ruthenium and the effect of calcination rate in the catalytic pyrolysis of waste tire with Ru/SBA-1 catalysts have been studied. SBA-1 was selected as the support since it was proven to be catalytically inactive and its structure retained after reaction. The presence of ruthenium sites strongly increased the yield of gaseous products, approximately 2 times as compared to thermal pyrolysis. And, ruthenium clusters were found to be the active sites for poly- and polar-aromatic hydrocarbons (PPAHs) reduction, leading to a good light oil production. However, they also decreased saturates in the derived oils.

The heating rates during the calcination step strongly influenced the catalytic activity of Ru/SBA-1 catalysts. Different heating rates resulted in the formation of different ruthenium particle sizes on the catalyst. And, the catalyst calcined with a heating rate of 5°C/min (denoted as 2.5Ru/SBA-1) exhibited the highest activity on the poly- and polar-aromatic reduction and on the consequent

light oil production. Catalyst characterization results indicated that the smallest mean ruthenium particle size and the strongest interaction between Ru and supported resulting in the highest sulfur tolerance and coke resistance were the cause for the highest activity of this catalyst.

7.2 MCM-41

A meso- and macro-pore type of zeolites was reported to promote the selectivity to propylene (Jung *et al.*, 2005). Additionally, mesoporous silica MCM-41 showed interesting results in waste plastic degradation (Seddegi *et al.*, 2002). Namely, the carbon number distribution shifted to lower number, and the authors also observed the carbenium ion cracking mechanism over this material. Furthermore, our previous study showed that the acid catalyst promoted not only cracking but also oligomerization reaction, and the higher the acid density, the latter reaction is more preferable (Dung *et al.*, 2009).

In the present study, a pure silica MCM-41 was first synthesized via silatrane route, and then 2%Ru/MCM-41 was prepared by the conventional impregnation technique. The prepared samples were used as catalysts in the pyrolysis of waste tire aiming at a high production of light olefins (ethylene and propylene) yield and simultaneously a high reduction of polycyclic aromatics in the derived oils.

The experimental results showed that the presence of catalysts strongly influenced the yield and nature of products. Namely, the gas yield increased at the expense of liquid yield. In addition, a considerable high yield of light olefins, 4 times higher than non-catalytic pyrolysis, can be achieved for Ru/MCM-41 catalyst. Furthermore, the uses of catalysts produced much lighter oil and there was a drastic increase in the concentration of single ring aromatics in accordance a reduction in polycyclic aromatic compounds in the derived oils. Ru/MCM-41 produced the lightest oil and the oil has the highest concentration of mono-aromatics. The high activity of catalysts, particularly Ru/MCM-41 is discussed in relation with the catalyst

characterization results obtained from various techniques including TPD-NH_3, H_2-chemisorption, XRD, N_2-adsorption/desorption analysis, and TPO as follows.

7.2.1 Catalyst characterization

The XRD patterns of the synthesized and metal-supported MCM-41 are illustrated in **Figure 7.9**. The XRD pattern of the synthesized MCM-41 is very similar to that reported in the literature (Thanabodeekij *et al.*, 2006), indicating the accomplishment of material synthesis. The catalyst composition analyzed by ICP shows a very good consistence between the targeted and true values of Ru loaded. Also, the XRD pattern of Ru-supported MCM-41 sample obviously indicates that the introduction of Ru does not affect the crystal structure of the parent mesoporous material. Moreover, in this pattern neither peak of Ru metal nor Ru compound is observed. This, together with the similar intensity of peaks as compared to MCM-41, suggests a high dispersion of Ru.

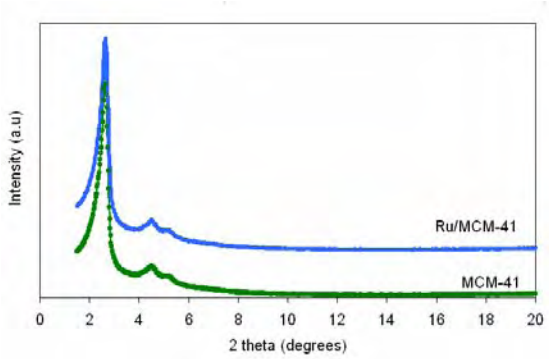

Figure 7.9 XRD patterns of MCM-41 and Ru-supported MCM-41 catalysts

Table 7.3 Physical-chemical properties of the studied catalysts

Samples	Ru (wt %)	Dispersion (%)	Surface area (m^2/g)	Pore diameter (nm)	Asphaltenes (g/g oil)	Coke (g/g catalyst)
MCM-41	-		1454	2.61	0.00064	0.084
Ru/MCM-41	2.02	65.2	1439	2.51	0.00022	0.124

The physical-chemical properties of the fresh catalysts and the amount of coke of the spent ones are displayed in **Table 7.3**. The BET surface area of the synthesized silica MCM-41 is very high and the average pore diameter is approximately 26Å, which well coincides with the data reported in Thanabodeekij *et al.*, (2006). The incorporation of Ru slightly decreases the surface area of the support in association with a reduction in average pore diameter, possibly caused by the diffusion of Ru into the pore. Ru/MCM-41 exhibits a TPR profile (not shown here) having a main reduction peak at 184°C, which is higher than Ru-supported on mesoporous silica doped with zirconium (Eliche-Quesada *et al.*, 2005), indicating stronger metal support interaction. As a result, H_2-chemisorption result indicates a high dispersion of ruthenium on the surface of zeolite support, 65%, which is well consistent with the XRD results.

Figure 7.10 shows the TPD-NH_3 profile of the MCM-41 and Ru/MCM-41 catalysts. It can be seen that the profile of MCM-41 shows 2 desorption peaks with maxima at 150°C and 350°C, respectively. These peaks are broad and low intensive suggesting a good distribution of the acidic sites as well as the low amount of acidic sites. As this zeolite material is composed of pure silica; thus, the acid sites must be contributed from the silanol groups lining the wall of the channels as suggested by Seddegi *et al.*, (2002). Namely, they found that the interactions between the bridging oxygen atoms lining the straight channels and the hydrogen atoms from the polyethylenic chain made the hydrocarbon fragment more basic and, thus, reactive with the silanol groups. This interaction stabilized the carbenium ion formation and allowed its further reactions. The incorporation of ruthenium to MCM-41 slightly decreases the intensity of the desorption peaks, possibly caused by the diffusion of ruthenium particles into the zeolite channels, thus blocking some acidic sites.

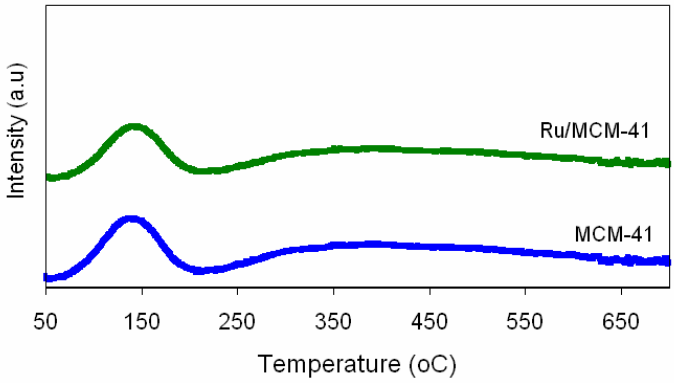

Figure 7.10 TPD-NH_3 profiles of prepared catalysts

Temperature-Programmed Oxidation (TPO) was used to determine the amount of coke deposited on the spent catalysts. TPO profiles (not shown here) of the spent catalysts showed two peaks with maxima located at around 300°C and 500°C. The peak located at low temperature (~300°C) is most likely due to the oxidation of adsorbed hydrocarbon species, which could be formed from condensed polycyclic compounds, whereas the peaks at basically 500°C – 600°C are corresponding to the oxidation of deposited carbon species (Zheng *et al.*, 2008), possibly including some carbon black. Consequently, the catalyst, to a certain extent, can be deactivated by coke deposition. Quantitative analysis showed there is a considerable amount of coke on the spent catalysts; and, Ru/MCM-41 catalyst has the highest amount of coke (**Table 7.3**).

7.2.2 Pyrolysis products

(a) Product yield

Figure 7.11 shows the yields of gas, liquid, and solid product with all catalysts prepared. It can be seen that in the non-catalytic pyrolysis, the yields (wt%) of solid, liquid and gas are approximately 47%, 42% and 11%, respectively. The solid product contains high concentration of carbon black (**Table 7.4**) and some other mineral matters initially present in the tire (Napoli *et al.*, 1997). Therefore, as expected, the yield of solid obtained from all runs is similar. This is attributed to the

fact that the pyrolysis conditions were kept constant and the tire was reported to be completely decomposed at 500°C (Berrueco *et al.*, 2005).

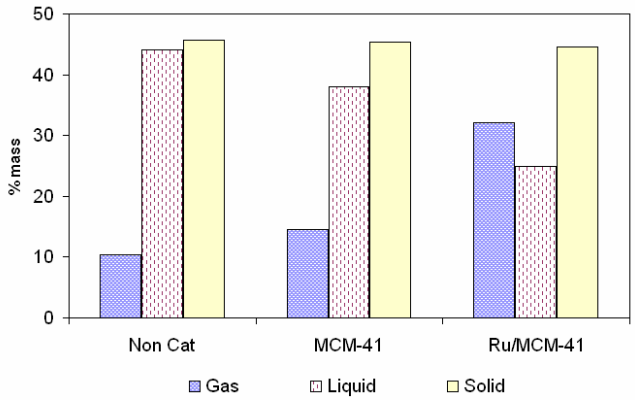

Figure 7.11 The yields of products obtained from thermal and catalytic pyrolysis

The use of catalysts strongly influences the yields of other products. For instance, the gas yield increases from ~ 11 %wt to about 15 %wt and 30 %wt when MCM-41 and Ru/MCM-41 were used, respectively. However, the yield of oil decreases for all prepared catalysts. As revealed from TPD-NH_3 analysis, there is a considerable amount of acidic sites on the surface of the pure silica MCM-41 used in this study. As a result, the presence of MCM-41 might promote the conversion of heavy compounds to the lighter ones due to its cracking activity (Dung *et al.*, 2009), leading to the increase in the yield of gaseous product. A further increase in the yield of gaseous product is observed with the use of Ru/MCM-41 catalyst. This might be attributed to the presence of bifunctionalities of the Ru/MCM-41 catalyst as explained as follows. It is well known that the aromatic compounds are predominant in the liquid product of waste tire pyrolysis (Laresgoiti *et al.*, 2004). The liquid analysis result in the current study also corroborates these results. In addition, the secondary cracking of aromatics is very difficult (Zhichang *et al.*, 2007). Meanwhile, an initial hydrogenation over the metal sites can make these aromatics more reactive for cracking and heteroatoms such as sulfur removal (Ali *et al.*, 2002). Therefore, it is proposed that ruthenium clusters on the support surface, which were reported to

have high hydrogenation activity (Ali *et al.*, 2002), hydrogenate the aromatics, producing (partial) hydrogenated compounds, which rapidly undergo cracking and/or ring-opening on the acid sites. Therefore, a higher amount HCs in the liquid product was cracked when the Ru/MCM-41 was used, resulting in a drastic decrease in the liquid yield as compared to MCM-41 and non-catalytic cases as seen in **Figure 7.11**.

Table 7.4 Hydrogen and carbon contents

	C (wt%)	**H (wt%)**	**H/C***
Non-cat			
Oil	83.7	10.8	**1.54**
Solid	90.6	1.8	-
Gas**	72.6	16.8	**2.77**
MCM-41			
Oil	82.9	11.1	**1.61**
Solid	90.9	1.8	-
Spent catalyst	6.9	0.4	-
Gas**	73.1	15.8	**2.59**
Ru/MCM-41			
Oil	82.1	13.2	**1.93**
Solid	91.2	1.4	-
Spent catalyst	10.9	0.6	-
Gas**	80.8	14.6	**2.17**

*Atomic ratio

** Determined by mass balance.

In this work, the gas analysis is based on hydrogen-free basis; thus, hydrogen is not hereby reported in the gas product. The obtained solid and liquid products were therefore analyzed for their hydrogen and carbon contents in order to

explain the source of hydrogen involved in the production of lighter products. The experimental results are given in **Table 7.4**. From the table, the H/C atomic ratio in the pyrolytic oil increases with the use of catalyst, particularly Ru/MCM-41, whereas that of gas product decreases. It is noted that hydrogen is known to be a co-product of hydrocarbon cracking. For example, the thermal cracking of naphtha gives about 16% H_2 as a co-product, and a tire pyrolysis could give hydrogen as high as 30% by volume (Aylon *et al.*, 2007). Therefore, the decrease in the H/C ratio of the gas (with the increase in this ratio of the pyrolytic oil) indicates the reduction of hydrogen in the gas product. Therefore, it implies that hydrogen in the gas phase, produced from the reactions, is also used in the reactions, contributing to the productions of lighter liquids and less polycyclic aromatics, when the catalysts were used.

(b) Gaseous product

GC analysis results reveal that the pyrolysis gas composes of methane, ethane, ethylene, propane, propylene, C_4-, C_5-, C_6-, C_7- and C_8-hydrocarbons. These compositions of gaseous products are presented in **Figure 7.12**. Such compositions are given as grams of gas component with respect to 100 grams of tire, so that the results with different catalysts can be compared, and information on how the catalysts affect the pyrolysis products may be inferred. It can be seen that for the thermal pyrolysis gas, the yield of C_4 exhibits a maximum value. The high yield of C_4 in the gas obtained from pyrolysis of waste tire was also reported in (Berrueco *et al.*, 2005). This might be attributed to the breakdown of the styrene-butadiene rubber, SBR, a main component of tire (Berrueco *et al.*, 2005). However, as compared to the results reported in the literatures (Laresgoiti *et al.*, 2002), the yield of methane obtained from thermal pyrolysis in our study is relatively higher, possible caused by the different reactor used. In our case, a semi-batch reactor was used and the upper zone of the reactor was also heated in the thermal pyrolysis case. Thus, this high temperature (350°C), to a certain extent, might promote the aromatization reactions (Williams and Taylor, 1993), leading to the production of higher amount of methane (Cypres and Bettens, 1989). This can be proved by the high aromatic content of the

derived oil (~50 wt%) despite the proportion of styrene (aromatic) to butadiene (non-aromatic) in the SBR of the tire is normally 25/75, suggesting that the aromatization reaction had occurred.

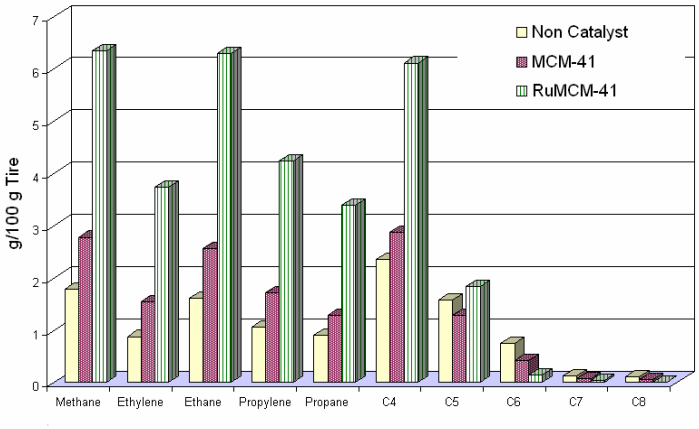

Figure 7.12 Compositions of pyrolysis gas

The introduction of catalyst, particularly Ru/MCM-41 causes an important increase in the yield of gas component having carbon number less than 5, whereas decreases the yield of heavy hydrocarbon ($C \geq 5$). In addition, the catalyst also enhances the selectivity toward light hydrocarbons ($C \leq 4$) in the gas product together with a reduction in heavy hydrocarbon selectivity. This suggests the presence of greater and deeper cracking reactions when the catalysts were used. Besides, Ru also was reported to have ability to crack C_3H_8 (Shiraga *et al.*, 2007). Therefore, in our case possibly Ru also cracks the heavy HCs into the gas product, leading to the higher yield of light hydrocarbons in the gas product as indicated in **Figure 7.12**.

Light olefins, i.e. ethylene and propylene, as mentioned in the introduction part, are among the most important chemicals. There, it is of interest if a catalyst could convert the waste tire to valuable oil and simultaneously to light olefins with a high yield. As one can see from **Figure 7.12**, the yield of light olefins increases with the treatment of catalysts, and the use of Ru/MCM-41 catalyst produces the highest yield of light olefins, approximate 4 times higher as compared

to non-catalytic pyrolysis. This beneficial influence of Ru/MCM-41 might be contributed from the combination effects of Ru and the support. Our previous study (Dung *et al.*, 2009) showed that the acidic catalyst promoted not only cracking but also aromatization/oligomerization reactions. The higher the acid density of the catalyst was, the more preferable the latter reaction occurred. Therefore, the mild acid properties of MCM-41 can promote the cracking reaction to a certain extent, but can not at the same time promote aromatization/oligomerization reactions. Additionally, further oligomerization is suppressed by the rapid elution of the cracking products due to the sizes in meso-pores, and thus high selectivity to propylene becomes possible (Jung *et al.*, 2005). On the other hand, the intermediates of many reactions occurred simultaneously during catalytic pyrolysis might quickly be hydrogenated over ruthenium clusters; thus, the reactions involving the consumption of light olefins, such as alkylation, hydride transfer, are possibly prevented. Also, the acidity of the pure silica MCM-41 was attributed to the silanol groups lining the channels (Seddegi *et al.*, 2002) and, Ru is highly dispersed on the surface of the acid zeolite support (**Table 7.3**). These result in a proper balance between the metal and acid sites, which is a crucial factor affecting the catalytic activity of the bifunctional catalyst (Lugstein *et al.*, 1999). Ru helps promoting the hydrogenation /dehydrogenation reactions, enhancing cracking reaction; thus, more olefins are produced. Therefore, a higher yield of light olefin is achieved. Finally, it should be emphasized that the high yield of light olefins obtained over Ru/MCM-41 catalyst can be compared with that obtained over ZSM-5 catalyst (Williams and Brindle, 2003) but with much lower amount of catalyst used (8 times less).

(c) Oil product

The influence of catalysts on the pyrolysis products can be further depicted by the change in the compositions as well as the distribution of hydrocarbons in the pyrolysis oils. **Figure 7.13** shows the carbon number distribution of the derived oils over C_5 – C_{50} for both thermal and catalytic pyrolysis. Accordingly, the carbon number distribution of the non-catalytic oil is wide but

mainly allocates in the range of C_{10} – C_{20}. The presence of catalyst produces the oil that has a narrower distribution and the peak tends to shift to lower carbon number. And, the highest and narrowest peak is observed over the oil obtained from catalytic pyrolysis with Ru/MCM-41. Besides, the uses of catalysts also lead to a drastic decrease in asphaltenes in the oils, as presented in **Table 7.3**. Thus, to this point, it is safe to conclude that catalytic pyrolysis produces much lighter oil with respect to thermal pyrolysis.

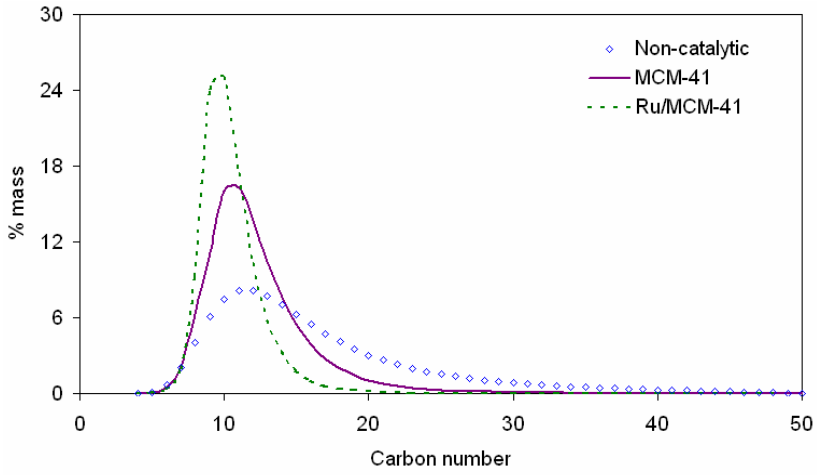

Figure 7.13 Carbon number distribution of pyrolysis oils

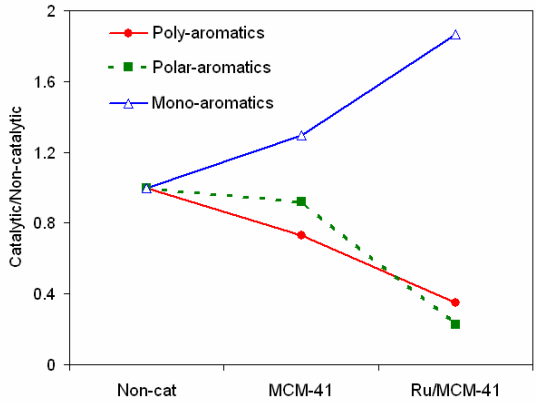

Figure 7.14 Compositions of pyrolysis oils obtained from non-catalytic and catalytic pyrolysis

On the other hand, it is of paramount importance to note that the stringent environmental regulations have limited the content of aromatics in the fuel oils, particularly polycyclic ones (Albertazzi *et al.*, 2003). Therefore, the derived oils were also subjected to analysis for their compositions by mean of the liquid adsorption chromatograph (Sebor *et al.*, 1999) and the results are presented in **Figure 7.14**.

Figure 7.14 displays the ratios of the contents of poly-, polar- and mono-aromatics in the catalytic oils to those in the non-catalytic oil. It can be seen that, for poly- and polar-aromatics, there exist a heavy drop of these ratios, indicating a drastic decrease in the contents of these compounds in the oils obtained from catalytic pyrolysis. In contrast, the yield of mono-aromatics in the liquid product increases with the treatment of catalysts, and reaches the highest value when Ru/MCM-41 was used. These results together with the shift of hydrocarbon distribution to the lower carbon number (**Figure 7.13**) suggest the conversion of polycyclic aromatics (higher carbon number) to the single ring aromatic compounds (lower carbon number). And the highest conversion is achieved with using bifunctional catalyst, Ru/MCM-41.

As revealed from TPD-NH_3 analysis, MCM-41 has a considerable amount of acidic sites on its surface and these sites might be attributed to the slight reduction in polycyclic aromatics, including poly- and polar-aromatics, in the derived oil as well as the shift to lower carbon number of hydrocarbon distribution (Dung *et al.*, 2009a). The presence of the ruthenium clusters on the surface of MCM-41 leads to a dramatic reduction of the polycyclic aromatics in the oil. It is well known that Ru-supported acidic zeolite catalysts exhibit high aromatic hydrogenation activity (Ali *et al.*, 2002). Therefore, polycyclic aromatics might be hydrogenated over ruthenium sites. And, due to the high dispersion of ruthenium (**Table 7.3**), the (partial) hydrogenated might be quickly transferred to the acidic sites of the support undergoing cracking and/or ring-opening reactions. More importantly, the hydrogenation of polycyclic aromatics is much preferable than their corresponding single ring aromatics (Corma *et al.*, 1997). Meanwhile, the hydrogenation of polycyclic

aromatics generally can be achieved only partial hydrogenation (Jacquin *et al.*, 2003). These phenomena probably explain the increase in the concentration of mono-aromatics at the expense of polycyclic aromatics observed when Ru/MCM-41 was used. And consequently, the produced oil has a much narrower carbon distribution, and the peak shifts to the lowest carbon number (**Figure 7.14**). However, although to a small extent, the high amount of coke generated on the spent catalysts should not be excluded for the reduction of polycyclic aromatics in the derived oils since this coke could have been formed from the condensation of polycyclic aromatics (Dung *et al.*, 2009a), as well as the polar-aromatics (Dung *et al.*, 2009b). Summarily, the catalytic pyrolysis with Ru/MCM-41 produced not only lighter oil, but also contains lower concentrations of poly- and polar-aromatics.

7.2.3. Conclusions

Catalytic pyrolysis of waste tire using a pure silica MCM-41 and Ru/MCM-41 catalysts have been investigated in relation to the yield and nature of the obtained products. It was found that the presence of catalysts caused a dramatic increase in the yield of gaseous product at the expense of the liquid yield, particularly for Ru/MCM-41. Additionally, the compositions of the gas obtained were shown to be strongly dependent on the catalysts. Especially, a considerable high yield of light olefins, i.e. ethylene and propylene, (4 times higher) was achieved over Ru/MCM-41.

In addition, catalytic pyrolysis using current catalysts produced much lighter oil as compared to non-catalytic oil. Moreover, the catalytic oils have higher concentration of single ring aromatics and less poly- and polar-aromatics. Ru-supported MCM-41 synthesized via silatrane route was considered as a good catalyst in the pyrolysis of waste tire, since it can obtain light oil with high concentration of single ring aromatics and low contents of polycyclic aromatics and simultaneously a high yield of light olefins. The high activity of Ru supported MCM-41 was attributed to: (i) the high dispersion of Ru as well as the nature of this metal to effectively catalyze hydrogenation reaction, and (ii) the suitable acid and topology properties of the support.

7.3 MCM-48

Mobil Composition of Matter (MCM) is the name given for a series of mesoporous materials. The MCM-48 is one of three phases of the mesoporous materials, which is cubic crystalline structure. The MCM-48 in this work was synthesized from silatrane route, and Ru metal was loaded by wetness impregnation. This work investigated the activity and selectivity of MCM-48 and Ru/MCM-48 used as the catalysts for waste tire pyrolysis. The results showed that Ru/MCM-48 improved the gas yield. In addition, the use of Ru/MCM-48 catalyst produced light olefins twice as much as non-catalytic pyrolysis. On the other hand, the catalyst helped to improve the oil quality by increasing light oil portion. Furthermore, it also reduced poly- and polar- aromatic compounds and sulfur content in the derived oil. Surface Area Analysis, XRD, and CHNS Analysis were performed to explain the experimental results. The details are discussed as follows.

7.3.1 Catalyst characterization

The XRD patterns of synthesized MCM-48 and Ru-supported MCM-48 are presented in Fig.1. Only one peak of the both samples is detected at $2\theta = 2.2°$, which is the unique peak. The peak corresponding of Ru metal is generally obtained at 38°, 42°, 44°, and 58° (Perring *et al.*, 1998). However, it is rarely detected because of low amount of metal loaded (0.7%wt). The loaded ruthenium metal does not affect the crystal structure.

The physical properties of fresh catalysts are shown in **Table 7.5**. The BET surface area and B.J.H. pore volume of the synthesized MCM-48 are 1,405 m^2/g and 0.87 cm^3/g, respectively. Moreover, the average pore diameter of synthesized MCM-48 is 35.9 Å. The covering of Ru metal causes the dramatic reduction in surface area. In addition, the reductions of pore volume and pore diameter are caused by Ru metal, which covers the pore of synthesized MCM-48.

Dr. Sirirat Jitkarnka
Associate Professor
The Petroleum and Petrochemical College
Chulalongkorn University

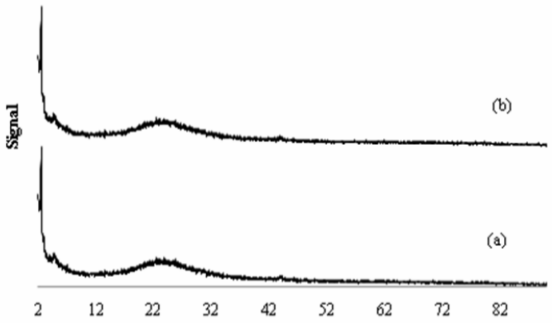

Figure 7.15 XRD Pattern of catalysts: (a) MCM-48, and (b) 0.7%Ru/MCM-48

Table 7.5 Physical properties of studied catalysts.

	Surface area (m^2/g)*	**Pore volume B.J.H. (cm^3/g)****	**Pore diameter (Å)****
MCM-48	1,405	0.87	35.87
0.7% Ru/MCM-48	915.7	0.63	32.94

***BET method, **B.J.H. method

7.3.2 Pyrolysis Products

According to **Figure 7.16**, the non-catalytic pyrolysis can produce that the yield of gas, oil, and solid char of approximately 13%, 40%, and 47%, respectively. The use of MCM-48 can produce the gas yield of about 23%, and its production is higher than the non-catalytic case by 10%. Furthermore, Ru metal loading on MCM-48 also improves the gas production by 3% higher than the MCM-48 case. Moreover, the synthesized MCM-48 and Ru-supported MCM-48 decrease the oil production. They can produce less oil than the non-catalytic case by 7%, and 8%, respectively. MCM-48 is synthesized by silatrane route; therefore, it is not an acidic material. However, the effect on gas production of synthesized MCM-48 is through the 3D pore structure (Rodtiguez *et al.*, 2001), which holds up the reactants inside its pore long enough that hydrocarbons have great mass transfer to undergo cracking reaction in the porous MCM-48. Moreover, the acidity of synthesized MCM-48 is less than other acidic zeolites such as MOR, and Beta; therefore, it has

the low amount of coke deposition. The activity of catalyst is maintained because of the low amount of coke deposition (Lan-Lan and Shuangxi, 2005). Furthermore, the Ru loading on the MCM-48 increases gas production. Ru metal, which is the metal sites, promotes the hydrogenation reaction of aromatic hydrocarbons, which are subsequently cracked and undergo ring-opening reaction in the pore of MCM-48.

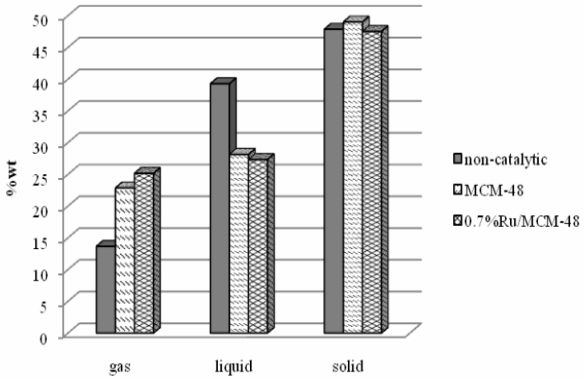

Figure 7.16 Product distribution of pyrolysis product from using 0.7% Ru/MCM-48 catalysts

The gas fractions are composed of methane, ethylene, ethane, propylene, propane, C4-, C5-, C6-, C7-, and C8-hydrocarbons. It was found that the gas consisted of 0.233% H_2, and 0.423% CO_x for the non-catalytic case (Alsobaai *et al.*, 2007). **Figure 7.17** shows the composition of pyrolytic gas obtained from this work. The use of synthesized MCM-48 can drastically improve methane, ethane, and especially C4-, and C5-hydrocarbons. The C4- and C5-hydrocarbons productions are high in the gas because tires originally consisted of high butadiene and isoprene; hence, hydrocarbons chains tend to be cracked to the monomers. Moreover, the increment of C5-hydrocarbon might be resulted from the 3D pore structure of MCM-48, which maintains hydrocarbon molecules, and then gas molecules combine with then to larger gas molecules. Ru loaded catalyst produces the same gas yields as those of the synthesized MCM-48, except C5-hydrocarbons. Ru/MCM-48 can produce the significantly high amount of C5-hydrocarbons as compared to the other gases. Ru metal was reported that it can crack heavy hydrocarbons to gas products

(Berrueco, *et al.*, 2005). The increment of C5-HCs occurs from Ru metal that cracks heavy HCs to gas product, but MCM-48 combines with resulted light gas with converting other gases to C5-HCs. According to **Figure 7.17**, MCM-48 and Ru/MCM-48 show that they can produce high light olefins, which consist of ethylene and propylene in the gas composition. They can convert invaluable waste tire to valuable products at a high yield of light olefins. When Ru metal is loaded on MCM-48, the Ru/MCM-48 can improve the efficiency on light olefins selectivity. Due to the non-acidity of synthesized MCM-48, it can preserve light olefins molecules, and these molecules are not over-cracked to other HCs. Additionally, the meso-pore of MCM-48 gives higher selectivity of propylene than that of ethylene. Although, Ru metal also converts heavy HCs to gas product, ethylene and propylene are still slightly improved due to the higher gas production by Ru.

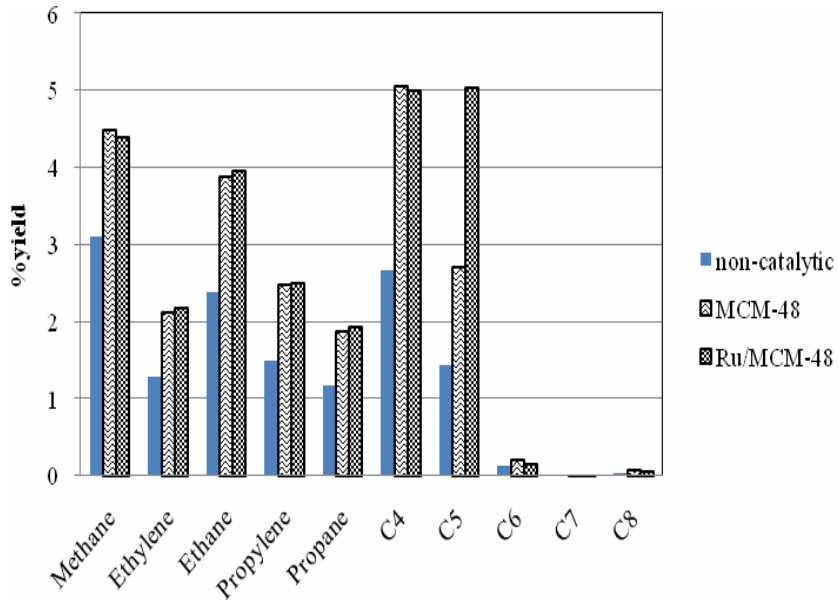

Figure 7.17 Composition of pyrolytic gas

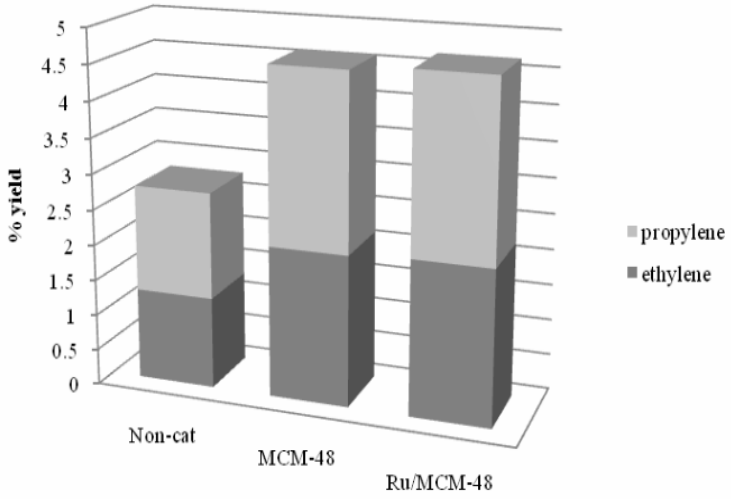

Figure 7.18 Light olefins production from using synthesized MCM-48 and Ru/MCM-48 catalysts

Furthermore, the catalysts can improve the quality of pyrolytic oils. As shown in **Table 7.6**, the amount of asphaltene is reduced with using the synthesized MCM-48 and Ru supported MCM-48. It can be seen that synthesized MCM-48 has cracking ability; accordingly, the large HCs such as poly- and polar-aromatic can be cracked to smaller molecules. Thus, the synthesized MCM-48 dramatically reduces asphaltene. However, the Ru-loaded MCM-48 does not reduce the amount of asphaltene as compared to synthesized MCM-48; instead it slightly increases asphaltene.

In **Figure 7.19**, the molecular fractions, obtained from the liquid chromatography column, indicate that the synthesized MCM-48 causes the increment of mono-, and di-aromatic HCs in accordance with decreasing saturated, poly-, and polar-aromatic HCs. As previously explained, the non-acidic MCM-48 has mild cracking activity with meso pore size allowing large molecules to enter; thus, the amounts of poly- and polar-aromatic slightly decrease. In addition, saturated HCs are found decreasing as well. On the other hand, Ru loading on the MCM-48 support can dramatically improve saturated HCs in accordance with decreasing all aromatic

compounds as compared to the synthesized MCM-48 case. Absolutely, Ru metal can promote high hydrogenation reaction. Consequently, multi-ring aromatics, especially poly- and polar-aromatic HCs, can be hydrogenated by the metal sites. It can be explained that saturated HCs are increased at the expense of aromatic compounds from using the Ru/MCM-48 catalyst. **Table 7.6** also shows that Ru/MCM-48 insignificantly reduces the amount of sulfur in oil, and sulfur deposition on the catalyst does not charge as compared to the non-catalytic case since the mild cracking activity of MCM-48, that cannot break C-S bonds in the pyrolytic oil. Due to less C-S bond cracking activity, sulfur deposition on the spent catalysts is low as well.

Table 7.6 The amount of asphaltene in oil, sulfur deposition on spent catalysts, and sulfur in oils

	%Asphaltene	**%Sulfur deposition on spent catalysts**	**%Sulfur in oils**
non-catalytic	0.71	-	0.73
MCM-48	0.2	0.43	0.69
Ru/MCM-48	0.28	0.43	0.69

Since the coke deposition on the catalyst is in the form of poly- and polar-aromatic HCs (Dung *et al.*, 2008), the amount of sulfur deposition on the catalyst is proportional to that of coke deposition. With low cracking activity, the amount of coke is low as well. It is summarized that catalytic pyrolysis with using Ru/MCM-48 not only improves gas and light olefins yield, but also reduce poly- and polar-aromatic in the pyrolytic oil.

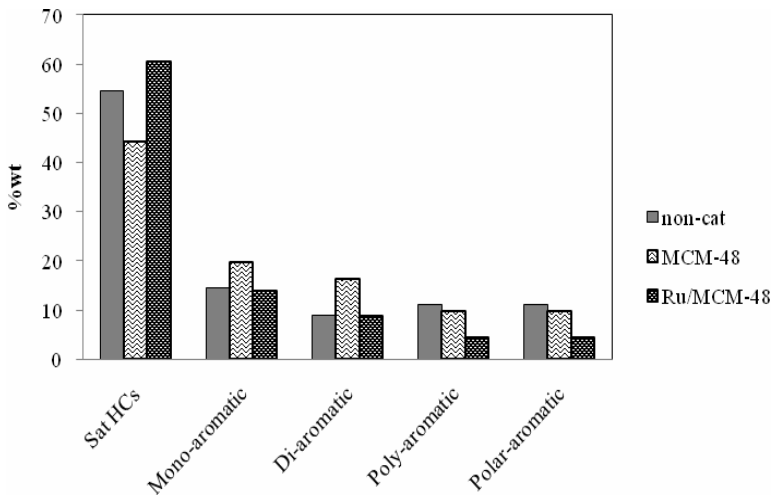

Figure 7.19 Molecular compounds in oils from using synthesized MCM-48 and Ru/MCM-48 catalysts

7.3.3 Conclusions

The catalytic pyrolysis of waste tire with using MCM-48 and 0.7% Ru/MCM-48 was performed in this work. The synthesized MCM-48 gave the dramatic improvement of gas production as compared to the non-catalytic case in accordance with decreasing the oil production, and Ru supported MCM-48 also increased the gas yield further from using pure MCM-48. Moreover, both MCM-48 and 0.7% Ru/MCM-48 enhanced the light olefins production.

Furthermore, the catalysts can improve the quality of oil. Ru/MCM-48 gave the lighter oil as compared to the non-catalytic case. In particular, the maltene from using Ru/MCM-48 catalyst had the high concentration of saturated-hydrocarbons and low poly-, and polar-aromatic hydrocarbons.

The high activity and selectivity of Ru/MCM-48 is attributed to that its mild cracking activity, maintaining light olefins. The 3D pore structure of MCM-48 allowed high mass transfer, which improved overall reaction. Moreover, Ru metal site has improved cracking activity

References

Aboul-Gheit, A.K., Aboul-Fotouh, S.M., and Aboul-Gheit, N.A.K., (2005). Hydroconversion of cycloexene using catalysts containing Pt, Pd, Ir and Re supported on H-ZSM-5 zeolite. Applied Catalysis A: General, 283, 157-164.

Aboul-Gheit, A.K., Aboul-Fotouh, S.M., and Aboul-Gheit, N.A.K., (2005). Effect of combining palladium, iridium or rhenium with platinum supported on H-ZSM-5 zeolite on their cyclohexene hydroconversion activites. Applied Catalysis A: General, 292, 144-153.

Adam, J., Blazso, M., Meszaros, E., Stocker, M., Nilson, M.H., Bouzga, A., Hustad, J.E., Gronli, M. and Oye, G. (2005). Pyrolysis of biomass in the presence of Al-MCM-41 type catalysts. Fuel, 84, 1494-1502.

Aguado, J., Serrano, D.P., San Miguel, G., Escola, J.M., and Rodrı´guez, J.M. (2006) Catalytic activity of zeolitic and mesostructured catalysts in the cracking of pure and waste polyolefins. Journal of Analytical and Applied Pyrolysis, 78, 153–161.

Akhmedov, V.M. and Al-Khowaiter, S.H. (2000) Hydroconversion of hydrocarbons over Ru-containing supported catalysts prepared by metal vapor method. Applied catalysis A: General, 197, 201-212.

Albertazzi, S., Ganzerla, R.,Gobbi, C., Lenarda, M., Mandreoli, M., Salatelli, E., Savini, P., Storaro, L., and Vaccari, A. (2003). Hydrogenation of naphthalene on noble-metal-containing mesoporous MCM-41 aluminosilicates. Journal of Molecular Catalysis A: Chemical, 200, 261–270.

Ali, M.A., Kimura, T., Suzuki, Y., Al-Saleh, M.A., Hamid, H., Inui, T. (2002) Hydrogen spillover phenomenon in noble metal modified clay-based hydrocracking catalysts. Applied Catalysis A: General, 27, 63-72.

Alsobaai, A.M., Zakaria, R., and Hameed, B.H. (2007). Hydrocracking of petroleum gas oil over NiW/MCM-48-USY composite catalyst. Fuel Processing Technology. 88, 921-928.

Álvarez-Rodríquez, J.A., Guerrero-Ruiz, A., Rodríguez-Ramos, I., and Arcoya-Martín, A. (2005). Modifications of the citral hydrogenation selectivities over Ru/KL-zeolite catalysts induced by the metal precursors. Catalysis Today, 107–108, 302–309.

Álvarez-Rodríquez, J.A., Guerrero-Ruiz, A., Rodríguez-Ramos, I., Arcoya-Martín, A., and Miriam Cerro-Alarcon. (2008). Effect of nickel precursor and the copper addition on the surface properties of Ni/KL-supported catalysts for selective hydrogenation of citral. Applied Catalysis A: General, 348, 241–250.

Álvarez-Rodríquez, J.A., Guerrero-Ruiz, A., Rodríguez-Ramos, I., and Arcoya-Martín, A. (2008). Structure changes on RuCu/KL bimetallic catalysts as evidenced by n-hexane reforming. Catalysis Today, 133–135, 793–799.

Antonakou, E., Lappas, A., Nilsen, M.H., Bouzga, A. and Stocker, M. (2006). Evaluation of various types of Al-MCM-41 materials as catalysts in biomass pyrolysis for the production of bio-fuels and chemicals. Fuel.

Arribas, M.A., Concepción, P. and Martinez, A. (2004a). The role of metal sites during the coupled hydrogenation and ring opening of tetralin on bifunctional Pt(Ir)/USY catalysts. Applied catalysis A: General, 267, 111-119.

Arribas, M.A., Corma, A., Diaz-Cabanas, M.J. and Martinez, A. (2004b). Hydrogenation and ring opening of tetralin over bifunctional catalysts based on the new ITQ-21 zeolite. Applied catalysis A: General, 273, 277-286.

Arribas,M.A., Corma,A., Díaz-Cabañas., and M.J., Martínaz, A. (2004c) Hydrogenation and ring opening of Tetralin over bifunctional catalysts based on the new ITQ-21 zeolite. Applied Catalyst A: General, 273, 227-286.

Aylón, E., Fernández-Colino, A., Murillo, R., Navarro, M.V., García T., and Mastral, A.M. (2009). Valorisation of waste tyre by pyrolysis in a moving bed reactor. Waste Management, 30, 1,220-1,224.

Baldovino-Medrano, V.G., Giraldo, S.A., and Centeno, A. (2008) The functionalities of Pt/γ-Al2O3 catalysts in simultaneous HDS and HDA reactions. Fuel 87, 1,917–1,926.

Barbier, J., Lamy-Pitara, E., Maracot, P., Boitiaux, J.P., Cosyns, J., Verna, F. (1990) Role of Sulfur in Catalytic Hydrogenation Reactions. Advanced in Catalysis, 37, 279-

Barbooti, M.M., Mohamed, T.J., Hussain, A.A. and Abas, F.O. (2004). Potimization of pyrolysis conditions of scrap tires under inert gas atmosphere. Journal Analytical and Applied Pyrolysis, 72, 165-170.

Barrer, R.M. and Villiger, H. (1969). Crystal structure of synthetic zeolite L. Crystallography, 128, 352−361.

Bécue, T., Maldonado-Hodar, F.J., Antunes, A.P., Silva, J.M., Ribeiro, M.F., Massiani, P., and Kermarec, M. (1999). Influence of Cesium in Pt/NaCsβ on the Physico-Chemical and Catalytic Properties of the Pt Clusters in the Aromatization of n-Hexane. Journal of Catalysis, 181, 244-255.

Benallal, B., Roy, C., Pakdel, C., Chabot, S., Poirier, M.A.(1995) Characterization of pyrolytic light naphtha from vacuum pyrolysis of used tyres comparison with petroleum naphtha. Fuel 74, 1589-1594.

Berrueco, C., Esperanza, E., Mastral, F.J., Ceamanos, J. and Garcia-Bacaicoa, P. (2005). Pyrolysis of waste tyres in an atmospheric static-bed batch reactor: Analysis of gases obtained. Journal of Analytical and Applied Pyrolysis, 74, 245-253.

Blasco, T., Corma, A., Díaz-Cabañas, Rey, F., Rius, J., Sastre, G., and Vidal-Moya, J.A. (2004) Synthesis, Characterization, and Framework Heteroatom Localization in ITQ-21. Journal of American Chemical Soceity, 126, 13,414-13,423.

Blow, C.M. and Hepburn. M. (1982) Rubber technology and manufacture, 2nd Edition, Butterworths, Norwich.

Boxiong, S., Chunfei, W., Binbin, G., Rui, W., Cai, L. (2007a) Pyrolysis of waste tyres with zeolite USY and ZSM-5 catalysts. Applied Catalysis B: Environmental, 73, 150-157.

Boxiong, S., Chunfei, W., Rui, W., Binbin, G. and Cai, L. (2007b). Pyrolysis of waste tyres: The influence of USY catalyst/tyre ratio on products. Journal Analytical and Applied Pyrolysis, 78, 243-249.

Can, F., Travert, A., Ruaux, V., Gilson, J.-P., Maugéa, F., Hub, R., Wormsbecher, R.F. (2007) FCC gasoline sulfur reduction additives: Mechanism and active sites. Journal of Catalysis, 249, 79–92.

Carter, J.L., McVicker, G.B., Weissman, W., Kmak., W.S., and Sinfelt, J.H. (1982). Bimetallic Catalysts; Application in Catalytic Reforming. Applied Catalysis, 3, 327-346.

Chaiyavech, P. and Grisadanurak, N. (2000) Petroleum Technology. pp. 55-56 Department of Chemical Technology, Faculty of Science, Chulalongkorn University.

Charoenpinijkarn, W., Suwankruhasn, M., Kesapabutr, B., Wongkasemjit, S., and Jamieson, A.M. (2001) Sol–gel processing of silatranes. European Polymer Journal, 37, 1,441-1,448.

Chen, F. and Qian, J. (2002) Studies on the thermal degradation of *cis*-1,4-polyisoprene. Fuel, 81, 2071–2077.

Choi, S-S. (2000). Characterization of bound rubber of filled styrene-butadiene rubber compounds using pyrolysis-gas chromatography. Journal of Analytical and Applied Pyrolysis, 55, 161-170.

Choosuton A. (2007). Development of Waste Tire Pyrolysis for the Production of Commercial Fuels: Effect of Noble Metals and Supports . M.S. Thesis, The Petroleum and Petrochemical College, Chulalongkorn University, Bangkok, Thailand.

Chupin, J., Gnep, J.N., Lacombe, S., and Guisnet, M. (2001) Influence of the metal and of the support on the activity and stability of bifunctional catalysts for toluene hydrogenation. Applied Catalysis A: General, 206, 43-56.

Contreras, R., Cuevas-Garcia, R., Ramirez J., Ruiz-Azuara, L., Gutierrez-Alejandre, A., Puente-Lee, I., Castillo-F P., and Salcedo-Luna, C. (2008). Transformation of thiophene, benzothiophene and dibenzothiophene over Pt/HMFI, Pt/HMOR and Pt/HFAU: Effect of reactant molecular dimensions and zeolite pore diameter over catalyst activity, Catalysis Today, 130, 320–326.

Corma, A., Martinez, A. and Martinez-Soria, V. (1997). Hydrogenation of Aromatics in diesel fuels on Pt/MCM-41 catalysts. Journal of Catalysis, 169, 480-489.

Corma, A. and Orchilliés, A.V. (2000) Current views on the mechanism of catalytic cracking. Microporous and Mesoporous Material, 35-36, 21-30.

Corma A.,. Gonz´ alez-Alfaro, V., and Orchill´esy, A. V. (2001) Decalin and Tetralin as Probe Molecules for Cracking and Hydrotreating the Light Cycle Oil. Journal of Catalysis, 200, 34–44.

Corma, A., Diaz-Cabanas, M.J., Martinez-Triguero,J., Rey, F., and Rius, J. (2002) A large-cavity zeolite with wide pore windows and potential as and oil refining catalyst. Nature , 418, 514-517.

Crisafulli, C., Scire, S., Minico, S., and Solarino, L. (2002) Ni–Ru bimetallic catalysts for the CO_2 reforming of methane. Applied Catalysis A: General, 225, 1-9.

Cunliffe, A.M. and Williams, P.T. (1998) Composition of oils derived from the batch pyrolysis of tyres. Journal of Analytical and Applied Pyrolysis, 44,131-152.

Cypres, R., and Bettens, B., in: G.L. Ferrero, G.L., and Maniatis, K. (Eds.), Pyrolysis and Gasification, Elsevier Applied Science, Barking, UK, 1989, 209.

Dai, X., Yin, X., Wu, C., Zhang, W., and Chen, Y. (2001). Pyrolysis of waste tires in a circulating fluidized-bed reactor. Energy, 26, 385-399.

Dean, J.A. Lange's Handbook of Chemistry, Fifteenth edition, McGrawHill, New York, 1999.

Diez, C., Martinez, O., Calvo, L.F., Cara, J. and Moran, A. (2004). Pyrolysis of tyres. Influence of the final temperature of the process on emission and calorific value of the product recovered. Waste Management, 24, 463-469.

Du, H., Fairbridge, C., Yang, H. and Ring, Z. (2005). The chemistry of selective ring-opening catalysts. Applied catalysis A: General, 294, 1-21.

Dũng, N.A, Wongkasemjit, S., and Jitkarnka, S. (2009). Effects of pyrolysis temperature and Pt-loaded catalysts on polar-aromatic content in tire-derived oil. Applied Catalysis B: Environmental, 91, 300–307.

Dũng, N.A., Mhodmonthin, A., Wongkasemjit, S., and Jitkarnka, S. (2008). Effects of ITQ-21 and ITQ-24 as zeolite additives on the oil products obtained

from the catalytic pyrolysis of waste tire. Journal Analytical and Applied. Pyrolysis, 85, 338–344.

Dupain, X., Rogier, L.J., Gamas, E.D., Makkee, M., Moulijn, J.A. (2003). Cracking behavior of organic sulfur compounds under realistic FCC conditions in a microriser reactor, Applied Catalysis A: General, 238, 223–238.

Ekinci, E., Yardim, F., Razvigorova, M., Minkova, V., Goranova. M., Petrov, N., and Budinova, T. (2002). Characterization of liquid products from pyrolysis of subbituminous coals. Fuel Processing Technology, 77-78, 309-315.

Eliche-Quesada, D., Merida-Robles, J.M., Rodríguez-Castellon, E., and Jiménez-Lopez, A. (2005) Ru, Os and Ru–Os supported on mesoporous silica doped with zirconium as mild thio-tolerant catalysts in the hydrogenation and hydrogenolysis/hydrocracking of tetralin. Applied Catalysis A: General, 279, 209-221.

Eliche-Quesada, D., Macias-Ortiz, M.I., Jimenez-Jimenez, J., Rodriguez-Castellon, E., and Jimenez-Lopez, J. (2006) Catalysts based on Ru/mesoporous phosphate heterostructures (PPH) for hydrotreating of aromatic hydrocarbons. Journal of Molecular Catalysis A: Chemical, 225, 41-48.

Eliche-Quesada, D., Meria-Robles, J.M., Rodriguez-Castellon, E., and Jimenez-Lopez. A. (2006) Influence of the incorporation of palladium on Ru/MCM hydrotreating catalysts. Applied Catalysis B: Environmental, 65, 118-126;

Eliche-Quesada, D., Rodríguez-Castellon, E., and Jiménez-Lopez, A. (2007) Hydrodesulfurization activity over supported sulfided ruthenium catalysts: Influence of the support. Microporous and Mesoporous Material, 99, 268-278.

Escobar, A.S., Pereira, M.M., and Cerqueira, H.S. (2008) Effect of iron and calcium over USY coke formation. Applied Catalysis A: General, 339, 61-67.

Fan, Y., Bao, X., Lei, D., Shi, G., Wei, W. and Xu, J. (2005). A novel catalyst system based on quadruple silicoaluminophosphate and aluminosilicate zeolite for gasoline upgrading. Fuel, 84, 435-442.

Fesi, A., Palinko, I. and Kiricsi, I. (1999). Ring opening and Dimerization reactions of methyl and dimethyloxiranes on HZSM-5 and CuHZSM-5 zeolite. Journal of Catalysis, 188, 385-392.

Friend and Chen, 1997 (loss of record)

Galvagno, S., Casu, S., Carsabianca, T., Calabrese, A. and Cornacchia, G. (2002). Pyrolysis process of the treatment of scrap tyres: Preliminary experimental results. Waste Management, 22, 917-923.

Galvagno, S., Casu, S., Casablanca, T., Calabrese, A., and Cornacchia, G. (2002) Pyrolysis process for the treatment of scrap tyres: preliminary experimental results. Waste Management, 22, 917-923.

Gao, S. and Schmidt, L.D. (1989) Effect of oxidation-reduction cycling on C_2H_6 hydrogenolysis: Comparison of Ru, Rh, Ir, Ni, Pt, and Pd on SiO_2. Journal of Catalysis, 115, 356-364.

Gault, 1981 (loss of record)

Gong Y., Dou T., Kang S., Li Q., and Hu Y. (2009). Deep-desulfurization of gasoline using Ag/BETA. Fuel processing technology, 90, 122-129.

Harris, S. and Chianelli, R.R. (1984) Catalysis by transition metal sulfides: The relation between calculated electronic trends and HDS activity. Journal of Catalysis, 86, 400 - 412.

Ishihara, A., Dumeignil, F., Lee, J., Mitsuhashi, K., Qian, E.W., and Kabe, T. (2005) Hydrodesulfurization of sulfur-containing polyaromatic compounds in light gas oil using noble metal catalysts. Applied Catalysis A: General, 289, 163-173.

Islas-Flores, C.A., Buenrostro-Gonzalez, E., and Lira-Galeana, C. (2006) Fractionation of petroleum resins by normal and reverse phase liquid chromatography. Fuel, 85, 1,842-1,850.

Jacobs, G., Alvarez, W.E., and Resasco, D.E. (2001). Study of preparation parameters of powder and pelletized Pt/KL catalysts for n-hexane aromatization, Applied Catalysis A: General, 267-282.

Jacquin, M., Jones, D.J., Rozière, J., Albertazzi, S., Vaccari, A., Lenarda, M., Storaro, L., and Ganzerla, R. (2003). Novel supported Rh, Pt, Ir and Ru mesoporous aluminosilicates as catalysts for the hydrogenation of naphthalene. Applied Catalysis A: General, 251, 131–141.

Jada, A. and Chaou, A.A. (2003). Surface properties of petroleum oil polar fraction as investigated by Zetametry and DRIFT spectroscopy. Journal of Petroleum Science and Engineering, 3, 287-296.

Jang, J. W., Yoo, T. S., Oh, J. H., and Iwasaki, I. (1998). Discarded tire recycling practices in the United States, Japan and Korea, Resources, Conservation and Recycling, 22, 1-14.

Jitkarnka, S., Chusaksri, B., Supaphol, B., and Magaraphan, R. (2007) Influences of thermal aging on properties and pyrolysis products of tire tread compound. Journal of Analytical and Applied Pyrolysis, 80, 269-276.

Jongpatiwut, S., Li, Z., Resasco, D.E., Alvarez ,W.E., Sughrue, E.L., and Dodwell, G.W. (2004). Competitive hydrogenation of poly-aromatic hydrocarbons on sulfur-resistant bimetallic Pt-Pd catalysts. Applied Catalysis A: General, 262, 241–253.

Jung, J.S., Park, J.W., and Seo, G. (2005). Catalytic cracking of n-octane over alkali-treated MFI zeolites, Applied Catalysis A: General, 288 149-157.

Kinger, G., and Vinek, H. (2001) *n*-Nonane hydroconversion on Ni and Pt containing HMFI, HMOR and HBEA. Applied Catalysis A: General, 218, 139-149.

Komvokis, V.G., Marnellos, G.E., Vasalos, I.A., and Triantafyllidis, K.S. (2009) Effect of pretreatment and regeneration conditions of Ru/γ-Al_2O_3 catalysts for N_2O decomposition and/or reduction in O_2-rich atmospheres and in the presence of NO_X, SO_2 and H_2O Applied Catalysis B: Environmental, 89, 627-634.

Krogh, A., Hagen, A., Hansen, T.W., Christensen, C.H., and Schmidt, I. (2003). Re/HZSM-5: a new catalyst for ethane aromatization with improved stability. Catalysis Communications, 4, 627-630.

Kumar, M., Saxena, A.K., Negi, B.S., and Viswanadham, N. (2008). Role of pore size analysis in development of zeolite reforming catalyst. Catalysis Today, 130, 501–508.

Lacroix, M., Boutarfa, N., Guillard, N., Vrinat, M., and Breysse, M. (1989) Hydrogenating properties of unsupported transition metal sulphides. Journal of Catalysis, 120, 473-477.

Lakhapatri, S.L., and Abraham, M.A. (2009). Deactivation due to sulfur poisoning and carbon deposition on Rh-Ni/Al_2O_3 catalyst during steam reforming of sulfur-doped n-hexadecane. Appiled catalysis A: General, 364, 113-121.

Lan-Lan, L., and Shuangxi, L. (2005). CuO-containing MCM-48 as catalysts for phenol hydroxylation. Catalysis Communication, 6, 762-765.

Laresgoiti, M.F., Caballero, B.M., Marco, I., Torres, A., Cabrero, M.J., and Chomón, M.J. (2004). Characterization of the liquid products obtained in tyre pyrolysis. Journal of Analytical and Applied Pyrolysis, 71, 917-934.

Laresgoiti, M.F., Marco, I., Torres, A., Caballero, B., Cabrero, M.A., and Chomón, M.J. (2000) Chromatographic analysis of the gases obtained in tyre pyrolysis. Journal of Analytical and Applied Pyrolysis, 55, 43-54.

Lee, J.K., and Rhee, H.K. (1998) Sulfur tolerance of zeolite beta-supported Pd−Pt catalysts for the isomerization of *n*-hexane. Journal of Catalysis, 177, 208-216.

Leflaive, P., Lemberton, J. L., Pérot, G., C. Mirgain, C., Carriat, J. Y., Colin, J. M. (2002) On the origin of sulfur impurities in fluid catalytic cracking gasoline—Reactivity of thiophene derivatives and of their possible precursors under FCC conditions. Applied Catalysis A: General, 227, 201-215

Leung, D.Y.C., Yin, X.L., Zhao, Z.L., Xu, B.Y. and Chen, Y. (2002). Pyrolysis of tire powder: influence of operation variables on the composition and yields of gaseous product. Fuel Processing Technology, 79, 141-155.

Li, B., Guo, W., Yuan, S., Hua, J., Wang, J., and Jiao, H. (2008). A theoretical investigation into the thiophene-cracking mechanism over pure Brønsted acidic zeolites, Journal of Catalysis, 253, 212–220.

Liu, Z.-W., Li Xiaohong, Asami Kenji, Fujimoto Kaoru. (2006) High performance Pd/beta catalyst for the production ofgasoline-range iso-paraffins via a modifiedFischer–Tropsch reaction. Applied Catalysis A: General, 300, 162–169.

Lu, et al., 2008 (loss of record)

Lucas, D.A., Valverde, L.J., Dorado, F., and Ramos, J.M. (2005). Hydroisomerisation of n-octane over platinum catalysts with or without binder. Applied Catalysis A: General, 282, 15-24.

Lucas, D.A., Ramos, J.M., Dorado, F., Sánchez, P., and Valverde, L.J. (2005). Influence of Si/Al ration in the hydroisomerization of n-octane over platinum and palladium beta zeolite-based catalysts with or without binder. Applied Catalysis A: General, 289, 205-213.

Lugstein, A., Jentys, A., and Vinek, H. (1999) Hydroisomerization and cracking of *n*-octane and C_8 isomers on Ni-containing zeolites. Applied Catalysis A: General, 176, 119-128.

M.J. (2000). Chromatographic analysis of the gases obtained in tyre pyrolysis. Journal of analytical and applied pyrolysis, 55, 43-54.

Marcilla, A., Gómez-Siurana, A., and Berenguer, D. (2006).Study of the influence of the characteristics of different acid solids in the catalytic pyrolysis of different polymers. Applied Catalysis A: General, 301, 222–231.

Mark, J.E., Erman, B., and Eirich, F. (1994) Science and technology of rubber, 2nd Edition, Academic Press, San Diego.

Mastral, A.M., Murillo, R., Callen, M.S., Garcia, T., and Snape, C.E. (2000) Influence of Process Variables on Oils from Tire Pyrolysis and Hydropyrolysis in a Swept Fixed Bed Reactor. Energy& Fuels, 14, 739-744.

Matsubayashi, N., Yasuda, H., Inamura, M., and Yoshimura, Y. (1998). EXAFS study on Pd-Pt catalyst supported on USY zeolite. Catalysis today, 45, 375-380.

Mazzieri, V., Coloma-Pascual, F., Arcoya, A., L'Argentière, P. C., Fígoli, N. S. (2003) XPS, FTIR and TPR characterization of Ru/Al_2O_3 catalysts Applied Surface Science, 210, 222-230

McKinley, J.B., In: Emett P.H., editor. Catalysis, vol. 5. Nework: Reinhold, 1957 McKinley and Emmett, 1957

Miguel, G.S., Aguado, J., Serrano, D.P. and Escola, J.M. (2006). Thermal and catalytic conversion of used tyre rubber and its polymeric constituent using Py-GC/MS. Applied Catalysis B: Environmental, 64, 209-219.

Mizutani, H., Korai, Y., and Mochida, I. (2007). Behavior of sulfur species present in atmospheric residue in fluid catalytic cracking, Fuel, 86, 2,898–2,905.

Murugan, S., Ramaswamy, M.C., and Nagarajan, G. (2009) Assessment of pyrolysis oil as an energy source for diesel engines. Fuel Processing Technology, 90, 67-74.

Naccache, C., Dutel, J.F., Che, M. (1973) Valence state of palladium in Y zeolite. Journal of Catalysis, 29, 179-181

Nacheff, M.S., Kraus, L.S., Ichikawa, M., Huffman, B.M., Butt, J.B., and Sachtler, W.M.H. (1987) Characterization and catalytic function of Re^0 and Re^{4+} in Re/Al_2O_3 and $PtRe/Al_2O_3$ catalysts. Journal of Catalysis, 106, 263-272.

Napoli, A., Soudais, Y., Lecomte, D., and Castillo, S. (1997) Scrap tyre pyrolysis: Are the effluents valuable products? Journal of Analytical and Applied Pyrolysis, 40-41, 373-382.

Navarro, R.M., Castano, P., Alvarez-Galvan, M.C., and Pawelec, B. (2009) Hydrodesulfurization of dibenzothiophene and a SRGO on sulfide $Ni(Co)Mo/Al_2O_3$ catalysts. Effect of Ru and Pd promotion. Catalysis Today, 15, 108-114.

Ojeda, J., Escalona, N., Fierro, J.L.G., Agudo, A.L., and Gil-Llambias, F.J. (2005) Effect of the preparation of Re/γ-Al_2O_3 catalysts on the HDS and HDN of gas oil. Applied Catalysis A: General, 281, 25-30.

Okal, J., and Kubicka, H. (1998) Influence of oxidation–reduction treatment on activity and selectivity of Re supported on γ-alumina. Applied Catalysis A: General, 171, 351-359.

Oliveira, M.L.M., Miranda, A.A.L., Barbosa, C.M.B.M., Cavalcante, C.L. Jr., Azevedo, D.C.S., and Rodriguez-Castellon, E. (2009). Adsorption desulfurization of model gasoline on NaY zeolites exchanged with Ag(I), Ni(II) and Zn(II). Fuel, 88, 1,885–1,892.

Onyestyak, G., Pal-Borbely, G., and Beyer, H.K. (2002) Cyclohexane conversion over H-zeolite supported platinum. Applied Catalysis A: General, 229, 63-74.

Pakdel, H., Pantea, D.M., and Roy, C. (2001) Production of *dl*-limonene by vacuum pyrolysis of used tires. Journal of Analytical and Applied Pyrolysis, 57, 91-107.

Pecoraro, T.A. and Chianelli, R.R. (1981) Hydrodesulfurization catalysis by transition metal sulfides. Journal of Catalysis, 67, 430 – 445.

Perring, L., Bussy, F., Gachon, J.C., and Peschotte, P. (1998). The Ruthenium-Silicon System. Alloy and compounds, 284, 198-205

Philippou, A. and Anderson, M.W. (1997) Solid-State NMR Investigation of Ethylbenzene Reactions over HMOR and Pt–HMOR Catalysts. Journal of Catalysis, 167, 266- 272.

Ponec, V. and Bond, G.C. (1995) Catalysis by Metals and Alloys, Elsevier, Amsterdam.

Poondi, D. and A.A. Vannice, A.A. (1996). Competitive Hydrogenation of Benzene and Toluene on Palladium and Platinum Catalysts, Journal of Catalysis, 161, 742-751.

Qu, W., Zhou, Q., Wang, Y-Z., Zhang, J., Lan, W-W., Wu, Y-H., Yang, J-W., and Wang, D-Z. (2006) Pyrolysis of waste tire on ZSM-5 zeolite with enhanced catalytic activities. Polymer Degradation and Stability, 91, 2389-2395.

Reddy, K.M. and Song, C. (1996). Synthesis of mesoporous zeolites and their application for catalytic conversion of polycyclic aromatic hydrocarbons. Catalysis Today, 31, 137-144.

Richardeau, D., Joly, G., Canaff, C., Magnoux, P., Guisnet, M., Thomas, M., and Nicolaos, A. (2004) Adsorption and reaction over HFAU zeolites of thiophene in liquid hydrocarbon solutions. Applied Catalysis A: General, 263, 49-61.

Rodreguez, I.M., Laresgoiti, M.F., Cabrero, M.A., Torres, A., Chomón, M.J., and Caballero, B. (2001) Pyrolysis of scrap tyres. Fuel Processing Technology, 72, 9-22.

Rodriguez-Castellon, E., Mérida-Robles, J., Díaz, L., Maireles-Torres, P., Jones, D.J., Rozière, J., and Jiménez-López, A. (2004) Hydrogenation and ring opening of tetralin on noble metal supported on zirconium doped mesoporous silica catalysts. Applied Catalysis A: General, 260, 9 -18.

Roldán, R., Romero, F.J., Jiménez-Sanchidrián, C., Marinas, J.M. and Gómez, J.P. (2005). Influence of acidity and pore geometry on the product distribution in the hydroisomerization of light paraffins on zeolites. Applied Catalysis A: General, 288, 104-115.

Roy, C., Chaala, A. and Darmstadt, H. (1999). The vacuum pyrolysis of used tires End-uses for oil and carbon black products. Journal of Analytical and Applied Pyrolysis, 51, 201-221.

Sachtler, W.M.H., Stakheev, A.Y. (1992) Electron-deficient palladium clusters and bifunctional sites in zeolites. Catal. Today, 12, 283-295.

Sajkowski, D.J., Lee, J.Y., Schwank, J., Tian, Y., and Goodwin Jr, J.W. (1986) The role of the zeolite in the hydrogenolysis of C_2 and C_3 hydrocarbons on RuNaY catalysts. Journal of Catalysis, 125, 549-560.

San Miguel, G., Aguado, J., Serrano, G.P., and Escola, J.M. (2006) Thermal and

catalytic conversion of used tyre rubber and its polymeric constituents using Py-GC/MS. Applied Catalysis B: Environmental, 64, 209-219.

Santikunaporn, M., Herrera, J.E., Jongpatiwut, S., Resasco, D.E., Alvarez, W.E. and Sughrue, Ed L. (2004). Ring opening of decalin and tetralin on HY and Pt/HY zeolite catalysts. Journal of Catalysis, 228, 100-113.

Sato, T., Kunimori, K., and Hayashi, S. (1999). Dynamics of benzene, cyclohexane and n-hexane in KL zeolite studied by ^{2}H NMR. Phys. Chem. Chem. Phys, 1(16), 3839-3843.

Šebor, G., Blažek, J., and Nemer, M.F. (1999) Optimization of the preparative separation of petroleum maltenes by liquid adsorption chromatography. Journal of Chromatography A, 847, 323-330.

Seddegi, Z.S., U. Budrthumal, U., Al-Arfaj, A.A., Al-Amer, A.M., and Barri, S.A.I. (2002). Catalytic cracking of polyethylene over all-silica MCM-41 molecular sieve, Applied Catalysis A: General. 225,167-176.

Shiraga, M., Li, D., Atake, I., Shishido, T., Oumi, Y., Sano, T., and Takehira, K. (2007). Partial oxidation of propane to synthesis gas over noble metals-promoted Ni-Mg(Al)O catalysts—High activity of Ru–Ni-Mg(Al)O catalyst. Journal of Applied Catalysis A: General, 318, 143-154.

Shulmann, 2002 (loss of record)

Sinfelt, J.H. (1983) Bimetallic Catalysts: Discovery, Concepts and Applications, Wiley, NewYork.

Speight, J.G. (2002) Handbook of Petroleum Product Analysis, New Jersey: John Wiley&Sons, Inc.

Speight, J.G. (2005) Petroleum Asphaltenes Part 1 Asphaltenes, Resins and the Structure of Petroleum. Oil and Gas Science and Technology. 59, 467-477.

Song, C., Garcés, J.M., and Sugi, Y. (2000). Shape Selective Catalysis: Chemicals Synthesis and Hydrocarbon Processing. Washington DC; ACS symposium series 738, 381-389.

Song, C. and Ma, X.(2003) New design approaches to ultra-clean diesel fuels by deep desulfurization and deep dearomatization. Applied Catalysis B: Environmental, 41, 207-238.

Stanislaus, A., and Cooper, B.H. (1994). Aromatic Hydrogenation Catalysis: A Review, Catalysis Reviews: Science and Engineering, 36, 75–123.

Tang, A.M., Cui, Y.N. and Le, T.T. (2007) A study on the thermal conductivity of compacted bentonites. Applied Clay Science, 41, 181-189.

Tanglumlert, W., Imae, T., White, T.J., and Wongkasemjit, S. (2008) Preparation of highly ordered Fe-SBA-1 and Ti-SBA-1 cubic mesoporous silica via sol-gel processing of silatrane. Materials Letters, 62, 4,545-4,548.

Teschner,D., Matusek,K., and Paál,Z. (2000). Reactivity of the hydrocarbon C–C bonds as a function of the reaction conditions in the conversion of C_6 alkanes and methylcyclopentane over Rh catalysts. Journal of Molecular Catalysis A: Chemical, 179, 201–212.

Teschner,D., Matusek,K., and Paál,Z. (2000). Ring Opening of Methylcyclopentane on Alumina-Supported Rh Catalysts of Different Metal Loadings. Journal of Catalysis, 192, 335-343.

Teschner, D., Duprez, D., and Paal, Z. (2002) Reactivity of the hydrocarbon C–C bonds as a function of the reaction conditions in the conversion of C_6 alkanes and methylcyclopentane over Rh catalysts. Journal of Molecular Catalysis: A Chemical, 179, 201-212.

Thanabodeekij, N., Sadthayanon, S., Gulari, E., and Wongkasemjit, S. (2006) Extremely high surface area of ordered mesoporous MCM-41 by atrane route. Materials Chemistry and Physics, 98, 31-137.

Torri, C., Lesci ,I.G., and Fabbri, D. (2008). Analytical study on the pyrolytic behaviour of cellulose in the presence of MCM-41 mesoporous materials. Journal of Analytical and Applied Pyrolysis, 85, 192–196.

Unapumnuk, K., Keener, Tim C., Liang, F., and Lu, M. (2008). Investigation into the removal of sulfur from tire derived fuel by pyrolysis. Fuel, 87, 951–956.

Uhl, F.M., Mckinney, M.A. and Wilkie, C.A. (2000). Polybutadiene cross-linked with various diols – effect on thermal stability. Polymer Degradation and Stability, 70, 417-424.

Vagif, M., Akhmedov, Soliman, H., Al-Khowaiter. (2000). Hydroconversion of hydrocarbons over Ru-containing supported catalysts prepared by metal vapor method. Applied Catalysis A:General, 197, 201-212.

Valla, J.A., Lappas, A.A., and Vasalos, I.A., Catalytic cracking of thiophene and benzothiophene: Mechanism and kinetics. Applied Catalysis A: General, 297, 90-101.

Wakui, K., Satoh, K.I., Sawada, G., Shiozawa, K., Matano, K.I., Suzuki, K., Hayakawa, T., Murata, K., Yoshimura, Y., and Mizukami, F. (1999). Catalytic cracking of n-butane over rare earth-loaded HZSM-5 catalysts. Applied Catalysis A: General, 42, 307-314.

Wang, S.H., and Griffiths, P.R. (1985) Resolution enhancement of diffuse reflectance i.r. spectra of coals by Fourier self-deconvolution: 1. C-H stretching and bending modes. Fuel, 64, 229-265.

Weitkamp, J., Raichle, A. and Traa, Y. (2001). Novel zeolite catalysis to create value from surplus aromatics: preparation of C_{2+}-n-alkanes, a high-quality synthetic steam cracker feed stock. Applied catalysis A: General, 222, 277-297.

Williams, P.T. and Besler, S. (1995) Pyrolysis-thermogravimetric analysis of tyres and tyre components. Fuel, 14, 1277-1283.

Williams,P.T. and Bottrill, R.P. (1995) Sulfur-polycyclic aromatic hydrocarbons in tyre pyrolysis oil. Fuel, 74(5), 736-742.

Williams, P.T. and Brindle, A.J. (2002) Catalytic pyrolysis of tyres: influence of Tyres: influence of catalyst temperature. Fuel, 81, 2425-2434.

Williams, P.T. and Brindle, A.J. (2003a) Aromatic chemicals from the catalytic pyrolysis of scrap tyres. Journal of Analytical and Applied Pyrolysis, 67, 143-164.

Williams, P.T. and Brindle, A.J. (2003b) Temperature selective condensation of tyre pyrolysis oils to maximize the recovery of single ring aromatic compounds. Fuel, 82, 1023-1031.

Williams, P.T. and Taylor, D.T. (1993) Aromatization of tyre pyrolysis oil to yield polycyclic aromatic hydrocarbons. Fuel, 72, 1469-1474.

Williams, P.T., Besler, S., and Taylor, D.T. (1990) The pyrolysis of scrap automotive tyres the influence of temperature and heating rate on product composition. Fuel, 69, 1474-1482.

Williams, M.F., B. Fonfe´, B., Woltza, C., Jentys, A., van Veen, J.A.R., Lercher, J.A. (2007) Hydrogenation of tetralin on silica–alumina-supported Pt catalysts II. Influence of the support on catalytic activity, Journal of Catalysis, 251, 497–506.

Wongkerd, T., Luengnaruemitchai, A., and Jitkarnka, J. (2008) Phase change of catalysts derived from a LDH-deoxycholate intercalated compound and its impacts on NO reduction from stationary source emissions Applied Catalysis B: Environmental, 78, 101-111.

Wu, J.C.S., Goodwin, J.G., and Davis, M. (1990) Zeolite A-supported Ru catalysts. Journal of Catalysis, 125, 488-500.

Yasuda, H., Sato, T., and Yoshimura, Y. (1999) Influence of the acidity of USY zeolite on the sulfur tolerance of Pd–Pt catalysts for aromatic hydrogenation. Catalysis Today, 50, 63-71.

Zheng, J., Guo, M., and Song, C. (2008) Characterization of Pd catalysts supported on USY zeolites with different SiO_2/Al_2O_3 ratios for the hydrogenation of naphthalene in the presence of benzothiophene. Fuel Processing Technology, 89, 467-474.

Zhicheng, S., Wenyuan, S., Yifang, Y., Xingpin, G., Ping, C., Zaiting, L., Xingtian, S., Xiaoming, Y., Wei, F., Meng, Z., and Mingyuan, H. U.S.Patent 5,380,690, 1995.

Outputs จากโครงการวิจัยที่ได้รับทุนจาก สกว.

Outputs จากโครงการวิจัยที่ได้รับทุนจาก สกว. สามารถแบ่งออกได้เป็นประเภทต่างๆ ดังต่อไปนี้

1. ผลงานวิจัยที่ตีพิมพ์ในวารสารวิชาการนานาชาติ

1.1 Dũng NA, Wongkasemjit S, **Jitkarnka S***. *Effects of Pyrolysis Temperature and Pt-Loaded Catalysts on Polar-Aromatic Content in Tire-Derived Oil*. Applied Catalysis B: Environmental, 2009; 91: 300–307.

1.2 Dũng NA, Mhodmonthin A, Wongkasemjit S , **Jitkarnka S***. *Effects of ITQ-21 and ITQ-24 as zeolite additives on the oil products obtained from the catalytic pyrolysis of waste tire*. Journal of Analytical and Applied Pyrolysis, 2009; 85: 338–344.

1.3 Dũng NA, Klaewkla R, Wongkasemjit S, **Jitkarnka S***. *Light olefins and light oil production from catalytic pyrolysis of waste tire*. Journal of Analytical and Applied Pyrolysis, 2009; 86: 281–286.

1.5 Dũng NA, Tanglumlert W, Wongkasemjit S, **Jitkarnka S***. *Roles of ruthenium on catalytic pyrolysis of waste tire and the changes of its activity upon the rate of calcinations*. Journal of Analytical and Applied Pyrolysis, 2010; 87: 256–262.

1.6 Witpathomwong C, Longloilert R, Wongkasemjit S, **Jitkarnka S***. *Improving Light Olefins and Light Oil Production Using Ru/MCM-48 in Catalytic Pyrolysis of Waste Tire*. Energy Procedia, ***In Press*** (Accepted from the 9th EMSES 2011).

1.7 Phopaisarn M, **Jitkarnka S***. *Influence of the Physical Mixture of Y and KL Zeolites on the Pyrolysis of Waste Tire.* International Journal of Global Warming, ***Manuscript on Revision***

2. ผลงานวิจัยที่ตีพิมพ์ในวารสารการประชุม วารสารเฉพาะทาง หรือการนำเสนอผลงานในที่ประชุมวิชาการ

2.1 <u>การนำเสนอผลงานในที่ประชุมวิชาการ</u>

(1) N.A. Dung, A. Mhodmonthin, S. Wongkasemjit, and **S. Jitkarnka***, “Effects of ITQ-21 and ITQ-24 as zeolite additives on the oil products obtained from the catalytic pyrolysis of waste tire”, Oral Presentation at 18th International Symposium on Analytical and Applied Pyrolysis, Lanzarote, Spain, 18-23 May 2008

(2) N.A. Dung, A. Choosuton, R. Magaraphan, and **S. Jitkarnka ***, “Catalytic pyrolysis of waste tire using Pt-supported HMOR and KL catalysts”, Poster presented at 14th International Congress in Catalysis: Catalysis as the Pivotal Technology for Future Society, Seoul, South Korea, July 13-18, 2008 (<u>Dung received the Young Scientist Award from the conference</u>)

(3) **Sirirat Jitkarnka**, “Catalyst Application in Tire Pyrolysis for Tailored Production of Fuels and Petrochemical Feedstocks”, Oral Presentation at The International Chulalongkorn University - Hiroshima University Joint Seminar on “Innovative Materials and Alternative & Green Energy, organized by Chulalongkorn University and Hiroshima University at Patumwan Princess Hotel, Bangkok, May 5, 2009

(4) Nguyễn Anh Dũng, Sujitra Wongkasemjit, and **Sirirat Jitkarnka***, “Effects of Pyrolysis Temperature and Pt-Loaded Catalysts on Polar-Aromatic Content in Tire-Derived Oil”, Poster presentation, การประชุม “นักวิจัยรุ่นใหม่...พบ... เมธีวิจัยอาวุโส สกว.” ครั้งที่ 9 ที่จะจัดขึ้น ณ โรงแรมฮอลิเดย์ อินน์ รีสอร์ท รีเจ้นท์ บีช ชะอำ จังหวัดเพชรบุรี ระหว่างวันที่ 15-17 ตุลาคม 2553

(4) **S. Jitkarnka***, N.A. Dung, S.Wongkasemjit, R. Klaewkla, W. Tanglumlert, “Ru-Supported Catalysts for Light Olefins and Light Oil Production from Catalytic Pyrolysis of Waste Tire”, Poster presentation, การประชุม “นักวิจัยรุ่นใหม่... พบ...เมธีวิจัยอาวุโส สกว.” ครั้งที่ 10 ที่จะจัดขึ้น ณ โรงแรมฮอลิเดย์ อินน์ รีสอร์ท รีเจ้นท์ บีช ชะอำ จังหวัดเพชรบุรี ระหว่างวันที่ 14-16 ตุลาคม 2553

2.2 การนำเสนอผลงานในวารสารเฉพาะทาง

(1) **Sirirat Jitkarnka**, “From Wastes to Fuels: The Astonishing Invention of “*Innovable*” Energy”, PTIT Focus, Volume 23 No. 1, January 2009, p.10.

2.3 ผลงานวิจัยที่ตีพิมพ์ในวารสารการประชุมวิชาการ (Proceedings)

(1) Thirapat Latthikawiboon, and **Sirirat Jitkarnka***, “Catalysis of Waste Tire over Y-Based Catalysts: Synergistic Effect between Pd-Pt”, In Proceedings of The 16th PPC Symposium on Petroleum, Petrochemicals, and Polymers and The 1st National Research Symposium on Petroleum, Petrochemicals, and Advanced Materials organized by The National Center of Excellence for Petroleum, Petrochemicals, and Advanced Materials and the Petroleum and Petrochemical College, Montien Hotel, Bangkok, April 22, 2010

(2) Mullika Phopaisarn, and **Sirirat Jitkarnka***, “Catalysis of Waste Tire over KL-Based Catalysts: Double Beds of KL and Y Zeolites”, In Proceedings of The 16th PPC Symposium on Petroleum, Petrochemicals, and Polymers and The 1st National Research Symposium on Petroleum, Petrochemicals, and Advanced Materials organized by The National Center of Excellence for Petroleum, Petrochemicals, and Advanced Materials and the Petroleum and Petrochemical College, Montien Hotel, Bangkok, April 22, 2010

(3) Palida Sritana, and **Sirirat Jitkarnka***, “Catalytic Pyrolysis of Waste Tire over HMOR-based Catalysts: Industrialized Ru/HMOR-based Catalyst”, In Proceedings of The 16th PPC Symposium on Petroleum, Petrochemicals, and Polymers and The 1st National Research Symposium on Petroleum, Petrochemicals, and Advanced Materials organized by The National Center of Excellence for Petroleum, Petrochemicals, and Advanced Materials and the Petroleum and Petrochemical College, Montien Hotel, Bangkok, April 22, 2010

(4) Mullika Phopaisarn and **Sirirat Jitkarnka***, “Influence of the physical mixture of Y and KL zeolites on the pyrolysis of waste tire”, Proceedings, 10th International Conference on Clean Energy (ICCE-2010) Famagusta, N. Cyprus, September 15-17, 2010. *(This article is recommended by the Organizing Committee*

of the International Conference on Clean Energy (ICCE-2010) to be published in the International Journal of Global Warming.)

(5) Palida Sritana and **Sirirat Jitkarnka***, “Coke formation on a Ru/HMOR based catalyst and its effect on waste tire pyrolysis products”, Proceedings of 10th International Conference on Clean Energy (ICCE-2010) Famagusta, N. Cyprus, September 15-17, 2010.

(6) Anusara Wehatoranawee and **Sirirat Jitkarnka***, “Effect of Silver Supported HMOR-zeolite on Waste Tire Pyrolysis Products”, ASCON 2010, October 12 – 14, 2010, Phuket, Thailand.

(7) Witpathomwong, C., Longloilert, R., Wongkasemjit, S., and **Jitkarnka*, S.**, “ Improving Light Olefins and Light Oil Production Using Ru/MCM-48 in Catalytic Pyrolysis of Waste Tire”, Proceedings of the 9th Eco-Energy and Material Science and Engineering Symposium 2011 (EMSES 2011), Wiang Inn Hotel, Chiang Rai, Thailand, May 25-28, 2011.

(8) Anusara Wehatoranaweea, and **Sirirat Jitkarnka***, “Catalytic Pyrolysis of Waste Tire over Ag-Loaded Catalysts: Effect of different zeolites”, In Proceedings of The 17th PPC Symposium on Petroleum, Petrochemicals, and Polymers and The 2nd National Research Symposium on Petroleum, Petrochemicals, and Advanced Materials organized by The National Center of Excellence for Petroleum, Petrochemicals, and Advanced Materials and the Petroleum and Petrochemical College, Queen Sirikit National Convention Center, Bangkok, April 26, 2011.

(9) Pisit Akarapatanakul, and **Sirirat Jitkarnka***, “Development of Industrialized Pd/BETA Based Catalysts for Waste Tire Pyrolysis”, Proceedings of The 17th PPC Symposium on Petroleum, Petrochemicals, and Polymers and The 2nd National Research Symposium on Petroleum, Petrochemicals, and Advanced Materials organized by The National Center of Excellence for Petroleum, Petrochemicals, and Advanced Materials and the Petroleum and Petrochemical College, Queen Sirikit National Convention Center, Bangkok, April 26, 2011.

(10) Chaiyaporn Witpathomwong, Sujitra Wongkasemjt, and **Sirirat Jitkarnka***, “Development of Industrialized Ru/HMOR-Based Catalysts for Waste Tire Pyrolysis: 0-20% of Ru/HMOR in Extrudates”, Proceedings of The 17th PPC

Symposium on Petroleum, Petrochemicals, and Polymers and The 2nd National Research Symposium on Petroleum, Petrochemicals, and Advanced Materials organized by The National Center of Excellence for Petroleum, Petrochemicals, and Advanced Materials and the Petroleum and Petrochemical College, Queen Sirikit National Convention Center, Bangkok, April 26, 2011.

(11) Ruktawee Mahanin, and **SiriratJitkarnka***, “Catalytic Pyrolysis of Waste Tire over MoO3-loaded KL Catalysts”, Proceedings of The 17th PPC Symposium on Petroleum, Petrochemicals, and Polymers and The 2nd National Research Symposium on Petroleum, Petrochemicals, and Advanced Materials organized by The National Center of Excellence for Petroleum, Petrochemicals, and Advanced Materials and the Petroleum and Petrochemical College, Queen Sirikit National Convention Center, Bangkok, April 26, 2011.

(12) Waleerat Pinket, and **Sirirat Jitkarnka***, “Catalytic Pyrolysis of Waste Tires over Cobalt Supported on KL”, Proceedings of The 17th PPC Symposium on Petroleum, Petrochemicals, and Polymers and The 2nd National Research Symposium on Petroleum, Petrochemicals, and Advanced Materials organized by The National Center of Excellence for Petroleum, Petrochemicals, and Advanced Materials and the Petroleum and Petrochemical College, Queen Sirikit National Convention Center, Bangkok, April 26, 2011.

3. การตีพิมพ์หนังสือและรางวัล

ศิริรัตน์ จิตการค้า. จากขยะสู่น้ำมัน: เทคโนโลยีผลิตพลังงานทางเลือกที่ดูแลสิ่งแวดล้อม. พิมพ์ครั้งที่ 1. สำนักพิมพ์แห่งจุฬาลงกรณ์มหาวิทยาลัย: โรงพิมพ์บริษัทเอเซียแปซิฟิคพริ้นติ้ง จำกัด, ธันวาคม 2551. 290 หน้า. (ได้รับรางวัลหนังสือวิชาการดีเด่นด้านสิ่งแวดล้อม **TTF Award ประจำปี 2552** จากมูลนิธิโตโยต้าประเทศไทย และมหาวิทยาลัยธรรมศาสตร์ รับรางวัลเมื่อ 11 มีนาคม 2553 ณ หอประชุมศรีบูรพา มหาวิทยาลัยธรรมศาสตร์ ท่าพระจันทร์)

4. ผลงานการผลิตบัณฑิตระดับบัณฑิตศึกษา

ระดับปริญญาเอก

ก. นาย เหงียน อาห์ ดุง สาขาเทคโนโลยีปิโตรเคมี หัวข้อวิทยานิพนธ์ ชื่อ Light Oil Production from Waste Tire Pyrolysis Using Noble Metal-Supported Catalysts, October 2009

ระดับปริญญาโท

ก. นาย ถิรภัทร์ ลัฐิกาวิบูลย์ หัวข้อวิทยานิพนธ์ ชื่อ Catalysis of Waste Tire over Y-Based Catalysts: Synergistic Effect between Pd-Pt, May 2010

ข. นางสาว มัลลิกา เผ่าไพศาล หัวข้อวิทยานิพนธ์ ชื่อ Catalysis of Waste Tire over KL-Based Catalysts: Double Beds of KL and Y Zeolites, May 2010

ค. นางสาว ปาลิดา ศรีธนะ หัวข้อวิทยานิพนธ์ ชื่อ Catalysis of Waste Tire over Ru/HMOR-Based Catalysts: Industrialized Ru/HMOR-Based Catalyst, May 2010

ง. นางสาว อนุสรา เวหาธรนาวี หัวข้อวิทยานิพนธ์ ชื่อ Catalytic Pyrolysis of Waste Tire over Ag-Loaded Catalysts, May 2011

จ. นาย ชัยพร วิทย์ปฐมวงศ์ หัวข้อวิทยานิพนธ์ ชื่อ Development of Industrialized Ru/MCM-48 and Ru/HMOR-Based Catalyst for Waste Tires Pyrolysis, May 2011

ฉ. นาย พิสิฐ อัครพัฒนากูล หัวข้อวิทยานิพนธ์ ชื่อ Development of Industriallized Pd/Beta based Catalysts for Waste Tire Pyrolysis, May 2011

ช. นางสาว รักทวี มหานิล หัวข้อวิทยานิพนธ์ ชื่อ Catalytic Pyrolysis of Waste Tire over KL-based Catalysts: The Effect of MoO3 and Re, May 2011

ซ. นางสาว วลีรัตน์ ปิ่นเกตุ หัวข้อวิทยานิพนธ์ ชื่อ Catalytic pyrolysis of waste tire over Rh, Ni and Co supported on KL zeolite and their bimetallic catalysts, May 2011

5. การนำผลงานวิจัยไปใช้ประโยชน์

5.1 <u>การใช้ประโยชน์ผลงานในเชิงสาธารณะและเชิงพาณิชย์</u>

มีการนำเอาผลงานที่เกิดขึ้นจากโครงการ องค์ความรู้ที่เกิดขึ้นจากโครงการ และผลงานที่ต่อเนื่องนั้น ไปเขียนเป็นหนังสือ เรื่อง <u>จากขยะสู่น้ำมัน: เทคโนโลยีผลิตพลังงานทางเลือกที่ดูแลสิ่งแวดล้อม</u>**.** ซึ่งได้รับรางวัลหนังสือวิชาการดีเด่นด้านสิ่งแวดล้อม **TTF Award ประจำปี 2552** จากมูลนิธิโตโยต้าประเทศไทย และมหาวิทยาลัยธรรมศาสตร์ จากการเขียนหนังสือเผยแพร่ ประกอบกับการได้รับรางวัลดังกล่าว ทำให้สร้างกระแสความสนใจให้กับบุคคลทั่วไป และบริษัทต่างๆ หลายบริษัทให้ความสนใจในการทำธุรกิจประเภทนี้เพิ่มมากขึ้น

5.2 <u>การใช้ประโยชน์ผลงานในเชิงนโยบาย</u>

มีการนำเอาผลงานที่เกิดขึ้นจากโครงการ องค์ความรู้ที่เกิดขึ้นจากโครงการ และผลงานที่ต่อเนื่องนั้น ไปต่อยอดทำงานวิจัยกับ บริษัท ไทยออยล์ จำกัด (มหาชน) ทำให้เกิดการเปลี่ยนแปลงในเชิงนโยบายของบริษัทฯ ในด้านพลังงานทดแทน และนโยบายด้านการทำงานวิจัยเพื่อพัฒนาธุรกิจใหม่ๆ ในอนาคต

ภาคผนวก

Applied Catalysis B: Environmental 91 (2009) 300–307

Contents lists available at ScienceDirect

Applied Catalysis B: Environmental

journal homepage: www.elsevier.com/locate/apcatb

Effects of pyrolysis temperature and Pt-loaded catalysts on polar-aromatic content in tire-derived oil

Nguyễn Anh Dũng, Sujitra Wongkasemjit, Sirirat Jitkarnka *

The Petroleum and Petrochemical College, Center of Excellence for Petroleum, Petrochemical and Advanced Materials, Chulalongkorn University, Chula 12, Pathumwan, Bangkok 10330, Thailand

ARTICLE INFO

Article history:
Received 17 October 2008
Received in revised form 26 May 2009
Accepted 27 May 2009
Available online 6 June 2009

Keywords:
Waste tire
Pyrolysis
Polar-aromatics
Pt
Zeolite

ABSTRACT

This study investigates the influences of pyrolysis temperatures and Pt-supported catalysts on polar-aromatic content in the oils obtained from pyrolysis of waste tire. These polar-aromatic compounds are mostly the sulfur-containing aromatics since oxygen is prohibited in pyrolysis. The experimental results indicated that pyrolysis temperatures strongly affected the polar-aromatic content in the derived oils. Namely, the increase in pyrolysis temperature in the tested range produced not only a higher amount of polar-aromatics but also heavier polar-aromatic compounds. All studied catalysts decreased the polar-aromatic content in the oils drastically. In addition, it was found that the introduction of the studied catalyst also led to the production of lighter polar-aromatic compounds with respect to that produced from thermal pyrolysis. Comparing the two acid catalysts, HBETA exhibited higher activity for polar-aromatic reduction as compared to HMOR, which was ascribed to its higher medium and strong acid site density, smaller particle size and 3D-structure. The Pt supported on HMOR and HBETA catalysts showed better polar-aromatic reduction activity than their corresponding acid catalysts. And, a slightly higher catalytic activity was observed over Pt/HBETA than Pt/HMOR, which was mainly due to the higher Pt dispersion of Pt/HBETA catalyst.

© 2009 Elsevier B.V. All rights reserved.

1. Introduction

The world production of waste tires is approximately 5×10^6 tons/year and nearly 65–70% of these wastes are eventually legally or illegally land-filled [1,2]. Along the years, different alternatives for waste tire recycling such as retreading, reclaiming, incineration, and grindings have been used. However, all of them have many drawbacks and/or limitations. Pyrolysis of waste tire might be considered as a non-conventional treatment, which recently has received renewed attention and attempts, since it can produce some high valuable products such as oil and petrochemicals.

Polar-aromatic compounds are the aromatic substances containing a sulfur, oxygen, or nitrogen atom in aromatic rings. And, in tire pyrolysis, most of polar-aromatics are obtained in the liquid product, and believed to be mostly sulfur-containing aromatics as oxygen is prohibited in pyrolysis. In the tire structure, after vulcanization sulfur is located at the allylic positions [3], and these sulfur atoms might be present as mono-sulfide, cyclic-sulfide or even dependent sulfide [4]. Our previous study showed that the breakdown of a tire molecule was initialized by breaking S–S bonds, and then spread out along the chains [5]. Nowadays, there has been a great interest in studying polar-aromatics, for instance aromatic-type sulfur-compounds, in fuels since some of them have been proven to be carcinogenic [6] and mutagenic [7], and may also give rise to toxic and corrosive SO_x in the exhaust streams of combustion plant using such fuels [8]. In refinery, sulfur-containing compounds are removed from fuels by hydrotreating or hydrodesulfurization process (HDS). Nevertheless, understanding how polar-aromatics are formed in the pyrolysis of waste tire helps finding the ways to prevent their formation and/or to eliminate them during pyrolysis. Williams and Bottrill [8] in 1995 studied the sulfur-polycyclic aromatic hydrocarbons in tire pyrolysis oil and reported the presence of a large number of sulfur-containing polycyclic aromatic hydrocarbons (HCs). Furthermore, Pakdel et al. [9] found thiophene derivatives in the liquid products obtained from tire pyrolysis. Several attempts to study the effects of waste tire pyrolysis conditions on the sulfur content in the products have been reported. In the study of Diez et al. in 2004 [10], it was found that the amount of sulfur liberated in the liquid and gas fractions after the pyrolysis process was greater as the final temperature rose. Moreover, they also reported that the presence of chlorine in the liquid and gas products was negligible, regardless of the final temperature of pyrolysis. The production of sulfur-containing polycyclic hydrocarbons in the pyrolytic oil was believed to occur

* Corresponding author. Tel.: +66 2 218 4148; fax: +66 2 215 4459.
E-mail address: sirirat.j@chula.ac.th (S. Jitkarnka).

0926-3373/$ – see front matter © 2009 Elsevier B.V. All rights reserved.
doi:10.1016/j.apcatb.2009.05.038

via the Diels–Alders reaction involving polycyclic aromatic hydrocarbon and sulfur [8].

Attempts have been made towards understanding the mechanism of the thermal degradation of different tire components. In many cases, the outcomes were what one may have expected. For example, the β-scission was found to be more preferable during the pyrolysis of natural rubber [11], polybutadiene [12], and styrene-butadiene rubber [13]. Corma et al. [14] reported the ability of acid zeolites for cracking mercaptans, thiophene and thiophene derivatives. The cracking of mercaptans might ultimately produce hydrogen sulfide and low molecular weight hydrocarbons. However, thiophenes and alkyl-thiophenes could hardly crack directly, but a prior partial saturation of the molecules via hydrogen transfer should give rise to cracking reactions. Moreover, most of the thiophenes converted mainly to coke, whereas the rest converted to gas and gasoline, but 2-methyl thiophene was more prompt to crack to give gas and gasoline. The high preference of thiophenes to convert into coke under cracking conditions was also reported in the study of Valla et al. [15].

Furthermore, Miguel et al. [16] found that the addition of acid catalysts did not affect the degradation temperature of the rubber, but it made a difference to the nature of the hydrocarbons obtained. They also reported that the greater the acidity was, the more aromatic hydrocarbons were produced. Platinum catalysts have been known as effective desulfurization catalysts [17], and noble metal catalysts are very active for hydrogenation reactions [18]. For deep HDS, the hydrogenating function of a catalyst is crucial because an initial hydrogenation of the refractory sulfur-containing molecules was found to reduce steric effects that impede the direct elimination of sulfur heteroatoms [19,20]. The known poisoning effect of Pt-based catalysts caused by the presence of sulfur-containing compounds in the feed might be overcome by the increase in the support acidity [21–25]. Moreover, in 2004, Santikunaporn et al. investigated the ring-opening of decalin and tetralin on HY and Pt/HY zeolite catalysts [26] and found that the production of ring-opening products was increased with the addition of Pt metal.

To our knowledge, there has been no research conducted to study the effect of pyrolysis temperature and catalysts on the polar-aromatic content in tire-derived oil. Thus, the purposes of this work were to study polar-aromatic formation in the pyrolytic oil obtained from the non-catalytic pyrolysis of waste tire at various temperatures, and to investigate the distinctive effects of Pt-supported HMOR and Pt-supported HBETA catalysts on the polar-aromatic formation. The influence of the catalysts on other issues is to be reported in separate paper.

2. Experimental

2.1. Catalyst preparation

Two zeolites, mordenite (MOR, H-form, Si:Al = 19) and BETA (NH_4-form, Si:Al = 27) supplied by the TOSOH Company (Singapore) were first calcined in air at 500 and 600 °C, respectively, with a heating rate of 5 °C min^{-1} for 3 h. Then, they were loaded with Pt using the incipient wetness impregnation technique to obtain 1 %wt Pt-supported catalysts. After that, the samples were pelletized, ground, and then sieved to a specific particle sizes of 400–425 μm. Finally, all catalysts were calcined in a flow of air at 500 °C for 3 h. Prior to catalytic activity measurement, the catalysts were reduced at 400 °C by H_2 for 3 h.

2.2. Catalyst characterization

XRD patterns were obtained using the Riguku D/Max 2200H using Cu Kα small radiation, and operated at 40 kV and 30 mA. The catalyst samples were scanned from 5° to 60° ($2\theta/\theta$) with a scanning speed of 5° min^{-1}. Hydrogen chemisorption was carried out using a conventional laboratory made-up system equipped with a TCD detector. Prior to performing the chemisorption at room temperature, an approximate 50 mg of sample was reduced using 5% hydrogen in nitrogen at the temperatures ramped up from room temperature to 800 °C with a heating rate of 10 °C min^{-1}. Temperature program desorption (TPD) using NH_3 was carried out in a TPD/TPR Micromeritics 2900 apparatus. Approximately 0.1 g of sample was first pretreated in He at 550 °C for 30 min. Then, the system was cooled to 100 °C, and the NH_3 adsorption was performed using NH_3/N_2 for 1.5 h followed by the introduction of He to remove the physically adsorbed NH_3 for 30 min at 100 °C. Finally, the system was cooled to 50 °C, and then the temperature program desorption was started from 50 to 600 °C with a heating rate of 5 °C min^{-1}. The composition of the bifunctional catalysts was determined by Inductively Coupled Plasma (ICP) technique using a PerkinElmer Optima 4300 PV machine after the dissolution of the catalysts. The surface area and pore size of the studied catalysts were characterized by N_2 physical adsorption using the Sorptomatic 2900 equipment. The Dupont TGA 2590 equipped with a thermal analyzer 2000, heated from 30 to 800 °C with the heating rate of 10 °C min^{-1} was employed to study the amount of coke in the used catalysts.

2.3. Pyrolysis of waste tire

Fig. 1 displays the experimental diagram. A tire sample was pyrolyzed in the lower zone of the reactor from room temperature to the final temperature of 500 °C with the heating rate of 10 °C min^{-1}. This pyrolysis zone was kept at the final temperature for 1 h to ensure the total conversion of tire. The evolved products were carried by a 25 ml min^{-1} nitrogen flow to the upper zone, where was controlled at 350 °C and packed with a catalyst. The obtained product was passed through an ice-salt condensing system containing 3 consecutive condensers in order to separate incondensable compounds from the liquid product. The solid and liquid products were weighed to determine the product distribution. The amount of gas was then determined by mass balance. The gas product collected in a Dual Valve Tedlar PVF bag purchased from Cole Parmer was analyzed by a GC, Agilent Technologies 6890 Network system, using an HP-PLOT Q column (300 mm × 0.32 mm ID and 20 μm film thicknesses) and an FID detector. The liquid product was first dissolved in n-pentane with the ratio of 40:1 to precipitate asphaltene prior to the determination of polar-aromatic content by liquid adsorption chromatography. Saturated hydrocarbons, mono-, di-, poly- and polar-aromatics in the obtained maltenes were fractionated by means of the liquid adsorption chromatography technique reported in details elsewhere [27]. Only polar-aromatic fraction was brought to analysis in this study. Finally, a Varian CP 3800 Simulated Distillation Gas Chromatograph equipped with FID and a 15 m × 0.25 mm × 0.25 μm WCOT fused silica capillary column (SIMDIST GC) was used to analyze the polar-aromatic fractions, according to the ASTM D2887 method, for simulated true boiling point curves and carbon number distribution. From the obtained true boiling point curve, a polar-aromatic portion was cut into ranges as follows: gasoline (<149 °C), kerosene (149–232 °C), gas oil or diesel (232–343 °C), light vacuum gas oil or fuel oil (343–371 °C), and heavy vacuum gas oil (>371 °C).

3. Results and discussion

3.1. Catalyst characterization

The XRD patterns of the Pt-supported catalysts and their corresponding supports are displayed in Fig. 2a and b. These

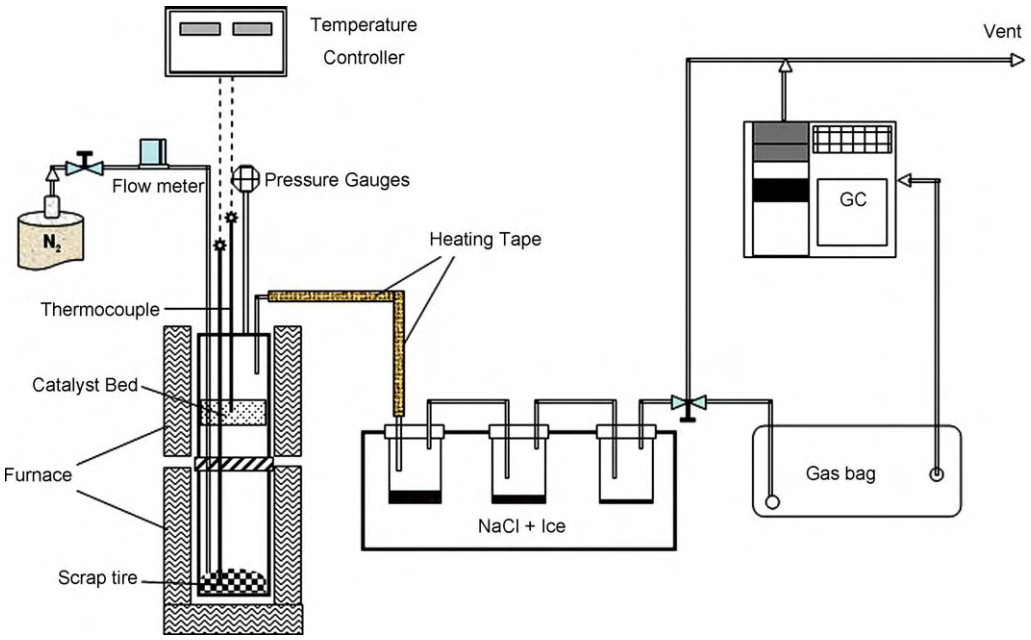

Fig. 1. Schematic experimental system of waste tire pyrolysis.

patterns indicate that the introduction of Pt to the zeolites did not affect the structure of the zeolites. However, due to the low amount of metal loaded on the catalysts, the peaks of Pt located at the 2θ of 39° and 46° [28] are then very small.

Fig. 3 illustrates the TPD-NH_3 profiles of HMOR and HBETA. Both profiles have two peaks. In the profile of HMOR, the taller peak appears at the temperature of around 190 °C, whereas the shorter peak locates at approximately 480 °C. For HBETA, the first peak is observed at around 290 °C and the second one emerged at the temperature of 480 °C. Obviously, according to the area under the peaks, HMOR possesses greater acid density than HBETA due to its lower Si:Al ratio. Meanwhile, the profile of HBETA exhibits the long-tail end, which is the characteristic of this zeolite [29]. In addition, TPD-NH_3 curve of HBETA shows higher amount of medium and strong acid sites (located at temperatures higher than 250 °C), as compared to that of HMOR. This higher medium and strong acid site density might be attributed to the dislodged Al of HBETA [29]. Moreover, it should be noted that, in this study, HBETA was pretreated by calcination at the higher temperature as compared to HMOR. This probably increases the amount of dislodged Al [30], resulting in the higher medium and strong acidic sites of HBETA as observed from ammonia desorption spectrum.

For all used catalysts, the TG results show two different weight loss positions corresponding to two different types of deposited hydrocarbons. The first one is observed at a lower temperature of around 290 °C, whereas the second one is located at around 500 °C. Between the two studied zeolites, the higher amount of coke was observed on HBETA, possibly due to its larger pore volume (Table 1). And, the amount of coke produced on Pt/HMOR and Pt/HBETA is comparable but this amount is higher than that produced on their corresponding acid catalysts.

The physical properties of the studied samples are also presented in Table 1. The amount of metal loaded was confirmed by using ICP technique. The obtained values of surface area of HMOR and HBETA samples displayed in the table are close to those supplied by the TOSOH, which are 380 and 630 $m^2\ g^{-1}$, respectively. Moreover, clearly the introduction of Pt led to a decrease in both surface area and pore volume. The decrease in surface area and pore volume suggests the diffusion of Pt into the pore of the zeolites and/or the pore blockage. The hydrogen chemisorption

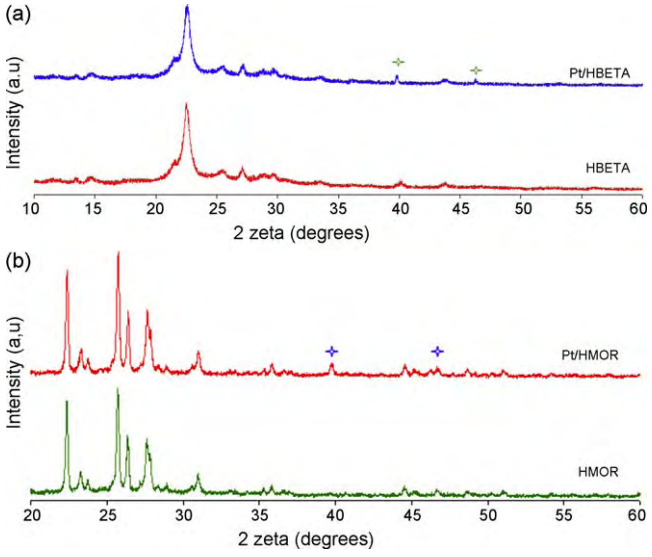

Fig. 2. (a) XRD patterns of HBETA and Pt/HBETA, and (b) XRD patterns of HMOR and Pt/HMOR.

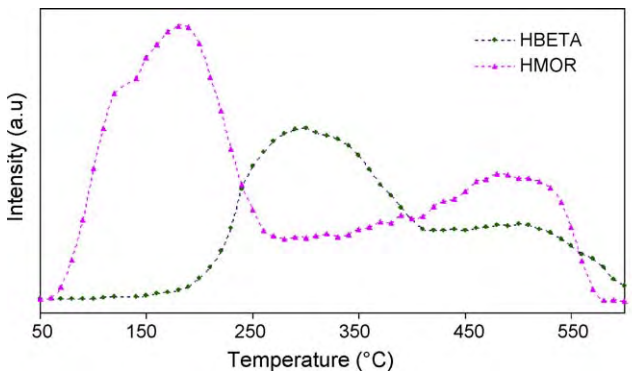

Fig. 3. TPD-NH_3 of HBETA and HMOR.

Table 1
Physical and chemical composition of the studied catalysts.

Catalyst	Pt (%wt)	Dispersion (%)[a]	Surface area ($m^2\ g^{-1}$)	Pore diameter (Å)	Pore volume ($cm^3\ g^{-1}$)	Particle size (μm)[b]	Coke ($g\ g^{-1}$ cat)
HMOR	–	–	372.5 ± 9.3	6.3[c]	0.20[c]	10–12	0.14
HBETA	–	–	618.3	7.5	0.68	3–6	0.22
Pt/HMOR	0.94	30.8	359.8	6.1	0.18	–	0.38
Pt/HBETA	1.01	42.1	608.5	7.1	0.67	–	0.33

[a] Determined by H_2 chemisorption.
[b] Supplied by TOSOH Corp.
[c] Determined by HK method [31].

results indicate that Pt is dispersed better on HBETA than on HMOR, possibly due to the higher surface area [32] of HBETA (Table 1). In addition, the slight decrease in pore volume together with the higher amount of coke generated over Pt-supported catalysts and the H_2 chemisorption results suggest that a considerable amount of Pt is located outside the zeolite crystals.

3.2. Polar-aromatic formation in the non-catalytic pyrolysis of waste tire

Prior to being able to explain how the catalysts can help reducing polar-aromatic contents, the formation of such compounds needs to be understood. This section is contributed to the discussion about how polar-aromatics can be formed during the pyrolysis of waste tire.

3.2.1. Polar-aromatic formation from thermal cracking of tire

The chemistry of sulfur vulcanization is so complex that, even today, only the main stages have been proven. After vulcanization, sulfur was combined in the network in a number of ways. Sulfur may be present as monosulfide, disulfide or polysulfide, but it may also be present as dependent sulfides, or cyclic-mono- and di-sulfides [4]. In addition, sulfur was found to attach to the rubber chains almost exclusively at the allylic positions [3]. Moreover, a typical tire compound contains natural rubber (NR), styrene-butadiene rubber (SBR), poly butadiene and butyl rubber [33]. Therefore, the rubber chains of tire should contain the aromatic rings originally from SBR as well as double bonds. In addition, in the SBR, the configuration of styrene monomers could be both block and random. And, the amount of bound styrene (%wt) is in the range from 10 to 45% [3], depending on the way the SBR was synthesized.

Several researches have investigated the thermal degradation of different rubbers. In the work of Chen and Qian [11], it was found that during the pyrolysis of natural rubber, β-scission was much more preferable because of the low bond dissociation energy, leaving the allylic radicals. The thermal cracking of polybutadiene also was reported to occur via β-scission [4]. Meanwhile, the thermal degradation of the styrene-butadiene rubber was favored to occur at the position (**a**) than at (**c**) in Scheme 1 as suggested by Choi [13], whereas no product resulting from the dissociation at the position (**b**) was observed. In addition, during the pyrolysis, not only the depolymerization but also the decomposition reaction to produce short chain hydrocarbon occurred [11].

In the present study, it was found that the polar-aromatics mainly distributed in the heavy fractions of the oils (light and heavy vacuum gas oils), which is in good agreement with some studies [9,34,35]. Scheme 2 shows several polar-aromatics found in the pyrolyzates from various references [9,34–36].

In order to ease further discussion about polar-aromatic formation/reduction with respect to the pyrolysis conditions and the presence of catalysts, an example of tire structure is hereby anticipated, as shown in Scheme 3, based upon the earlier discussion on the possible cracking positions having been proposed to occur during the pyrolysis of waste tire [11–13] and upon our experimental results.

Sulfur, which is originally present in the tire rubber approximately by 1.7 %wt [37], is the source for the formation of sulfur-containing compounds during pyrolysis. In addition, oxygen is prohibited in pyrolysis. Consequently, polar-aromatics found in pyrolysis oil are mostly sulfur-containing aromatics. In the study of Jitkarnka et al. [5], it was reported that the breakdown of a tire molecule would initially occur at the S–S bonds, and then spread

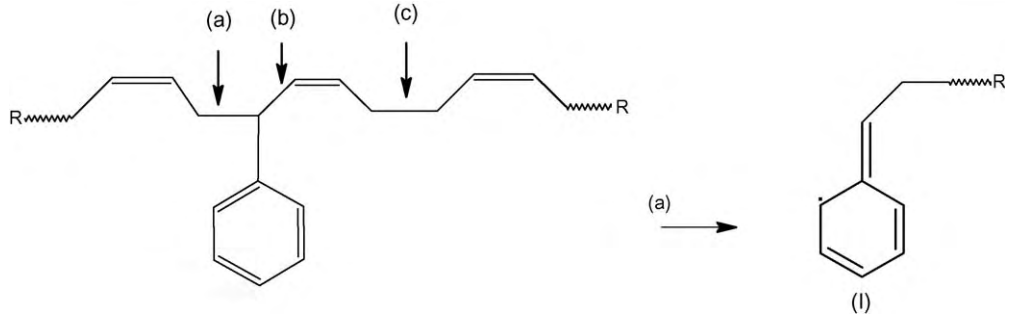

Scheme 1. All cracking positions on the SBR chain and the product (**I**) obtained from cracking at the most probable position (**a**) [13].

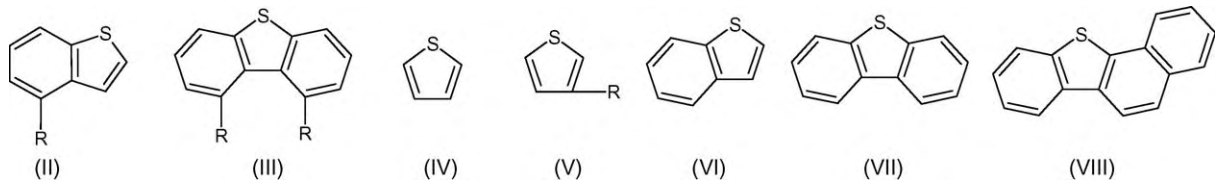

Scheme 2. Some polar-aromatics found in pyrolytic oils [9,34–36].

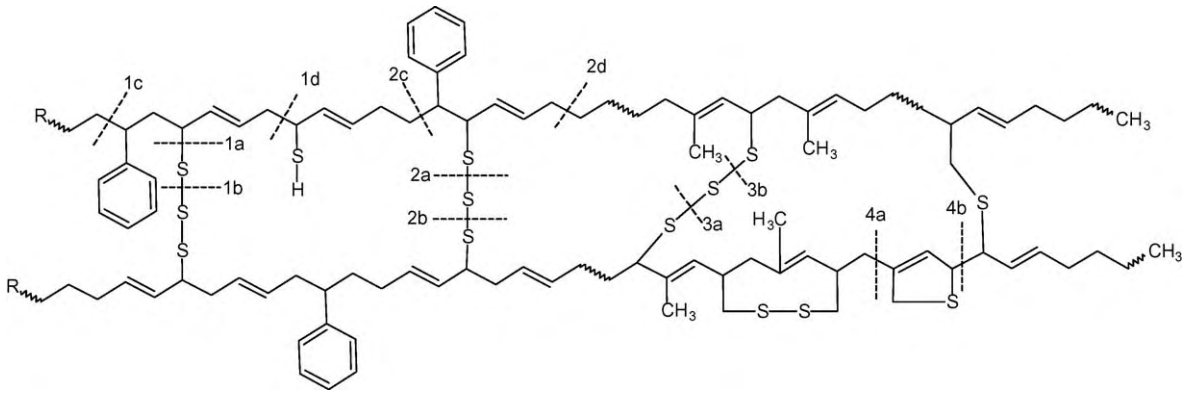

Scheme 3. A tire molecule (adapted from [4,8,33]) accompanied with the proposed possible cracking positions during pyrolysis [5,11–13].

out along the free rubber chains. According to the dissociation energy of the S–S, C–S and C–C bonds, which are 429, 699 and 607 kJ mol^{-1}, respectively [38], the free sulfur might easily be produced by the cracking of tire molecule at the positions **1a**, **1b**, **2a**, **2b**, **3a**, and **3b**.

The thermal cracking reaction could simultaneously occur at any position from **1** to **4**. The scissions occurring at the positions **1a**, **b**, **c**, and **d** result in the formation of Species (**I**) [13] and some free sulfurs. After that, Species (**I**) might react with the generated free sulfurs under the presence of ethylene via the Diels–Alders reaction [8], followed by cyclization and dehydrogenation [35] to form (**II**). Consequently, Species (**II**) can further react with the produced olefins [34], and then again cyclizes yielding Species (**III**) as shown in Scheme 4.

The production of hydrogen sulfide [39,40] in the gas product could be explained by the reactions displayed in Scheme 5. Initialized by the simultaneous cracking of tire molecule at positions **1d** and **2c** in Scheme 3, the product could then be stabilized by hydrogen coming from potential H-donor structures [34], followed by cracking to produce hydrogen sulfide and light olefins such as ethylene and propylene [41].

In contrast, with the presence of potential H-donor compounds during the pyrolysis [34], the produced H_2S might be added to the olefins generated by the thermal cracking to form thiols, which suffer the cyclization and dehydrogenation into thiophenic compounds [42,43].

The cracking of the rubber chain at the positions **2a**, **b**, **c** and **d** followed by the free radical stabilization and the cyclization reaction on the chain [44] could lead to the formation of alkylbenzothiophene (**II**). Moreover, thiophene, which could be directly produced via the cracking reaction at positions **4a** and **b**, might undergo hydrogen transfer reaction [34]. And then, the obtained product subsequently reacts with the available olefins [15,44], followed by cyclization and dehydrogenation [34], generating benzothiophene (**V**). Further reactions could also occur, leading to the formation of polycyclic polar-aromatic compound, **VIII**, as shown in Scheme 6.

3.2.2. Effect of temperature on polar-aromatic production

The effect of pyrolysis temperature on polar-aromatic production was also investigated in the present study. The results show that under the pyrolysis temperature of 500 °C, the amount of polar-aromatics account for approximately 11 %wt of the obtained oil product. And, when the pyrolysis temperature increased, the amount of polar-aromatics increased as shown in Fig. 4.

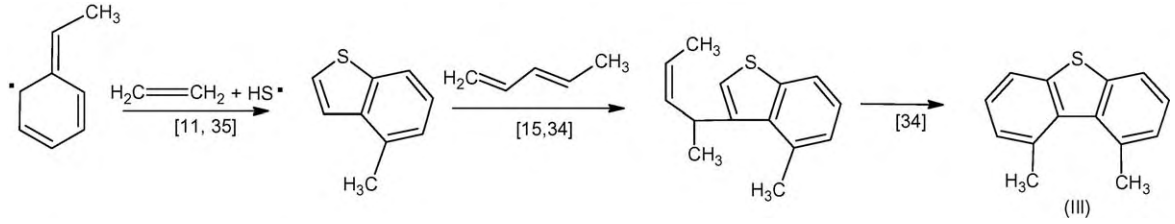

Scheme 4. An example of polar-aromatic formation via a consecutive reaction with free sulfurs.

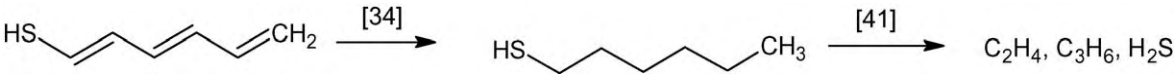

Scheme 5. An example of hydrogen sulfide production via hydrogenation followed by cracking.

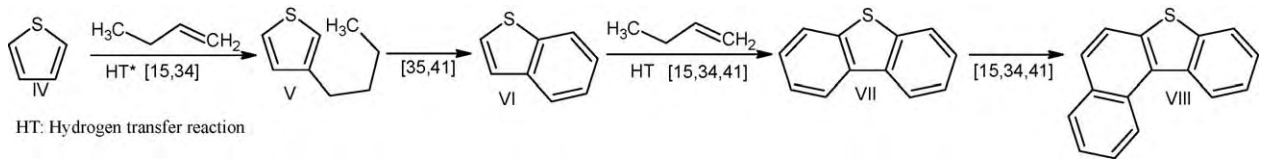

Scheme 6. An example of polycyclic polar-aromatic formation initialized by the direct cracking of tire.

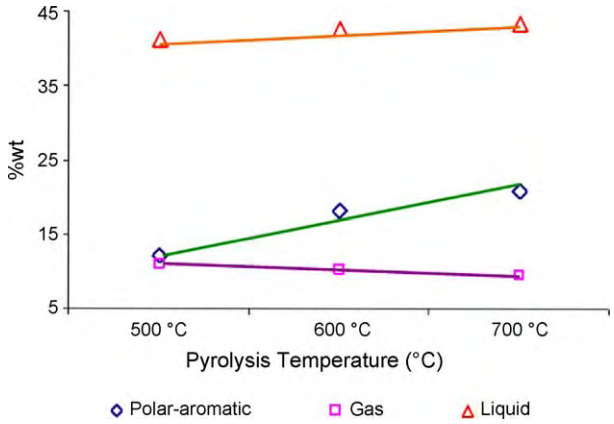

Fig. 4. Effect of pyrolysis temperature on the yield of gaseous and liquid products in association with the weight-percentage of polar-aromatics in the liquid product.

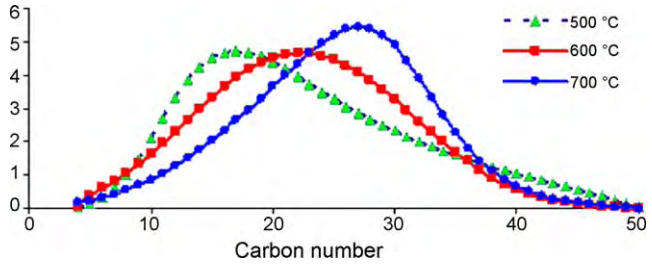

Fig. 5. Effect of pyrolysis temperature on the carbon number distribution of polar-aromatic compounds.

From the results, it can be explained that at higher temperatures, more free radicals are generated at a greater rate, so many of them combine with one another. As a consequence, more aliphatic chains link to polar-aromatic structures as in Scheme 4, and then these chains might undergo cyclization reactions resulting in the production of much heavier polar-aromatic hydrocarbons as in Scheme 6. The decrement of gas product as observed in Fig. 4 is also the consequence of the poly-aromatic formations. The shift of the peak to the higher carbon number with temperature shown in Fig. 5 can be the evidence confirming the formation of bigger size poly-aromatic compounds in the oil products.

In summary, the formation of polar-aromatics could mainly be attributed to (i) the combinations of available olefins and free sulfurs, (ii) the combination of sulfur-containing compounds with olefins, via the Diels–Alders reactions, and (iii) the direct cracking of tire molecule where the S atoms resided. Therefore, in order to reduce polar-aromatics in the pyrolytic oils without the introduction of hydrogen, one can either prevent them from formation via such means or force them by any means to crack into lower molecules and eventually to hydrogen sulfide as in Scheme 5.

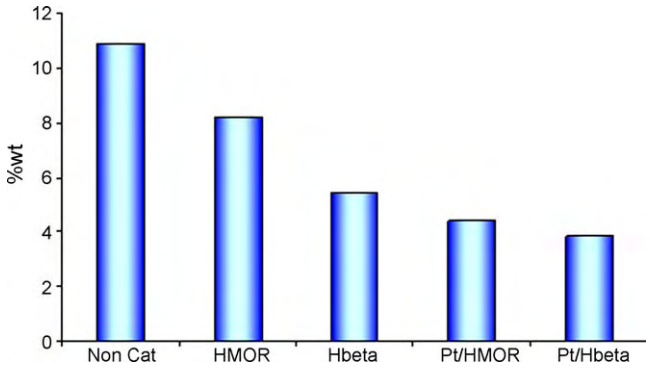

Fig. 6. Effect of catalysts on the polar-aromatic content in the pyrolytic oils.

3.3. Effects of the catalysts

Fig. 6 shows the percentages of the polar-aromatics in the pyrolytic oils obtained from the experiments run with different catalysts. From the figure, it is clear that HMOR and HBETA zeolites help decrease the amount of polar-aromatics by approximately 30 and 50 %wt, respectively, as compared to the non-catalytic case. The introduction of Pt on the zeolites led to a further decrease in the content of polar-aromatics. And, the lowest polar-aromatic content is observed when Pt/HBETA catalyst was used.

Fig. 7 shows the simulated distillation of the obtained polar-aromatic portions, which were cut, according to the boiling points, into gasoline (<149 °C), kerosene (149–232 °C), gas oil or diesel (232–343 °C), light vacuum gas oil or fuel oil (343–371 °C), and heavy vacuum gas oil (>371 °C). According to the figure, one can see that polar-aromatics from the non-catalytic pyrolysis are mainly distributed in the range of gas oil and vacuum gas oil. The introduction of the catalysts alters the distribution of polar-aromatics to a range of lighter fractions. Especially, when the bifunctional catalysts were used, polar-aromatic compounds in the HVGO range decreased remarkably. And, polar-aromatics are highly distributed in the kerosene range, instead of the gas oil range as having occurred when the corresponding zeolites were used. Besides, a small amount of polar-aromatics in the gasoline range is obtained in the case of HBETA. This might be attributed to the fact that HBETA has two channels 7.6 × 6.4 Å in diameter, and a third channel that is only 5.5 × 5.5 Å wide [16], so that deep cracking of polar-aromatics might have occurred producing H_2S and light hydrocarbons in the gaseous product.

Fig. 8 shows the shift of carbon number distribution of polar-aromatics to lower carbon numbers in conjunction with the narrower distribution when the catalysts were used. Many studies have proven that acid catalysts are able to crack thiophene, benzothiophene, and their derivatives to lower molecular weight substances [15,45]. Once polar-aromatics are formed, acid catalysts can crack them into smaller molecules, and possibly

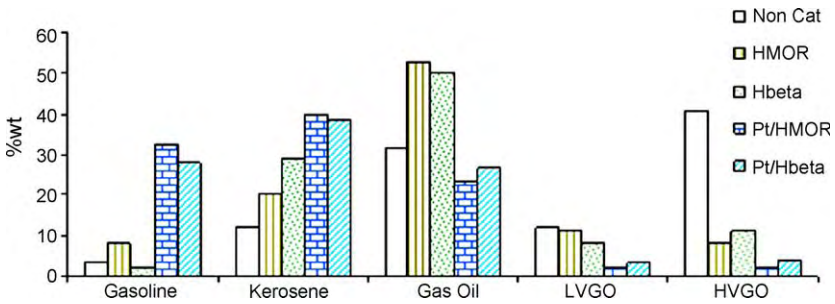

Fig. 7. Effect of catalyst on polar-aromatic distribution in petroleum fractions.

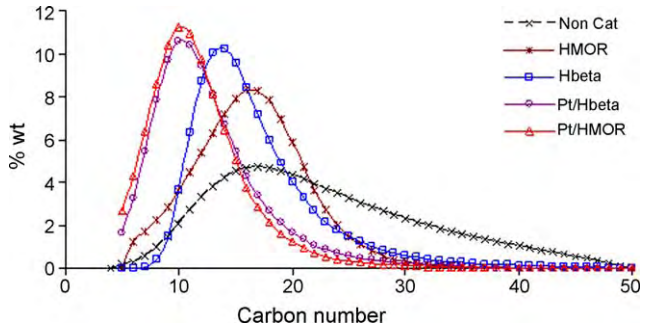

Fig. 8. Effect of catalysts on the carbon number distribution of polar-aromatic compounds.

open aromatic rings, consequently reducing the total amount of the polar-aromatics in the pyrolytic oil.

As presented in this work, between the two zeolites, HBETA exhibits higher activity than HMOR in reducing the size of polar-aromatics as illustrated by the lower average carbon number (Fig. 8) as well as the quantity of the compounds (Fig. 6). The higher activity of HBETA as compared to HMOR might be attributed to its better cracking activity caused by the combination effects of its higher total amount of medium and strong acid sites (Fig. 3), its smaller crystalline (Table 1), and especially its large sinusoidal pore systems [46,47]. Moreover, its larger pore diameter favors the diffusion of larger molecules into inner pores; thus, a higher amount of reactants including polar-aromatics might be cracked to smaller compounds.

Additionally, it was reported that acid catalysts displayed the activity not only on cracking polar-aromatics or sulfur-containing compounds but also on the cracking of a hydrogenated aromatic intermediate, as in Scheme 7a [14]. Prior to being converted to a polar-aromatic compound, Species (**I**) might be stabilized and cracked to produce lighter HCs, preventing the reactions in Scheme 6 from occurring. In addition, the presence of acid catalysts was found to convert long chain alkyl-thiophenes to shorter alkyl-thiophenes by cracking the alkyl chain of the former [14,15] as shown in Scheme 7b, resulting in the prevention of the formation of Species (**VI**) from (**V**) as illustrated in Scheme 6.

Table 1 has shown that HBETA forms higher amount of coke than HMOR. This could be attributed to the higher total amount of medium and strong acid sites, and particularly its larger pore volume that favors the condensation of an aromatic compound to form coke [48]. Corma et al. [14] also suggested a possible pathway to form coke from alkyl-benzothiophenes (Species **II**). In addition, the highest amount of coke is produced when the bifunctional catalysts were used, suggesting that possibly polar-aromatics are partially diminished by the formation of coke instead.

As shown in Scheme 4, the formation of polar-aromatics involves the interaction with accessible olefins. Consequently, if a catalyst can help eliminating these compounds, the polar-aromatic formation can be prevented. And, interestingly, that was indeed the case when the bifunctional catalysts were used. Although the HBETA zeolite alone displays much higher polar-aromatic reduction than the HMOR zeolite does (Fig. 8); with the introduction of Pt, the polar-aromatic reduction activity of the two emerged bifunctional catalysts is found comparable. Consequently, the presence of Pt on the surface of the catalyst results in the

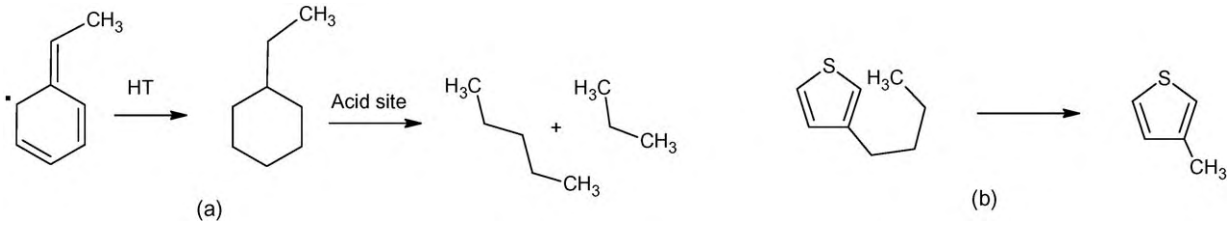

Scheme 7. Examples of polar-aromatic reduction by acid catalysts [14,15].

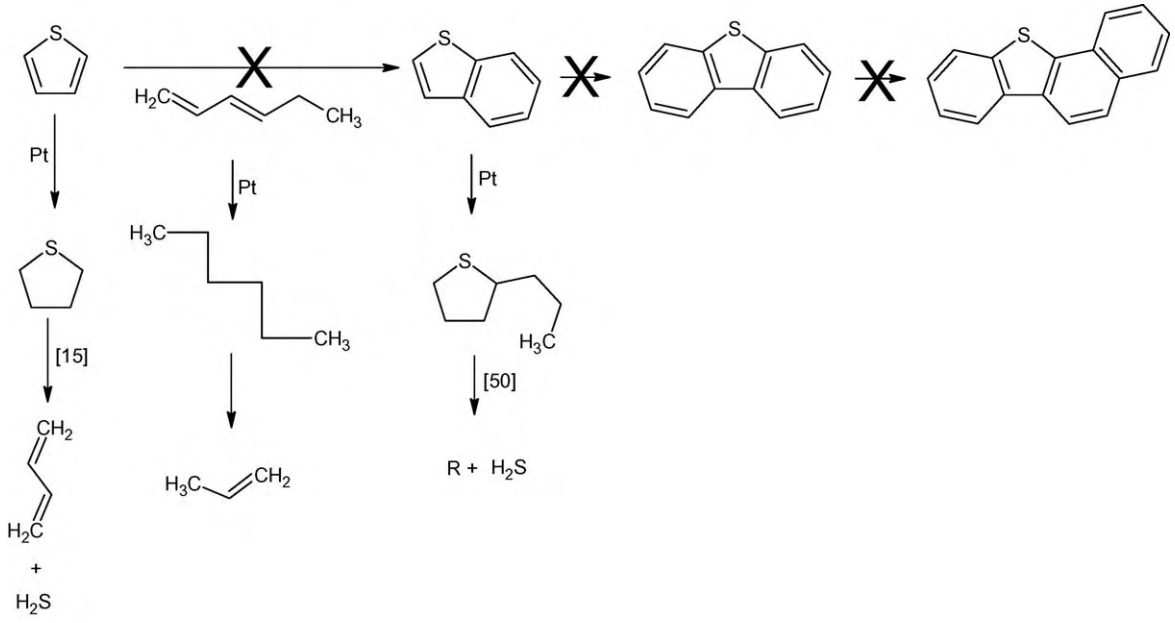

Scheme 8. Examples of some prevented and favored reactions by a bifunctional catalyst.

prevention of polar-aromatic formation. This could be attributed to the high hydrogenation activity of Pt [18,49] that helps converting olefins and other unsaturated intermediates to saturated HCs, instead of being combined with one another to form heavier polycyclic polar-aromatic compounds as in Scheme 6. In addition, these hydrogenated compounds might further undergo cracking reactions, and then, are converted into lighter polar-aromatics or sulfur-containing compounds or even into H_2S in association with the formation of short-chain hydrocarbons. That explains the shift of the peak to the lower carbon number (Fig. 8) when Pt-supported catalysts were present. Therefore, it is possible that the rate of the hydrogenation catalyzed by Pt metal is faster than the rate of the combination reaction (as in Scheme 6 to yield heavier polar-aromatic compounds), leading to the reduction of polar-aromatic compounds in the pyrolytic oils. To visualize the previous explanation, Scheme 8 gives some examples of the prevented and favored reactions if thiophene, reported as a sulphur-compound among other thiophene compounds found in tire-derived oil [9,34–36], is present with the catalysts. Furthermore, as mentioned earlier, the polar-aromatic reduction activity of Pt/HBETA was slightly higher than Pt/HMOR. This could be attributed to the higher surface area of HBETA (Table 1), resulting in the better dispersion of Pt (Table 1) [32], and leading to a better hydrogenation activity.

Finally, the bifunctional catalysts can also decrease the amount of polar-aromatic hydrocarbons in the pyrolytic oil via the cracking reactions. Once polar-aromatics are formed, they might be hydrogenated on the Pt sites, followed by cracking on the acid sites [50,51].

4. Conclusions

The complex structure of the tire makes it difficult to understand the multi-reactions occurring under the pyrolysis. In this study, the polar-aromatic formation in the pyrolysis of waste tire has been proposed. And pyrolysis temperature was found to strongly influence polar-aromatic content in the derived oil. The increase in the pyrolysis temperature led to an increment of polar-aromatic content, and also a shift of polar-aromatic distribution to the higher carbon number. The use of acid zeolites decreased polar-aromatic content dramatically. And, HBETA showed higher polar-aromatic reduction activity as compared to HMOR, which was ascribed to its acidic properties, small crystal size and 3D-structure. Especially, the introduction of Pt on the zeolites led to a further decrease in the polar-aromatic content. Pt/HBETA showed a slightly higher polar-aromatic reduction activity as compared to its counterpart, Pt/HMOR, which was explained by its higher metal dispersion.

The major role of Pt was to enhance the hydrogenation reactions, resulting in the conversion of polar-aromatics and their precursors to saturated HCs. Consequently, these compounds might undergo the cracking reactions catalyzed by the acid function of the catalysts, thus reducing the amount of the polar-aromatics.

Acknowledgements

The following agencies are acknowledged for their mutual financial support: The Petroleum and Petrochemical Consortium, the Thailand Research Fund (TRF), the "*Syntheses and Applications of Organometallics*" Research Unit of Chulalongkorn University, and The Graduate Scholarship Program for Faculty Members from Neighboring Countries of Chulalongkorn University.

References

[1] S. Boxiong, W. Chunfei, G. Binbin, W. Rui, Liangcai, Appl. Catal. B 73 (2007) 150–157.
[2] S. Galvagno, S. Casu, T. Casabianca, A. Calebrese, G. Cornacchia, Waste Manage. 22 (2002) 917–923.
[3] J.E. Mark, B. Erman, F. Eirich, Science and Technology of Rubber, 2nd Edition, Academic Press, San Diego, 1994.
[4] C.M. Blow, C. Hepburn, Rubber Technology and Manufacture, 2nd Edition, Butterworths, Norwich, 1982.
[5] S. Jitkarnka, B. Chusaksri, P. Supaphol, R. Magaraphan, J. Anal. Appl. Pyrolysis 80 (2007) 269–276.
[6] M.L. Lee, M. Novotny, K.D. Bartle, Analytical Chemistry of Polycyclic Aromatic Compounds, Academic Press, New York, 1981.
[7] R.A. Pelroy, D.L. Stewart, Y. Tominga, M. Iwao, R.N. Castle, M.L. Lee, Mutat. Res. 117 (1981) 31.
[8] P.T. Williams, R.P. Bottrill, Fuel 74 (1995) 736–742.
[9] H. Pakdel, D.M. Pantea, C. Roy, J. Anal. Appl. Pyrolysis 57 (2001) 91–107.
[10] C. Diez, O. Martinez, L.F. Calvo, J. Cara, A. Moran, Waste Manage. 24 (2004) 463–469.
[11] F. Chen, J. Qian, Fuel 81 (2002) 2071–2077.
[12] F.M. Uhl, M.A. McKinney, C.A. Wilkie, Polym. Degrad. Stab. 70 (2000) 417–424.
[13] S. Choi, J. Anal. Appl. Pyrolysis 55 (2000) 161–170.
[14] A. Corma, C. Martínez, G. Ketley, G. Blair, Appl. Catal. A: Gen. 208 (2001) 135–152.
[15] J.A. Valla, A.A. Lappas, I.A. Vasalos, Appl. Catal. A: Gen. 297 (2006) 90–101.
[16] G.S. Miguel, J. Aguado, D.P. Serrano, J.M. Escola, J.M. Rodríguez, Appl. Catal. B: Environ. (2006) 209–219.
[17] V.G. Baldovino-Medrano, S.A. Giraldo, A. Centeno, Fuel 87 (2008) 1917–1926.
[18] M.F. Williams, B. Fonfé, C. Woltza, A. Jentys, J.A.R. van Veen, J.A. Lercher, J. Catal. 251 (2007) 497–506.
[19] J.B. McKinley, in: P.H. Emmett (Ed.), Catalysis, vol. 5, Reinhold, New York, 1957.
[20] T.A. Pecoraro, R.R. Chianelli, J. Catal. 67 (1981) 430–445.
[21] A. Stanislaus, B.H. Cooper, Catal. Rev. Sci. Eng. 36 (1994) 75–123.
[22] H. Du, C. Fairbridge, H. Yang, Z. Ring, Appl. Catal A: Gen. 294 (2005) 1–21.
[23] H. Yasuda, Y. Yoshimura, Catal. Lett. 46 (1997) 43.
[24] N. Matsubayashi, H. Yasuda, M. Imamura, Y. Yoshimura, Catal. Today 45 (1998) 375.
[25] R.M. Navarro, B. Pawelec, J.M. Trejo, R. Mariscal, L.L.G. Fierro, J. Catal. 189 (2000) 184.
[26] M. Santikunaporn, J.E. Herrera, S. Jongpatiwut, D.E. Resasco, W.E. Alvarez, Ed L. Sughrue, J. Catal. 228 (2004) 100–113.
[27] G. Sebor, J. Blaz ek, M.F. Nemer, J. Chromatogr. A 847 (1999) 323–330.
[28] A.D. Schmitz, G. Bowers, C. Song, Catal. Today 31 (1996) 45–56.
[29] F. Lonyi, J. Valyon, Thermochim. Acta (2001) 53–57.
[30] Y. Miyamoto, N. Katada, M. Niwa, Micro. Meso. Mater. 40 (2000) 271–281.
[31] Horvath, Kawazoe, J. Chem. Eng. Japan 16 (1983) 47.
[32] C. Song, X. Ma, Appl. Catal. B: Environ. 41 (2003) 207–239.
[33] P.T. Williams, S. Besler, Fuel 14 (1995) 1277–1283.
[34] I.M. Rodriguez, M.F. Laresgoiti, M.A. Cabrero, A. Torres, M.J. Chomón, B. Caballero, Fuel Process. Technol. 72 (2001) 9–22.
[35] M.F. Laresgoiti, B.M. Caballero, I.M. Rodriguez, A. Torres, M.A. Cabrero, M.J. Chomón, J. Anal. Appl. Pyrolysis 71 (2004) 917–934.
[36] K. Unapumnuk, T.C. Keener, M. Lu, F. Liang, Fuel 87 (2008) 951–956.
[37] P.T. Williams, A.J. Brindle, J. Anal. Appl. Pyrolysis 62 (2003) 143–164.
[38] J.A. Dean, Lange's Handbook of Chemistry, 15th Edition, McGrawHill, 1999.
[39] D.Y.C. Leung, X.L. Yin, Z.L. Zhao, B.Y. Xu, Y. Chen, Fuel Process. Technol. 79 (2002) 141–155.
[40] E. Aylon, R. Murillo, A. Fernandez-Colino, A. Aranda, T. Garcıa, M.S. Callen, A.M. Mastral, J. Anal. Appl. Pyrolysis 79 (2007) 210–214.
[41] X. Dupain, L.J. Rogier, E.D. Gamas, M. Makkee, J.A. Moulijn, Appl. Catal. A: Gen. 238 (2003) 223–238.
[42] P. Leflaive, J.L. Lemberton, G. Pérot, C. Mirgain, J.Y. Carriat, J.M. Colin, Appl. Catal. A: Gen. 227 (2002) 201–215.
[43] H. Mizutani, Y. Korai, I. Mochida, Fuel 86 (2007) 2898–2905.
[44] P.T. Williams, D.T. Taylor, Fuel 72 (1993) 1469–1474.
[45] B. Li, W. Guo, S. Yuan, J. Hua, J. Wang, H. Jiao, J. Catal. 253 (2008) 212–220.
[46] Yun Je Lee, Jong-Ho Kim, Seok Han Kim, Suk Bong Hong, Gon Seo, Appl. Catal. B: Environ. 83 (2008) 160–167.
[47] A. Corma, J. Martınez-Triguero, C. Martınez, J. Catal. 197 (2001) 151.
[48] D. Richardeau, G. Joly, C. Canaff, P. Magnoux, M. Guisnet, M. Thomas, A. Nicolaos, Appl. Catal. A: Gen. 263 (2004) 49–61.
[49] A. Philippou, M.W. Anderson, J. Catal. 167 (1997) 266–272.
[50] F. Can, A. Travert, V. Ruaux, J.-P. Gilson, F. Maugéa, R. Hub, R.F. Wormsbecher, J. Catal. 249 (2007) 79–92.
[51] R. Contreras, R. Cuevas-Garcia, J. Ramirez, L. Ruiz-Azuara, A. Gutierrez-Alejandre, I. Puente-Lee, Castillo-F P., C. Salcedo-Luna, Catal. Today 130 (2008) 320–326.

Provided for non-commercial research and education use.
Not for reproduction, distribution or commercial use.

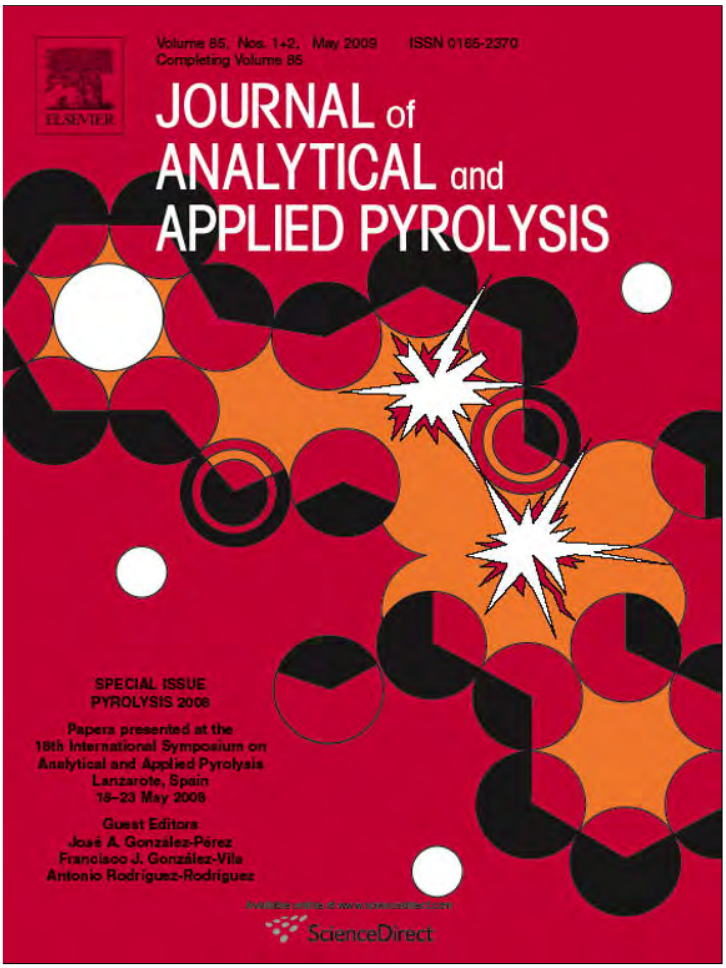

This article appeared in a journal published by Elsevier. The attached copy is furnished to the author for internal non-commercial research and education use, including for instruction at the authors institution and sharing with colleagues.

Other uses, including reproduction and distribution, or selling or licensing copies, or posting to personal, institutional or third party websites are prohibited.

In most cases authors are permitted to post their version of the article (e.g. in Word or Tex form) to their personal website or institutional repository. Authors requiring further information regarding Elsevier's archiving and manuscript policies are encouraged to visit:

http://www.elsevier.com/copyright

Author's personal copy

J. Anal. Appl. Pyrolysis 85 (2009) 338–344

Contents lists available at ScienceDirect

Journal of Analytical and Applied Pyrolysis

journal homepage: www.elsevier.com/locate/jaap

Effects of ITQ-21 and ITQ-24 as zeolite additives on the oil products obtained from the catalytic pyrolysis of waste tire☆

N.A. Dũng, A. Mhodmonthin, S. Wongkasemjit, S. Jitkarnka *

The Petroleum and Petrochemical College, Center of Excellence for Petroleum, Petrochemicals, and Advanced Materials, Chulalongkorn University, Chula Soi 12, Phaya Thai, Bangkok 10330, Thailand

ARTICLE INFO

Article history:
Received 25 June 2008
Accepted 17 October 2008
Available online 5 November 2008

Keywords:
Waste tire
Pyrolysis
ITQ-21
ITQ-24
MOR

ABSTRACT

The effects of ITQ-21 and ITQ-24 as zeolite additives on the catalytic pyrolytic oil using HMOR were investigated. The research was started by studying the effect of HMOR and its amount represented by the catalyst-to-tire ratio, and then followed by the effects of addition of the two ITQ zeolites into HMOR. The results showed that, with increasing the catalyst-to-tire ratio, the gasoline and kerosene yield increased in accordance with the reduction of the heavier fractions, and the concentration of the saturated hydrocarbons in the pyrolytic oil was found to be higher. However, increasing the catalyst-to-tire ratio decreased the yield of liquid product. The two ITQ zeolite additives have strong effects on the pyrolytic oil. For example, as compared with the case of pure HMOR, adding ITQ-21 enhanced the production of kerosene whereas the introduction of ITQ-24 resulted in the higher concentration of aromatic compounds in the derived oil. In addition, the use of catalyst was found to enhance the selectivity of mono-aromatic in the light fraction, but adding ITQ zeolites caused a reduction in the selectivity of HMOR toward the production of mono-aromatics. The differences on the effects of the two ITQ zeolites were explained in relation with the catalyst characterization results. It was found that, the acid properties and topology played very important roles on the influences of these additives.

© 2008 Elsevier B.V. All rights reserved.

1. Introduction

Pyrolysis has been proposed as a viable tire recycling technology which recently been receiving renewed attention. Pyrolysis generates oil which has a high calorific value, ~42 MJ kg^{-1}, and has been successfully combusted in an engine [1]. In addition, the oil has been shown to be aromatic, and contains a high concentration of potentially valuable chemical feedstock [2]. However, there are some obstacles to the use of the oil as a recycle product without refinery complex due to the low quality and variability of properties. Therefore, there has been great interest in process development such as the introduction of catalyst treatment.

Williams and Brindle [3] investigated the effect of catalytic temperature in the pyrolysis of scrap tire using ZSM5 and Y type zeolite catalysts. They found that there was a dramatic increase in the concentration of certain single ring aromatic compounds in the derived oil after using the catalysts. Similar results were reported in the study of Miguel et al. [4]. Besides, the pore size and silica to alumina ratio of the zeolite catalysts affected strongly on the production and selectivity of aromatic compounds in the pyrolysis of waste tire [5]. However, the oil has been investigated for its potential as a chemical feedstock rather than fuel.

ITQ-21, a zeolite with a three-dimensional pore network containing 1.18 nm wide cavities, each of which is accessible through six circular and 0.74 nm wide windows, is the great discovery of the researchers of Instituto de Tecnologıa Quımica, Universidad Politecnica de Valencia, Spain [6,7]. ITQ-21 has been used as a catalyst, and exhibited a high catalytic activity and selectivity for valuable products in preliminary oil refining tests [6]. Moreover, ITQ-21 catalyst yielded the lowest olefin content in gasoline as compared with USY and Beta zeolite catalysts in the cracking of light vacuum gas oil [6]. Furthermore, ITQ-24 has a tridirectional pore system of intercrossing 12 member ring (MR) and 10MR channels. The first set of 12MR straight channel runs perpendicularly to the *ab* plane with a pore aperture of approximately 7.7 Å × 5.6 Å. A second set of 12MR sinusoidal channels is placed along the *a* axis with a pore aperture of 7.2 Å × 6.2 Å. Finally, there is a third 10MR channel system that intersects perpendicularly to both 12MR channel systems with a

☆ Presented at 18th International Symposium on Analytical and Applied Pyrolysis, Lanzarote, Spain, 18–23 May 2008.

* Corresponding author. Tel.: +66 2 218 4148; fax: +66 2 215 4459.
E-mail address: Sirirat.j@chula.ac.th (S. Jitkarnka).

0165-2370/$ – see front matter © 2008 Elsevier B.V. All rights reserved.
doi:10.1016/j.jaap.2008.10.020

Author's personal copy

pore opening of 5.7 Å × 4.8 Å. This particular topology should make the ITQ has high shape selectivity. In addition, the ITQ series were found to have high thermal stability and high resistance to pore blockage [8] as well as high acidity [6]. ITQ-21 has been used as a zeolite additive in catalysts used for many types of reaction including cracking [9–11] due to its acid property. However, no report on using the ITQ zeolite as an additive has been found in the application of waste tire pyrolysis.

Therefore, in this paper, the two ITQ-21 and ITQ-24 zeolites were successfully synthesized and used as zeolite additives of a commercial HMOR zeolite. The catalysts were tested for their activity on waste tire pyrolysis. The effects of ITQs on the pyrolytic oils were investigated.

2. Experimental

2.1. Catalyst preparation and characterization

The ITQ zeolites were freshly prepared in the laboratory. The accomplishment of ITQ series synthesis was confirmed by means of XRD and XRF techniques in accordance with comparison to Refs. [6,7]. XRD patterns were obtained using the Riguku D/Max 2200H with a scanning speed of 0.02 °/min and 2θ from 5° to 60°. X-ray fluorescence (XRF) technique was employed to obtain the chemical composition of the studied materials. FTIR spectroscopic analysis of the synthesized materials was conducted using a Bruker instrument (EQUINOX55) with a resolution of 4 cm^{-1}. The surface area and pore size distribution of the studied catalysts were characterized by N_2 physical adsorption using the Sorptomatic 2900 equipment.

To prepare a catalyst for testing the cracking activity, the MOR zeolite, supplied by TOSOH company, was first calcined at 500 °C for 5 h. Then, the ITQ series were physically mixed with the calcined HMOR zeolite to a specific amount of 2 wt%. Finally, the mixture was pellitized and sieved to obtain a particle size in the range of 400–425 μm.

Temperature program desorption (TPD) using NH_3 was carried out in a TPD/TPR Micromeritics 2900 equipment. Approximately 0.1 g of sample was first pretreated in He at 550 °C for 30 min. Then, the system was cooled down to 100 °C, and the NH_3 adsorption was performed using NH_3/N_2 for 1.5 h followed by the introduction of He to remove the physically adsorbed and gaseous NH_3 for 30 min at 100 °C. Finally, the system was cooled down to 50 °C, and then the temperature program desorption was started from 50 to 600 °C with a heating rate of 5 °C min^{-1}.

Temperature program oxidation (TPO) using a Micromeritics 2900 machine was performed from room temperature to 900 °C with a heating rate of 10 °C min^{-1} and hold for 30 min. The amount of coke was then determined from the area under the peak and calculated by the software supplied with the machine.

2.2. Pyrolysis of waste tire

A tire sample was first pyrolyzed in the lower zone of the reactor from room temperature to a final temperature of 500 °C with a heating rate of 10 °C min^{-1}. This pyrolysis zone was kept at the final temperature for 1 h to ensure the total conversion of tire. The evolved product was carried by a 30 ml min^{-1} nitrogen flow to the upper zone controlled at 350 °C and packed with a catalyst. The obtained product was next passed through an ice-salt condensing system containing 3 condensers in order to separate incondensable compounds from the liquid product. The experimental system is shown in Fig. 1. The solid and liquid products were weighed to determine the product distribution. The amount of gas was then determined by mass balance. The gaseous product collected in a Dual Valve Tedlar PVF bag purchased from Cole Parmer was analyzed by a GC, Agilent Technologies 6890 Network system, using an HP-PLOT Q column (300 mm × 0.32 mm ID and 20 μm film thicknesses) and an FID detector. For asphaltene separation, the liquid product was first dissolved in n-pentane with the ratio of 40:1 to precipitate asphaltene. Saturated hydrocarbons, mono-, di-, poly- and polar-aromatics in the obtained maltenes were fractionated by means of the liquid adsorption chromatography [12]. Finally, a Varian CP 3800 Simulated Distillation Gas Chromatograph equipped with FID and a 15 m × 0.25 mm × 0.25 μm WCOT fused silica capillary column (SIMDIST GC) was used to analyze the obtained maltene and hydrocarbon fractions according to the ASTM D2887 method.

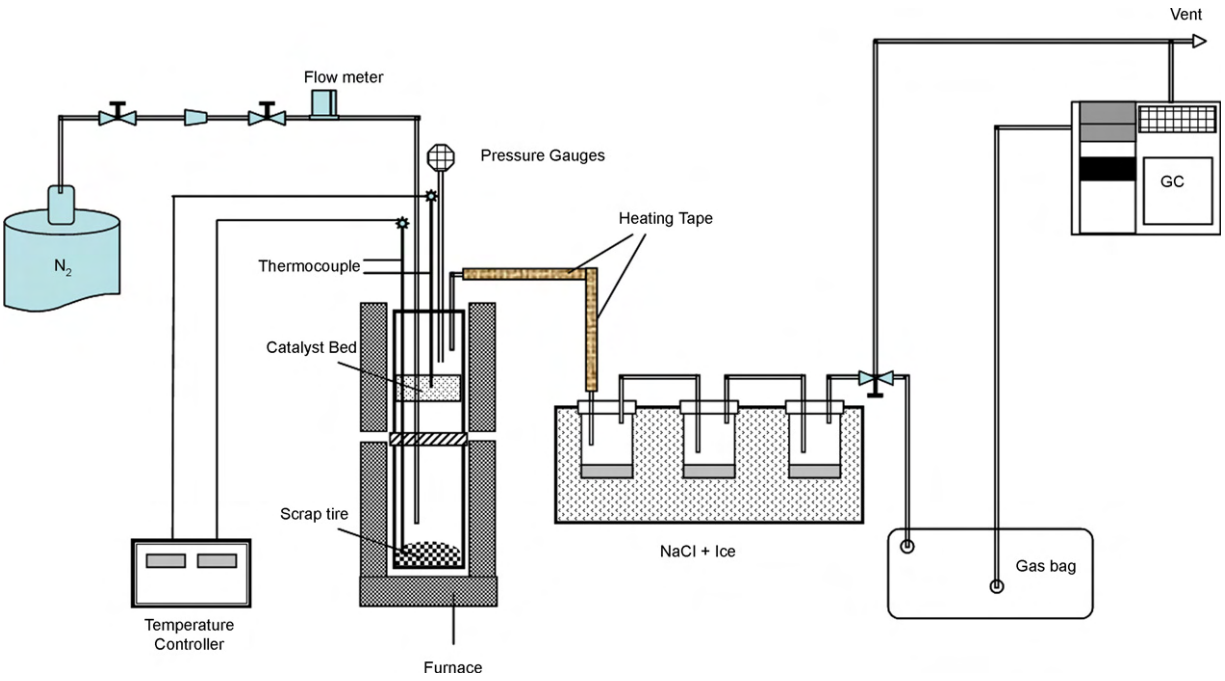

Fig. 1. Schematic of experimental pyrolysis system.

Author's personal copy

3. Results and discussion

3.1. Catalyst characterization

Fig. 2 shows the XRD patterns of the synthesized ITQ-21 (Fig. 2a) as compared to that of ITQ-21 from the reference (Fig. 2b) [6]. The figure indicates the success in the synthesis of ITQ-21 zeolite. Similarly, Fig. 3a and b illustrates the XRD patterns of the synthesized ITQ-24 and that of Ref. [7], also confirming the successful synthesis of ITQ-24. However, it is important to note that slightly broader peaks are observed in the XRD patterns of the synthesized materials. This is probably due to the fact that these materials were synthesized in fluoride media; thus, during calcination the evacuation of the occluded F^- could occur, resulting in a partial destruction of double-4-ring (D4R) cages and then leading to the slightly broader peaks in the XRD patterns [13].

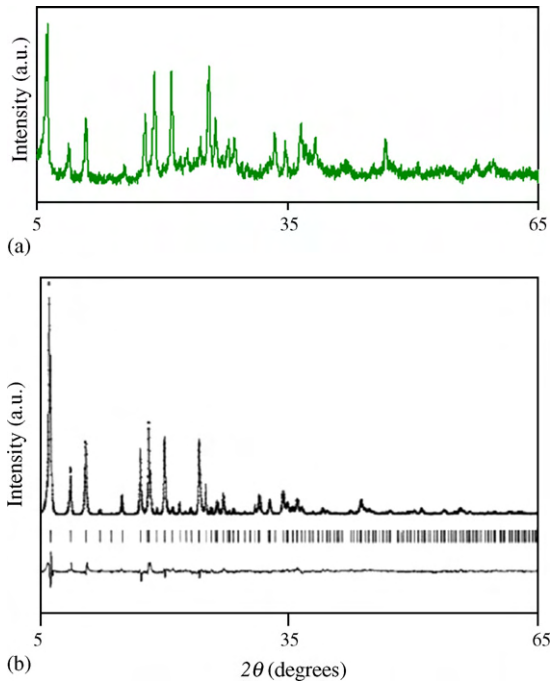

Fig. 2. XRD patterns of (a) synthesized ITQ-21 and (b) Ref. [6].

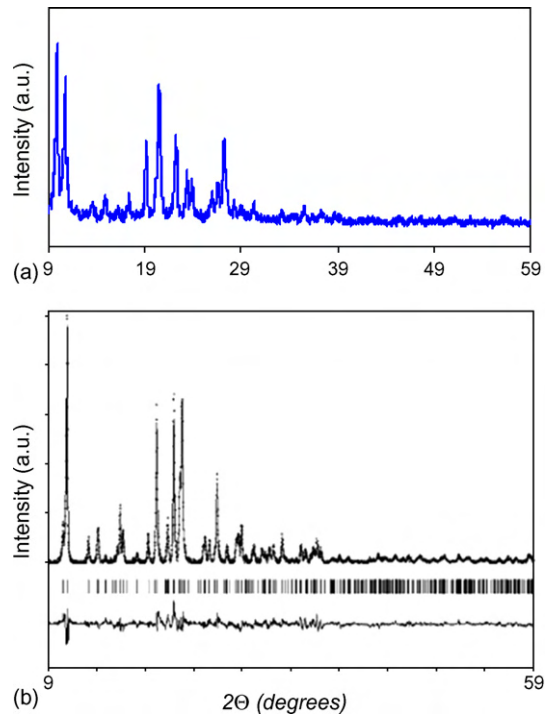

Fig. 3. XRD patterns of (a) synthesized ITQ-24 and (b) Ref. [7].

Table 1
Physical properties of the studied catalysts.

Material	Dimension	MR	SiO_2:Al_2O_3	Surface area ($cm^2\ g^{-1}$)	Mean pore diameter[a] (Å)
HMOR	1D	12	19.0[b]	372.5 ± 9.3	6.3 ± 0.3
ITQ-24	3D	12	33.3	356.6 ± 7.8	7.9 ± 0.4
ITQ-21	3D	12	47.5	453.3 ± 8.2	6.5 ± 0.4

[a] Determined by Horvath Kawazoe Poresizes method.
[b] From TOSOH Co., Ltd.

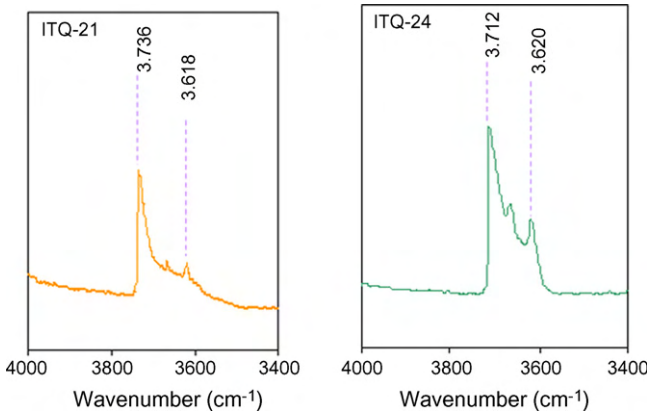

Fig. 4. FTIR spectra in the OH region of the synthesized ITQ zeolites.

Surface area, pore size distribution, the amount of coke and the Si:Al of all catalysts are displayed in Table 1. ITQ-24 has the largest pore size whereas HMOR zeolite has the lowest pore size. And, the two synthesized zeolites have higher Si:Al ratio with respect to HMOR, and the highest ratio belongs to the ITQ-21 zeolite.

The FTIR spectra of the calcined ITQ materials in the OH region are displayed in Fig. 4. All the synthesized materials show an absorption at around 3620 cm^{-1}, which is attributed to an acid bridging hydroxyl groups [6,7]. The spectra are very similar to those of Refs. [6,7]; thus, the success in synthesis of ITQ series in this study can then be assured.

Fig. 5 shows the TPD–NH_3 results of the studied catalysts, which indicate that the catalysts are fairly different on acid property. The

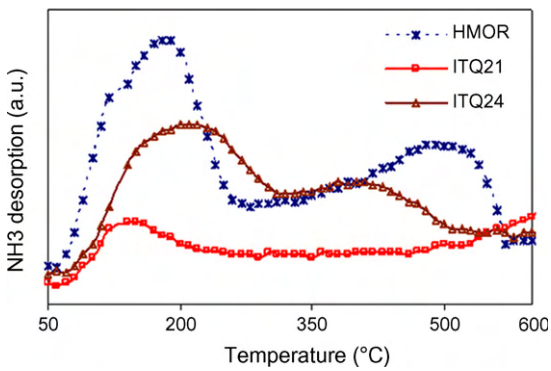

Fig. 5. TPD–NH_3 of the studied catalysts.

Author's personal copy

Table 2
Effect of HMOR-to-tire ratio on the product distribution, coke and asphaltenes.

HMOR:tire ratio	Gas (wt%)	Liquid (wt%)	Solid (wt%)	Coke ($g\,g^{-1}$ catalyst)	Asphaltenes ($g\,g^{-1}$ oil)
Non-catalyst	10.3	44.0	45.6	–	0.0059
0.13	11.9	41.8	46.3	0.19	0.0030
0.25	12.2	41.3	46.6	0.23	0.0027
0.33	17.6	35.2	47.8	0.33	0.0023

HMOR sample displays two desorption peaks at 175 and 485 °C. Similar observation was reported elsewhere [14]. ITQ-21 has low acidity, as determined from the area under the peak. On contrary, ITQ-24 shows two broaden peaks locating at 200 and 390 °C. Finally, based on the area under the peaks, one can see that HMOR has the highest acid density among the three zeolites.

3.2. Pyrolysis of waste tire

3.2.1. Effect of the catalyst-to-tire ratio

In order to see a great influence of catalysts, the appropriate amount of catalyst used in the catalytic pyrolysis of waste tire was first investigated. The effect of HMOR and its amount, represented by the catalyst-to-tire ratio, was thus studied by varying the ratio. Table 2 shows the influence of catalyst-to-tire ratio on the product yields, the coke formation on the catalysts, and the asphaltenes in the pyrolytic oils. The yield of gas increases significantly at the expense of oil yield with the increase in the catalyst-to-tire ratio. It is known that the catalytic activity can be improved, up to an extent, with the increase of catalyst quantity. Therefore, more hydrocarbons were cracked into the lower molecular weight compounds resulted from the greater effect of the catalyst. As a result, increasing in the catalyst to tire ratio decreased the amount of asphaltenes in the pyrolytic oil. However, there is not much different in the amount of asphaltenes obtained from the case of catalyst-to-tire ratio of 0.25 and 0.33.

Moreover, when the obtained oil was further analyzed, it was found that, as compared with the non-catalytic pyrolysis, HMOR generated higher saturated hydrocarbon. With the increasing catalyst-to-tire ratio, the yield of saturated hydrocarbons increases gradually, and then reaches a plateau at the catalyst-to-tire ratio of 0.25 as shown in Fig. 6. In practice, when the amount of catalyst increases, the amount of acid sites increases, or in other words, the surface acidity increases, resulting in an improvement of the catalytic activity. In addition, it is elucidated that aromatic and alkene species have a greater predisposition to being involved in pathways to coke formation because of their ability to easily be

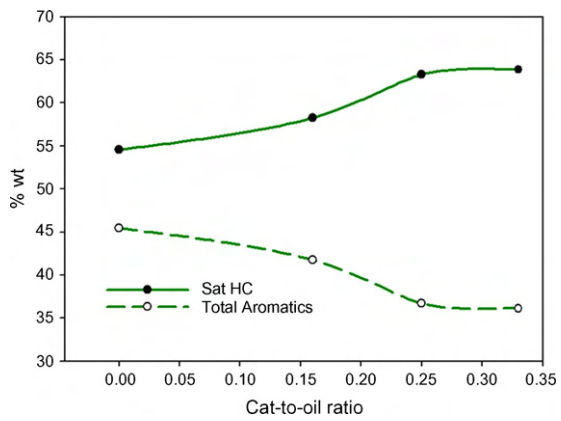

Fig. 6. Effect of catalyst-to-tire ratio on the composition of oil product.

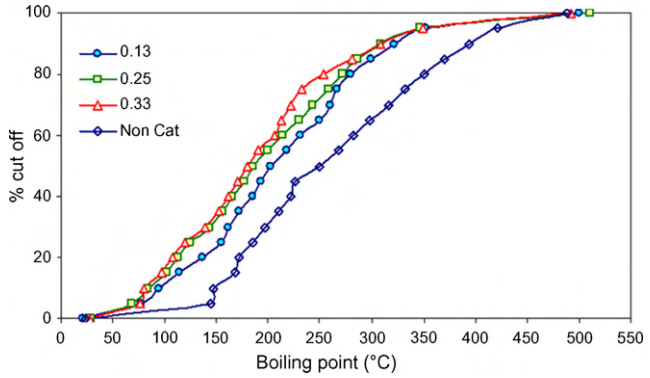

Fig. 7. Effect of catalyst-to-tire ratio on the simulated TBP curves of the oils.

involved in hydrogen transfer and cyclization reactions [15]. Therefore, an increase in the catalyst-to-tire ratio in the testing range can enhance either the cracking of the heavy compounds including aromatic compounds into lower molecular-weight hydrocarbons or the coke formation from aromatic hydrocarbons. This contributes to the fact that the amount of coke is found to increase with the catalyst-to-tire ratio as illustrated in Table 2.

In order to examine the liquid products as fuels, the true boiling point (TBP) curves of the pyrolytic oils obtained from using the different amounts of HMOR are plotted in Fig. 7. It demonstrates that the curve shifts to the lower temperature, indicating that lighter oil is produced with an increasing catalyst-to-tire ratio. Consequently, the catalyst-to-tire ratio affects strongly toward the production of light valuable oil fractions.

Fig. 8 indicates the simulated distillation of oils comprised of gasoline (<149 °C), kerosene (149–232 °C), gas oil or diesel (232–343 °C), fuel oil (343–371 °C), and heavy vacuum gas oil (>371 °C). Each fraction was classified according to its boiling point range. With respect to the non-catalytic pyrolysis, the introduction of HMOR led to the increase in the gasoline and kerosene yields at the expense of the heavier fractions, which is attributed to the cracking activity of the catalyst. Moreover, when the catalyst-to-tire ratio increases, the most affected fractions are gasoline and gas oil, which change in the opposite way from one another. For example, the yield of gasoline increases from 25.1 to 35.1 wt% with the increasing catalyst-to-tire ratio from 0.13 to 0.33 whereas the gas oil yields decreases from 32 to 22.4 wt%. As mentioned previously, the activity increased with the increase in catalyst. Therefore, the higher catalyst-to-tire ratio resulted in higher cracking activity that led to the higher production of gasoline in accordance with the decrease in gas oil fraction. However, unlike gasoline, the kerosene fraction only slightly increases with the catalyst-to-tire ratio. It is possible that the pore size of HMOR favors the diffusion of small

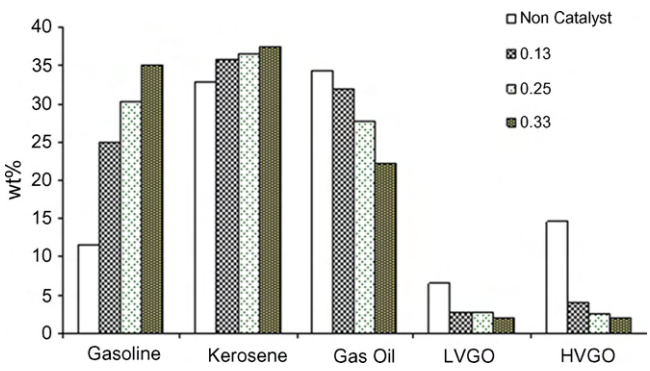

Fig. 8. Effect of catalyst-to-tire ratio on the pyrolytic oil fractions.

Author's personal copy

Table 3
Effect of ITQ additives on product distribution, coke formation, and asphaltene production.

Catalyst	Gas (wt%)	Liquid (wt%)	Solid (wt%)	Coke (g g^{-1} catalyst)	Asphaltenes (g g^{-1} oil)
Non-catalyst	10.3	44.0	45.6	–	0.0059
HMOR	14.7	40.3	45.0	0.23	0.0027
HMOR + 2% ITQ-24	12.0	42.4	45.6	0.29	0.0042
HMOR + 2% ITQ-21	13.8	41.0	45.2	0.15	0.0030

molecules which are in the range of gasoline fraction out of the pores, and thus more gasoline is produced.

From the previous results, it was realized that the catalyst-to-tire ratio of 0.33 gave the highest gasoline and kerosene production. However, its liquid yield was much lower than that obtained from the ratio of 0.25. Hence, the catalyst-to-tire ratio of 0.25 was selected for the further study.

3.2.2. Effect of the ITQ series as additives

Table 3 shows the product distribution, coke formation on the catalysts, and asphaltene production in the pyrolytic oils obtained from using various catalysts. It can be observed that the addition of the two ITQ additives slightly affects the product distribution. However, the asphaltene reduction activity of HMOR is found to decrease by adding ITQ zeolite additives. This is owing to the reduction of cracking activity with the introduction of the ITQ additives due to their lower density, yielding the mixtures with a slightly lower acid density.

Fig. 9 shows the TPB curves of the obtained oils from the introduction of ITQ additives. It demonstrates that when all catalysts are used, the curves shift to lower temperatures, meaning that the oils obtained from using all catalyst are lighter than that obtained from non-catalytic case. However, the addition of the two ITQs makes the curve shifts to higher temperatures as compared to that of the HMOR case. Therefore, the ITQ addition reduced cracking activity of HMOR. Among the studied catalysts, the HMOR + 2% ITQ-21 produced the heaviest oil.

The effect of the ITQ addition can be further depicted from the petroleum cuts. Fig. 10 displays the petroleum fractions obtained from using various catalysts. From the figure, one can see that the heavy fractions (gas oil and VGOs) are decreased in accordance with the increase in lighter fractions with the presence of the acid catalysts. Therefore, the acid catalysts cracked the heavy molecules into the lighter ones. However, with the addition of the ITQ zeolites, the yields of these heavy fractions slightly increase with respect to those obtained from the pure HMOR. This is attributed to the decrease in the cracking activity by the dilution of HMOR by the ITQ zeolites, and thus the total acidity of the mixtures is decreased because the ITQs have higher Si:Al ratio (Table 1) than HMOR [16].

Moreover, it is noted that the main differences caused by adding the two ITQ zeolites into HMOR are the yields of gasoline and kerosene, whereas those of the heavier fractions are comparable. In details, the gasoline yield drops from 30.4 wt% (in the case of HMOR) to 26.4 wt% with the addition of ITQ-24, and further decreases to 20.1 wt% when ITQ-21 was mixed. On contrary, with respect to HMOR, adding ITQ-21 produces the higher yield of kerosene, but adding ITQ-24 gives less. From the result of catalyst characterization, the two ITQ zeolites have larger pore sizes than that of HMOR (Table 1). In general, a larger pore size can enable larger and/or more reactants to diffuse into its inner pore and react, and allow larger products to diffuse out of the pore. In case of ITQ-24, its channels have different sizes, and contain a 12 member ring sinusoidal ones whereas those are uniform for the ITQ-21 structure [6,7]. Therefore, ITQ-21 should give a more homogeneous electric field gradient in the channels than ITQ-24 does. Similar effect of the topology on cracking activity of a catalyst was reported elsewhere [10]. This, together with the lower Si:Al ratio of ITQ-24, makes it possible to enhance the cracking activity to a certain extent, resulting in the reduction of kerosene yield as compared with HMOR and HMOR + ITQ-21. Meanwhile, ITQ-21 has very low cracking activity (due to its high Si:Al ratio or low acid density) associated with its large pore size, thus enhancing the selectivity toward the production of kerosene when added into HMOR. The selectivity of ITQ-21 toward hydrocarbon molecules in the kerosene range due to its appropriate pore size was also reported in the study of Arribas et al. [17]. Conclusively, the higher yield of kerosene and lower yield of gasoline were obtained with the addition of 2%ITQ-21. This is also in a good agreement with the experimental result showing that the yield of gasoline is higher when ITQ-24 was used as an additive instead of ITQ-21. From these results, it can be expected that using ITQ-21 alone possibly enhance the production of kerosene from waste tire pyrolysis.

In order to obtain the effects of the ITQ series as additives on the chemical composition of the oil, the liquid products were separated using liquid adsorption chromatography [12] into saturated hydrocarbons, mono-, di-, poly- and polar-aromatics. Olefins cannot be obtained using the procedure [12]. The yields of different types of hydrocarbons in the oil are demonstrated in Fig. 11. In the figure, total aromatics are meant to be all types of aromatics, including poly-aromatics as well. The sum of saturated and total aromatic hydrocarbons was made to 100%. However, the yield of poly-aromatics is plotted separately in the same graph to depict its change toward the use of catalysts. It is observed that the total aromatics in the oil are found to decrease with the treatment

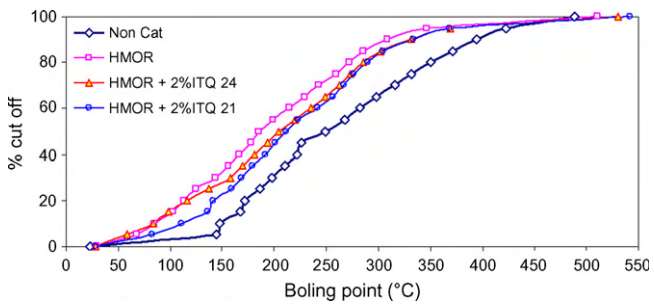

Fig. 9. Effect of zeolite additives on the TBP curves of the pyrolytic oils.

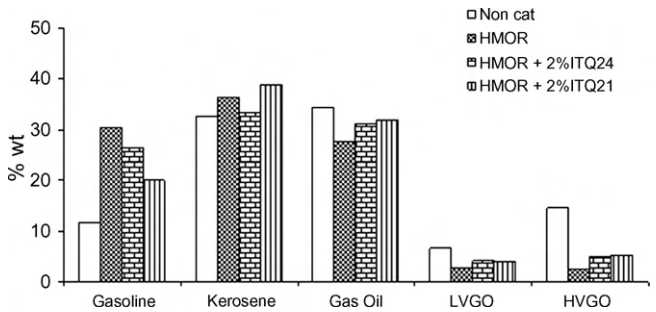

Fig. 10. Petroleum fractions of pyrolytic oil obtained from using various catalysts.

Author's personal copy

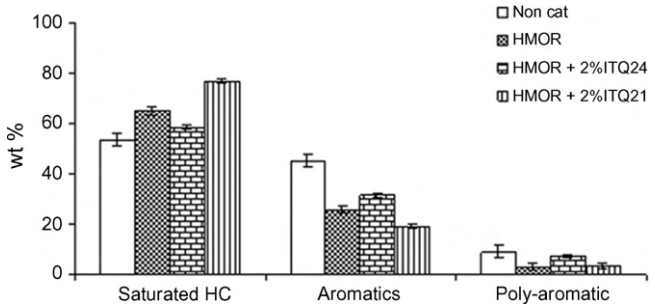

Fig. 11. Composition of the pyrolytic oil obtained from different catalysts.

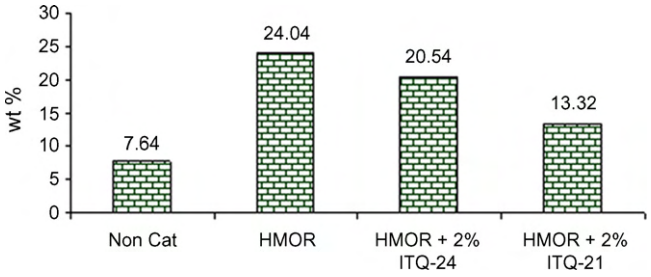

Fig. 12. Selectivity of mono-aromatic in the light fraction.

of the acid catalysts. This reduction could be attributed to the cracking of the heavy compounds including aromatics to the lighter non-aromatic ones, to the formation of coke, or to the dealkylation of the aromatic compounds [18], resulting in the increase in saturated hydrocarbons.

As compared with HMOR, the addition of the two ITQs shows the opposite effect toward one another on the production of different types of hydrocarbons. In details, the yield of total aromatic hydrocarbons produced by HMOR is 24.9 wt%. Addition of 2 wt% ITQ-21 decreases the yield to 20.8 wt%. On contrary, aromatic yield increases from 24.9 to 30.3 wt% by the introduction of 2 wt% ITQ-24 into HMOR. Lee et al. [19] in 1998 studied the cracking of VGO on the dealuminated mordenites, and found that the aromatic compounds were formed via the cyclization of olefins produced in the cracking process. Moreover, it is well known that the product of waste tire pyrolysis contains a considerable amount of olefins including conjugated olefins, aromatics, etc, and these compounds might undergo cyclization followed by dehydrogenation to produce aromatics when the acid catalyst was used [3,20]. Besides, it has been known that the pore size plays a very important role in the activity of catalyst due to the shape selectivity [21–23]. Furthermore, Boxiong et al. [5] studied the pyrolysis of waste tire using ZSM5 and USY, and found that USY with a larger pore size produced a higher amount of aromatics in the light fraction than ZSM5. Therefore, the larger pore size of ITQ-24, as compared to ITQ-21, should be responsible for the higher amount of aromatic produced in the case of HMOR + 2%ITQ-24. The larger pore size of ITQ-24 possibly enables the formation the heavier aromatics from olefins or the lighter ones. More poly-aromatic were also produced with the addition of ITQ-24 as compared with the pure HMOR.

Moreover, Liu et al. [24] studied the aromatization performance of a cracking catalyst, and suggested a pathway for aromatic formation from olefins in which a catalyst with a high hydrogen transfer index would produce more aromatic due to its high dehydrogenation activity. Additionally, the low hydrogen transfer activity of ITQ-21 was reported by Corma et al. [6]. Hence, the dilution of HMOR by the addition of ITQ-21 with lower acid density, due to its higher Si:Al ratio, consequently decreased the acid density of the whole mixture. As a result, the hydrogen transfer activity of the system decreased, thus decreasing the capacity for hydride ions and resulting in high cracking activity rather than dehydrogenation. In addition, it is noteworthy that ITQ-21 has smaller pore as compared to ITQ-24, leading to the lower aromatic formation due to steric restriction. Consequently, the lower concentration of aromatic compounds in the pyrolytic oil was produced when ITQ-21 was used as an additive. There were also several studies reporting the increase of aromatic content with decreasing Si:Al ratio [3,5,24,25]. Furthermore, when coke formation was examined, it was found that the amount of coke produced was in the order: HMOR + 2%ITQ-24 > HMOR > HMOR + 2%ITQ-21 (Table 3), which is in a very good agreement with the previous discussion. Since the aromatic species have a great predisposition to being involved in pathways to coke formation [15]. Therefore, the catalyst, which has high aromatic formation activity, can lead to a high potential of coke formation. Consequently, the addition of ITQ-24 into HMOR allowing the aromatic formation activity to occur more easily resulted in the highest amount of coke observed whereas the lowest amount was found in the case of adding ITQ-21.

3.2.3. Selectivity of mono-aromatic in the light fraction (boiling point <232 °C)

Because of the high economic values of the mono-aromatics in the light fraction, many studies have been carried out to investigate the production of these compounds in the catalytic pyrolysis of waste tire [3–5]. Therefore, the selectivity of mono aromatic in the light fraction (boiling point <232 °C) of the various catalysts was determined, and the obtained results were displayed in Fig. 12.

From this figure, it is found that the introduction of acid catalysts increases the selectivity toward mono-aromatics. However, the selectivity decreases from 24.0% to 20.5% and 13.3% with the addition of 2 wt% ITQ-24 and ITQ-21 into HMOR, respectively. This reduction is attributed to, again, the dilution of the acidity since the two ITQ zeolites have lower acid density than HMOR. The higher selectivity of HMOR + 2% ITQ-24 with respect to HMOR + 2% ITQ-21 is owing to the lower Si:Al ratio of ITQ-24, resulting in the better aromatization activity as discussed previously.

4. Conclusions

The catalyst-to-tire ratio strongly affected the oil product. The gasoline and kerosene fraction increased in accordance with the reduction of heavier fractions with increasing the catalyst-to-tire ratio. However, the increase in the ratio also caused a reduction in the oil yield. Both ITQ-21 and ITQ-24 zeolite additives have shown significant influences on the catalytic pyrolysis of waste tire using HMOR as the base case. The addition of these additives not only affected the yield of petroleum fractions but also the composition of the derived oil. Less gasoline was produced when the ITQ zeolites were introduced into HMOR regardless of the type of the studied ITQs. However, adding ITQ-21 enhanced the production of kerosene whereas adding ITQ-24 was found to decrease the yield of kerosene. In addition, the addition of two ITQs showed the opposite effect to one another on the production of aromatic hydrocarbons in the oil. With respect to HMOR, when ITQ-24 was used as an additive, the higher concentration of aromatics was observed whereas the concentration was decreased by adding ITQ-21. Finally, diluting the catalyst by adding ITQ zeolites led to the reduction of the selectivity of single-ring aromatics in the light fractions. The difference effects of the two ITQ zeolites were believed to come from their different acid properties and topology.

Author's personal copy

Acknowledgments

This work was supported by the Petroleum and Petrochemical Technology Consortium, the Thailand Research Fund, the Chulalongkorn University's Research Unit of "Syntheses and Applications of Organometallics", and The Graduate Scholarship Program for Faculty Members from Neighboring countries, Chulalongkorn University, Thailand.

References

[1] P.T. Williams, R.P. Bottrill, A.M. Cunliffe, Trans. Inst. Chem. Eng. B: Process. Sar. Environ. Protect. 76 (1998) 291.
[2] P.T. Williams, S. Besler, Fuel 74 (1995) 1277.
[3] P.T. Williams, Alexander J. Brindle, J. Anal. Appl. Pyrol. 67 (2003) 143.
[4] G.S. Miguel, J. Aguado, D.P. Serrano, J.M. Escola, Appl. Catal. B: Environ. 64 (2006) 209.
[5] S. Boxiong, W. Chunfei, G. Binbin, W. Rui, Liangcai, Appl. Catal. B: Environ. 73 (2007) 150.
[6] A. Corma, M.J. Diaz Cabinas, J. Martinez-Trigueru, F. Rey, J. Rius, Nature 418 (2002) 514.
[7] R. Castaneda, A. Corma, V. Fornes, F. Rey, J. Rius, J. Am. Chem. Soc. 125 (2003) 7820.
[8] M.A. Camblor, P.A. Barrett, M. Díaz-Cabañas, L.A. Villaescusa, M. Puche, T. Boix, E. Pérez, H. Koller, Micropor. Mesopor. Mater. 48 (2001) 11.
[9] J.S. Buchanan, Catal. Today 55 (2000) 207.
[10] A. Corma, J. Martınez-Triguero, C. Martınez, J. Catal. 197 (2001) 151.
[11] A. Corma, J. Martınez-Triguero, J. Catal. 165 (1997) 102.
[12] G. Sebor, J. Blaz ek, M.F. Nemer, J. Chromatogr. A 847 (1999) 323.
[13] T. Blasco, A. Corma, M.J. Diaz-Cabans, F. Rey, J. Rius, G. Sastre, J.A. Vidal-Moya, J. Am. Chem. Soc. 126 (2004) 13414.
[14] N. Labhsetwar, H. Minamino, M. Mukherjee, T. Mitsuhashi, S. Rayalu, M. Dhakad, H. Haneda, J. Subrt, S. Devotta, J. Mol. Catal. A: Chem. 261 (2007) 213.
[15] P.B. Venuto, T.E. Habib, Fluid Catalytic Cracking with Zeolite Catalysts, Marcel Dekker, New York, 1979.
[16] K. Yoo, E.C. Burckle, P.G. Smirniotis, J. Catal. 211 (2002) 6.
[17] M.A. Arribas, A. Corma, M.J. Dıaz-Cabanas, A. Martínez, Appl. Catal. A: Gen. 273 (2004) 277.
[18] J.M. Serra, E. Guillon, A. Corma, J. Catal. 227 (2004) 459.
[19] K.H. Lee, Y.W. Lee, B.H. Ha, J. Catal. 178 (1998) 328.
[20] P.T. Williams, D.T. Taylor, Fuel 72 (1993) 1469.
[21] A. Corma, V.I. Costa-Vaya, M.J. Dıaz-Cabanas, F.J. Llopis, J. Catal. 207 (2002) 46.
[22] R. Roldan, F.J. Romero, C.J. Sanchidrian, J.M. Marinas, J.P. Gomez, Appl. Catal. A: Gen. 288 (2005) 104.
[23] A. Corma, M. Davis, V. Fornes, V. Gonzalez-Alfaro, R. Lobo, A.V. Orchill, J. Catal. 167 (1997) 438.
[24] C. Liu, Y. Denga, Y. Pan, Y. Gub, B. Qiao, X. Gaob, J. Mol. Catal. A: Chem. 215 (2004) 195.
[25] C.W. Kuehler, M.L. Occelli, P. O'Connor (Eds.), Fluid Cracking Catalysts, American Chemical Society, Marcel Dekker, New York, 1998.

Provided for non-commercial research and education use.
Not for reproduction, distribution or commercial use.

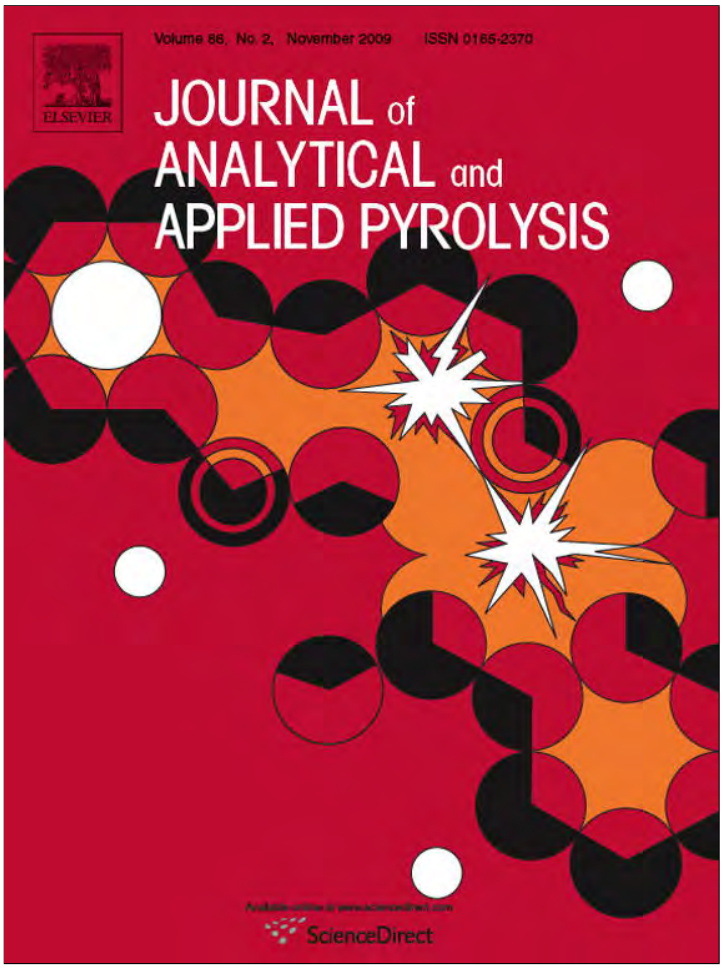

This article appeared in a journal published by Elsevier. The attached copy is furnished to the author for internal non-commercial research and education use, including for instruction at the authors institution and sharing with colleagues.

Other uses, including reproduction and distribution, or selling or licensing copies, or posting to personal, institutional or third party websites are prohibited.

In most cases authors are permitted to post their version of the article (e.g. in Word or Tex form) to their personal website or institutional repository. Authors requiring further information regarding Elsevier's archiving and manuscript policies are encouraged to visit:

http://www.elsevier.com/copyright

Author's personal copy

J. Anal. Appl. Pyrolysis 86 (2009) 281–286

Contents lists available at ScienceDirect

Journal of Analytical and Applied Pyrolysis

journal homepage: www.elsevier.com/locate/jaap

Light olefins and light oil production from catalytic pyrolysis of waste tire

Nguyễn Anh Dũng, Raweewan Klaewkla, Sujitra Wongkasemjit, Sirirat Jitkarnka *

The Petroleum and Petrochemical College, Center of Excellence for Petroleum, Petrochemicals, and Advanced Materials, Chulalongkorn University, Soi Chulalongkorn 12, Phayathai Road, Pathumwan, Bangkok 10330, Thailand

ARTICLE INFO

Article history:
Received 28 April 2009
Accepted 21 July 2009
Available online 29 July 2009

Keywords:
Waste tire
Pyrolysis
Ru
Silica MCM-41
Light olefin
Aromatics

ABSTRACT

This paper investigates the catalytic activity of MCM-41 synthesized via silatrane route and Ru/MCM-41 in waste tire pyrolysis. The experimental results showed that the presence of catalysts strongly influenced the yield and nature of products. Namely, the gas yield increased at the expense of liquid yield. In addition, a considerable high yield of light olefins, 4 times higher than non-catalytic pyrolysis, can be achieved for Ru/MCM-41 catalyst. Furthermore, the uses of catalysts produced much lighter oil and there was a drastic increase in the concentration of single ring aromatics in accordance to a reduction in polycyclic aromatic compounds in the derived oils. Ru/MCM-41 produced the lightest oil and the oil has the highest concentration of mono-aromatics. The high activity of catalysts, particularly Ru/MCM-41 was discussed in relation with the catalyst characterization results obtained from various techniques including TPD-NH_3, H_2-chemisorption, XRD, N_2-adsorption/desorption analysis, and TPO.

© 2009 Elsevier B.V. All rights reserved.

1. Introduction

Light olefins, i.e. ethylene and propylene, are important chemicals in synthesis processes because of their high chemical activity during reactions. The world demand and production of light olefins are higher than those of any other chemicals [1]. Currently, light olefin production mainly comes from steam crackers and refinery fluid catalytic cracking (FCC) unit. Although the capacity of light olefins is going to be drastically enhanced in the coming years, it will still cover only a small part of the light olefin demand; thus, other sources have to be developed [2]. Moreover, the gradually depletion of petroleum reserves has created interest in finding alternative source of energy. Meanwhile, the increasing amount of waste tire produced annually exposes a serious problem for both environment and human beings.

Recently, the pyrolysis of wastes has been considered as a promising alternative for dealing with this issue. Many studies have shown that the pyrolysis of waste tire produces not only valuable oil but also a high yield of gaseous product [3,4]. However, the gas product has mainly been studied for its application as combustion gas [3] rather than for light olefins sources since the yield of light olefins was low, whereas the oils were shown to contain high concentration of polycyclic aromatics, thus preventing it from being used as fuel [5].

Catalysts have been applied in several studies for upgrading the quality and quantity of the products obtained from waste tire pyrolysis [6–8]. In general, an acid catalyst increases the gas yield at the expense of the yield of liquid oil. For example, Boxiong et al. studied the effect of catalyst-to-tire ratio, and found that the gas yield increased with increasing the amount of Y catalyst used [7]. Similarly, Williams and Brindle reported the increment of gas yield after catalysis treatment using two types of zeolites, Y and ZSM-5, as catalysts [8]. Although the authors, to a certain extent, achieved an increase in the yield of single ring aromatics, but the production of light olefins was low. In addition, the amount of catalysts used [8] was quite high (catalyst-to-feed ratio of 2), particularly if considering the practical/industrial application.

On the other hand, a meso- and macro-pore type of zeolites was reported to promote the selectivity to propylene [9]. Additionally, mesoporous silica MCM-41 showed interesting results in waste plastic degradation [10]. Namely, the carbon number distribution shifted to lower number, and the authors also observed the carbenium ion cracking mechanism over this material. Furthermore, our previous study showed that the acid catalyst promoted not only cracking but also oligomerization reaction, and the higher the acid density, the latter reaction is more preferable [11].

Noble metal-supported zeolite catalysts are widely used since metals can catalyze the hydrogenation of the feedstock, making it more reactive for cracking and heteroatoms (sulfur, oxygen) removal [12]. Additionally, noble metal catalysts can achieve a high level of aromatic hydrogenation at moderate hydrogen pressures [13,14]. And the Ru-supported catalyst was found to have a better sulfur tolerance than Pt, Pd, or Pd–Pt catalysts due to

* Corresponding author. Tel.: +66 22 18 41 48; fax: +66 22 15 44 59.
E-mail address: sirirat.j@chula.ac.th (S. Jitkarnka).

0165-2370/$ – see front matter © 2009 Elsevier B.V. All rights reserved.
doi:10.1016/j.jaap.2009.07.006

Author's personal copy

the low density of states at the Fermi level of this metal [15]. Moreover, the hydrogenation of polycyclic aromatics is more preferable than their corresponding mono-aromatics [16], and partial hydrogenation is generally the main route [17]. Furthermore, due to the size of the polycyclic aromatics a large pore material consequently should be used as the support of the bifunctional catalyst.

In the present study, a pure silica MCM-41 was first synthesized via silatrane route, and then 2%Ru/MCM-41 was prepared by the conventional impregnation technique. The prepared samples were used as catalysts in the pyrolysis of waste tire aiming at a high production of light olefins (ethylene and propylene) yield and simultaneously a high reduction of polycyclic aromatics in the derived oils.

2. Experimental

2.1. Catalyst preparation

To synthesize pure silica MCM-41, silatrane was first synthesized using the method of Wongkasemjit's group [18]. Silatrane precursor was added to a solution containing hexadecyltrimethyl ammonium bromide (CTAB, purchased from Sigma Chemical Co.), sodium hydroxide (NaOH, Sigma Chemical Co.), and triethanolamine (TEA, Carlo Erba Reagent) followed by adding water with vigorous stirring [19]. The obtained crude product was filtered and washed with water to obtain a white solid. Then, the white solid was dried at room temperature and calcined at 580 °C for 6 h to obtain mesoporous MCM-41.

2 wt% Ru-supported catalyst was prepared by the conventional wetness impregnation technique. An appropriate amount of precursor solution of $RuCl_3{\cdot}xH_2O$, purchased from Fluka was dropped stepwise to the MCM-41, followed by drying in an oven at 110 °C for 3 h then calcined at 580 °C for 2 h with a heating rate of 10 °C min^{-1}. Subsequently, it was pellitized and sieved to obtain a particle size in the range of 400–425 μm. Prior to catalytic activity testing, the catalyst was reduced by hydrogen at 400 °C for 3 h. A complete reduction of ruthenium species was confirmed by temperature-programmed reduction (TPR) since there was no peak found in the TPR profile of the reduced sample.

2.2. Catalyst characterization

The crystalline phases present in these samples were determined from the X-ray diffraction patterns (XRD). The diffractograms were recorded on a Riguku D/Max 2200H apparatus with a scanning speed of 0.5° min^{-1} and 2θ from 1.5° to 60°. The composition of the Ru on the support was determined by the inductively coupled plasma (ICP) technique using a Perkin Elmer Optima 4300 PV machine after the dissolution of the catalyst. The surface area and pore size distribution of the studied catalysts were characterized by N_2 physical adsorption using the Sorptomatic 2900 equipment.

Hydrogen chemisorption of the reduced sample was carried out in a Micromeritics 2900 apparatus at room temperature, after the pre-treatment of sample at 150 °C (10 °C min^{-1}) for 1 h, under a flow of helium. Dispersion data was calculated by assuming a stoichiometry H/Ru = 1 [14].

Temperature-programmed desorption (TPD) using NH_3 was carried out in a TPD/TPR Micromeritics 2900 machine. Approximately 0.1 g of sample was first pre-treated in He at 550 °C for 30 min. Then, the system was cooled to 100 °C, and the NH_3 adsorption was performed using NH_3/N_2 for 1.5 h followed by the introduction of He to remove the physically adsorbed NH_3 for 30 min at 100 °C. Finally, the system was cooled to 50 °C, and then the temperature-programmed desorption was started from 50 °C to 600 °C with a heating rate of 5 °C min^{-1}.

Table 1
Elemental composition of the tire sample.

	H	C	S	Others[a]
wt%	84.5	7.4	1.7	4.7

[a] Determined by mass balance.

Temperature-programmed oxidation (TPO) using the same Micromeritics 2900 machine was performed from room temperature to 900 °C (10 °C min^{-1}), and the final temperature was hold for 30 min. The amount of coke was then determined from the area under the curve and calculated by the software supplied with the machine.

2.3. Pyrolysis of waste tire

2.3.1. Waste tire sample

The waste tire used in this study was a used passenger car tire (about 50,000 km mileage). The tire was cut into pieces by a cutting machine and then sieved to the particle sizes of 8–18 mesh. Elemental analysis (Table 1) shows that the fed tire contains mainly hydrogen and carbon. The portion named as "Others" in the table might be other elements originally present in the additives, steel, and some other inorganic compounds in the tire sample [20].

The tire sample also was analyzed by thermal-gravimetric analysis (TGA), and the obtained results are presented in Fig. 1. Accordingly, the data obtained from the two runs are similar. The decomposition of tire begins at around 200 °C and ends at approximately 500 °C. The non-volatile organic and inorganic compounds become the solid product of pyrolysis (~50 wt%).

2.3.2. Pyrolysis of waste tire

The pyrolysis reactor employed in this work is comprised of lower and upper zones of 11.45 cm height each with the diameter of 7.60 cm. The temperature of the two zones was independently controlled. The detail of pyrolysis experiments was described elsewhere [11]. Briefly, a 30 g tire sample was pyrolyzed in the lower zone of the reactor from room temperature to the final temperature of 500 °C (at 10 °C min^{-1}). The evolved product was carried by a nitrogen flow to the upper zone packed with a catalyst (at the catalyst-to-tire ratio of 1/4), and controlled at 350 °C. The obtained product was next passed through an ice-salt condensing system containing three condensers in order to separate incondensable compounds from the liquid product. The solid and liquid products were weighed to determine the product distribution. The amount of gas was then determined by mass balance. The gaseous

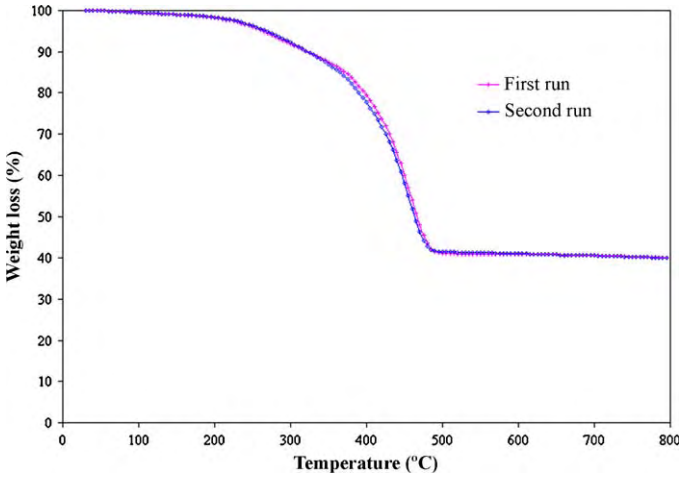

Fig. 1. TG analysis of the feed tire sample.

Author's personal copy

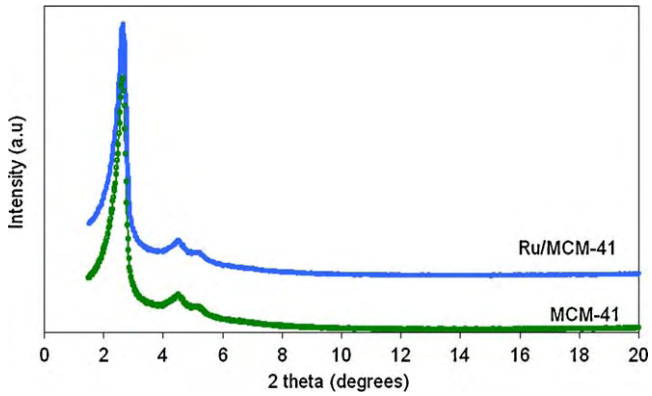

Fig. 2. XRD patterns of MCM-41 and Ru-supported MCM-41 catalysts.

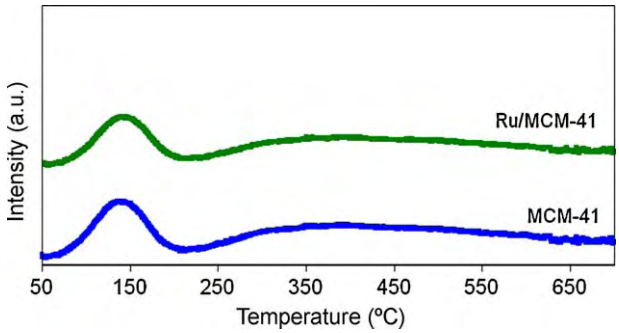

Fig. 3. TPD-NH_3 profiles of prepared catalysts.

product collected in a Dual Valve Tedlar PVF bag purchased from Cole Parmer was analyzed by a GC, Agilent Technologies 6890 Network system, equipped with an HP-PLOT Q column and an FID. The liquid product was first dissolved in n-pentane with the ratio of 40:1 to precipitate asphaltenes. The maltenes was subsequently obtained after asphaltene removal. Then, a Varian CP 3800 simulated distillation gas chromatograph equipped with FID and a 15 m × 0.25 mm × 0.25 μm WCOT fused silica capillary column (SIMDIST GC) was used to analyze the obtained maltenes according to the ASTM D2887 method for simulated true boiling point curves. Finally, the maltenes was also analyzed for its compositions, based on hydrocarbon types, including saturate, mono-, di-, poly-, and polar-aromatics by liquid adsorption chromatography [21]. The pyrolysis products were also analyzed for their hydrogen and carbon contents by elemental analysis using a LECO (US) machine.

3. Results and discussion

3.1. Catalyst characterization

The XRD patterns of the synthesized and metal-supported MCM-41 are illustrated in Fig. 2. The XRD pattern of the synthesized MCM-41 is very similar to that reported in the literature [19], indicating the accomplishment of material synthesis. The catalyst composition analyzed by ICP shows a very good consistence between the targeted and true values of Ru loaded. Also, the XRD pattern of Ru-supported MCM-41 sample obviously indicates that the introduction of Ru does not affect the crystal structure of the parent mesoporous material. Moreover, in this pattern neither peak of Ru metal nor Ru compound is observed. This, together with the similar intensity of peaks as compared to MCM-41, suggests a high dispersion of Ru .

The physical–chemical properties of the fresh catalysts and the amount of coke of the spent ones are displayed in Table 2. The BET surface area of the synthesized silica MCM-41 is very high and the average pore diameter is approximately 26 Å, which well coincides with the data reported in Ref. [19]. The incorporation of Ru slightly decreases the surface area of the support in association with a reduction in average pore diameter, possibly caused by the diffusion of Ru into the pore. Ru/MCM-41 exhibits a TPR profile (not shown here) having a main reduction peak at 184 °C, which is higher than Ru-supported on mesoporous silica doped with zirconium [22], indicating stronger metal support interaction. As a result, H_2-chemisorption result indicates a high dispersion of ruthenium on the surface of zeolite support, 65%, which is well consistent with the XRD results.

Fig. 3 shows the TPD-NH_3 profile of the MCM-41 and Ru/MCM-41 catalysts. It can be seen that the profile of MCM-41 shows two desorption peaks with maxima at 150 °C and 350 °C, respectively. These peaks are broad and low intensive suggesting a good distribution of the acidic sites as well as the low amount of acidic sites. As this zeolite material is composed of pure silica; thus, the acid sites must be contributed from the silanol groups lining the wall of the channels as suggested by Seddegi et al. [10]. Namely, they found that the interactions between the bridging oxygen atoms lining the straight channels and the hydrogen atoms from the polyethylenic chain made the hydrocarbon fragment more basic and, thus, reactive with the silanol groups. This interaction stabilized the carbenium ion formation and allowed its further reactions. The incorporation of ruthenium to MCM-41 slightly decreases the intensity of the desorption peaks, possibly caused by the diffusion of ruthenium particles into the zeolite channels, thus blocking some acidic sites.

Temperature-programmed oxidation (TPO) was used to determine the amount of coke deposited on the spent catalysts. TPO profiles (not shown here) of the spent catalysts showed two peaks with maxima located at around 300 °C and 500 °C. The peak located at low temperature (~300 °C) is most likely due to the oxidation of adsorbed hydrocarbon species, which could be formed from condensed polycyclic compounds, whereas the peaks at basically 500–600 °C are corresponding to the oxidation of deposited carbon species [23], possibly including some carbon black. Consequently, the catalyst, to a certain extent, can be deactivated by coke deposition. Quantitative analysis showed there is a considerable amount of coke on the spent catalysts; and, Ru/MCM-41 catalyst has the highest amount of coke (Table 2).

3.2. Pyrolysis products

3.2.1. Product yield

Fig. 4 shows the yields of gas, liquid, and solid product with all catalysts prepared. It can be seen that in the non-catalytic pyrolysis, the yields (wt%) of solid, liquid and gas are approximately 47%, 42% and 11%, respectively. The solid product contains high concentration of carbon black (Table 3) and some other mineral matters initially present in the tire [24]. Therefore, as

Table 2
Physical–chemical properties of the studied catalysts.

Samples	Ru (wt%)	Dispersion (%)	Surface area (m^2/g)	Pore diameter (nm)	Asphaltenes (g/g oil)	Coke (g/g catalyst)
MCM-41	–		1454	2.61	0.00064	0.084
Ru/MCM-41	2.02	65.2	1439	2.51	0.00022	0.124

Author's personal copy

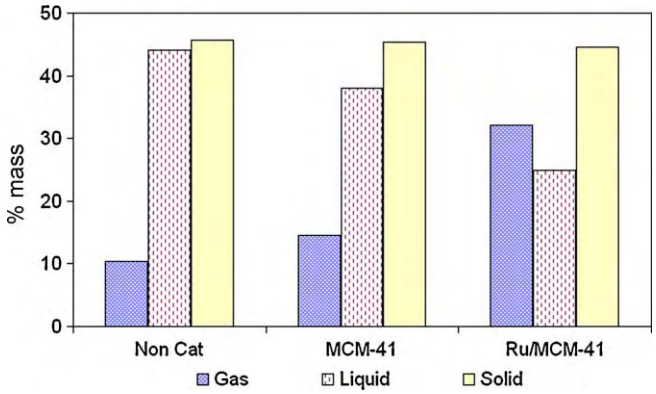

Fig. 4. The yields of products obtained from thermal and catalytic pyrolysis.

expected, the yield of solid obtained from all runs is similar. This is attributed to the fact that the pyrolysis conditions were kept constant and the tire was reported to be completely decomposed at 500 °C [3].

The use of catalysts strongly influences the yields of other products. For instance, the gas yield increases from ~11 wt% to about 15 wt% and 30 wt% when MCM-41 and Ru/MCM-41 were used, respectively. However, the yield of oil decreases for all prepared catalysts. As revealed from TPD-NH_3 analysis, there is a considerable amount of acidic sites on the surface of the pure silica MCM-41 used in this study. As a result, the presence of MCM-41 might promote the conversion of heavy compounds to the lighter ones due to its cracking activity [11], leading to the increase in the yield of gaseous product. A further increase in the yield of gaseous product is observed with the use of Ru/MCM-41 catalyst. This might be attributed to the presence of bifunctionalities of the Ru/MCM-41 catalyst as explained as follows. It is well known that the aromatic compounds are predominant in the liquid product of waste tire pyrolysis [25]. The liquid analysis result in the current study also corroborates these results (see Section 3.2.3). In addition, the secondary cracking of aromatics is very difficult [26]. Meanwhile, an initial hydrogenation over the metal sites can make these aromatics more reactive for cracking and heteroatoms such as sulfur removal [12]]. Therefore, it is proposed that ruthenium clusters on the support surface, which were reported to have high hydrogenation activity [12], hydrogenate the aromatics, producing (partial) hydrogenated compounds, which rapidly undergo cracking and/or ring-opening on the acid sites. Therefore, a higher amount HCs in the liquid product was cracked when the Ru/MCM-41 was used, resulting in a drastic decrease in the liquid yield as compared to MCM-41 and non-catalytic cases as seen in Fig. 4.

In this work, the gas analysis is based on hydrogen-free basis; thus, hydrogen is not hereby reported in the gas product. The obtained solid and liquid products were therefore analyzed for their hydrogen and carbon contents in order to explain the source of hydrogen involved in the production of lighter products. The experimental results are given in Table 3. From the table, the H/C atomic ratio in the pyrolytic oil increases with the use of catalyst, particularly Ru/MCM-41, whereas that of gas product decreases. It is noted that hydrogen is known to be a co-product of hydrocarbon cracking. For example, the thermal cracking of naphtha gives about 16% H_2 as a co-product, and a tire pyrolysis could give hydrogen as high as 30% by volume [27]. Therefore, the decrease in the H/C ratio of the gas (with the increase in this ratio of the pyrolytic oil) indicates the reduction of hydrogen in the gas product. This implies that hydrogen in the gas phase, produced from the reactions, is also used in the reactions, contributing to the productions of lighter liquids and less polycyclic aromatics, when the catalysts were used.

Table 3
Hydrogen and carbon contents.

	C (wt%)	H (wt%)	H/C[a]
Non-cat			
Oil	83.7	10.8	1.54
Solid	90.6	1.8	
Gas[b]	72.6	16.8	2.77
MCM-41			
Oil	82.9	11.1	1.61
Solid	90.9	1.8	
Spent catalyst	6.9	0.4	
Gas[b]	73.1	15.8	2.59
Ru/MCM-41			
Oil	82.1	13.2	1.93
Solid	91.2	1.4	
Spent catalyst	10.9	0.6	
Gas[b]	80.8	14.6	2.17

[a] Atomic ratio.
[b] Determined by mass balance.

3.2.2. Gaseous product

GC analysis results reveal that the pyrolysis gas composed of methane, ethane, ethylene, propane, propylene, C_4-, C_5-, C_6-, C_7- and C_8-hydrocarbons. These compositions of gaseous products are presented in Fig. 5. Such compositions are given as grams of gas component with respect to 100 g of tire, so that the results with different catalysts can be compared, and information on how the catalysts affect the pyrolysis products may be inferred. It can be seen that for the thermal pyrolysis gas, the yield of C_4 exhibits a maximum value. The high yield of C_4 in the gas obtained from pyrolysis of waste tire was also reported in Ref. [3]. This might be attributed to the breakdown of the styrene–butadiene rubber, SBR, a main component of tire [3]. However, as compared to the results reported in the literatures [28], the yield of methane obtained from thermal pyrolysis in our study is relatively higher, possible caused by the different reactors used. In our case, a semi-batch reactor was used and the upper zone of the reactor was also heated in the thermal pyrolysis case. Thus, this high temperature (350 °C), to a certain extent, might promote the aromatization reactions [29], leading to the production of higher amount of methane [30]. This can be proved by the high aromatic content of the derived oil (~50 wt%) despite the proportion of styrene (aromatic) to butadiene (non-aromatic) in the SBR of the tire is normally 25/75, suggesting that the aromatization reaction had occurred.

The introduction of catalyst, particularly Ru/MCM-41 causes an important increase in the yield of gas component having carbon number less than 5, whereas decreases the yield of heavy

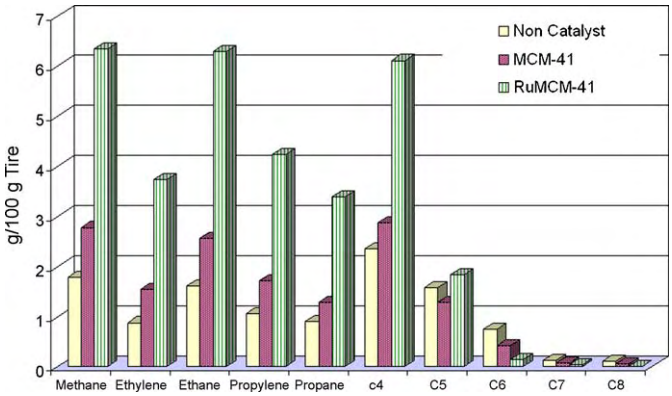

Fig. 5. Compositions of pyrolysis gas.

Author's personal copy

hydrocarbon ($C \geq 5$). In addition, the catalyst also enhances the selectivity toward light hydrocarbons ($C \leq 4$) in the gas product together with a reduction in heavy hydrocarbon selectivity. This suggests the presence of greater and deeper cracking reactions when the catalysts were used. Besides, Ru also was reported to have ability to crack C_3H_8 [31]. Therefore, in our case possibly Ru also cracks the heavy HCs into the gas product, leading to the higher yield of light hydrocarbons in the gas product as indicated in Fig. 5.

Light olefins, i.e. ethylene and propylene, as mentioned in the introduction part, are among the most important chemicals. Therefore, it is of interest if a catalyst could convert the waste tire to valuable oil and simultaneously to light olefins with a high yield. As one can see from Fig. 5, the yield of light olefins increases with the treatment of catalysts, and the use of Ru/MCM-41 catalyst produces the highest yield of light olefins, approximate 4 times higher as compared to non-catalytic pyrolysis. This beneficial influence of Ru/MCM-41 might be contributed from the combination effects of Ru and the support. Our previous study [11] showed that the acidic catalyst promoted not only cracking but also aromatization/oligomerization reactions. The higher the acid density of the catalyst was, the more preferable the latter reaction occurred. Therefore, the mild acid properties of MCM-41 can promote the cracking reaction to a certain extent, but cannot at the same time promote aromatization/oligomerization reactions. Additionally, further oligomerization is suppressed by the rapid elution of the cracking products due to the sizes in meso-pores, and thus high selectivity to propylene becomes possible [9]. On the other hand, the intermediates of many reactions occurred simultaneously during catalytic pyrolysis might quickly be hydrogenated over ruthenium clusters; thus, the reactions involving the consumption of light olefins, such as alkylation, hydride transfer, etc., are possibly prevented. Also, the acidity of the pure silica MCM-41 was attributed to the silanol groups lining the channels [10] and, Ru is highly dispersed on the surface of the acid zeolite support (Table 1). These result in a proper balance between the metal and acid sites, which is a crucial factor affecting the catalytic activity of the bifunctional catalyst [32]. Ru helps promoting the hydrogenation/dehydrogenation reactions, enhancing cracking reaction; thus, more olefins are produced. Therefore, a higher yield of light olefin is achieved. Finally, it should be emphasized that the high yield of light olefins obtained over Ru/MCM-41 catalyst can be compared with that obtained over ZSM-5 catalyst [8] but with much lower amount of catalyst used (8 times less).

3.2.3. Oil product

The influence of catalysts on the pyrolysis products can be further depicted by the change in the compositions as well as the distribution of hydrocarbons in the pyrolysis oils. Fig. 6 shows the carbon number distribution of the derived oils over C_5–C_{50} for both thermal and catalytic pyrolysis. Accordingly, the carbon number distribution of the non-catalytic oil is wide but mainly allocates in the range of C_{10}–C_{20}. The presence of catalyst produces the oil that has a narrower distribution and the peak tends to shift to lower carbon number. And, the highest and narrowest peak is observed over the oil obtained from catalytic pyrolysis with Ru/MCM-41. Besides, the uses of catalysts also lead to a drastic decrease in asphaltenes in the oils, as presented in Table 1. Thus, to this point, it is safe to conclude that catalytic pyrolysis produces much lighter oil with respect to thermal pyrolysis.

On the other hand, it is of paramount importance to note that the stringent environmental regulations have limited the content of aromatics in the fuel oils, particularly polycyclic ones [33]. Therefore, the derived oils were also subjected to analysis for their compositions by means of the liquid adsorption chromatograph [21] and the results are presented in Fig. 7.

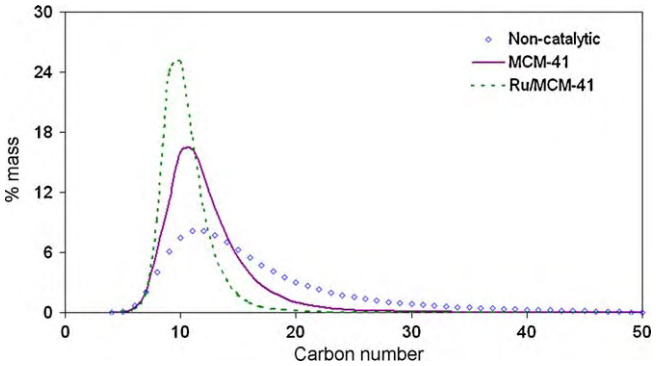

Fig. 6. Carbon number distribution of pyrolysis oils.

Fig. 7 displays the ratios of the contents of poly-, polar- and mono-aromatics in the catalytic oils to those in the non-catalytic oil. It can be seen that, for poly- and polar-aromatics, there exist a heavy drop of these ratios, indicating a drastic decrease in the contents of these compounds in the oils obtained from catalytic pyrolysis. In contrast, the yield of mono-aromatics in the liquid product increases with the treatment of catalysts, and reaches the highest value when Ru/MCM-41 was used. These results together with the shift of hydrocarbon distribution to the lower carbon number (Fig. 6) suggest the conversion of polycyclic aromatics (higher carbon number) to the single ring aromatic compounds (lower carbon number). And the highest conversion is achieved with using bifunctional catalyst, Ru/MCM-41.

As revealed from TPD-NH_3 analysis, MCM-41 has a considerable amount of acidic sites on its surface and these sites might be attributed to the slight reduction in polycyclic aromatics, including poly- and polar-aromatics, in the derived oil as well as the shift to lower carbon number of hydrocarbon distribution [11]. The presence of the ruthenium clusters on the surface of MCM-41 leads to a dramatic reduction of the polycyclic aromatics in the oil. It is well known that Ru-supported acidic zeolite catalysts exhibit high aromatic hydrogenation activity [12]. Therefore, polycyclic aromatics might be hydrogenated over ruthenium sites. And, due to the high dispersion of ruthenium (Table 1), the (partial) hydrogenated might be quickly transferred to the acidic sites of the support undergoing cracking and/or ring-opening reactions. More importantly, the hydrogenation of polycyclic aromatics is much preferable than their corresponding single ring aromatics [16]. Meanwhile, the hydrogenation of polycyclic aromatics generally can be achieved only partial hydrogenation [17]. These phenomena

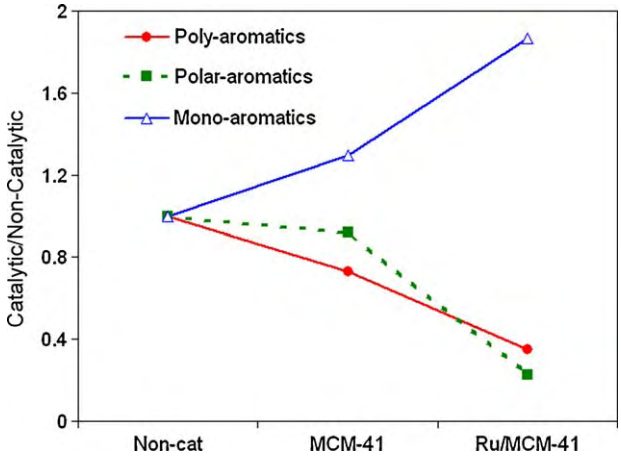

Fig. 7. Compositions of pyrolysis oils obtained from non-catalytic and catalytic pyrolysis.

Author's personal copy

probably explain the increase in the concentration of mono-aromatics at the expense of polycyclic aromatics observed when Ru/MCM-41 was used. And consequently, the produced oil has a much narrower carbon distribution, and the peak shifts to the lowest carbon number (Fig. 6). However, although to a small extent, the high amount of coke generated on the spent catalysts should not be excluded for the reduction of polycyclic aromatics in the derived oils since this coke could have been formed from the condensation of polycyclic aromatics [11], as well as the polar-aromatics [34]. Summarily, the catalytic pyrolysis with Ru/MCM-41 produced not only lighter oil, but also contains lower concentrations of poly- and polar-aromatics.

4. Conclusions

Catalytic pyrolysis of waste tire using a pure silica MCM-41 and Ru/MCM-41 catalysts has been investigated in relation to the yield and nature of the obtained products. It was found that the presence of catalysts caused a dramatic increase in the yield of gaseous product at the expense of the liquid yield, particularly for Ru/MCM-41. Additionally, the compositions of the gas obtained were shown to be strongly dependent on the catalysts. Especially, a considerable high yield of light olefins, i.e. ethylene and propylene (4 times higher) was achieved over Ru/MCM-41.

In addition, catalytic pyrolysis using current catalysts produced much lighter oil as compared to non-catalytic oil. Moreover, the catalytic oils have higher concentration of single ring aromatics and less poly- and polar-aromatics. Ru-supported MCM-41 synthesized via silatrane route was considered as a good catalyst in the pyrolysis of waste tire, since it can obtain light oil with high concentration of single ring aromatics and low contents of polycyclic aromatics and simultaneously a high yield of light olefins.

The high activity of Ru-supported MCM-41 was attributed to (i) the high dispersion of Ru as well as the nature of this metal to effectively catalyze hydrogenation reaction, and (ii) the suitable acid and topology properties of the support.

Acknowledgements

Thailand Research Fund (TRF) and the Commissions on Higher Education, the Petroleum and Petrochemical Consortium, the Research Unit of "Syntheses and Applications of Organometallics", and The Graduate Scholarship Program for Faculty Members from Neighboring Countries, Chulalongkorn University, Thailand, are acknowledged for the mutual financial support.

References

[1] D. Rensheng, W. Fei, J. Yan, Chem. Eng. Technol. 25 (2002) 711–718.
[2] A. Corma, F.V. Melo, L. Sauvanaud, F. Ortega, Catal. Today 107–108 (2005) 699–706.
[3] G.C. Berrueco, E. Esperanza, F.J. Mastral, J. Ceamanos, P. Garcıa-Bacaicoa, J. Anal. Appl. Pyrol. 74 (2005) 245–253.
[4] I.M. Rodriguez, M.F. Laresgoiti, M.A. Cabrero, A. Torres, M.J. Chomon, B. Caballero, Fuel Process. Technol. 72 (2001) 9–22.
[5] S. Murugan, M.C. Ramaswamy, G. Nagarajan, Fuel Process. Technol. 90 (2009) 67–74.
[6] S. Boxiong, W. Chunfei, G. Binbin, W. Rui, Liangcai, Appl. Catal. B: Environ. 73 (2007) 150–157.
[7] S. Boxiong, W. Chunfei, L. Cai, G. Binbin, W. Rui, J. Anal. Appl. Pyrol. 78 (2007) 243–249.
[8] P.T. Williams, A.J. Brindle, J. Anal. Appl. Pyrol. 67 (2003) 143–164.
[9] J.S. Jung, J.W. Park, G. Seo, Appl. Catal. A: Gen. 288 (2005) 149–157.
[10] Z.S. Seddegi, U. Budrthumal, A.A. Al-Arfaj, Appl. Catal. A: Gen. 225 (2002) 167–176.
[11] N.A. Dũng, A. Mhodmonthin, S. Wongkasemjit, S. Jitkarnka, J. Anal. Appl. Pyrol. 85 (2009) 338–344.
[12] M.A. Ali, T. Kimura, Y. Suzuki, M.A. Al-Saleh, H. Hamid, T. Inui, Appl. Catal. A: Gen. 227 (2002) 63–72.
[13] D. Eliche-Quesada, J.M. Meria-Robles, E. Rodriguez-Castellon, A. Jimenez-Lopez, Appl. Catal. B: Environ. 65 (2006) 118–126.
[14] D. Eliche-Quesada, M.I. Macias-Ortiz, J. Jimenez-Jimenez, E. Rodriguez-Castellon, A. Jimenez-Lopez, J. Mol. Catal. A: Chem. 255 (2006) 41–48.
[15] E. Rodriguez-Castellon, J. Merida-Robles, L. Diaz, p. Maireles-Torres, J.J. Jones, J. Roziere, A. Jemenez-Lopez, Appl. Catal. A: Gen. 260 (2004) 9–18.
[16] A. Corma, A. Martinez, V. Martinez-Soria, J. Catal. 169 (1997) 480–489.
[17] M. Jacquin, D.J. Jones, J. Roziere, S. Albertazzi, A. Vaccari, M. Lenarda, L. Storaro, R. Ganzerla, Appl. Catal. A: Gen. 251 (2003) 131–141.
[18] W. Charoenpinijkarn, M. Sawankruhasn, B. Kesapabutr, S. Wongkasemjit, A.M. Jamieson, Eur. J. Polym. 37 (2001) 1441–1448.
[19] N. Thanabodeekij, S. Sadthayanon, E. Gulari, S. Wongkasemjit, Mater. Chem. Phys. 98 (2006) 131–137.
[20] D.C.K. Ko, E.L.K. Mui, K.S.T. Lau, G. McKay, Waste Manage. 24 (2004) 875–888.
[21] G. Sebor, J. Blaz ek, M.F. Nemer, J. Chromatogr. A 847 (1999) 323–330.
[22] D. Eliche-Quesada, J.M. Merida-Robles, E. Rodríguez-Castellon, A. Jiménez-Lopez, Appl. Catal. A: Gen. 279 (2005) 209–221.
[23] J. Zheng, J. Guo, C. Song, Fuel Process. Technol. 89 (2008) 467–474.
[24] A. Napoli, Y. Soudais, D. Lecomte, S. Castillo, J. Anal. Appl. Pyrol. 40–41 (1997) 373–382.
[25] M.F. Laresgoiti, B.M. Caballero, I. de Marco, A. Torres, M.A. Cabrero, M.J. Chomón, J. Anal. Appl. Pyrol. 71 (2004) 917–934.
[26] L. Zhichang, M. Xianghai, X. Chunming, G. Jensen, Chin. J. Chem. Eng. 15 (2007) 309–314.
[27] E. Aylon, R. Murrilo, A. Fernandez-Colino, A. Aranda, T. Garcia, M.S. Callen, A.M. Mastral, J. Anal. Appl. Pyrol. 79 (2007) 210–214.
[28] M.F. Laresgoiti, I. Marco, A. Torres, B. Caballero, M.A. Cabrero, M.J. Chomon, J. Anal. Appl. Pyrol. 55 (2000) 43–54.
[29] P.T. Williams, D.T. Taylor, Fuel 72 (1993) 1469–2147.
[30] R. Cypres, B. Bettens, in: G.L. Ferrero, K. Maniatis (Eds.), Pyrolysis and Gasification, Elsevier Applied Science, Barking, UK, 1989, p. 209.
[31] M. Shiraga, D. Li, I. Atake, T. Shishido, Y.I. Oumi, Tsuneji, K. Takehira, Appl. Catal. A: Gen. 318 (2007) 143–154.
[32] A. Lugstein, A. Jentys, H. Vinek, Appl. Catal. A: Gen. 176 (1999) 119–128.
[33] S. Albertazzi, R. Ganzerla, C. Gobbi, M. Lenarda, M. Mandreoli, E. Salatelli, P. Savini, L. Storaro, A. Vaccari, J. Mol. Catal. A: Chem. 200 (2003) 261–270.
[34] N.A. Dũng, S. Wongkasemjit, S. Jitkarnka, Effects of pyrolysis temperature and Pt-loaded catalysts on polar-aromatic content in the tire-derived oil, Appl. Catal. B: Environ., DOI:10.1016/j.apcatb.2009.05.038.

Provided for non-commercial research and education use.
Not for reproduction, distribution or commercial use.

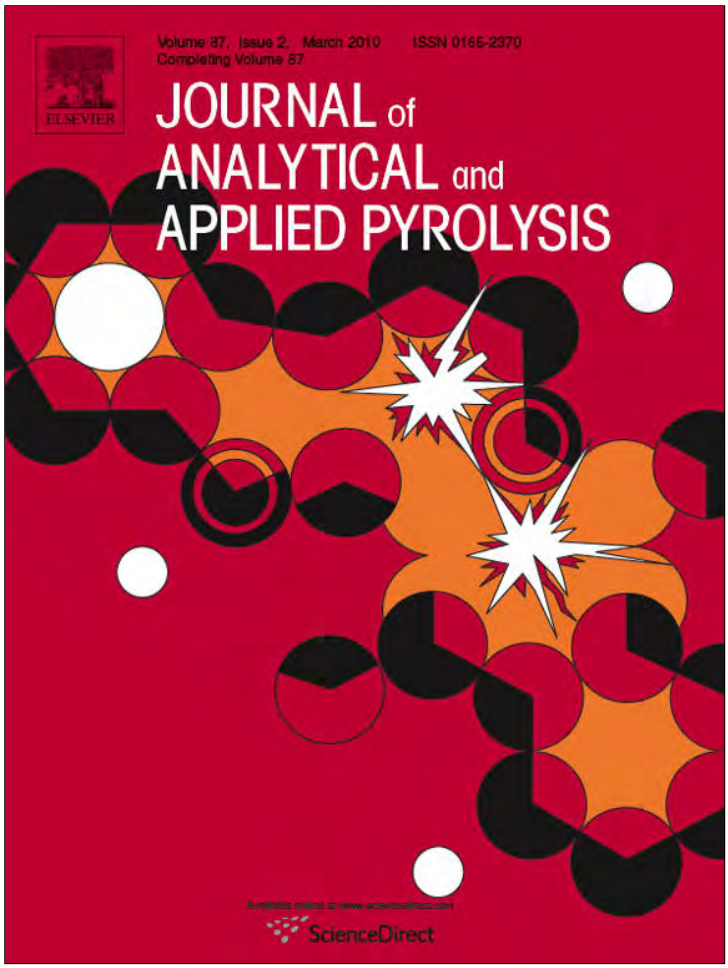

This article appeared in a journal published by Elsevier. The attached copy is furnished to the author for internal non-commercial research and education use, including for instruction at the authors institution and sharing with colleagues.

Other uses, including reproduction and distribution, or selling or licensing copies, or posting to personal, institutional or third party websites are prohibited.

In most cases authors are permitted to post their version of the article (e.g. in Word or Tex form) to their personal website or institutional repository. Authors requiring further information regarding Elsevier's archiving and manuscript policies are encouraged to visit:

http://www.elsevier.com/copyright

Author's personal copy

J. Anal. Appl. Pyrolysis 87 (2010) 256–262

Contents lists available at ScienceDirect

Journal of Analytical and Applied Pyrolysis

journal homepage: www.elsevier.com/locate/jaap

Roles of ruthenium on catalytic pyrolysis of waste tire and the changes of its activity upon the rate of calcination

Nguyễn Anh Dũng, Walairat Tanglumlert, Sujitra Wongkasemjit, Sirirat Jitkarnka *

The Petroleum and Petrochemical College, Center of Excellence for Petroleum, Petrochemical, and Advanced Materials, Chulalongkorn University, Soi Chulalongkorn 12, Phayathai Road, Pathumwan, Bangkok, 10330, Thailand

ARTICLE INFO

Article history:
Received 17 August 2009
Accepted 26 January 2010
Available online 4 February 2010

Keywords:
Waste tire
Pyrolysis
Ruthenium
SBA-1
Particle size

ABSTRACT

The catalytic pyrolysis of waste tire with Ru/SBA-1 catalysts was studied. The roles of ruthenium were elucidated since the support, a pure silica SBA-1 synthesized via silatrane route, was proven to be catalytically inactive and its structure retained after pyrolysis. Ruthenium clusters increased the yield of gaseous products, approximately 2 times as compared to thermal pyrolysis, at the expense of the liquid yield. They also decreased poly- and polar-aromatics and consequently produced lighter oil. The heating rates (1 °C/min, 5 °C/min, and 10 °C/min) during calcination were found to strongly influence the activity of the Ru/SBA-1 catalysts. The catalyst calcined with a heating rate of 5 °C/min exhibited the highest activity on poly- and polar-aromatics reduction and light oil production. The highest activity of this catalyst was attributed to its smallest mean ruthenium particle size and its highest sulfur tolerance.

© 2010 Elsevier B.V. All rights reserved.

1. Introduction

The main advantage of tire pyrolysis is that all of its products, *i.e.* a carbonaceous char, oil and a gas fraction, have potential to be utilized [1]. Among them, pyrolytic oil has attracted much more attentions due to its high heating value [2] and its property, which was reported to be similar, to a certain extent, to that of commercial naphtha [3]. However, the major obstacle that has limited the application of this oil as fuel is its high concentration of aromatics, especially polycyclic aromatic compounds [3]. Moreover, pyrolytic oil has been shown to contain a considerable amount of polar-aromatics, which are mostly sulfur-containing compounds [4]. And the low resistance to sulfur poisoning is one of the major drawbacks of noble metal-supported catalysts. Interestingly, sulfur tolerance may be enhanced by modifying the physicochemical characteristics of the metal atoms by (i) using acidic carriers, (ii) alloying with other metals, or (iii) changing the metal particle size [5]. Different metal particle sizes can be obtained by controlling the catalyst preparation conditions/methods [6].

Recently, we have reported the high activity of Ru-supported mesoporous MCM-41 for poly- and polar-aromatics reduction, and simultaneously for the production of light oil from waste tire pyrolysis [7]. The high activity of Ru/MCM-41 catalyst was proposed to be the combination effects of its bifunctionality contributed from metal and acid sites. However, the complex structure of tire, together with the presence of the bifunctionality of the catalysts, makes it difficult to distinguish the role(s) of metal and acid sites during catalytic pyrolysis. Meanwhile, understanding the role of each individual site might help designing a better catalyst.

This study was carried out to investigate the roles of ruthenium during waste tire pyrolysis. The influence of calcination rate on the activity of Ru-based catalysts was also studied.

2. Experimental

2.1. Catalyst preparation

To synthesize SBA-1 (*Santa Barbara Airport* No. 1), a mesoporous molecular sieve, silatrane was first synthesized using the method of Wongkasemjit's group [8]. The silatrane precursor was added to a solution containing NaOH, and H_2SO_4, followed by adding a solution of water and cetyl trimethyl ammonium bromide (CTAB) with vigorous stirring [9]. Water was added to this mixture prior to aging at room temperature for 2 days to form a white precipitate. The product was filtered and washed with water. Then, the white solid was dried at room temperature and calcined at 580 °C for 6 h (0.5 °C/min) to obtain the mesoporous SBA-1.

Ru-supported catalysts were prepared using conventional wetness impregnation technique. An appropriate amount of precursor solution of $RuCl_3{\cdot}xH_2O$, purchased from FLUKA, was dropped to the SBA-1 to obtain 1 wt% of Ru, followed by drying in an oven at 110 °C for 3 h. In order to study the influence of the

* Corresponding author. Tel.: +66 22 18 41 48; fax: +66 22 15 44 59.
E-mail address: Sirirat.j@chula.ac.th (S. Jitkarnka).

0165-2370/$ – see front matter © 2010 Elsevier B.V. All rights reserved.
doi:10.1016/j.jaap.2010.01.004

Author's personal copy

calcinations rate, the obtained dried sample was divided into 3 portions, which were calcined under different heating rates (1 °C/min, 5 °C/min, and 10 °C/min) from room temperature to 580 °C. Subsequently, all samples were pelletized and sieved to obtain particle sizes in the range of 400–425 μm. Prior to catalytic activity testing, all catalysts were reduced by hydrogen at 400 °C for 3 h.

2.2. Catalyst characterization

X-Ray diffraction (XRD) patterns were obtained using the Riguku D/Max 2200H with a scanning speed of 0.5°/min and 2θ from 1.5° to 60°. The composition of the Ru on the support was determined by the Inductively Coupled Plasma (ICP) technique (PerkinElmer Optima 4300 PV). The surface area, pore volume and pore size distribution of the studied catalysts were characterized by N_2 physical adsorption using a Sorptomatic 2900 equipment. Carbon monoxide chemisorption was carried out in a Micromeritics 2900 apparatus at room temperature, after the *in situ* reduction of sample at 500 °C (10 °C/min) for 1 h, under a flow of H_2. Dispersion data was calculated by assuming a stoichiometry of CO/Ru = 1 [10]. Scanning Electron Microscopy (SEM) and Transmission Electron Microscopy (TEM) images were recorded by a JEOL 2010 and JEM 2100 instrument, respectively. For determination of particle size by TEM, the mean size of Ru particles was calculated on the basis of size measurements of 300–500 for each sample. Temperature programmed techniques including H_2-TPR, TPD-H_2, and TPO were conducted using the same Micromeritics 2900. For TPD-H_2, about 0.1 g of sample was first pretreated in He at 550 °C for 30 min. Then, the system was cooled to 30 °C, and the H_2 adsorption was performed for 1 h, followed by He purging for 30 min. The TPD-H_2 was started from 30 °C to 500 °C with a heating rate of 5 °C/min. TPR-H_2 of Ru-supported catalysts was conducted from room temperature to 500 °C with a heating rate of 5 °C/min after pre-treatment of sample at 150 °C under He flow for 1 h. TPO was performed from room temperature to 900 °C (10°C/min), and the final temperature was held for 30 min. The amount of coke was then determined from the area under the curve and calculated by the software equipped with the machine. The sulfur contents in waste tire and in the spent catalysts were determined by elemental analysis (LECO, US).

2.3. Pyrolysis of waste tire

The details of waste tire sample and pyrolysis process including sample amount, reactor size, and so on was described in [7,11]. Briefly, a tire sample was pyrolyzed in the lower zone of the reactor (500 °C), and then the evolved product was carried to the upper zone (350 °C) packed with a catalyst. The obtained product was next passed through a condensing system to separate incondensable compounds from the liquid product. The solid and liquid products were weighed to determine the product distribution. The amount of gas was then determined by mass balance. The gaseous product was analyzed by a GC equipped with an FID on the H_2- and CO_x-free basis (only hydrocarbons were detected). The liquid product was first dissolved in n-pentane to precipitate asphaltenes. The obtained maltenes was analyzed by FTIR and liquid adsorption chromatography using the methods and conditions described in [12], in which saturated hydrocarbons, mono-, di-, poly-, and polar-aromatics were fractionated. Finally, a SIMDIST GC was used to analyze the obtained maltenes and hydrocarbon fractions according to the ASTM D2887 method to determine the simulated true boiling point (TBP) curves. The curves were then cut into petroleum fractions, based on their boiling point ranges, including naphtha (<200 °C), kerosene (200–250 °C), gas oil (250–370 °C), and residue (>370 °C).

3. Results and discussion

3.1. SBA-1 as the selected support

In order to clearly determine the roles of ruthenium and the effect of calcination rate on the activity of Ru-supported catalyst in the catalytic pyrolysis of waste tires, a selected support should not play any role on chemical reactions. Additionally, to obtain a high metal dispersion for a metal-supported catalyst, the use of a zeolite, especially the one having large surface area, is commonly suggested. Moreover, a pure silica material has been shown to be inactive for the conversion of used tire rubber into hydrocarbon products [13]. Consequently, in this study, a silica SBA-1 was first synthesized *via* the silatrane route [9]. The accomplishment of the material synthesis was confirmed by XRD and N_2 physical adsorption results. The surface area and pore volume of the synthesized SBA-1 are 1428 m^2/g and 0.72 cm^3/g, respectively, which are similar to the values from the reference [9].

The experiment results of thermal and catalytic pyrolysis using SBA-1 as a catalyst are depicted in Fig. 1. It can be seen that the yield of solid product is similar in both runs (Fig. 1A). This is because of the fact that the pyrolysis conditions were kept constant and the tire was reported to be completely decomposed at 500 °C [14]. As compared to non-catalytic case, the use of SBA-1 insignificantly influences the product yields because the yields of gas and liquid products in the two runs are comparable. In addition, the concentrations of saturated hydrocarbons, mono-, di-, poly- and polar-aromatics, analyzed by liquid adsorption chromatography, of the two derived oils are quite similar (Fig. 1B). Furthermore, the TBP curves of the two oils are mostly overlapped (Fig. 1C). Thus, it is safe to conclude that SBA-1 is catalytically inactive for waste tire pyrolysis.

3.2. Roles of ruthenium during catalytic pyrolysis of waste tire

1%Ru-supported SBA-1 catalyst was prepared, and its catalytic activity was tested for understanding the role of ruthenium in the waste tire pyrolysis. The amount of ruthenium loaded on the SBA-1 support is confirmed by ICP analysis. No loss in the crystallinity of the SBA-1 is detected in the XRD pattern of the prepared 1%Ru/SBA-1 sample. Note that the SBA-1 was proven to be catalytically inactive for waste tire pyrolysis; thus, from this point, the

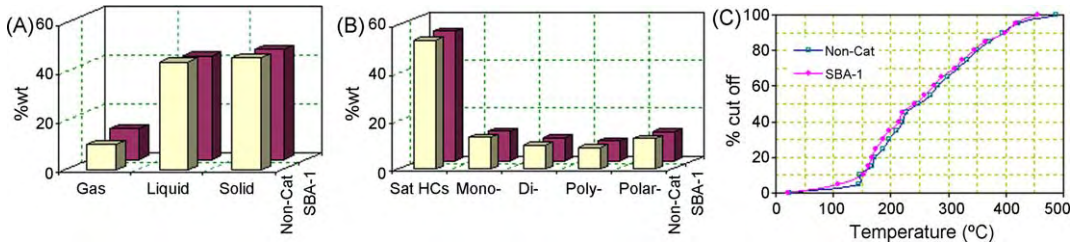

Fig. 1. Effects of SBA-1 on the pyrolysis products: (A) product distribution, (B) liquid compositions, and (C) true boiling point curves.

Author's personal copy

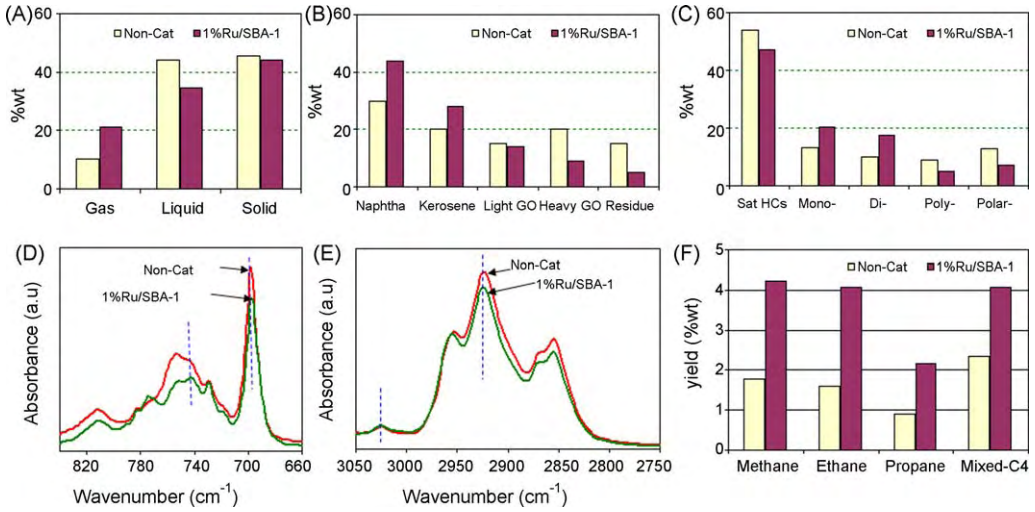

Fig. 2. Effects of 1%Ru/SBA-1 on the pyrolysis products: (A) product distribution, (B) petroleum cuts, (C) liquid composition, and (D) light alkanes yield.

influences of 1%Ru/SBA-1 will be presented by comparing directly to the thermal pyrolysis.

The results of experiments with and without 1%Ru/SBA-1 are given in Fig. 2. The results include the product yields, petroleum cuts, and compositions of the derived oils. Fig. 2A shows that 1%Ru/SBA-1 decreases the yield of oil in accordance with an increase in the yield of gaseous products. Namely, the gas yield increases from ~10 wt% to ~20 wt%. Fig. 2B shows the petroleum fractions in the pyrolysis oils. A high concentration of heavy fractions, *i.e.* residues and gas oil (GO), is observed in the non-catalytic oil. The presence of 1%Ru/SBA-1 catalyst shifts the TBP curves to lower temperature, resulting in the increase in light fractions. The content of light fraction (boiling point $< 250\,^{\circ}C$) increases from approximate 50 wt% to over 70 wt%. Fig. 2C indicates that 1%Ru/SBA-1 strongly influences the compositions of the pyrolysis oils. As compared to non-catalytic oil, the contents of poly- and polar-aromatic hydrocarbons (PPAHs) are much lower. The reduction of these heavy HCs caused by the presence of Ru-based catalysts is further confirmed by observing the results obtained from FTIR analysis (Fig. 2D). This figure presents the FTIR spectra of the oils in the wave number corresponding to the polycyclic aromatic range [15,16]. The intensity of peaks at 700 cm^{-1} and 740 cm^{-1} in the spectrum of the oil produced over 1%Ru/SBA-1 is obviously lower than that of the non-catalytic case, indicating a lower concentration of polycyclic HCs [16].

The formation of PPAHs from the pyrolysis of waste tire was reported to occur through the Diels-Alders reaction and aromatization [4,17,18]. And a poly-aromatic compound, such as phenanthrene, was formed after the formation of naphthalene, a di-aromatic compound. Moreover, no evidence proving the direct formation of aromatics from cyclization of alkanes was observed [17]. The presence of ruthenium clusters in this study drastically decreases PPAHs (Fig. 2C). Due to the fact that the nature of ruthenium is highly active for catalyzing hydrogenation reaction [5]; thus, it might decrease PPAHs either by: (i) converting their intermediates to smaller molecules preventing their formation (*first route*), or: (ii) transforming them to other types of molecules, most likely through hydrogenating (*second route*).

If the first route is really the case, then the content of di-aromatics, intermediates of PPAHs, should be lower with respect to the thermal pyrolysis. However, for 1%Ru/SBA-1 catalyst, the reduction of PPAHs is accompanied with the increase in di-aromatics; thus, the occurrence of the first route is unlikely. Moreover, it has been reported that the hydrogenation of poly-aromatics is more preferable than their di-aromatic intermediates [19], and generally yields partial hydrogenated products [20]. This, together with the higher concentration of di-aromatics (for 1%Ru/SBA-1) with respect to thermal pyrolysis (Fig. 2C), suggests that the reduction of PPAHs is more likely to occur by the second route. However, it should be noted that no evidence disproving the first route has been found. Therefore, it can be concluded that ruthenium decreases PPAHs by both ways, but the second route is more likely.

The presence of ruthenium clusters also decreases saturates in the derived oil (Fig. 2C). This is well consistent with the results obtained from FTIR analysis (Fig. 2E). The peak at 3030 cm^{-1} corresponds to the C–H stretch aromatic C, whereas the peak at 2920 cm^{-1} belongs to the CH stretch aliphatic [15]. And, the ratio between the intensity (I) of peak at 3030 cm^{-1} and 2920 cm^{-1} ($I_{3030cm} - 1/I_{2920cm} - 1$) is proportional to the relative concentration of saturates in oil [21]. It can be seen that as compared to thermal pyrolysis, this ratio increases when 1%Ru/SBA-1 was used, indicating a lower concentration of saturates in the derived oil. Usually, Ru-based catalyst is a good catalyst for hydrogenolysis reaction of hydrocarbons [5]. And, a consequence of hydrogenolysis generally is the production of light alkanes [22]. From the gas analysis from both thermal and catalytic pyrolysis in Fig. 2F, the yields of methane, ethane, propane and mix-C_4 increase dramatically when 1%Ru/SBA-1 was used. Therefore, those saturates might be converted to the light gases, speculatively indicating that the deep hydrogenolysis reactions might have occurred [23], reducing saturates in the oil.

Up to this point, it has been proven that ruthenium cluster strongly influences the pyrolysis products, SBA-1 is catalytically inactive, and there is no loss of the crystallinity of this support after incorporation with ruthenium. However, the topology and/or morphology of a zeolite can be changed during reaction [24], which can also be the cause of catalytic activity change [24,25]. Therefore, it is essential to analyze the spent 1%Ru/SBA-1 catalyst to see if any change in the structure of the support has occurred, which would have contributed to the change on the activity. The coke deposited on the spent 1%Ru/SBA-1 was first removed by oxidation. Then, it was subject to analysis by means of XRD and SEM. It can be seen that its XRD pattern is similar to the fresh catalyst (Fig. 3A). Actually, no difference can be observed. And, the SEM image of the spent catalysts depicted in Fig. 3B reveals the preservation of the SBA-1 morphology. Therefore, it is safe to conclude that the structure of SBA-1 did not change during pyrolysis. As a consequence, the catalytic activity of 1%Ru/SBA-1 is only attributed to the ruthenium contribution.

Author's personal copy

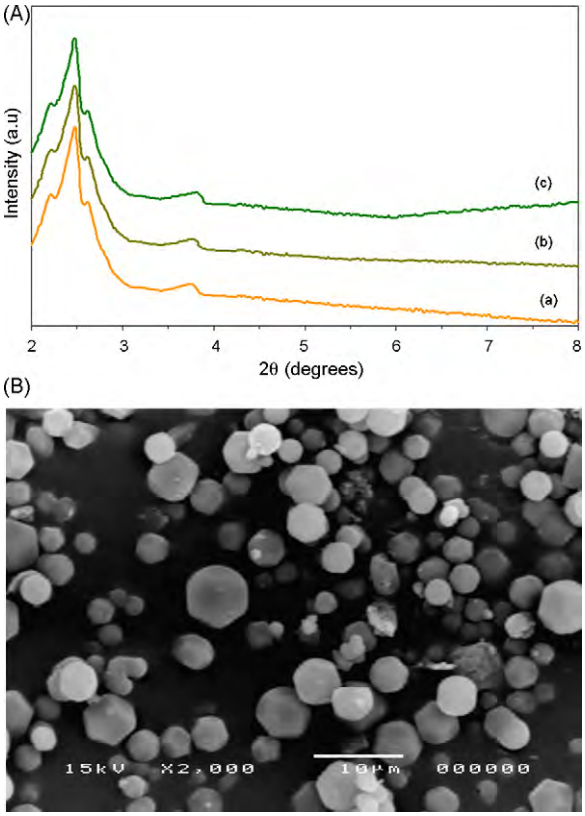

Fig. 3. (A) XRD patterns (a) SBA-1, (b) Fresh 1%Ru/SBA-1, and (c) Spent 1%Ru/SBA-1 after coke removal; (B) SEM images Spent 1%Ru/SBA-1 after coke removal.

Conclusively, ruthenium strongly increases the yield of gas in accordance with a reduction of the oil yield. Moreover, the presence of ruthenium also produces much lighter oil by decreasing poly- and polar-aromatics. Saturates in oil is also lessened possibly due to the high hydrogenolysis activity of ruthenium clusters.

3.3. Influences of catalyst preparation

3.3.1. Catalyst characterization

Table 1 summarizes the physical–chemical properties of the studied Ru-based catalysts. The catalysts prepared with a calcination rate of 1 °C/min, 10 °C/min, and 5 °C/min are denoted as 4.0Ru/SBA-1, 4.5Ru/SBA-1, and 2.5Ru/SBA-1, respectively. The number in front of the sample name stands for its mean diameter of ruthenium particles obtained from TEM for each rate of calcination. A typical TEM image of the studied catalysts is illustrated in Fig. 4. From ICP analysis, the percentage of Ru in all samples is well consistent with the targeted value. Meanwhile, the surface area and pore volume of all samples decrease with the addition of ruthenium. However, the mean pore diameter of 4.0Ru/SBA-1 and 4.5Ru/SBA-1 samples is higher than that of SBA-1,

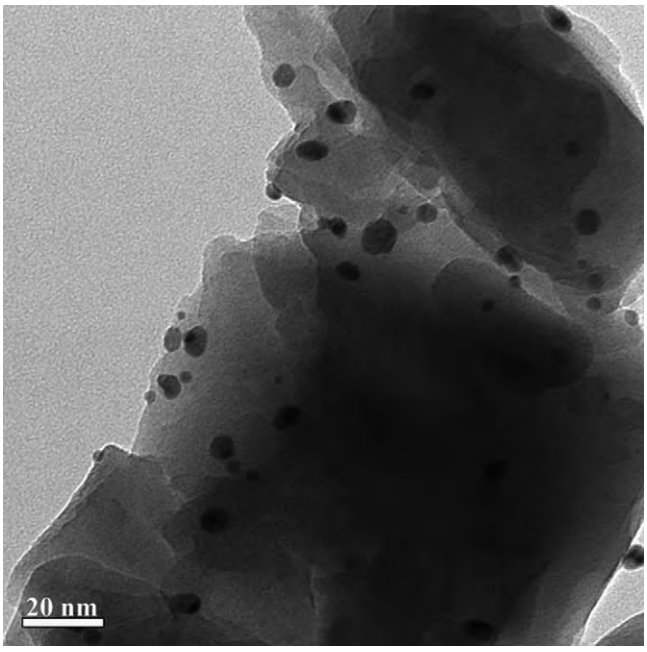

Fig. 4. TEM image of 4.5Ru/SBA-1.

possibly caused by the blockage of small pores by ruthenium particles leading to the increment of mean diameter. The pore blockage might also be the reason for the reduction in total pore volume.

The metal particle size or the consequent dispersion is strongly dependent on the preparation condition (Table 1). The sample prepared under the highest heating rate during calcination has the biggest particle size, as determined by CO-chemisorption and TEM. The average particle size obtained from TEM is slightly lower than that obtained from CO-chemisorption for the same sample. However, the trend of the mean ruthenium particle size variation is identical.

H_2-TPR profiles of Ru-supported catalysts are displayed in Fig. 5. From the figure, the two profiles of 2.5Ru/SBA-1 and 4.5Ru/SBA-1 present two overlapped reduction peaks at 195 °C and 230 °C whereas that of 4.0Ru/SBA-1 shows a narrower peak between the two peaks with a little shoulder at 195 °C. The first peak at low temperature (around 195 °C) is assigned to the Ru^{3+}/Ru^{o} single step reduction, whereas the second peak located at high temperature (~230 °C) comes from the reduction of RuO_2 [5]. The H_2-consumption curve of 2.5Ru/SBA-1 sample is broad, possibly due to the reduction of highly dispersed ruthenium species located in different environments; and its high temperature peak is the clearest, indicating a high amount of ruthenium oxide. The signals of the 4.0Ru/SBA-1 and 4.5Ru/SBA-1 are clearly narrower than 2.5Ru/SBA-1, probably due to the poor dispersion of ruthenium in the two samples, leading to the formation of bigger particles, which is well consistent with CO-chemisorption and TEM results (Table 1). Moreover, all samples have similar ruthenium content;

Table 1
Physical–chemical properties of Ru-supported catalysts.

	Ru (wt%)	Pore volume (cm^3/g)	Surface area (m^2/g)	Pore diameter (nm)	Dispersion (%)	Mean Ru particle size (nm)[a]	
						TEM	CO-chemisorption
SBA-1	–	0.72	1428	2.17	–	–	–
4.5Ru/SBA-1	1.02	0.67	1387	2.19	26.6	4.49	4.85
4.0Ru/SBA-1	0.98	0.68	1396	2.22	29.8	3.99	4.33
2.5Ru/SBA-1	0.99	0.71	1405	2.13	48.8	2.56	2.64

[a] Volume–area mean diameter.

Author's personal copy

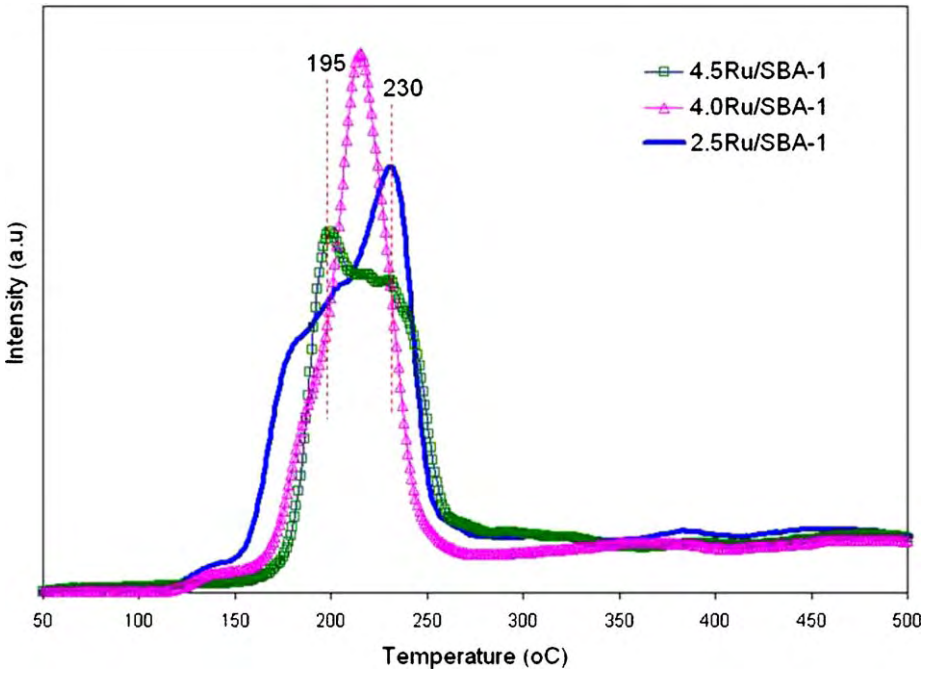

Fig. 5. TPR-H_2 profiles of calcined Ru/SBA-1 catalysts.

thus, the location of the peaks indicates the degree of metal support interaction. The stronger the metal support interaction, the more difficult it is to reduce the metal. And, a strong interaction between metal and support helps prevent sintering during reaction, resulting in a slower deactivation of the catalyst [5]. Among all samples, 2.5Ru/SBA-1 has the strongest interaction between metal and support indicated by its highest temperature of the reduction peak. This can be attributed to its smallest clusters of RuO_2 that has strong ruthenium–oxygen–silica interactions [26,27].

In order to investigate the H_2 uptake of the reduced catalysts, the Ru-supported samples were subjected to TPD-H_2 analysis. The results are displayed in Fig. 6. All samples show one hydrogen chemisorption peak locating at a temperature below 200 °C. However, the location of the peak is different from sample to sample. The peak of TPD-H_2 profile of 2.5Ru/SBA-1 is located at the highest temperature. Considering the intensity of the peak which is the indication of hydrogen adsorption on the metal sites, the observed trend is 2.5Ru/SBA-1 >> 4.0Ru/SBA-1 > 4.5Ru/SBA-1. This is well consistent with the results obtained from CO-chemisorption and TEM. Namely, the sample, which shows the higher hydrogen uptake, has smaller ruthenium particles. When the particle is smaller, there exists the greater amount of accessible ruthenium atoms for hydrogen to adsorb; thus, increasing total hydrogen uptake.

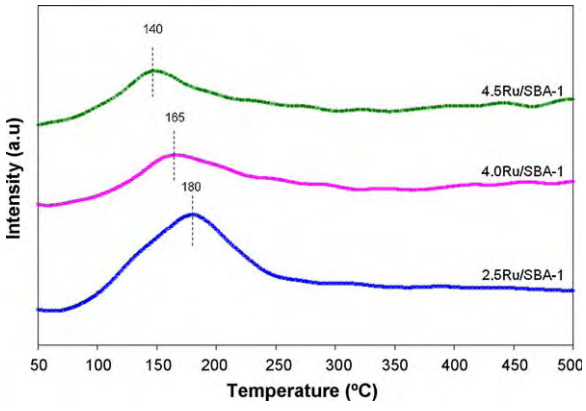

Fig. 6. TPD-H_2 profiles of Ru/SBA-1 samples: (a) 2.5Ru/SBA-1, (b) 4.0Ru/SBA-1, and (c) 4.5Ru/SBA-1.

3.3.2. *Influences of ruthenium particle size*

As demonstrated in the previous section, the different heating rates during calcination resulted in the formation of different ruthenium particle sizes on the catalysts. As such, this section presents the influences of ruthenium particle size on the yield and nature of the obtained products, which are summarized in Fig. 7.

Fig. 7A illustrates the product distribution obtained from using Ru/SBA-1 catalysts having various ruthenium particle sizes. The size of ruthenium particle strongly affects the yield of gaseous product. The gas yield increases gradually at the expense of the yield of oil with decreasing ruthenium particle size. For instance, the yield of gaseous product increases from around 15 wt% to almost 25 wt% whereas the oil yield drops from around 40 wt% to 30 wt% when the ruthenium particle size decreases from 4.5 nm to 2.5 nm. The influence of ruthenium particle can be further depicted by the petroleum cuts as shown in Fig. 7B. The decrease in ruthenium particle size causes a shift of hydrocarbons from heavy fractions, *i.e.* residues and GO to lighter fractions, naphtha and kerosene. And the highest selectivity toward light fractions is observed over the smallest ruthenium particle containing sample, 2.5Ru/SBA-1. Fig. 7C depicts the compositions of the derived oils, which reveals that the sample having the smallest ruthenium particle exhibits the highest activity for the reduction of PPAH compounds in the derived oil. And, increasing ruthenium particle size decreases the activity on PPAH reduction. The mechanism of hydrogenation reaction of aromatics was reported to involve the dissociative adsorption of H_2 on the metal sites [28]. Meanwhile, as revealed from catalyst characterization, the sample having smaller ruthenium particle size possesses higher hydrogen uptake (Fig. 6). Therefore, 2.5Ru/SBA-1 exhibit higher hydrogenation activity as compared to the other Ru-supported catalysts due to its smallest ruthenium particle size (Table 1). As a consequence, the lowest concentration of PPAHs was detected in the oil obtained from using this catalyst.

Author's personal copy

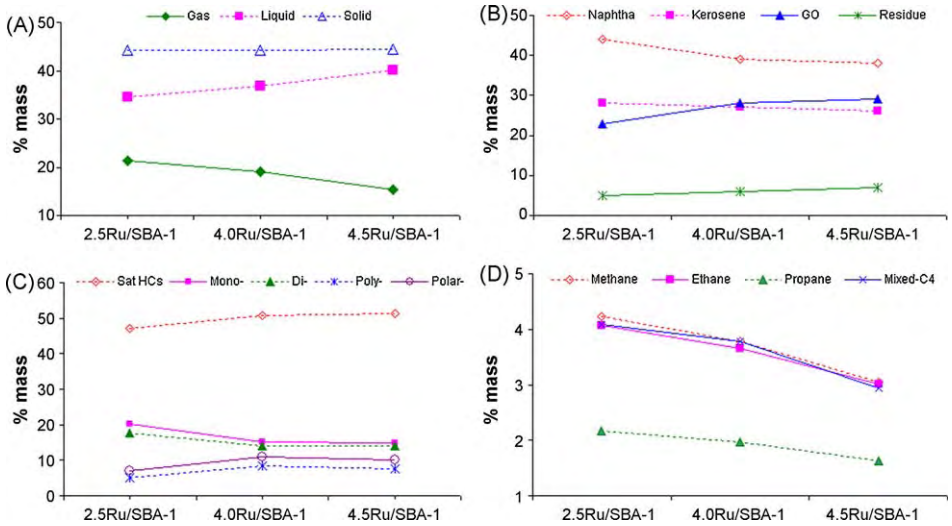

Fig. 7. Influences of ruthenium particle size on pyrolysis products: (A) product distribution, (B) petroleum cuts, (C) liquid compositions, and (D) light alkanes yield.

As elucidated in Section 3.2, the ruthenium sites are the active sites for the reduction of PPAHs and saturates in the derived oils, possibly by hydrogenation and hydrogenolysis reactions, respectively. Moreover, the sample with the smallest particle size produces the oil having the highest selectivity toward light fractions, *i.e.* naphtha and kerosene (Fig. 7B), in accordance with the lowest concentration of PPAHs (Fig. 7C). Besides, the yields of light alkane hydrocarbons in gaseous products increase gradually with decreasing ruthenium particle size (Fig. 7D). These observations suggest the existence of greater hydrogenation and hydrogenolysis reactions [23] as the metal particle size decreases due to the increase of ruthenium specific surface area. Therefore, it is likely that the decreasing ruthenium particle enhances hydrogenation reactions, then, the hydrogenated species might be further converted into lower molecular weight compounds by thermal cracking and/or hydrogenolysis reactions. That explains the increment in light oil production with decreasing ruthenium particle size. In addition, the greater hydrogenolysis reactions also explain the decrease in saturated HC content in the obtained oils (Fig. 7C). FTIR experiment (not shown here) further confirms the reduction in saturates in oil with decreasing ruthenium particle size.

The results of TPO experiments of spent SBA-1 and Ru-based catalysts are presented in Fig. 8. SBA-1 sample shows a main oxidation peak at 300–400 °C, whereas the TPO curves of all Ru/SBA-1 samples consist of two peaks located at around 300 °C and 500 °C. The first peak located at low temperature (~300 °C) is most likely due to the oxidation of adsorbed hydrocarbon species formed from condensed polycyclic compounds [29] and/or possibly comes from the oxidation of ruthenium metal. And the second peaks at 500–600 °C, corresponding to the oxidation of deposited carbon species [29], are obviously distinguishable. In addition, a shift of the second peaks to higher temperature with decreasing ruthenium particle size is observed.

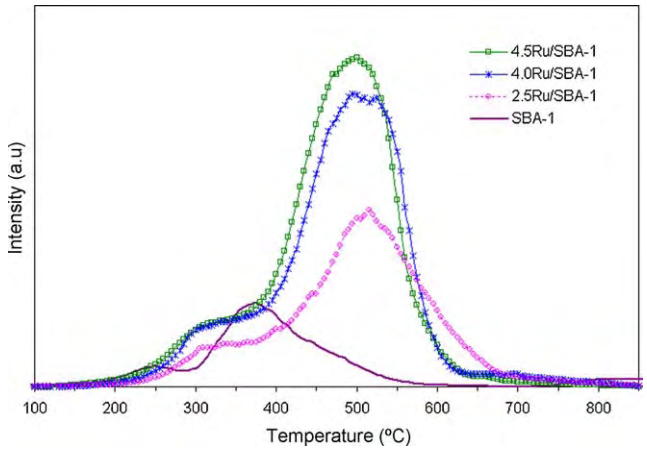

Fig. 8. TPO profiles of the spent Ru/SBA-1 catalysts.

The quantitative TPO analysis data calculated the temperatures in the range of 250–850 °C are shown in Table 2. It is clearly seen that all Ru-based catalysts produce the higher amount of coke than SBA-1. And, the amount of coke increases in the following order: SBA-1 < 2.5Ru/SBA-1 < 4.0Ru/SBA-1 < 4.5Ru/SBA-1.

Elemental analysis gives the sulfur content in the feed (waste tire) is 1.77 ± 0.01 wt%. Consequently, a considerable amount of sulfur-containing polar-aromatic compounds was produced from waste tire pyrolysis (Fig. 7C). The sulfur-containing compounds can deactivate the noble metal-supported catalysts by the strong bonding between sulfur and metal atoms [5,30]. The metal support interaction plays an important role in changing the strength of the bonding interaction between sulfur and metal [20,30–32]. In addition, a stronger interaction between metal and support also helps prevent sintering during reaction, resulting in a slower deactivation of the catalyst [5]. Besides, the sulfur tolerance might also be enhanced by changing the metal particle size [5]. According to the results of elemental analysis for sulfur contents in the spent catalysts given in Table 2, 2.5Ru/SBA-1 exhibits the highest sulfur tolerance among Ru-supported catalysts due to its lowest sulfur content, which is probably caused by its strongest interaction between metal and support and smallest ruthenium particle. Consequently, 2.5Ru/SBA-1 exhibits the highest catalytic activity with the least coke formation. The other samples, which have bigger ruthenium particles, display much lower catalytic activity due to their low dispersion and resistance to coke formation.

Table 2
Coke and sulfur in the spent catalysts.

Spent catalysts	SBA-1	2.5Ru/SBA-1	4.0Ru/SBA-1	4.5Ru/SBA-1
Coke (g/g cat)	0.027	0.061	0.098	0.112
Sulfur (wt%)	–	1.33	1.91	1.99

Author's personal copy

4. Conclusions

The roles of ruthenium and the effect of calcination rate in the catalytic pyrolysis of waste tire with Ru/SBA-1 catalysts have been studied. SBA-1 was selected as the support since it was proven to be catalytically inactive and its structure retained after reaction. The presence of ruthenium sites strongly increased the yield of gaseous products, approximately 2 times as compared to thermal pyrolysis. And, ruthenium clusters were found to be the active sites for poly- and polar-aromatic hydrocarbons (PPAHs) reduction, leading to a good light oil production. However, they also decreased saturates in the derived oils.

The heating rates during the calcination step strongly influenced the catalytic activity of Ru/SBA-1 catalysts. Different heating rates resulted in the formation of different ruthenium particle sizes on the catalyst. And, the catalyst calcined with a heating rate of 5 °C/min (denoted as 2.5Ru/SBA-1) exhibited the highest activity on the poly- and polar-aromatic reduction and on the consequent light oil production. Catalyst characterization results indicated that the smallest mean ruthenium particle size and the strongest interaction between Ru and supported resulting in the highest sulfur tolerance and coke resistance were the cause for the highest activity of this catalyst.

Acknowledgements

Center of Excellence for Petroleum, Petrochemical, and Advanced Materials, The Petroleum and Petrochemical College, Chulalongkorn University, Thailand Research Fund (TRF), Office of Commissions on Higher Education, the Chulalongkorn University's Research Unit of "Syntheses and Applications of Organometallics", and The Graduate Scholarship Program for Faculty Members from Neighboring Countries, Chulalongkorn University, are acknowledged for the partial financial support.

References

[1] P.T. Williams, A.J. Brindle, J. Anal. Appl. Pyrolysis 67 (2003) 143–164.
[2] A.M. Cunliffe, P.T. Williams, J. Anal. Appl. Pyrolysis 44 (1998) 131–152.
[3] B. Benallal, C. Roy, H. Pakdel, S. Chabot, M.A. Poirier, Fuel 74 (1995) 1589–1594.
[4] N.A. Dũng, S. Wongkasemjit, S. Jitkarnka, Appl. Catal. B: Environ. 91 (2009) 300–307.
[5] D. Eliche-Quesada, J.M. Merida-Rboles, E. Rodriguez-Caslellon, A. Jimenz-Lopez, Appl. Catal. B: Environ. 65 (2006) 118–126.
[6] H.–H. Chen, S.-C. Shen, X. Chen, S. Kawi, Appl. Catal. B: Environ. 50 (2004) 37–47.
[7] N.A. Dũng, S. Wongkasemjit, S. Jitkarnka, J. Anal. Appl. Pyrolysis 86 (2009) 281–286.
[8] W. Charoenpinijkarn, M. Sawankruhasn, B. Kesapabutr, S. Wongkasemjit, A.M. Jamieson, Eur. J. Polym. 37 (2001) 1441–1448.
[9] W. Tanglumlert, T. Imae, T.J. White, S. Wongkasemjit, Matter. Lett. 62 (2008) 4545–4548.
[10] T. Mitsui, K. Tsutsui, T. Matsui, R. Kikuchi, K. Eguchi, Appl. Catal. B: Environ. 81 (2008) 56–63.
[11] N.A. Dũng, A. Mhodmonthin, S. Wongkasemjit, S. Jitkarnka, J. Anal. Appl. Pyrolysis 85 (2009) 338–344.
[12] G. Sebor, J. Blaz ek, M.F. Nemer, J. Chromatogr. A 847 (1999) 323–330.
[13] G.S. Miguel, J. Aguado, D.P. Serrano, J.M. Escola, Appl. Catal. B: Environ. 64 (2006) 209–219.
[14] C. Berrueco, E. Esperanza, F.J. Mastal, J. Ceamanos, P. Garcia-Baicaicoa, J. Anal. Appl. Pyrolysis 74 (2005) 245–253.
[15] C.A. Islas-Flores, E. Buenrostro-Gonzalez, C. Lira-Galeana, Fuel 85 (2006) 1845–1850.
[16] C. Jager, F. Huisken, H. Mutschke, Th. Henning, W. Poppitz, I. Voicu, Carbon 45 (2007) 2981–2994.
[17] P.T. Williams, D.T. Taylor, Fuel 72 (1993) 1469–2147.
[18] P.T. Williams, R.P. Bottrill, Fuel 74 (1995) 736–742.
[19] S. Jongpatiwut, Z. Li, D.E. Resasco, W.E. Alvarez, Ad.L. Sughrue, G.W. Dodwell, Appl. Catal. A: Gen. 262 (2004) 241–253.
[20] M. Jacquin, D.J. Jones, J. Roziere, S. Albertazzi, A. Vaccari, M. Lenarda, L. Storaro, R. Ganzerla, Appl. Catal. A: Gen. 251 (2003) 131–141.
[21] S.H. Wang, P.R. Griffiths, Fuel 64 (1985) 229–265.
[22] G. Kinger, H. Vinek, Appl. Catal. A: Gen. 218 (2001) 139–149.
[23] V.M. Akhmedov, S. Al-Khowaiter, Appl. Catal. A: Gen. 197 (2000) 201–212.
[24] T. Wongkerd, A. Luengnaruemitchai, S. Jitkarnka, Appl. Catal B: Environ. 78 (2008) 101–111.
[25] Y.J. Lee, J.-H. Kim, S.H. Kim, S.B. Hong, G. Seo, Appl. Catal. B: Environ. 83 (2008) 160–167.
[26] A. Mazzieri, F. Coloma-Pascual, A. Arcoya, P.C. L'Argentiere, N.S. Figoli, Appl. Surf. Sci. 210 (2003) 222–230.
[27] V.G. Komvokis, G.E. Marnellos, I.A. Vasalos, K.S. Triantafyllidis, Appl. Catal. B: Environ. 89 (2009) 627–634.
[28] H. Du, C. Fairbridge, H. Yang, Z. Ring, Appl. Catal. A: Gen. 294 (2005) 1–21.
[29] J. Zheng, J. Guo, C. Song, Fuel. Process. Technol. 89 (2008) 467–474.
[30] C. Naccache, M. Primet, M.V. Mathieu, J. Catal. 121 (1973) 266.
[31] W.M.H. Sachtler, A.Y.u. Stakneev, Catal. Today 12 (1992) 283–295.
[32] D. Poondi, A.A. Vannice, J. Catal. 161 (1996) 742–751.

Available online at www.sciencedirect.com

ScienceDirect

Energy Procedia 00 (2011) 000–000

Energy Procedia

www.elsevier.com/locate/procedia

9th Eco-Energy and Materials Science and Engineering Symposium

Improving Light Olefins and Light Oil Production Using Ru/MCM-48 in Catalytic Pyrolysis of Waste Tire

Chaiyaporn Witpathomwong[a], Rujirat Longloilert[a], Sujitra Wongkasemjit[a,b] and Sirirat Jitkarnka[a,b,]a*

[a]*The Petroleum and Petrochemical College, Chulalongkorn University, Soi Chulalongkorn 12, Phayathai Road, Phathumwan, Bangkok 10330, Thailand*
[b]*Center for Petroleum, Petrochemicals, and Advanced Materials, Chulalongkorn University, Soi Chulalongkorn 12, Phayathai Road, Phathumwan, Bangkok 10330, Thailand*

Abstract

Mobil Composition of Matter (MCM) is the name given for a series of mesoporous materials. The MCM-48 is one of three phases of the mesoporous materials, which is cubic crystalline structure. The MCM-48 in this work was synthesized from silatrane route, and Ru metal was loaded by incipient wetness impregnation. This work investigated the activity and selectivity of MCM-48 and Ru/MCM-48 used as the catalysts for waste tire pyrolysis. The results showed that Ru/MCM-48 improved the gas yield. In addition, the use of Ru/MCM-48 catalyst produced light olefins twice as much as the non-catalytic pyrolysis. On the other hand, the catalyst helped to improve the oil quality by increasing light oil portion. Furthermore, it also reduced poly- and polar-aromatic compounds and sulfur content in the derived oil. Surface area analysis, XRD, and CHNS analysis were performed to explain the experimental results.

© 2010 Published by Elsevier Ltd. All right reserved

Keywords: Pyrolysis; Waste tires; Light olefins; Ruthenium; Silica MCM-48; Aromatics;

1. Introduction

Tires are non-biodegradable materials resulting in many problems such as landfill, hazardous, and environmental problems. Pyrolysis is an effective choice to manage the waste tire problem. It is a thermal decomposition of large molecular weight molecules to lower molecular weight products in the absence of

* Corresponding author. Sirirat Jitkarnka, Tel.:+662-218-4148; fax: +662-215-4459.
E-mail address: sirirat.j@chula.ac.th

oxygen. In general, the products of tire pyrolysis can be separated into liquid, gas and solid char. The light olefins are one of the fractions in the gas product from the pyrolysis of waste tire. They can be used as petrochemical feedstock and raw material of plastic industry. The use of catalyst can improve the quality of the product from pyrolysis. Ru/MCM-41 has been found to increase the gas yield (light olefins) due to its high cracking and dehydrogenating activity [1]. In 2008, Basagiannis and Verykios [2] studied the influence of the carrier on the steam reforming of acetic acid over Ru-based catalysts. They found that Ru can help increase the catalytic activity toward lower temperatures and higher hydrogen production rates. Moreover, Ru/HMOR can produce the high amount of light olefins and gas yield as studied by Dũng *et al.*, [1]. Later, it was found that 0.7% Ru supported HMOR can provide the highest light olefins yield [3]. Furthermore, the use of Ru/MCM-41 in the catalytic pyrolysis can produce 4 times higher light olefins yield than the non-catalytic case [1].

In particular, Mobil Composition of Matter (MCM) is the name given for a series of mesoporous materials that were first synthesized in 1992. The MCM-48 is a one of three phases of mesoporous MCMs which are MCM-41(hexagonal), MCM-48 (cubic), and MCM-50 (lamellar). The MCM-48 used in this work is the cubic mesoporous hydroxylated silicate, which consists of sub-micron-sized crystallites [4]. Since it is a mesoporous material that is in the same series of MCM-41, whose pore size has been proven appropriate to crack large molecules of HCs and preserve light olefins formation, MCM-48 might have high potential to be used as a support for light olefins production as well. Consequently, 0.7%wt ruthenium metal supported on MCM-48 was used as a catalyst for potentially producing light olefins from waste tire pyrolysis.

2. Experimental Setup

2.1. Catalyst preparation

The silica MCM-48 was synthesized by silatrane route. Silatrane was first synthesized using the method of Wongkasemjit's group [5]. Silatrane precursor was added to hexadecyltrimethyl ammonium bromide (CTAB, purchased from Sigma Chemical Co.), and sodium hydroxide (NaOH, sigma Chemical Co.). After that, water was added with vigorous stirring, and gel was kept in an autoclave 16 hr at 140°C. The obtained crude product was filtered and washed with water to keep a white solid. The ratio of chemicals: Si/CTAB/NaOH/H_2O was 1:0.3:0.5:62. Next, the white solid was dried at room temperature and calcined at 550 °C for 6 hours with the ramping rate of 0.5°C/min to obtain mesoporous MCM-48. For the Ru metal loading, the precursor solution of ruthenium (III) chloride hydrate was dropped on the support using the impregnation technique. The 0.7%Ru was loaded to 5 g. of the support, which needed 0.0719 g of $RuCl_3$. After that, the wet support was dried in an oven at 110°C for 3 hours and calcined in a furnace at 500°C for 3 hours with the heating rate of 10°C/min to obtain the catalysts in an oxide form. Then, the catalyst was reduced with H_2 at 400°C for 1-2 hours in order to convert the metal oxide form to metal element.

$$RuO_2 + H_2 \longrightarrow Ru + H_2O$$

2.2. Catalyst Characterization

The crystalline phase of the catalysts was examined using the X-ray diffraction pattern. X-ray diffraction (XRD) patterns were taken by using a Rigaku, Rint X-Ray diffractometer system (RINT 2200)

with Cu tube for generating CuKα radiation (1.5406 Å) and nickel filter. In this experiment, XRD determines the structure of catalysts and crystal size on the supports. A catalyst sample was ground to be fine and homogeneous particles, and then packed in a glass specimen holder. The data from XRD were analyzed and recorded by an on-line computer at the scanning speed of 0.5° min-1 and 2θ from 2° to 90°. The surface area, pore volume, and pore size of the studied catalysts were determined by N_2 physical adsorption with the Sorptomatic 2900 instrument. The percentage composition of sulfur in oil products and sulfur deposition on the spent catalysts were performed by using a LECO® Elemental Analyzer (TruSpec®S). The oil product of 0.1–1 g was absorbed on an aid support, which was put in a ceramic boat. The analyzed temperature of sulfur furnace was 1,350 °C.

2.3. Pyrolysis of Waste Tire

10 gram of waste tire sample was loaded, and was pyrolyzed at 500ºC in the lower zone of the pyrolysis reactor as in [6]. 2.5 gram of catalyst was packed and heated at 350 °C in the upper zone. The pyrolysis product was carried by a nitrogen flow, and was swept to the condensers. The non-condensable product was passed through the condensers and collected in the gas sampling bag. The solid and liquid products were weighed to determine the gas quantity by mass balance. The gas product was analyzed by a Gas Chromatography; Agilent Technologies 6890 Network GC system. The oil product was separated into maltene and asphaltene by adding n-pentane into the pyrolytic oil at the ratio of 40:1. Then, the maltenes were fractionated into saturated hydrocarbons, mono-, di-, poly-, and polar-aromatics by liquid adsorption chromatography [4].

3. Results and Discussion

MCM-48 is a mesoporous material, which has the 3D pore structure. The XRD patterns of synthesized MCM-48 and Ru-supported MCM-48 are presented in Fig.1. Only one peak of the both samples is detected at 2θ = 2.2°, which is the unique peak. The peaks corresponding of Ru metal are generally obtained at 38°, 42°, 44°, and 58° [7]. However, they are rarely detected because of low amount of Ru loading (0.7%wt). The loaded ruthenium metal does not affect the crystal structure.

The physical properties of fresh catalysts are shown in Table 1. The BET surface area and B.J.H. pore volume of the synthesized MCM-48 are 1,405 m^2/g and 0.87 cm^3/g, respectively. Moreover, the average pore diameter of synthesized MCM-48 is 35.9 Å. The covering of Ru metal causes the dramatic reduction in the surface area. In addition, the reduction of pore volume and pore diameter is caused by Ru metal, which covers the pore of synthesized MCM-48.

Table 1 Physical properties of studied catalysts.

	Surface area (m^2/g)*	Pore volume (cm^3/g)**	Pore diameter (Å)**
MCM-48	1,405	0.87	35.87
0.7% Ru/MCM-48	915.7	0.63	32.94

*****BET method, ******B.J.H. method

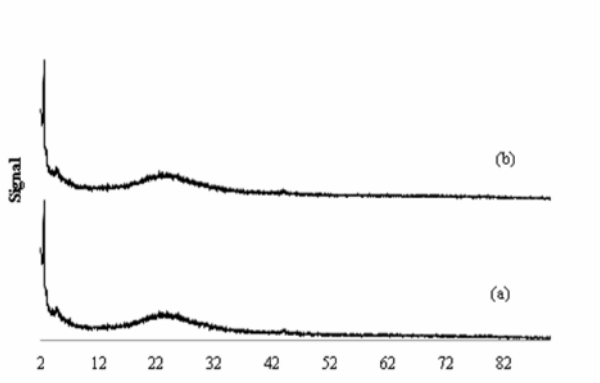

Fig.1. XRD pattern of catalysts: (a) MCM-48; and (b) 0.7%Ru/MCM-48

3.1. Pyrolysis Products

According to Fig.2, the non-catalytic pyrolysis can produce the yield of gas, oil, and solid char of approximately 13%, 40%, and 47%, respectively. The use of MCM-48 can produce the gas yield of about 23%, and its production is higher than the non-catalytic case by 10%. Furthermore, Ru metal loading on MCM-48 also improves the gas production by 3% higher than the MCM-48 case. Moreover, the synthesized MCM-48 and Ru/MCM-48 decrease the oil production. They can produce less oil than the non-catalytic case by 7%, and 8%, respectively. MCM-48 was synthesized by silatrane route; therefore, it is not an acidic material. However, the effect on gas production of synthesized MCM-48 is through the 3D pore structure [8], which holds up the reactants inside at a long enough time that hydrocarbons have great mass transfer to undergo cracking reaction in the porous MCM-48. Moreover, the acidity of synthesized MCM-48 is less than other acidic zeolites such as HMOR, and HBeta; therefore, it has the low amount of coke deposition. The activity of catalyst is maintained because of the low amount of coke deposition [9]. Furthermore, the Ru loading on the MCM-48 increases the gas production. Ru metal, providing the metal sites, promotes the hydrogenation reaction of aromatic hydrocarbons, which are subsequently cracked and undergo ring-opening reaction in the pore of MCM-48.

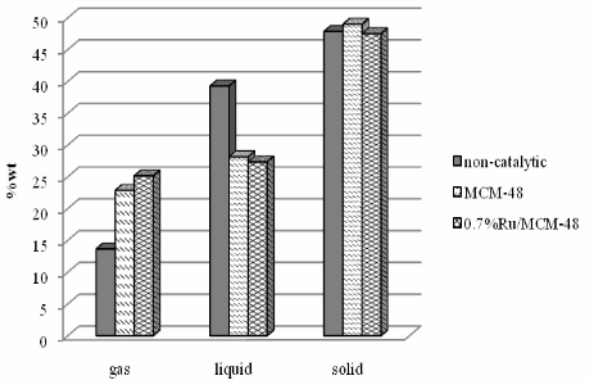

Fig.2. Product distribution of pyrolysis products from using 0.7% Ru/MCM-48 catalysts

3.2. Gaseous Products

The gas obtained from tire pyrolysis are, in general, composed of methane, ethylene, ethane, propylene, propane, C4-, C5-, and some traces of C6-, C7-, and C8-hydrocarbons. It was found that the gas also consisted of 0.233% H_2, and 0.423% CO_x for the non-catalytic case [10]. Fig.3. shows the composition of pyrolytic gas obtained from this work. The use of synthesized MCM-48 can drastically improve methane, ethane, and especially C4-, and C5-hydrocarbons. The C4- and C5-hydrocarbons productions are high in the gas because the tire is originally made from some butadiene and isoprene; hence, hydrocarbons chains tend to be cracked to the monomers. Moreover, the increment of C5-hydrocarbon might be resulted from the 3D pore structure of MCM-48, which holds up hydrocarbon molecules, then allowing some small gas molecules combine to larger gas molecules. Ru loaded catalyst produces the same gas yields as those of the MCM-48, except that of C5-hydrocarbons. Ru/MCM-48 can produce the significantly high amount of C5-hydrocarbons as compared to that of the other gases. It was reported that Ru metal can crack heavy hydrocarbons to gas products [11]. The increment of C5-HCs shown in the result consequently occurs from Ru metal that selectively cracks heavy HCs to C5s. According to Fig.4, MCM-48 and Ru/MCM-48 can produce high light olefins, which consist of ethylene and propylene in the gas. They can convert invaluable waste tire to valuable products at a high yield of light olefins. When Ru metal is loaded on MCM-48, the Ru/MCM-48 can improve the selectivity of light olefins. Due to the non-acidity of synthesized MCM-48, light olefins molecules can be preserved, because they are not further cracked to other HCs. Additionally, the meso-pore of MCM-48 gives higher selectivity of propylene than that of ethylene. With Ru metal, the yields of ethylene and propylene are slightly improved in conjunction with the higher gas production.

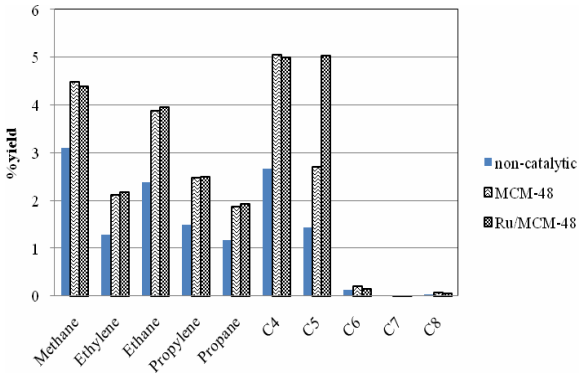

Fig.3. Composition of pyrolytic gas

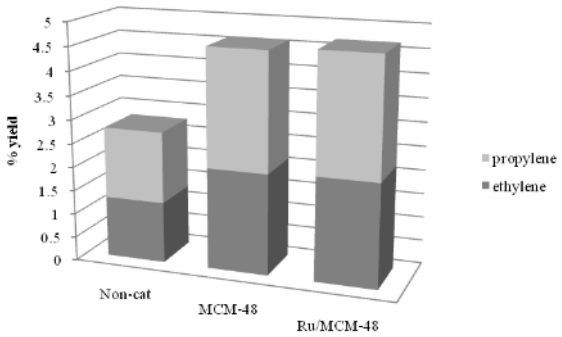

Fig.4. Light olefins production from using synthesized MCM-48 and Ru/MCM-48 catalysts

3.3. Pyrolytic Oil

Furthermore, the catalysts can improve the quality of pyrolytic oils. As shown in Table 2, the amount of asphaltene is significantly reduced with using the synthesized MCM-48 and Ru/MCM-48. It can be seen that the MCM-48 has cracking ability; accordingly, the large HCs such as poly- and polar-aromatic can be cracked to smaller molecules. Thus, the MCM-48 dramatically reduces asphaltene. However, the Ru-loaded MCM-48 does not further reduce the amount of asphaltene as compared to the unloaded MCM-48; instead it slightly increases asphaltene.

In Fig.5, the molecular fractions, obtained from the liquid chromatography, in the oils indicate that the synthesized MCM-48 causes the increment of mono-, and di-aromatic HCs in accordance with decreasing saturated, poly-, and polar-aromatic HCs. As previously explained, the non-acidic MCM-48 has mild cracking activity with meso pore sizes, allowing large molecules to enter; thus, the amounts of poly- and polar-aromatics slightly decrease. In addition, saturated HCs are found decreasing as well. On the other hand, Ru loading on the MCM-48 support can dramatically improve saturated HCs in accordance with decreasing all aromatic compounds, indicating that Ru metal can promote high hydrogenation reaction. Consequently, multi-ring aromatics, especially poly- and polar-aromatic HCs, can be hydrogenated on the metal sites. Therefore, saturated HCs are increased at the expense of aromatic compounds from using the Ru/MCM-48 catalyst. Table 2 also shows that MCM-48 and Ru/MCM-48 insignificantly reduce the amount of sulfur in oil, because the sulfur slightly changes as compared to the non-catalytic case. This indicates the mild cracking activity of MCM-48 and the low activity of Ru on breaking C-S bonds in the pyrolytic oil. Due to the low C-S bond cracking activity, sulfur deposition on the spent catalysts is low as well.

Table 2 Amount of asphaltene in oil, sulfur deposition on spent catalysts, and sulfur in oils

	%Asphaltene	%Sulfur deposition on spent catalysts	%Sulfur in oils
Non-catalytic	0.71	-	0.73
MCM-48	0.2	0.43	0.69
Ru/MCM-48	0.28	0.43	0.69

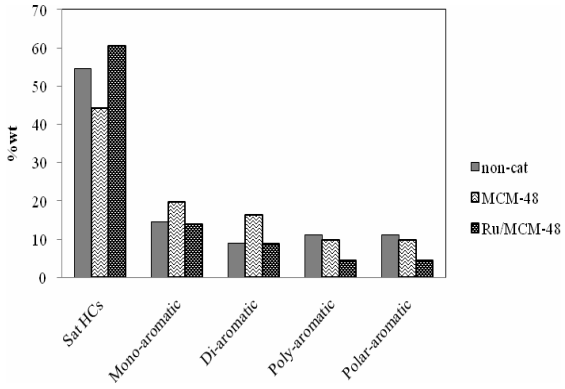

Fig.5. Molecular compounds in oils from using synthesized MCM-48 and Ru/MCM-48 catalysts

4. Results and Discussion

The catalytic pyrolysis of waste tire with using MCM-48 and 0.7% Ru/MCM-48 was performed in this work. The synthesized MCM-48 gave the dramatic improvement of gas production as compared to the non-catalytic case in accordance with decreasing the oil production, and Ru-supported MCM-48 also further increased the gas yield from using the pure MCM-48. Both MCM-48 and 0.7% Ru/MCM-48 enhanced the light olefins production. Furthermore, the catalysts can improve the quality of oil. Ru/MCM-48 gave the lighter oil as compared to the non-catalytic case. In particular, the maltene from using Ru/MCM-48 catalyst had the high concentration of saturated-hydrocarbons and low poly-, and polar-aromatic hydrocarbons.

The high activity and selectivity of Ru/MCM-48 is attributed to its mild cracking activity, preventing light olefins from over-cracking. The 3D pore structure of MCM-48 allowed high mass transfer, which improved overall reaction. Moreover, the Ru metal sites improved cracking and hydrogenation activities.

Acknowledgements

The authors would like to thank the Petroleum and Petrochemical College, the Wongkasemjit's group, Thailand Research Fund, the Commissions on Higher Education, and the National Center of Excellence for Petroleum, Petrochemicals, and Advanced Materials, Chulalongkorn University, Thailand.

References

[1] Dũng NA, Raweewan K, Wongkasemjit S, and Jitkarnka S. Light olefins and light oil production from catalytic pyrolysis of waste tire. *J Anal Appl Pyrol* 2009;**86**:281–286.

[2] Basagiannis AC, Verykios XE. Influence of the carrier on steam reforming of acetic acid over Ru-based catalysts. *Appl Catal B Envir* 2008;**82**:77–88.

[3] Kongkadee K. Effect of Metals loaded on zeolite supports on tire pyrolysis products: Ru on HMOR and HZSM5. *M.S. Thesis* 2008 The Petroleum and Petrochemical College, Chulalongkorn University, Bangkok, Thailand.

[4] Viveka A. Michael W, Tetsu O, Michael J, Malin B. Cubosome Description of the Inorganic Mesoporous Structure MCM-48. *Chem Mater* 1997;**9**:2,066-2,070.

[5] Longloilert R, Chaisuwan T, Luengnaruemitchai A, Wongkasemjit S. Synthesis of MCM-48 from silatrane via sol–gel process. *J Sol-Gel Sci Technol* 2011; doi:10.1007/s10971-011-2409-8

[6] Dũng NA, Wongkasemjit S, Jitkarnka S. Effects of pyrolysis temperature and Pt-loaded catalysts on polar-aromatic content in tire-derived oil. *J Anal Appl Pyrol* 2008;**91**:300-307.

[7] Perring L, Bussy F, Gachon JC, Peschotte P. The Ruthenium-Silicon System. *Alloy and compounds* 1998;**284**:198-205.

[8] Rodriguez M, Laresgoiti MF, Cabrero MA, Torres A, Chomón MJ, Caballero B. Pyrolysis of scrap tyres *Fuel Proc Technol* 2001;**72**:9–22.

[9] Lan-Lan L, Shuangxi L. CuO-containing MCM-48 as catalysts for phenol hydroxylation. *Catal Comm* 2005;**6**:762-765.

[10] Alsobaai AM, Zakaria R, Hameed BH. Hydrocracking of petroleum gas oil over NiW/MCM-48-USY composite catalyst. *Fuel Proc Technol* 2007;**88**:921-928.

[11] Berrueco C, Esperanza E, Mastral FJ, Ceamanos J, Garcı´a-Bacaicoa P. Pyrolysis of waste tyres in an atmospheric static-bed batch reactor: Analysis of the gases obtained. *J Anal Appl Pyrol* 2005;**74**:245–253.

[12] Dũng NA, Mhodmonthin A, Wongkasemjit S, Jitkarnka S. Effects of ITQ-21 and ITQ-24 as zeolite additives on the oil products obtained from the catalytic pyrolysis of waste tire. *J Anal Appl Pyrol* 2008;**85**:338–344.

Our reference: Version Number: 1/2009

ELSEVIER Ltd
PUBLISHING AGREEMENT

PLEASE PROVIDE US WITH THE FOLLOWING INFORMATION, REVIEW OUR POLICIES AND THE PUBLISHING AGREEMENT AND INDICATE YOUR ACCEPTANCE OF THE TERMS

Article entitled: Improving Light Olefins and Light Oil Production Using Ru/MCM-48 in Catalytic Pyrolysis of Waste Tire

Corresponding author: Sirirat Jitkarnka

To be published in The Procedia: Energy Procedia

I hereby assign to **ELSEVIER Ltd** the copyright in the manuscript identified above and any supplemental tables, illustrations or other information submitted therewith that are intended for publication as part of or as a supplement to the manuscript (the "Article") in all forms and media (whether now known or hereafter developed), throughout the world, in all languages, for the full term of copyright, effective when and if the article is accepted for publication. This transfer includes the right to provide the Article in electronic and online forms and systems. No revisions, additional terms or addenda to this Agreement can be accepted without our express written consent. Authors at institutions that place restrictions on copyright assignments, including those that do so due to policies about local institutional repositories, are encouraged to obtain a waiver from those institutions so that the author can accept our publishing agreement.

I confirm that I have read and understand the full list of rights retained by authors and also agree to the other *General Terms of Publication* (see below).

YOUR STATUS

☐ **I am the sole author of the manuscript**
Please indicate if any of the below also apply to you:
☐ I am a UK Government employee electing to transfer copyright
☐ I am a UK, Canadian or Australian Government employee and Crown Copyright is claimed
☐ I am a US Government employee and there is no copyright to transfer
☐ I am a contractor of the US Government under contract number: .....

☒ **I am one author signing on behalf of all co-authors of the manuscript**
Please indicate if any of the below also apply to you and your co-authors:
☐ We are all US Government employees and there is no copyright to transfer
☐ I am a US Government employee but some of my co-authors are not
☐ I am not a US Government employee but some of my co-authors are
☐ The work was performed by contractors of the US Government under contract number:.....
☐ We are all UK Government employees electing to transfer copyright
☐ We are all UK, Canadian or Australian Government employees and Crown Copyright is claimed
☐ I am not claiming Crown Copyright but some of my co-authors are employees of the UK, Canadian or Australian Government

☐ **The article is a 'work made for hire' and I am signing as an authorized representative of my employer.**
Name and job title of assignee if different from Corresponding Author: .....
Please indicate if any of the below also apply to you:
☐ The article is authored by US Government employees and there is no copyright to transfer
☐ The work was performed by contractors of the US Government under contract number: .....
☐ The article is authored by UK, Canadian or Australian Government employees and Crown Copyright is claimed

FUNDING

☐ **No funding was received for the research reported in the article**

☐ **The research reported in the article was funded by the US National Institutes of Health**

☐ **The research reported in the article was funded by the Brazilian Government**

☒ **The research reported in the article was funded by other agencies**
For information on funding agencies and our arrangements with funding bodies in general please visit www.elsevier.com/fundingbodyagreements.

Please mark **one or more** of the above boxes (as appropriate) and then sign and date the document

Signed: _____ Name printed: Dr. Sirirat Jitkarnka

Title and Company (if employer representative) : Associate Professor, The Petroleum and Petrochemical College, Chulalongkorn U.

Date: 13 July 2011

How we use your information: Our staff at Elsevier Ltd and its affiliated companies worldwide will be contacting you concerning the publishing of your article and occasionally for marketing purposes.

☒ Please tick the box if you do not wish to receive news, promotions and special offers about our products and services.

Influence of the physical mixture of Y and KL zeolites on the pyrolysis of waste tire

(This paper is recommended by the Organizing Committee of the International Conference on Clean Energy (ICCE-2010) to be published in the IJGW.)

Abstract

Catalysts can assist in waste tire pyrolysis process for the production of valuable products. A new type of acid-base catalysts can play an important role on modifying the product yields and the compositions of hydrocarbon products. Therefore, the advantage of acid (cracking) and basic (isomerization) catalysts could be simultaneously taken by using the combination of these catalysts in a pyrolysis reactor. The influence of the physical mixing of acid (Y) and basic (KL) zeolites was studied, aiming to produce the molecules of higher valuable products. The ratio of the two zeolites was varied from 0 to 1.0. From the results, it was clear that the yields of the light olefins and cooking gas obtained from the zeolite mixtures were higher than those of the catalytic pyrolysis with an individual zeolite. Especially, the mixture at the $Ø_{KL}$ = 0.25 gives the highest activity on the light olefins and cooking gas production. Moreover, it was found that the physical mixture at $Ø_{KL}$ = 0.75 produced the highest naphtha fraction.

Keywords: waste tire; cracking; pyrolysis; catalytic pyrolysis; Y zeolite; KL zeolite; acid catalyst; basic catalyst; light olefins; cooking gas; oil; tire-derived oil; naphtha; kerosene; gas oil.

Copyright © 200x Inderscience Enterprises Ltd.

Author

1 Introduction

The transportation in Thailand has been more convenient nowadays. Many roads have been constructed, which lead to the change in major types of transportation in Thailand. People tend to travel by cars, buses, etc. That is why there are a large number of cars having been produced. Consequently, materials which are soon to become some parts of cars have been launched increasingly to the market as well. One of the main parts of vehicles is tire. In 2005, Pollution Control Department in Thailand reported that there were about 1.7 million tons per year of tires produced in Thailand (Pollution Control Department, 2010). These tires become one of the most serious problems due to their non-biodegradation.

Acid-base catalysts used in the pyrolysis of waste tire is greatly interesting because they can reduce polyaromatic hydrocarbons in the oil due to its high activity and selectivity for the hydrogenation and ring opening of aromatic hydrocarbons (Choosuton, 2007). Some research work on the characteristics and activity of catalysts has been published. For example, Hattori (1995) investigated the the reaction mechanisms of heterogeneous basic catalysts. And, he found that KL can drive the aromatization reaction. Moreover, William *et al.* (2003) studied the effect of ZSM-5 and Y Zeolites with different pore sizes and Si/Al ratios in pyrolysis of waste tire. The result showed that the oil products contained high single-ring aromatic compounds such as toluene, benzene, and xylene when the Y zeolite with low Si/Al ratio was used. They also found that lower pore size zeolite (ZSM-5) produced lower amount aromatic compounds as compared with large pore size zeolite (Y zeolite).

According to the above literature reviews, the influence of the catalyst mixing between acid (Y zeolite) and basic (KL zeolite) catalyst was of interest in this work because the high isomerization activity of KL, the aromatization activity of KL and the cracking activity of Y can be simultaneously taken for advantages. Therefore, an attempt has been made here to study the influences of the catalyst mixing between acid (Y zeolite) and basic (KL zeolite) catalysts in order to expectedly produce molecules of higher value from the pyrolysis of waste tire

2 Experimental

2.1. Pyrolysis experiment

A tire sample was loaded at the lower zone of the reactor as in Dung *et al.*, (2009a, 2009b). KL and Y zeolites were purchased from Tosoh Company, and calcined at 500 °C prior to uses. The catalysts were physically mixed

with various ratios (0.25 to 1.0). Then, for each experiment a catalyst mixture was loaded to the upper zone of the reactor. After that, the reactor was closed and positioned in a furnace chamber, and nitrogen was then passed through the reactor to purge oxygen inside the system at a flow rate 30 ml/min for 30 minutes. Heating via an external electrical heater was subsequently started, and the temperature was controlled to the final temperature of the upper catalyst zone of 300 °C, and the lower pyrolysis zone of 500 °C with the ramping rate of 10 °C/min. The temperature was held at the final temperatures for 90 minutes at the atmospheric pressure.
The liquid products were collected in the condensers placed into the iced-bath. And, the non-condensable products or gaseous products were collected in a gas-sampling bag. The mass of tires and liquid products, before and after pyrolysis, were determined by weighing. The liquid products were first separated into maltene (n-pentane soluble) compounds and asphaltene (n-pentene insoluble) by adding n-pentane into the oils products at the ratio of 40:1. Hydrocarbon fractions in obtained maltenes were fractionated by using liquid adsorption chromatography technique. Then, the obtained maltene and hydrocarbon fractions were also analyzed by a Varian CP-3800 stimulated distillation gas chromatography (SIMDIST GC), equipped with FID. Each fraction was classified according to its boiling point range, which are naphtha (<200 °C), kerosene (200 - 250 °C), light gas oil (250–300 °C), heavy gas oil (300–370 °C), and long residue (>370 °C) (Dung *et al.*, 2009a, 2009b). The gaseous products were analyzed by Agilent Technologies 6890 Network GC system, using HP-PLOT Q column: 30 m x 0.32 mm diameter and 20 μm film thicknesses.

2.2. Catalyst characterization

The specific surface area and total pore volume of the prepared catalysts were determined by Brunauer-Emmet-Teller (BET) method using Thermo Finnigan/Sorptomatic 1990, which N_2 gas was used as the adsorbate. Acidic and basic site strengths of each catalyst were determined by Hammett indicators. The basic Hammett indicators (for acid site strength) used were methyl red (pK_a = 4.8), p-dimethylaminoazobenzene (pK_a = 3.3), crystal violet (pK_a = 0.8), 2-bromo-4,6-dinitroaniline (pK_a = -6.6), p-nitrotolulene (pK_a = -11.35). The acid Hammett indicators (for basic site strength) used were bromothymol blue (pK_{BH+} = 7.2), phenolphthalein (pK_{BH+} = 8.2) 2,4 dinitroaniline (pK_{BH+} = 15). About 30 mg of a catalyst sample was shaken with 1 ml of the solution of a Hammett indicator diluted in methanol and benzene for acidic and basic tests, and left to equilibrate for 2 h until no further color change was observed. The H_0 value of a sample at acid site was determined by the smallest value, which

had been subjected to a color change and having a H_0 value less than 7.0. Moreover, the H_0 value of a sample at the base site was determined by the greatest H_0, which had been subjected to a color change and having a H_0 value more than 7.0 (Singh and Fernando, 2008).

3 Results and Discussion

The catalytic pyrolysis of scrap tires was carried out with the two zeolites (Y and KL) packed in the reactor (the upper zone) in the physical mixture manner. The effects of mixing ratio were investigated. And, $Ø_{KL}$, defined as the weight fraction of KL in the following equations, was varied (0, 0.25, 0.5, 0.75, and 1).

$$Ø_{KL} = \frac{W_{KL}}{W_{KL} + W_Y} \quad ; \text{and } Ø_Y = 1 - Ø_{KL} \tag{1}$$

where W_{KL} is the weight of KL, and W_Y is the weight of Y in a mixture.

3.1 Physical Properties of Catalysts

The physical properties of the physical mixtures of Y and KL zeolites are summarized in Table 1.The BET surface area of pure Y and KL were about 296.7 and 578.2 m^2/g, respectively. Acid and basic strength of the physical mixtures are shown in Table 1. H_0 of KL zeolite is between 7.2–9.3, indicating the formation of strong basic sites on its surface. The Y zeolite and the physical mixture at $Ø_{KL}$ = 0.25 exhibited a high acid strength ($0.8 < H_0 \leq 3.3$). Moderate acid strength ($3.3 < H_0 \leq 4.8$) belongs to the physical mixtures of $Ø_{KL}$ = 0.5 and 0.75.

3.2 Effect of physical mixture on pyrolysis products

3.2.1. Product yields

The product yields are reported in terms of the gas to oil ratio as shown in Figure 1. The results presented in the figure include the non-catalytic case and each of pure zeolite cases. It could be seen that the gas-to-liquid ratio (G/L) of physical mixture cases is higher than the pure zeolite cases. Similar results regarding product yields have been reported by Shen *et al*. (2006), on which the presence of USY zeolite served to reduce the oil yield and then increase the gas yield, with the formation of coke on the catalyst. They suggested that the low Si/Al ratio of USY catalyst resulted

in high surface activity. Thus, it was clear that there were more reactants available to be cracked into the gaseous fraction. Moreover, for this work, the G/L ratio passes through the maxima at $Ø_{KL}$ = 0.75, and then decreases as the amount of KL zeolite increases. Consequently, the physical mixture at $Ø_{KL}$ = 0.75 exhibites the best performance in terms of the G/L ratio as compared to the pure zeolites. The solid yield remains almost constant throughout all experiments at around 44% (not shown in the figure), which means that the tire rubber is completely decomposed at 500 °C.

3.2.2. Light olefins and cooking gas production

The yields of the light olefins and cooking gas obtained from physical mixtures are also higher than the non-catalytic case and than the catalytic pyrolysis with pure zeolites ($Ø_{KL}$ = 0 and 1) as shown in Figure 2. This could be suggested that the different properties of the two catalysts in terms of their acidic and basic surfaces can influence the production of gases. However, the physical mixture of $Ø_{KL}$ = 0.25 was the best combination of catalysts to produce apparently the high amount of propane with a considerable amount of C_4 hydrocarbons, which was thus the best choice for cooking gas (propane and C_4) production. Moreover, it is found that this weight fraction also provides a high amount of ethylene and propylene. Hence, the physical mixture at the $Ø_{KL}$ = 0.25 could be the best catalyst combination to produce light olefins as well.

3.2.3. Liquid product

The effect of using the two zeolites simultaneously packed in the reactor on the quanlity of petroluem fractions is illustrated in Figure 3. The results show that the two catalysts with various packing ratios strongly affect the amount of naphtha. For example, the physical mixture at $Ø_{KL}$ = 0.75 gave the highest yield of naphtha (~ 48%) and also the lowest yields of residue (~ 4%) among the other mixture ratios. This could be suggested that the physical mixtures have higher cracking activity than using each separate zeolite, resulting in the higher yield to naphtha fraction. However, kerosene and LGO are still presented in the lowest yield at $Ø_{KL}$ = 0.25 and 0.75 when compared to a pure single zeolite.

It could be also suggested that the physica mixtures have higher cracking activity than using each separate zeolite, resulting in the higher yields to light olefins, cooking gas, and naphtha. Ou *et al.* (2006) studied the performance of ethylene and propylene production from a catalyst consisting of the combination of acid catalysts (SAPO-34 and SAPO-11). The results showed that the mixed catalyst gave a high conversion of ethylene, propylene, and butylenes that are higher than the sum of yields

of the individual components. And, they also suggested that the natural binary composition have the appropriate acid strength for reactions such as cracking. However, the basic catalyst can also drive a wide variety of hydrocarbon reactions such as double bond migration, dehydrogenation, hydrogenation, and isomerization via the carbanion intermediate (Hattori, 1995).

The saturated hydrocarbons and total aromatic compounds in maltene were analyzed by using liquid column chromatography. Figure 4 shows the effect of physical mixting on chemical composition in maltene. The results show that the physical mixtures provide the higher amount of saturated hydrocarbons and then the lower total aromaic compounds than the pure zeolite cases. Moreover, the yield of saturated hydrocrbons is slightly dropped with the increase of KL zeolite from $Ø_{KL}$ = 0.25 to 1. And, the aromatic compounds increase with the addition of KL zeolite.

Wakui *et al.*, (1999) suggested that the Brönsted acid sites and carbanion intermediate from basic sites act as active hydrogenation for alkenes at high reaction temperatures. As a result, for this work, the overall reaction can be predominated by the hydrogenation of heavy hydrocarbon molecules, leading to the large amount of saturated hydrocarbons in maltene fraction. In addition, the physical mixtures gave the highest saturated hydrocarbons. It can be postulated that the physical mixing provide a modest hydrogenation activity, as proposed by Kani *et al.*, (1992), who stated that Brönsted acid sites can act as active hydrogenation sites for alkenes at high temperatures.

Asphaltene formation can be used as another criterion to determine the quality of liquid product. The results can be observed in Figure 5. The main observation is that all catalysts, especially the physical mixture of $Ø_{KL}$ = 0.25, can drastically reduce asphaltene in the oil products. It is suggested that the complex molecules of asphaltene are possibly cracked on the active sites of catalysts.

4 Conclusions

The catalytic pyrolysis of waste tire was performed in a bench-scaled autoclave reactor. Y and KL zeolites were packed in the physically mixing style (Y + KL). The ratio of the two zeolites was varied from 0.25 to 1.0. Other parameter; the amount of used of tire, the amount of catalyst, the particle size of catalyst, the pyrolysis temperature, the holding time, and the heating rate were fixed at 30 g, 7.5 g, 8-18 mesh, 500 °C, 2 hr, 10 °C/min, respectively.

The physical mixing of zeoites significantly influenced the quality of pyrolysis products, and it is and easy and promising way to compromise

between acid and basic preparation of catalysts and make simultaneous use out of them. As a result, the mixture at $Ø_{KL}$ = 0.25 can produce the highest amount light olefins and cooking gas production. In addition, the physical mixtures of the two zeolites were also selective for naphtha production. The higher cracking activity of catalyst mixtures as compared to the individual one might be attributed to the collaboration of acidity and basicity.

Nomenclature

LGO Light gas oil
HGO Heavy gas oil

Greek Letters

$Ø_{KL}$ Weight fraction of KL

References

Choosuton, A. (2007) 'Development of Waste Tire Pyrolysis for the Production of Commercial Fuels: Effect of Noble Metals and Supports' M.S. Thesis book, The Petroleum and Petrochemical College, Chulalongkorn University, Bangkok, Thailand.

Dũng, N.A., Mhodmonthin, A., Wongkasemjit, S., Jitkarnka, S. (2009a) 'Effects of ITQ-21 and ITQ-24 as zeolite additives on the oil products obtainedfrom the catalytic pyrolysis of waste tire', *J. Anal. Appl. Pyrol.*, Vol. 85, pp. 338 344.

Dũng, N.A., Wongkasemjit, S., Jitkarnka, S. (2009b) 'Effects of pyrolysis temperature and Pt-loaded catalysts on polar-aromaticcontent in tire-derived oil', *Appl. Catal. B: Environ.*, Vol. 91, pp. 300 307.

Hattori, H. (1995) 'Heterogeneous Basic Catalysis', *Chem. Rev.*, Vol. 95, pp.537 558.

Kanai, J., Martens, J.A., Jacobs, P.A. (1992) 'On the Nature of the Active Sites for Ethylene Hydrogenation in Metal-Free Zeolites', *J. of Catal.*, Vol. 133, pp. 527 543.

Ou, J.D., Risch, M.A., Aronson, B.J. (2006) 'Combined oxydehydrogenation and cracking catalyst for production of olefins', U.S. Patent 7,145,051 B2, Dec. 5, 2006.

Pollution Control Department, Ministry of Natural Resources and Environment, THAILAND (2010) http://ptech.pcd.go.th/p2/ waste-util-article-view.php?aid=49.

Shen, B., Wu, C., Wang, R., Guo, B., Liang, C. (2006) 'Pyrolysis of scrap tyres with zeolite USY', Hazardous Materials B, Vol. 137, pp.1065 1073.

Singh, A.K., and Fernando, S.D. (2008) 'Transesterification of Soybean Oil Using Heterogeneous Catalysts', *Energy & Fuels*, Vol. 22, pp.2067 2069.

Wakui, K., Satoh, K.I., Sawada, G., Shiozawa, K., Matano, K.I., Suzuki, K., Hayakawa, T., Murata, K., Yoshimura, Y., Mizukami, F. (1999) 'Catalytic cracking of n-butane over rare earth-loaded HZSM-5 catalysts', *Appl. Catal. A: Gen.*, Vol. 42, pp.307 314.

Williams, P.T., Brindle, A.J. (2003) 'Aromatic chemicals from the catalytic pyrolysis of scrap tyres', *J. of Anal. and Appl. Pyrol.*, Vol.67, pp.143 164.

Caption of Tables

Table 1 Physical properties of the catalysts and their physical mixtures.

Caption of Figures

Figure 1 G/L ratio at various weight fractions of KL.

Figure 2 Effects of physical mixing and the weight fraction of KL on light olefins and cooking gas production.

Figure 3 Effect of physical mixing on petroleum fractions in maltenes.

Figure 4 Chemical composition in maltene obtained from the physical mixtures of zeolites (Y and KL) with various weight fractions of KL.

Figure 5 Weight fraction of asphaltene in pyrolytic oils obtained from using the physical mixtures of zeolites.

Table 1

Catalyst	Surface area (m^2/g)	Pore volume (cm^3/g)	Acid/Base site strength, (H_0)
Y	578.2	0.58	$0.8 < H_0 \leq 3.3$
$Ø_{KL}$ = 0.25	507.8*	0.53*	$0.8 < H_0 \leq 3.3$
$Ø_{KL}$ = 0.5	437.5*	0.49*	$3.3 < H_0 \leq 4.8$
$Ø_{KL}$ = 0.75	367.1*	0.44*	$3.3 < H_0 \leq 4.8$
KL	296.7	0.39	$7.2 < H_0 \leq 9.3$

*Weight average

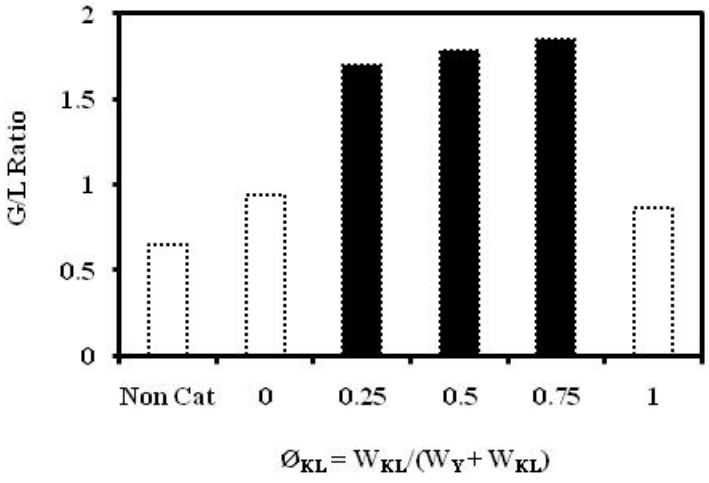

Figure 1

Author

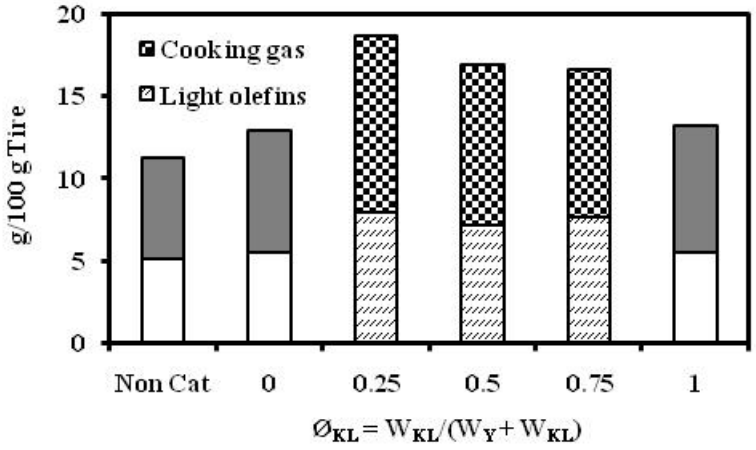

Figure 2

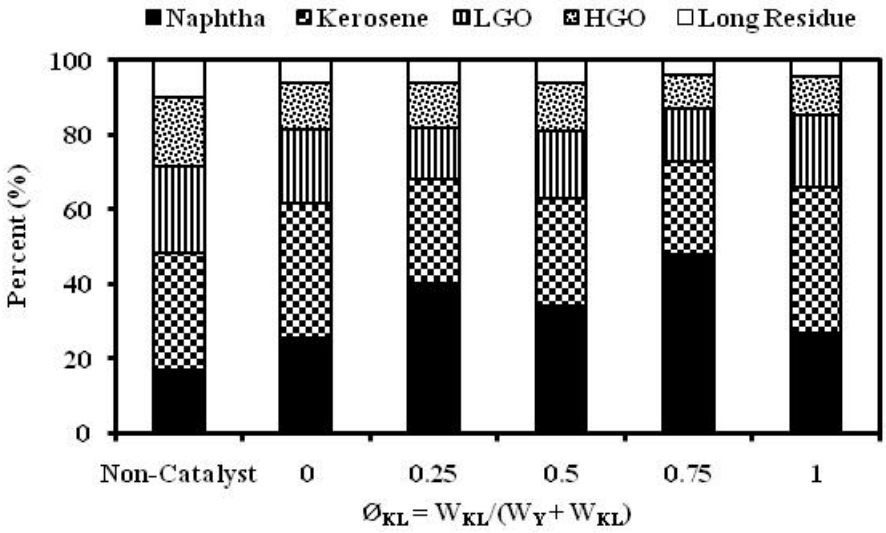

Figure 3

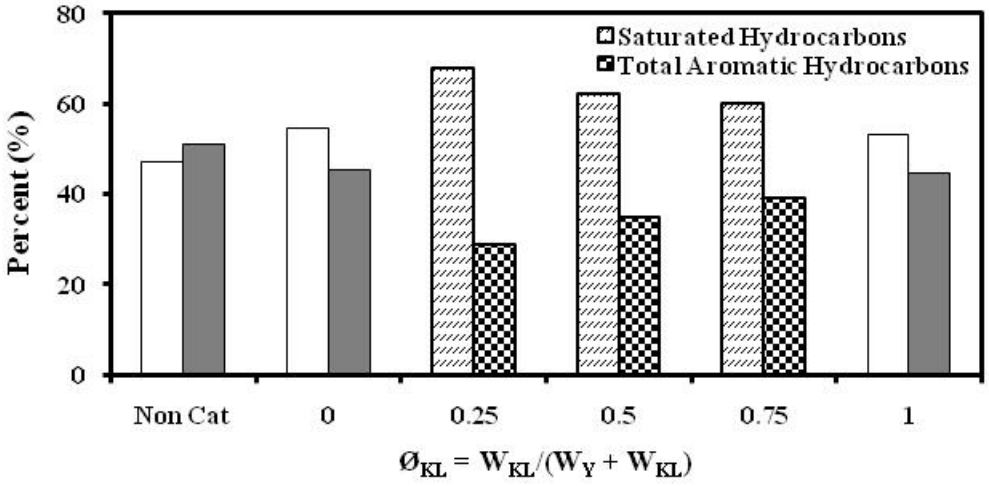

Figure 4

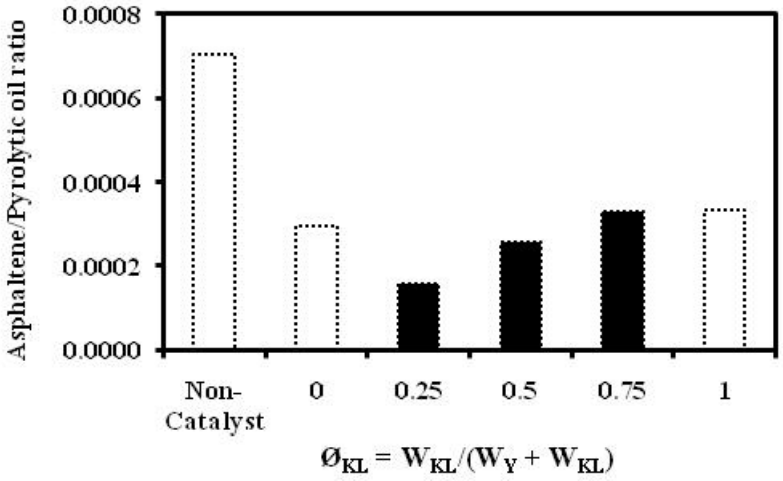

Figure 5

.